Dynamics of Quantum-Classical Hybrid Systems with Timescale Separation

Dissertation

zur Erlangung des Doktorgrades

an der Fakultät für Mathematik, Informatik und Naturwissenschaften

Fachbereich Physik

der Universität Hamburg

vorgelegt von

Nicolas Tom Daniel Lenzing

Hamburg, Januar 2025

Gutachter der Dissertation:	Prof. Dr. Michael Potthoff
	Prof. Dr. Alexander Lichtenstein
Zusammensetzung der Prüfungskommission:	Prof. Dr. Dorota Koziej
	Prof. Dr. Alexander Lichtenstein
	Prof. Dr. Michael Potthoff
	Prof. Dr. Michael Thorwart
	Prof. Dr. Tim Wehling
Vorsitzende der Prüfungskommission:	Prof. Dr. Dorota Koziej
Datum der Disputation:	17.12.2024
Vorsitzender Fach-Promotionsausschuss PHYSIK:	Prof. Dr. Wolfgang J. Parak
Leiter des Fachbereichs PHYSIK:	Prof. Dr. Markus Drescher
Dekan der Fakultät MIN:	Prof. Dr.-Ing. Norbert Ritter

Abstract

In this thesis, the real-time dynamics of quantum-classical spin-impurity models with timescale separation is investigated. These models consist of a small number (≤ 10) of classical impurity spins that are exchange-coupled to a quantum mechanical host system. It is assumed that the dynamics of the host system is fast compared to that of the classical spins.

The timescale separation motivates the introduction of an adiabatic constraint to the Hilbert space of the host system. One can distinguish a strict adiabatic constraint, where the host is restricted to the ground state only, and a relaxed constraint, which additionally includes a few of the lowest excited states. The incorporation of either constraint into the theory via a Lagrangian formulation yields a geometrical spin torque in the effective spin equations of motion that is not present in other treatments of effective spin dynamics, like, for example, the Landau-Lifshitz-Gilbert equation. This geometrical spin torque can have a strong influence on the spin dynamics, e.g., lead to an anomalous precession frequency, and is proportional to the spin-Berry curvature of the host system. The concrete form of the spin-Berry curvature, and thus the geometrical spin torque, strongly depends on the type of constraint used. While some effects can already be captured with the strict adiabatic constraint, it is found that for certain systems and parameter regimes the relaxation of the constraint is crucial.

For weak quantum-classical exchange coupling J the geometrical spin torque can also be derived by perturbation theory. It is then an effect of order J^2. However, it is shown that an interplay of correlation, spontaneous symmetry breaking, and Goldstone modes can strongly boost the geometrical spin torque and lead to a sizable long-range effect.

Finally, the adiabatic constraint can be treated using statistical mechanics, which results in the so-called adiabatic response theory. Applied to spin systems, this yields a spin-Berry curvature consistent with the Lagrangian approach and, for weak-J, is in agreement with linear response results. Importantly, both the linear and adiabatic response approaches give expressions for another essential effect of spin dynamics, the Gilbert damping. Usually, Gilbert damping is simply represented by a scalar quantity but it may be a highly nonlocal tensor in some cases. It is found that the nonlocal elements of the Gilbert damping can have a strong impact on the relaxation dynamics and may even counterintuitively cause longer relaxation times. The magnitude of the effect depends on the number of impurity spins and also their relative spatial locations.

Zusammenfassung

Diese Arbeit untersucht die Realzeitdynamik von quanten-klassischen Spin-Störstellen Modellen mit Zeitskalenseparation. Die Modelle bestehen dabei aus einer kleinen Anzahl (≤ 10) von klassischen Störstellenspins, die an ein quantenmechanisches Substrat gekoppelt sind. Es wird durchweg angenommen, dass die Dynamik des Substrats schnell ist im Vergleich zur Zeitskala, auf der die Spindynamik abläuft.

Die Zeitskalenseparation motiviert die Einführung einer adiabatischen Zwangsbedingung auf dem Hilbertraum des Substrats. Hierbei kann man zwischen einer strengen adiabatischen Zwangsbedingung, bei der das Substrat auf seinen Grundzustand beschränkt wird, und einer gelockerten adiabatischen Zwangsbedingung, welche ein paar der niedrigsten angeregten Zustände miteinbezieht, unterscheiden. Wenn man diese Zwangsbedingung in einer Lagrangeschen Formulierung der Theorie einbezieht, ergibt sich ein geometrisches Spindrehmoment in den effektiven Bewegungsgleichungen, das in anderen Behandlungen der effektiven Spindynamik, wie z. B. der Landau-Lifshitz-Gilbert-Gleichung, nicht vorhanden ist. Dieses geometrische Spindrehmoment kann einen starken Einfluss auf die Spindynamik haben, zum Beispiel in Form einer anomalen Präzessionsfrequenz, und ist proportional zur Spin-Berry Krümmung des Substrats. Die konkrete Form der Spin-Berry Krümmung, und somit des geometrischen Spindrehmoments, hängt stark von der Art der Zwangsbedingung ab. Während einige Effekte bereits im Rahmen einer strikten adiabatischen Näherung beschrieben werden können, findet man, dass für gewisse Systeme und Paramterregime die Lockerung der Zwangsbedingung notwendig ist.

Für schwache quanten-klassische Austauschkopplung J kann das geometrische Spindrehmoment auch perturbativ, mittels der adiabatisch-modifizierten linearen Antworttheorie hergeleitet werden. Hier ist es ein Effekt der Ordnung J^2. Es wird jedoch gezeigt, dass ein Zusammenspiel von Korrelation, spontaner Symmetriebrechung und Goldstone-Moden das geometrische Spindrehmoment stark erhöhen und damit einen beträchtlichen und langreichweitigen Effekt zur Folge haben kann.

Schließlich kann die adiabatische Zwangsbedingung auch im Rahmen der statistischen Mechanik behandelt werden, was in der sogenannten adiabatischen Antworttheorie resultiert. Angewendet auf Spinsysteme erhält man eine Spin-Berry Krümmung, die konsistent mit den Resultaten aus dem Lagrange Formalismus und der linearen Antworttheorie ist. Insbesondere liefern die Antworttheorien auch Ausdrücke für einen anderen wichtigen Effekt der Spindynamik, die Gilbertdämpfung. Normalerweise wird diese als skalare Größe dargestellt, jedoch kann sie auch die Form eines hochgradig nicht-lokalen Tensors annehmen. Man findet, dass die nicht-lokalen Elemente des Gilbertdämpfungs-Tensors einen starken Enfluss auf die Relaxationsdynamik haben und kontraintuitiv die Relaxationszeit sogar vergrößern können. Die Stärke dieses Effekts hängt hierbei von der Anzahl der Störstellenspins und ihren relativen Abständen zueinander ab.

Contents

1 – List of Publications

This cumulative thesis is based on three publications [I], [II], and [III]. These publications are listed chronologically below and are also presented in the thesis in that order. Publication [I] is presented in the last section of chapter 4, while publication [II] is found in the second section of chapter 5. Both publications deal with the geometrical spin torque, which is closely related to the spin-Berry curvature $\underline{\Omega}$. Chapter 4 introduces adiabatic spin dynamics (ASD) theory. This is applied to a system of a single classical spin coupled to a one-dimensional tight-binding model. In publication [I] ASD is extended to non-Abelian spin dynamics (NA-SD) theory, which is then tested for the same system. Chapter 5 starts with the calculation of $\underline{\Omega}$ for a host system of a ferromagnetic Heisenberg model using spin wave and linear response theory (LRT). This approach is then adapted in publication [II] for an antiferromagnetic Heisenberg model. The last publication [III] is presented at the end of chapter 6, after the introduction of adiabatic response theory (ART). This publication deals with the calculation of the Gilbert damping via the two different theories ART and LRT and subsequently computes and compares the corresponding spin dynamics, with the Rudermann-Kittel-Kasuya-Yosida (RKKY) interaction playing a minor role.

Publications:

[I] N. Lenzing, A. I. Lichtenstein, and M. Potthoff, Emergent non-Abelian gauge theory in coupled spin-electron dynamics, Physical Review B **106**, 094433 (2022).

[II] N. Lenzing, D. Krüger, and M. Potthoff, Geometrical torque on magnetic moments coupled to a correlated antiferromagnet, Physical Review Research **5**, L032012 (2023).

[III] N. Lenzing, D. Krüger, and M. Potthoff, Microscopic theory of spin friction and dissipative spin dynamics, Physical Review B **111**, 014402 (2025).

Declaration of Contribution

[I] N. Lenzing wrote the computer code, performed the numerical simulations, created all plots, and did the analytical calculations. All authors participated in the planning of the project, the analysis of the numerical results, and the writing of the paper.

[II] N. Lenzing wrote the computer code, performed the numerical simulations, and created all plots for the spin wave theory part of the paper. He also conducted the analytical calculations for that part of the paper. All authors participated in the planning of the project, the analysis of the numerical results, and the writing of the paper.

[III] N. Lenzing wrote the computer code, performed the numerical simulations, created all plots, and did the analytical calculations for all parts except section VIJ. All authors participated in the planning of the project, the analysis of the numerical results, and the writing of the paper.

2 – Introduction

The discovery of the electron in 1897 by Sir Joseph John Thomson and the accurate measurement of its charge in 1909 by Robert Andrews Millikan and Harvey Fletcher in their famous oil drop experiment [1] paved the way for the research area of electronics. Put simply, electronics uses the charge of the electron to store and transport information, and thus operate technical devices. A pivotal advancement that furthered modern electronics was the invention of the point-contact transistor by John Bardeen, Walter Brattain and William Shockley in 1947 at Bell Labs. In the following decades, transistors gradually replaced vacuum tubes as the leading electronic component and nowadays most devices are solid-state based. Two of the main advantages of transistors over vacuum tubes were that they are more compact and have a better scalability, thus facilitating the construction of smaller devices. In particular, this was crucial for integrated circuits also known as computer chips. Over the years, the number of transistors in an integrated circuit grew exponentially, as conjectured by Gordon Moore in the famous Moore's law, enabling the rapid increase of computing power, which shapes today's digital age. It is predicted, however, that this growth will stop in the near future, due to (fundamental) physical limitations. Therefore, it is prudent to look for other means with which to drive technological progress.

One such opportunity lies in the field of spintronics [2–5]. In contrast to conventional electronics, the focus is not only on the charge of the electron but includes its spin degrees of freedom as well. Early works in this direction study, for instance, the mobility of an electron in a ferromagnetic material. It is found that the mobility is spin-dependent [6]. A pioneering moment for spintronics was the discovery of the giant magnetoresistance (GMR) [7, 8] that enabled the efficient control of electron movement by means of their spin. It is observed in magnetic multilayer structures of alternating ferromagnetic and nonmagnetic metallic layers. The GMR is the effect that the electrical resistivity depends on the relative orientation, i.e., parallel or antiparallel, between the magnetic layers. A concrete example for such a multilayer structure is a spin valve [9], which is a trilayer structure, where a nonmagnetic metallic layer is sandwiched between two magnetic layers. One of the magnetic layers is pinned, i.e., the magnetic moments are fixed by an external field, while the other is free. Spin valves have already been used successfully in real world applications such as sensors [10]. Another promising platform for spintronics is that of magnetic tunnel junctions (MTJ) [11], which differ from spin valves in that the nonmagnetic layer is insulating instead of metallic. Here, one observes tunneling magnetoresistance (TMR), which is similar to GMR. Magnetic tunnel junctions are key for magnetic random access memory (MRAM) [12, 13], which is believed to potentially combine short access times with less power consumption and nonvolatility, i.e., it does not require power to maintain the stored information [14]. Apart from novel storage devices there is also research into novel logic devices using MTJ [15, 16], which promise high-speed operations [16, 17]. The advancement of spintronics is closely connected to nanomagnetism [12] and relies on the understanding of the effects that govern spin dynamics on

the atomistic scale, which is the overarching topic of this thesis.

One of the first widely used equations to describe spin dynamics theoretically is the Landau-Lifshitz-Gilbert (LLG) equation [18,19], which describes the real-time dynamics of magnetic moments in an (effective) magnetic field while also including damping effects. It is the successor of the Landau-Lifshitz equation, whose phenomenological damping term was modified by Gilbert to eliminate problems that existed for large damping. Hence, the prefactor α of the damping term is commonly referred to as Gilbert damping. While the Gilbert damping parameter is often treated as a scalar, it is actually a nonlocal, potentially nonuniform, tensor $\underline{\alpha}$ [20–22]. The nonlocalities can have a significant impact on the spin dynamics [23] and are also a major topic in publication [III]. As mentioned above, the Gilbert damping and the LLG equation were originally a phenomenological description of spin dynamics and were used only in the context of the macrospin approximation in micromagnetics [24], where the magnetisation of entire domains is represented by a single classical macrospin $\boldsymbol{S}$. However, this treatment glosses over many physical details and is often insufficient to accurately explain all the relevant interactions like spin inertia effects [25–31] and the RKKY interaction [32–34]. The RKKY interaction is an indirect exchange coupling that is mediated by conduction electrons and has to be understood from an atomistic point of view. Thus, it is preferable to derive $\underline{\alpha}$ and LLG-like equations by an atomistic approach using first principles [27,31,35–45]. In these kinds of derivations, the usual starting point is a lattice Hamiltonian describing an electronic host system to which spins are coupled, i.e., a kind of Kondo model [46,47]. These models have already been applied in the context of the nonequilibrium dynamics of spin-valve-like structures under an external current, see for example [48–50].

This thesis deals exclusively with impurity models, where only a few (≤ 10) spins are coupled to the host system. To get an effective LLG-like equation of motion for the impurity spins, one has to "integrate out" the electrons. This can be done via linear response theory (LRT) [45,51], where the influence of the host gets absorbed into the magnetic susceptibility $\underline{\chi}$ from which, for instance, the Gilbert damping can be computed [45,52–54]. The effective spin-only theory greatly simplifies the computation of the spin dynamics since the dynamics of the host is not considered explicitly but is contained in $\underline{\chi}$. This approach will be explained in chapter 3 and is applied to a ferromagnetic Heisenberg system in chapter 5. It is also the method used in publication [II]. However, it is sensible, where possible, to compare the results of the effective theory against results of the full theory including both spin and host dynamics, to gauge the validity of the effective theory away from the domain where the full theory is feasible. Computationally, it is very advantageous to treat the impurity spins as classical vectors of fixed length, an approximation that will be used throughout this thesis and is quite common in spin dynamics, cf. [45,48,49,55–57]. How to compute the dynamics of quantum-classical impurity systems will be discussed in chapter 3.

An important consideration that is a main topic in this thesis, but is completely absent in the LLG equation, is the treatment of different timescales. Arguably, the most prominent example in physics is found in molecular dynamics. Here, it is common to assume a timescale separation between nuclei and electrons due to their mass difference [58,59]. This justifies a separation of the total wavefunction into an electronic part and a nuclear part, which is

known as the Born-Oppenheimer approximation [58,60]. If additionally the nuclei are treated as classical point particles, their dynamical equations reduce to those of classical particles in a potential, given by the effective potential of the electrons. The electrons, on the other hand, are still treated as quantum particles but now their equations of motion depend on the nuclei only parametrically through their classical position vectors. In quantum-classical impurity problems considered here, one has an analogous situation with a timescale separation between fast electronic and slow spin degrees of freedom. Another approximation that is regularly invoked in the context of timescale separation is the adiabatic approximation [61–63]. It assumes that at every instance of time t the state of the fast variables is given by the ground state for the instantaneous configuration of the slow variables. While in the case of the quantum-classical impurity models, this is a holonomic constraint on the electronic host system, it has a feedback effect on the dynamics of the spins. Namely, there is a geometrical spin torque that enters the effective spin-only equations of motion. Such feedback effects are connected to the Berry curvature [64–66] and have been explored for spin systems [67–69]. A theoretical framework is given by adiabatic spin dynamics (ASD) theory [56], which will be introduced in chapter 4. ASD demonstrates that the inclusion of the adiabatic constraint into the theory has to be done via a Lagrangian formulation, i.e., the geometrical spin torque is non-Hamiltonian as opposed to the Hamiltonian spin torques in the LLG equation. However, in some cases, constraining the electrons to the ground state might be too strict of an approximation to capture all the relevant physics, e.g., inertia effects [29], and one has to relax the constraint to include a certain number of the lowest excited states. How this is done systematically is explained in publication [I], where the extension of ASD called non-Abelian spin dynamics (NA-SD) theory is worked out.

Timescale separation can be applied not only to coupled electron-spin systems, but also to systems exclusively containing spins. In [70] this is done for a purely classical system consisting of different types of spins, "slow" and "fast", coupled via an isotropic Heisenberg exchange interaction. Similar to the quantum-classical electron-spin case this yields an additional spin torque. In Chapter 5 this is discussed in the context of a quantum-classical spin-spin model with a classical impurity spin coupled to a Heisenberg model. Due to the interplay of correlations, spontaneous symmetry breaking, and gapless Goldstone modes one expects a large geometrical spin torque. Although this turns out to be false for the ferromagnetic case, see section 5.1, the description serves as a good basis for the understanding of publication [II], where an analogous procedure is applied to an antiferromagnetic host.

A weakness of ASD and NA-SD is that both are only valid at zero temperature and do not produce an expression for the Gilbert damping. These problems can be addressed using adiabatic response theory (ART) [71, 72] that is introduced in chapter 6. It formulates the adiabatic approximation in a finite temperature, statistical mechanics framework and provides expressions for both, Gilbert damping and geometrical spin torque. ART describes the response of a system to a slow perturbation, in contrast to linear response, which applies to weak perturbations, but for certain situations both theories can be shown to yield qualitatively the same results. This is taken up in publication [III], which deals with dissipative spin dynamics and compares the results for ART and LRT after putting both on equal footing.

3 – Quantum-Classical Spin Dynamics

The classical approximation of quantum mechanical quantities is an ubiquitous theme in theoretical physics. Arguably, this is known best from molecular dynamics [58], where the coordinates of the nuclei are usually treated as classical variables. However, it is also common for magnetic moments, which can be modelled as classical spins. The focus of this work is on magnetic moments coupled to a system of itinerant electrons, where treating the magnetic moments as classical spins results in a quantum-classical hybrid model. The main motivation for a classical treatment comes from the fact that this simplifies analytical and numerical calculations, however, at the expense of quantum phenomena of the magnetic moments, such as the Kondo effect [46]. This chapter introduces the quantum-classical spin models that are used throughout this thesis and explains how to generally compute quantum-classical dynamics.

3.1 – Hamiltonian and Equations of Motion

A generic quantum-classical spin Hamiltonian $\hat{H}(\boldsymbol{S})$, with M classical spins coupled to a quantum system, has the form

$$\hat{H}(\boldsymbol{S}) = \hat{H}_{\mathrm{qu}} + \hat{H}_{\mathrm{int}}(\boldsymbol{S}) + H_{\mathrm{cl}}(\boldsymbol{S}), \tag{3.1}$$

where $\boldsymbol{S} \equiv (\boldsymbol{S}_1, \ldots, \boldsymbol{S}_M)$ describes the entirety of classical spins, which in this work are typically of fixed length $S_m = |\boldsymbol{S}_m| = 1$. The Hamiltonian consists of three parts: $\hat{H}_{\mathrm{qu}}$ is the quantum part, in this work typically a system of itinerant electrons, H_{cl} the classical part, e.g., interactions among the classical spins or with an external magnetic field, and $\hat{H}_{\mathrm{int}}$ describes the interaction between the quantum and classical degrees of freedom. The interaction term is a quantum operator that depends parametrically on the classical degrees of freedom. The classical approximation of the spins can be reasonable, e.g., for large spin quantum numbers [30, 73].

All models considered in this thesis are models on a discrete lattice. The interaction term always takes the prototypical form

$$\hat{H}_{\mathrm{int}} = J \sum_m \hat{\boldsymbol{s}}_{i_m} \boldsymbol{S}_m(t), \tag{3.2}$$

which is a quantum-classical version of the multi-impurity Kondo, or s-d exchange [74], interaction. Here $\hat{\boldsymbol{s}}_{i_m}$ is a local magnetic moment of the quantum subsystem at lattice site i_m and J denotes the quantum-classical exchange interaction, which is assumed to be equally strong at every lattice site. Note also that the classical spins are explicitly time-dependent. Assuming that $\hat{H}_{\mathrm{qu}}$ describes a noninteracting system, the treatment of $\boldsymbol{S}_m$ as either a classical vector or a quantum operator makes the difference between a free or a correlated problem, i.e., if the computational complexity of the system scales polynomial

or exponentially with the system size. In the latter case, one would deal with a Kondo (multi-)impurity problem, which has to be solved using advanced numerical techniques. For a single impurity or a one dimensional system one can use the density matrix renormalisation group method [75–77], but even then accessing long timescales is difficult. Nevertheless, it is prudent to study cases for which a comparison between quantum-classical and full-quantum dynamics is possible, in order to estimate the reliability of the quantum-classical results in regimes where a full quantum solution is not achievable [30, 56].

The dynamics of the quantum system is governed by the Schrödinger equation

$$i\hbar\frac{d}{dt}\left|\Psi(t)\right\rangle = \left[\hat{H}_{\mathrm{qu}} + \hat{H}_{\mathrm{int}}(\boldsymbol{S}(t))\right]\left|\Psi(t)\right\rangle, \tag{3.3}$$

where $\left|\Psi(t)\right\rangle$ is the multi-particle wavefunction. In the case of a noninteracting quantum part $\hat{H}_{\mathrm{qu}}$, one is effectively on a one-particle level and it is thus possible to describe the system dynamics via the one-particle reduced density matrix

$$\rho_{i\sigma i'\sigma'}(t) := \langle c^{\dagger}_{i'\sigma'}(t)c_{i\sigma}(t)\rangle \tag{3.4}$$

with the fermionic creation and annihilation operators $c^{\dagger}_{i\sigma}$ and $c_{i\sigma}$. As usual i, i' refer to lattice sites and σ, σ' denote the spin projection with respect to the quantisation axis, which in this thesis is always the z axis. Concretely, the quantum part of the Hamiltonian takes the general form $\hat{H}_{\mathrm{qu}} = \sum_{ii'\sigma\sigma'} T_{ii'\sigma\sigma'} c^{\dagger}_{i\sigma} c_{i'\sigma'}$ with hopping amplitudes $T_{ii'\sigma\sigma'}$. Since the local magnetic moments can be expressed as $\hat{\boldsymbol{s}}_{i_m} = \frac{\hbar}{2} \sum_{\sigma\sigma'} c^{\dagger}_{i_m,\sigma} \boldsymbol{\tau}_{\sigma\sigma'} c_{i_m,\sigma'}$, with the vector of Pauli matrices $\boldsymbol{\tau} := (\tau_x, \tau_y, \tau_z)^{\mathsf{T}}$, the interaction term is also bilinear in c-operators and we can formulate the model in terms of an effective hopping matrix $\underline{T}^{\mathrm{eff}}$ as

$$\begin{aligned}\hat{H}_{\mathrm{qu}} + \hat{H}_{\mathrm{int}} &= \sum_{ii'\sigma\sigma'} T^{\mathrm{eff}}_{ii'\sigma\sigma'}(t) c^{\dagger}_{i\sigma} c_{i'\sigma'}\\ &=: \sum_{ii'\sigma\sigma'} \left(T_{ii'\sigma\sigma'} + \frac{J}{2}\delta_{ii'}[\boldsymbol{S}_i(t)\boldsymbol{\tau}]_{\sigma\sigma'}\right) c^{\dagger}_{i\sigma} c_{i'\sigma'},\end{aligned} \tag{3.5}$$

where we set $\hbar = 1$. The elements of the hopping matrix $\underline{T}$ and the quantum-classical coupling J determine the timescale on which the electron and spin dynamics take place, respectively. The dynamics of the one-particle reduced density matrix is given by a von Neumann equation

$$i\frac{d}{dt}\underline{\rho}(t) = \left[\underline{T}^{\mathrm{eff}}(t), \underline{\rho}(t)\right]. \tag{3.6}$$

There exist several schemes to compute the dynamics of classical degrees of freedom in a quantum-classical setup, the most common of which is the Ehrenfest dynamics [78–80]. Here, the expectation values of the quantum mechanical quantities are taken when deriving the equations of motion (EOM) of the classical degrees of freedom. The time evolution of functions depending on classical observables is then given by the Poisson bracket with the expectation value of the full Hamiltonian (3.1). For functions in classical physics depending on spin degrees of freedom, one has to use a generalised version of the Poisson bracket [81, 82]

that is defined as

$$\{f, g\} = \sum_i \left[\frac{\partial f}{\partial \boldsymbol{q}_i} \frac{\partial g}{\partial \boldsymbol{p}_i} - \frac{\partial g}{\partial \boldsymbol{q}_i} \frac{\partial f}{\partial \boldsymbol{p}_i} - \frac{\partial f}{\partial \boldsymbol{S}_i} \left(\boldsymbol{S}_i \times \frac{\partial g}{\partial \boldsymbol{S}_i} \right) \right], \tag{3.7}$$

where $f = f(\{\boldsymbol{q}_i\}, \{\boldsymbol{p}_i\}, \{\boldsymbol{S}_i\})$ and $g = g(\{\boldsymbol{q}_i\}, \{\boldsymbol{p}_i\}, \{\boldsymbol{S}_i\})$ denote two classical functions depending on (generalised) position, momentum, and spin variables. Using this generalised Poisson bracket, the EOM of the mth classical spin is given by

$$\dot{\boldsymbol{S}}_m = \{\boldsymbol{S}_m, \langle \hat{H} \rangle_t\} = \frac{\partial \langle \hat{H} \rangle_t}{\partial \boldsymbol{S}_m} \times \boldsymbol{S}_m. \tag{3.8}$$

In the case of the Kondo-like interaction term (3.2), this yields

$$\dot{\boldsymbol{S}}_m = J \langle \hat{\boldsymbol{s}}_{i_m} \rangle_t \times \boldsymbol{S}_m + \frac{\partial H_{\mathrm{cl}}}{\partial \boldsymbol{S}_m} \times \boldsymbol{S}_m, \tag{3.9}$$

where for noninteracting $\hat{H}_{\mathrm{qu}}$ the expectation value of the local magnetic moment $\hat{\boldsymbol{s}}_{i_m}$ can be computed as $\langle \hat{\boldsymbol{s}}_{i_m} \rangle = \frac{1}{2} \sum_{\sigma\sigma'} \rho_{i_m \sigma i_m \sigma'}(t) \boldsymbol{\tau}_{\sigma\sigma'}$. In the case of an interacting system one has to use the full multi-particle wavefunction $|\Psi(t)\rangle$.

An approximation that will play a central role is the adiabatic approximation. It leads to a geometrical spin torque when analytically evaluating $\frac{\partial \langle \hat{H} \rangle}{\partial \boldsymbol{S}_m}$ giving new physical insight concerning the feedback of the quantum system on the classical spin dynamics. This will be explored in chapter 4 and is the topic of publication [I].

3.2 – Linear Response Theory

Concerning the quantum-classical coupling strength J, it is often sensible to assume it as weak compared to the nearest-neighbour hopping amplitude or other couplings. In the weak-J regime, one can use linear response theory [51,83] to compute the expectation value $\langle \hat{\boldsymbol{s}}_{i_m} \rangle_t$. Linear response theory is generally applicable to calculate the response of a system under small time-dependent perturbations. This is described by a Hamiltonian of the form

$$\hat{H}'(t) = \hat{H}_0 + \lambda(t) \hat{H}_1, \tag{3.10}$$

where the unperturbed Hamiltonian $\hat{H}_0$ is time-independent and $\lambda(t)$, describing the time-dependent coupling to $\hat{H}_1$, is small for all t. The time-dependent expectation value of an observable $\hat{A}$ with regard to the full Hamiltonian $\hat{H}'$ can then be expressed as

$$\langle \hat{A} \rangle_t = \langle \hat{A} \rangle^{(0)} - i \int_{-\infty}^{t} dt' \lambda_B(t') \left\langle \left[\hat{A}(t), \hat{H}_1(t') \right] \right\rangle^{(0)} \tag{3.11}$$

discarding terms of order $\mathcal{O}(\lambda^2)$. This is Kubo's formula [51]. Here $\langle \hat{A} \rangle^{(0)}$ is the expectation value with regard to $\hat{H}_0$. Furthermore, $\hat{H}_1$ is now expressed in the interaction picture and thus time-dependent. In terms of the quantum-classical Hamiltonian introduced in (3.1) and (3.2) one has $\hat{H}_0 = \hat{H}_{\mathrm{qu}} + H_{\mathrm{cl}}$ and a sum of multiple time-dependent perturbations $\lambda_m(t) \hat{H}_m$ with $\lambda_m(t) = J\boldsymbol{S}_m(t)$ and $\hat{H}_m = \hat{\boldsymbol{s}}_{i_m}$. Using (3.11), the expectation value of the local magnetic

moment at site i_m is

$$\langle \hat{\boldsymbol{s}}_{i_m} \rangle_t = \langle \hat{\boldsymbol{s}}_{i_m} \rangle^{(0)} - iJ \int_{-\infty}^{t} dt' \left\langle \left[\hat{\boldsymbol{s}}_{i_m}(t), \sum_{m'} \hat{\boldsymbol{s}}_{i_{m'}}(t') \boldsymbol{S}_{m'}(t') \right] \right\rangle^{(0)}$$

$$= \langle \hat{\boldsymbol{s}}_{i_m} \rangle^{(0)} + J \sum_{m'} \int_{-\infty}^{t} dt' \underline{\chi}_{mm'}(t, t') \boldsymbol{S}_{m'}(t') \tag{3.12}$$

with the magnetic susceptibility χ defined by

$$\chi_{m\alpha, m'\alpha'}(t, t') = -i\Theta(t - t') \left\langle \left[\hat{s}_{i_m}^{\alpha}(t), \hat{s}_{i_{m'}}^{\alpha'}(t') \right] \right\rangle^{(0)}. \tag{3.13}$$

Using that $\langle \hat{A} \rangle^{(0)} = \frac{1}{Z} \text{Tr} \left[e^{\beta \hat{H}_0} \hat{A} \right]$ and $\hat{s}_{i_m}(t) = e^{i\hat{H}_0 t} \hat{s}_{i_m} e^{-i\hat{H}_0 t}$, one can show that the susceptibility is homogenous, i.e., $\chi_{m\alpha, m'\alpha'}(t, t') = \chi_{m\alpha, m'\alpha'}(t - t')$, see Appendix A.

If one assumes the electron dynamics to be much faster than the spin dynamics, the magnetic susceptibility will be strongly peaked at $t' \approx t$ [45]. A Taylor expansion of $\boldsymbol{S}_m(t')$ around $t' = t$ yields $\boldsymbol{S}_m(t') = \boldsymbol{S}_m(t) + (t' - t)\dot{\boldsymbol{S}}_m(t) + \mathcal{O}((t' - t)^2)$. Due to $\chi_{m\alpha, m'\alpha'}(t - t')$ being peaked at $t' \approx t$, the first two terms are sufficient when inserting into (3.12). This gives

$$\langle \hat{\boldsymbol{s}}_{i_m} \rangle_t = \langle \hat{\boldsymbol{s}}_{i_m} \rangle^{(0)} + J \sum_{m'} \boldsymbol{S}_{m'}(t) \int_{-\infty}^{t} dt' \underline{\chi}_{mm'}(t - t') + J \sum_{m'} \dot{\boldsymbol{S}}_{m'}(t) \int_{-\infty}^{t} dt'(t' - t) \underline{\chi}_{mm'}(t - t')$$

$$= \langle \hat{\boldsymbol{s}}_{i_m} \rangle^{(0)} + J \sum_{m'} \boldsymbol{S}_{m'}(t) \int_{-\infty}^{t} d\tau \underline{\chi}_{mm'}(\tau) - J \sum_{m'} \dot{\boldsymbol{S}}_{m'}(t) \int_{-\infty}^{t} d\tau \tau \underline{\chi}_{mm'}(\tau), \tag{3.14}$$

where the second equality follows from the integral transformation $t' \to \tau = t - t'$. In the limit $t \to \infty$ the integrals can be written in terms of the Fourier transform of the susceptibility

$$\chi_{m\alpha, m'\alpha'}(\omega) = \int_{-\infty}^{\infty} d\omega e^{i\omega\tau} \chi_{m\alpha, m'\alpha'}(\tau) = \int_{0}^{\infty} d\omega e^{i\omega\tau} \chi_{m\alpha, m'\alpha'}(\tau), \tag{3.15}$$

where the lower bound of integration can be set to zero since the susceptibility contains a $\Theta(\tau)$. Note that the limit $t \to \infty$ is only executed for the integral and not for the classical spins $\boldsymbol{S}_{m'}(t)$. For the expectation value, one gets

$$\langle \hat{\boldsymbol{s}}_{i_m} \rangle_t = \langle \hat{\boldsymbol{s}}_{i_m} \rangle^{(0)} + J \sum_{m'} \underline{\chi}_{mm'}(\omega) \bigg|_{\omega=0} \boldsymbol{S}_{m'}(t) + iJ \sum_{m'} \partial_\omega \underline{\chi}_{mm'}(\omega) \bigg|_{\omega=0} \dot{\boldsymbol{S}}_{m'}(t) \tag{3.16}$$

such that the EOM are

$$\dot{\boldsymbol{S}}_m(t) = \left(J \langle \hat{\boldsymbol{s}}_{i_m} \rangle^{(0)} + J^2 \sum_{m'} \underline{\chi}_{mm'}(\omega) \bigg|_{\omega=0} \boldsymbol{S}_{m'}(t) + iJ^2 \sum_{m'} \partial_\omega \underline{\chi}_{mm'}(\omega) \bigg|_{\omega=0} \dot{\boldsymbol{S}}_{m'}(t) \right) \times \boldsymbol{S}_m(t). \tag{3.17}$$

As a matrix in the multi-indices (m, α) and (m', α') the susceptibility can be split into a

symmetric and an antisymmetric part as $\chi_{m\alpha,m'\alpha'} = \chi^S_{m\alpha,m'\alpha'} + \chi^A_{m\alpha,m'\alpha'}$ with

$$\chi^S_{m\alpha,m'\alpha'} = \frac{1}{2}(\chi_{m\alpha,m'\alpha'} + \chi_{m'\alpha',m\alpha}) \tag{3.18}$$

$$\chi^A_{m\alpha,m'\alpha'} = \frac{1}{2}(\chi_{m\alpha,m'\alpha'} - \chi_{m'\alpha',m\alpha}), \tag{3.19}$$

i.e., symmetric and antisymmetric with respect to the multi-indices (m,α) and (m',α'). The symmetric part of the second term in (3.17) is the familiar RKKY coupling [32–34]

$$J^{\text{RKKY}}_{mm'\alpha\alpha'} := J^2 \chi^S_{m\alpha,m'\alpha'}(0), \tag{3.20}$$

which is an indirect exchange interaction between local magnetic moments, that may be mediated by magnetic ions or localised electrons in partially filled electron shells [84]. Including this term already on the Hamiltonian level, gives a term of the form

$$J^2 \sum_{mm'} \boldsymbol{S}_m \underline{\chi}^S_{mm'}(0) \boldsymbol{S}_{m'}. \tag{3.21}$$

It is important to note that, actually, the symmetric part of the magnetic susceptibility can itself be split into two different contributions. One part is symmetric not only with regard to the simultaneous exchange of (m,α) with (m',α') but also under the individual exchanges $m \leftrightarrow m'$ and $\alpha \leftrightarrow \alpha'$. This is the RKKY interaction from equation (3.20). The other part is antisymmetric under both of the individual exchanges. This latter part, which we will denote by $\underline{D}_{mm'}$, is thus an antisymmetric 3×3 matrix in the spin indices for fixed m and m'. For the cross product it holds that

$$\boldsymbol{v} \times \boldsymbol{S} = \underline{A}(\boldsymbol{v})\boldsymbol{S} \quad \text{with} \quad \underline{A} := \begin{pmatrix} 0 & -v_z & v_y \\ v_z & 0 & -v_x \\ -v_y & v_x & 0 \end{pmatrix}, \tag{3.22}$$

with any real 3-vector $\boldsymbol{v}$. Hence, one can write

$$J^2 \sum_{mm'} \boldsymbol{S}_m \underline{D}_{mm'} \boldsymbol{S}_{m'} = J^2 \sum_{mm'} \boldsymbol{S}_m (\boldsymbol{D}_{mm'} \times \boldsymbol{S}_{m'}) = J^2 \sum_{mm'} \boldsymbol{D}_{mm'} (\boldsymbol{S}_{m'} \times \boldsymbol{S}_m), \tag{3.23}$$

where in the last equality we used the cyclic property of the triple product. With the 3-vector $\boldsymbol{D}_{mm'}$ changing sign under exchange of m and m', this term is in fact a Dzyaloshinski-Moriya [85, 86] or antisymmetric exchange [87] interaction. However, for the models considered here it is zero. This is because their respective hopping matrices are spin-diagonal and spin-independent and therefore the corresponding magnetic susceptibilities are symmetric in the spin indices.

The third term in (3.17) can be split into a symmetric and an antisymmetric part in exactly

the same way and one can define

$$\underline{\alpha}_{mm'} := -iJ^2 \partial_\omega \underline{\chi}^S_{mm'}(\omega)\Big|_{\omega=0} \tag{3.24}$$

$$\underline{\Omega}^{(0)}_{mm'} := -iJ^2 \partial_\omega \underline{\chi}^A_{mm'}(\omega)\Big|_{\omega=0}, \tag{3.25}$$

where $\underline{\alpha}_{mm'}$ is the well-known Gilbert damping and $\underline{\Omega}^{(0)}_{mm'}$ produces a non-Hamiltonian spin torque and has a geometric nature. It is closely related to the Berry curvature with regard to the parameter space of classical spin variables, as will be discussed in section 4.4.

3.3 − Lehmann Representation

For analytical and numerical calculations, it is convenient to express the magnetic susceptibility in terms of (multi-particle) eigenenergies and eigenstates. This can be done by inserting an identity operator via the completeness relation $\mathbb{1} = \sum_n |n\rangle \langle n|$. From now on we omit the superscript (0) and it is understood that all expectation values are taken with regard to the eigenstates of $\hat{H}_0$. This yields

$$\begin{aligned}
\chi_{m\alpha,m'\alpha'}(t) &= -i\Theta(t) \left\langle \left[\hat{s}^\alpha_{i_m}(t), \hat{s}^{\alpha'}_{i_{m'}}(0) \right] \right\rangle \\
&= -i\Theta(t) \operatorname{Tr}\left[\frac{1}{Z} e^{-\beta \hat{H}_0} (\hat{s}^\alpha_{i_m}(t) \hat{s}^{\alpha'}_{i_{m'}}(0) - \hat{s}^{\alpha'}_{i_{m'}}(0) \hat{s}^\alpha_{i_m}(t)) \right] \\
&= -i\Theta(t) \frac{1}{Z} \sum_{nn'} e^{-\beta E_n} (\langle n| \hat{s}^\alpha_{i_m}(t) |n'\rangle \langle n'| \hat{s}^{\alpha'}_{i_{m'}} |n\rangle - n \leftrightarrow n') \\
&= -i\Theta(t) \frac{1}{Z} \sum_{nn'} e^{-\beta E_n} (e^{i(E_n - E_{n'})t} \langle n| \hat{s}^\alpha_{i_m} |n'\rangle \langle n'| \hat{s}^{\alpha'}_{i_{m'}} |n\rangle - n \leftrightarrow n') \tag{3.26}
\end{aligned}$$

with eigenenergies E_n and eigenstates $|n\rangle$ of $\hat{H}_0$ and the inverse temperature β. The notation $n \leftrightarrow n'$ symbolises that the second term in the brackets is equal to the first after exchanging n and n'. Computing the Fourier transform involves the integral $\int_{-\infty}^\infty dt e^{i(\omega + E_n - E_{n'})t} \Theta(t)$ which does not exist as an integral over complex functions. However, instead we can treat the integrand as the integral kernel of a distribution, i.e., see how it acts as a linear functional

$$\tilde{\Theta}[\varphi] = \int_{-\infty}^\infty d\omega \tilde{\Theta}(\omega)\varphi(\omega), \tag{3.27}$$

where $\varphi(\omega)$ is any test function. We can then regularise the integral as

$$\begin{aligned}
\int_0^\infty dt \lim_{\eta \to 0^+} e^{i(\omega + E_n - E_{n'} + i\eta)t} &\mapsto \lim_{\eta \to 0^+} \int_0^\infty dt e^{i(\omega + E_n - E_{n'} + i\eta)t} \\
&= \lim_{\eta \to 0^+} \frac{1}{i(\omega + E_n - E_{n'}) - \eta} e^{i(\omega + E_n - E_{n'})t} e^{-\eta t} \Big|_0^\infty \\
&= \lim_{\eta \to 0^+} \frac{i}{(\omega + E_n - E_{n'}) + i\eta} \\
&= \frac{i}{(\omega + E_n - E_{n'}) + i0^+}. \tag{3.28}
\end{aligned}$$

Thus, the Fourier transform of $\chi_{m\alpha,m'\alpha'}(t)$ is given by

$$\chi_{m\alpha,m'\alpha'}(\omega) = \frac{1}{Z} \sum_{nn'} e^{\beta E_n} \left(\frac{\langle n| \hat{s}^{\alpha}_{i_m} |n'\rangle \langle n'| \hat{s}^{\alpha'}_{i_{m'}} |n\rangle}{\omega + (E_n - E_{n'}) + i0^+} - \frac{\langle n| \hat{s}^{\alpha'}_{i_{m'}} |n'\rangle \langle n'| \hat{s}^{\alpha}_{i_m} |n\rangle}{\omega + (E_{n'} - E_n) + i0^+} \right). \quad (3.29)$$

It is important to note that one cannot simply identify $i0^+ = 0$ at this stage in general. Instead, both sums have to be computed and in the resulting expression the regularisation term might then be set to zero if the thermodynamic limit is taken beforehand [23]. Symmetrisation and antisymmetrisation of (3.29) yield

$$\chi^{S}_{m\alpha,m'\alpha'}(\omega) = \frac{1}{Z} \sum_{nn'} e^{\beta E_n} \mathrm{Re}\left\{ \langle n| \hat{s}^{\alpha}_{i_m} |n'\rangle \langle n'| \hat{s}^{\alpha'}_{i_{m'}} |n\rangle \right\} \left(\frac{1}{\omega + (E_n - E_{n'}) + i0^+} - n \leftrightarrow n' \right)$$

$$\chi^{A}_{m\alpha,m'\alpha'}(\omega) = \frac{i}{Z} \sum_{nn'} e^{\beta E_n} \mathrm{Im}\left\{ \langle n| \hat{s}^{\alpha}_{i_m} |n'\rangle \langle n'| \hat{s}^{\alpha'}_{i_{m'}} |n\rangle \right\} \left(\frac{1}{\omega + (E_n - E_{n'}) + i0^+} + n \leftrightarrow n' \right). \quad (3.30)$$

Interestingly, the symmetric part vanishes if $i0^+$ can be neglected. The Gilbert damping and the spin torque from above are easily calculated to be

$$-i\partial_\omega \chi^{S}_{m\alpha,m'\alpha'}(\omega)\Big|_{\omega=0} = -\frac{2}{Z} \sum_{nn'} e^{\beta E_n} \mathrm{Re}\left\{ \langle n| \hat{s}^{\alpha}_{i_m} |n'\rangle \langle n'| \hat{s}^{\alpha'}_{i_{m'}} |n\rangle \right\} \mathrm{Im}\left\{ \frac{1}{(E_n - E_{n'} + i0^+)^2} \right\}$$

$$-i\partial_\omega \chi^{A}_{m\alpha,m'\alpha'}(\omega)\Big|_{\omega=0} = -\frac{2}{Z} \sum_{nn'} e^{\beta E_n} \mathrm{Im}\left\{ \langle n| \hat{s}^{\alpha}_{i_m} |n'\rangle \langle n'| \hat{s}^{\alpha'}_{i_{m'}} |n\rangle \right\} \mathrm{Re}\left\{ \frac{1}{(E_n - E_{n'} + i0^+)^2} \right\}, \quad (3.31)$$

which in the zero temperature limit ($\beta \to \infty$) become

$$-i\partial_\omega \chi^{S}_{m\alpha,m'\alpha'}(\omega)\Big|_{\omega=0} = -2 \sum_{n} \mathrm{Re}\left\{ \langle 0| \hat{s}^{\alpha}_{i_m} |n\rangle \langle n| \hat{s}^{\alpha'}_{i_{m'}} |0\rangle \right\} \mathrm{Im}\left\{ \frac{1}{(E_0 - E_n + i0^+)^2} \right\}$$

$$-i\partial_\omega \chi^{A}_{m\alpha,m'\alpha'}(\omega)\Big|_{\omega=0} = -2 \sum_{n} \mathrm{Im}\left\{ \langle 0| \hat{s}^{\alpha}_{i_m} |n\rangle \langle n| \hat{s}^{\alpha'}_{i_{m'}} |0\rangle \right\} \mathrm{Re}\left\{ \frac{1}{(E_0 - E_n + i0^+)^2} \right\}, \quad (3.32)$$

where $|0\rangle$ denotes the ground state of $\hat{H}_0$.

In the case of a noninteracting quantum system, the Fourier transform of the magnetic susceptibility and its ω derivative evaluated at zero can be expressed in terms of single-particle quantities. To compute the susceptibility, one has to compute expectation values of the form $\langle \hat{s}^{\alpha}_{ir}(t)\hat{s}^{\alpha'}_{i'r'}(0)\rangle$, where the indices r and s denote orbital degrees of freedom. For a noninteracting system, these expectation values can be calculated analytically using Wick's theorem [88, 89]. With this, it is possible to express higher order correlation functions in terms of single-particle correlations. Wick's theorem can be stated as

$$\langle \mathcal{T}(d_{\alpha_1}(\tau_1) \cdots d_{\alpha_n}(\tau_n)) \rangle = \{\text{sum over all fully contracted terms}\} \quad (3.33)$$

with the time-ordering operator $\mathcal{T}$ and $d_\alpha(\tau)$ denoting either an annihilation or a creation

operator whose time-dependence is given by $d_\alpha(\tau) = e^{i\hat{H}_0\tau}d_\alpha e^{-i\hat{H}_0\tau}$. For operators at the same time the ordering operator puts creators to the left of annihilators. Under $\mathcal{T}$ all fermionic creation and annihilation operators anticommute such that

$$\mathcal{T}(d_{i_1}\cdots d_{i_s}) = (-1)^p d_{k_1}\cdots d_{k_s}, \tag{3.34}$$

where the operators on the right hand side of the equation are properly ordered and p is the number of permutations needed to go from $(i_1, \ldots, i_s)$ to $(k_1, \ldots, k_s)$.

A contraction always pairs two operators to give

$$\overset{\frown}{d_i d_j} := \langle \mathcal{T}(d_i d_j)\rangle, \tag{3.35}$$

which is a complex number. In order to compute $\langle \hat{s}_{ir}^\alpha(t)\hat{s}_{i'r'}^{\alpha'}(0)\rangle$, one needs to calculate the two-particle expectation value $\langle c_{ir\sigma}^\dagger(t)c_{ir\sigma'}(t)c_{i'r'\tau}^\dagger(0)c_{i'r'\tau'}(0)\rangle$. Assuming that $t > 0$, it is

$$\begin{aligned}
\langle c_{ir\sigma}^\dagger(t)c_{ir\sigma'}(t)c_{i'r'\tau}^\dagger(0)c_{i'r'\tau'}(0)\rangle &= \overset{\frown}{c_{ir\sigma}^\dagger(t)c_{ir\sigma'}(t)}\,\overset{\frown}{c_{i'r'\tau}^\dagger(0)c_{i'r'\tau'}(0)}\\
&\quad + \overset{\frown}{c_{ir\sigma}^\dagger(t)c_{i'r'\tau'}(0)}\,\overset{\frown}{c_{ir\sigma'}(t)c_{i'r'\tau}^\dagger(0)}\\
&= \langle c_{ir\sigma}^\dagger(t)c_{ir\sigma'}(t)\rangle\langle c_{i'r'\tau}^\dagger(0)c_{i'r'\tau'}(0)\rangle\\
&\quad + \langle c_{ir\sigma}^\dagger(t)c_{i'r'\tau'}(0)\rangle\langle c_{ir\sigma'}(t)c_{i'r'\tau}^\dagger(0)\rangle\\
&=: I_{iri'r'}^{\sigma\sigma'\tau\tau'}(t). \tag{3.36}
\end{aligned}$$

To evaluate the one-particle correlation functions, one can use the following identities:

$$c_\alpha(\tau) = e^{iH_0\tau}c_\alpha e^{-iH_0\tau} = \sum_\beta \left(e^{-i\underline{T}\tau}\right)_{\alpha\beta}c_\beta \tag{3.37}$$

$$c_\alpha^\dagger(\tau) = (e^{iH_0\tau}c_\alpha e^{-iH_0\tau})^\dagger = \sum_\beta c_\beta^\dagger \left(e^{i\underline{T}\tau}\right)_{\beta\alpha} \tag{3.38}$$

$$\langle c_\alpha(\tau)c_\beta^\dagger(\tau')\rangle = \sum_{\gamma\delta}\left(e^{-i\underline{T}\tau}\right)_{\alpha\gamma}\langle c_\gamma c_\delta^\dagger\rangle\left(e^{i\underline{T}\tau'}\right)_{\delta\beta} \tag{3.39}$$

$$\langle c_\gamma c_\delta^\dagger\rangle = \sum_k U_{\gamma,k}\frac{1}{1 + e^{-\beta(\varepsilon(k)-\mu)}}U_{k,\delta}^\dagger = \left(\frac{1}{1 + e^{-\beta(\underline{T}-\mu)}}\right)_{\gamma\delta} = (1 - \rho)_{\gamma\delta} \tag{3.40}$$

$$\langle c_\gamma^\dagger c_\delta\rangle = \sum_k U_{\delta,k}\frac{1}{e^{\beta(\varepsilon(k)-\mu)} + 1}U_{k,\gamma}^\dagger = \left(\frac{1}{e^{\beta(\underline{T}-\mu)} + 1}\right)_{\delta\gamma} = \rho_{\delta\gamma} \tag{3.41}$$

with the one-particle reduced density matrix $\rho_{\alpha\beta}$. For the time being, it is useful to introduce multi-indices α, β, γ and δ to combine lattice, orbital, and spin degrees of freedom, such that for instance $\alpha = (i, r, \sigma)$. Also $\underline{U}$ is the matrix that diagonalises the hopping matrix

$\underline{T} = \underline{U}\,\underline{\varepsilon}\,\underline{U}^\dagger$. With these relations, a general single-particle correlation function is given by

$$\langle c_\alpha(\tau) c_\beta^\dagger(\tau') \rangle = \sum_{\gamma\delta} \sum_k \left(e^{-i\underline{T}\tau}\right)_{\alpha\gamma} U_{\gamma,k} \frac{1}{1+e^{-\beta(\varepsilon(k)-\mu)}} U_{k,\delta}^\dagger \left(e^{i\underline{T}\tau'}\right)_{\delta\beta}$$

$$= \sum_{\gamma\delta} \sum_{k,k',k''} U_{\alpha,k'} e^{-i\varepsilon(k')\tau} U_{k',\gamma}^\dagger U_{\gamma,k} \frac{1}{1+e^{-\beta(\varepsilon(k)-\mu)}} U_{k,\delta}^\dagger U_{\delta,k''} e^{i\varepsilon(k'')\tau'} U_{k'',\beta}^\dagger$$

$$= \sum_k U_{\alpha,k} \frac{e^{-i\varepsilon(k)(\tau-\tau')}}{1+e^{-\beta(\varepsilon(k)-\mu)}} U_{k,\beta}^\dagger. \tag{3.42}$$

with $\varepsilon_{kk} \equiv \varepsilon(k)$, i.e., $\underline{\varepsilon}$ is a diagonal matrix in k. Analogously, it is

$$\langle c_\alpha^\dagger(\tau) c_\beta(\tau') \rangle = \sum_k U_{\beta,k} \frac{e^{i\varepsilon(k)(\tau-\tau')}}{e^{\beta(\varepsilon(k)-\mu)}+1} U_{k,\alpha}^\dagger. \tag{3.43}$$

Plugging this into (3.36) and going back to explicitly writing out the spatial, orbital, and spin indices, one ends up with the expression

$$I_{iri'r'}^{\sigma\sigma'\tau\tau'}(t) = \sum_{\substack{k,\nu,a \\ k',\nu',a'}} \frac{U_{ir\sigma',k\nu a} U_{k\nu a,ir\sigma}^\dagger U_{i'r'\tau',k'\nu'a'} U_{k'\nu'a',i'r'\tau}^\dagger}{(1+e^{-\beta(\varepsilon_{\nu a}(k)-\mu)})(1+e^{-\beta(\varepsilon_{\nu'a'}(k')-\mu)})}$$

$$+ \sum_{\substack{k,\nu,a \\ k',\nu',a'}} \frac{U_{i'r'\tau',k\nu a} U_{k\nu a,ir\sigma}^\dagger e^{i\varepsilon_{\nu a}(k)t} U_{ir\sigma',k'\nu'a'} U_{k'\nu'a',i'r'\tau}^\dagger e^{-i\varepsilon_{\nu'a'}(k')t}}{(1+e^{-\beta(\varepsilon_{\nu a}(k)-\mu)})(e^{\beta(\varepsilon_{\nu'a'}(k')-\mu)}+1)}. \tag{3.44}$$

With this, the expectation value of two spin operators is easily computed as

$$\langle \hat{s}_{ir}^\alpha(t) \hat{s}_{i'r'}^{\alpha'}(0) \rangle = \frac{1}{4} \sum_{\substack{\sigma\sigma' \\ \tau\tau'}} \sigma_{\sigma\sigma'}^\alpha \sigma_{\tau\tau'}^{\alpha'} I_{iri'r'}^{\sigma\sigma'\tau\tau'}(t). \tag{3.45}$$

For the susceptibility, which depends on the expectation value of the commutator, one needs the adjoint $\langle \hat{s}_{i'r'}^{\alpha'}(0) \hat{s}_{ir}^\alpha(t) \rangle$ as well. Here it is useful to note that $\langle \hat{A} \rangle = \langle \hat{A}^\dagger \rangle^*$. Since the Pauli matrices are Hermitian, it is $(\sigma_{\sigma\sigma'}^\alpha)^* = \sigma_{\sigma'\sigma}^\alpha$. Thus, one gets

$$\left\langle \left[\hat{s}_{ir}^\alpha(t), \hat{s}_{i'r'}^{\alpha'}(0) \right] \right\rangle = \frac{1}{4} \sum_{\substack{\sigma\sigma' \\ \tau\tau'}} \sigma_{\sigma\sigma'}^\alpha \sigma_{\tau\tau'}^{\alpha'} (I_{iri'r'}^{\sigma\sigma'\tau\tau'}(t) - (I_{iri'r'}^{\sigma'\sigma\tau'\tau}(t))^*). \tag{3.46}$$

In taking the difference $I_{iri'r'}^{\sigma\sigma'\tau\tau'}(t) - (I_{iri'r'}^{\sigma'\sigma\tau'\tau}(t))^*$ the time-independent terms cancel

$$I_{iri'r'}^{\sigma\sigma'\tau\tau'}(t) - (I_{iri'r'}^{\sigma'\sigma\tau'\tau}(t))^* = \sum_{\substack{k,\nu,a \\ k',\nu',a'}} \frac{U_{i'r'\tau',k\nu a} U_{k\nu a,ir\sigma}^\dagger U_{ir\sigma',k'\nu'a'} U_{k'\nu'a',i'r'\tau}^\dagger e^{i(\varepsilon_{\nu a}(k)-\varepsilon_{\nu'a'}(k'))t}}{(1+e^{-\beta(\varepsilon_{\nu a}(k)-\mu)})(e^{\beta(\varepsilon_{\nu'a'}(k')-\mu)}+1)}$$

$$- \sum_{\substack{k,\nu,a \\ k',\nu',a'}} \frac{U_{ir\sigma,k\nu a} U_{k\nu a,i'r'\tau'}^\dagger U_{i'r'\tau,k'\nu'a'} U_{k'\nu'a',ir\sigma'}^\dagger e^{-i(\varepsilon_{\nu a}(k)-\varepsilon_{\nu'a'}(k'))t}}{(1+e^{-\beta(\varepsilon_{\nu a}(k)-\mu)})(e^{\beta(\varepsilon_{\nu'a'}(k')-\mu)}+1)}$$

$$=: \tilde{I}_{iri'r'}^{\sigma\sigma'\tau\tau'}(t). \tag{3.47}$$

The magnetic susceptibility expressed in single-particle quantities is therefore given by

$$\chi_{ir\alpha,i'r'\alpha'}(t) = -\frac{i}{4}\Theta(t)\sum_{\substack{\sigma\sigma'\\\tau\tau'}}\sigma^{\alpha}_{\sigma\sigma'}\sigma^{\alpha'}_{\tau\tau'}\tilde{I}^{\sigma\sigma'\tau\tau'}_{iri'r'}(t). \tag{3.48}$$

From this expression the symmetric and the antisymmetric part as well as the Fourier transform can be readily computed. Since the time dependence of $\chi_{ir\alpha,i'r'\alpha'}(t)$ comes from the Heaviside function and the phase factors $e^{i(\varepsilon_{\nu a}(k)-\varepsilon_{\nu'a'}(k'))t}$, the integral can be computed in the same way as in the multi-particle case.

4 − Adiabatic Spin Dynamics

In quantum mechanics the approximation of an observable as a classical variable is often accompanied by another approximation, the so-called adiabatic approximation. This is again familiar from molecular dynamics, where it is often applied together with the Born-Oppenheimer approximation [58]. The adiabatic approximation is an approximation concerning the time evolution of a quantum system with time-dependent parameters and assumes that the system is in the same energy eigenstate, usually the ground state, for all times and corresponding instantaneous parameter configurations. The theoretical justification for the applicability of the adiabatic approximation is given by the adiabatic theorem [61–63]. In the following, it will be distinguished between strict and relaxed adiabatic approximations. The former restrict the quantum subsystem to the (single) ground state, while the latter include more than just a single state resulting in a state space of more than one dimension.

This chapter introduces the adiabatic spin dynamics (ASD) theory [56], which incorporates the strict adiabatic approximation into quantum-classical spin dynamics. It starts by briefly explaining the adiabatic theorem and then formulates the adiabatic constraint in the context of quantum-classical spin dynamics. To correctly apply this constraint to the quantum-classical spin models from chapter 3, one has to formulate those systems in terms of a quantum-classical Lagrangian. The EOM of the classical spins, which are derived via the Euler-Lagrange equations, show an additional spin torque, that results from a finite spin-Berry curvature. This spin torque also connects to the non-Hamiltonian spin torque derived above by linear response theory.

In some cases, the strict adiabatic approximation can be too restrictive to capture all relevant physics and the constraint has to be relaxed. This is done via an extension of ASD called non-Abelian spin dynamics (NA-SD), which is developed in publication [I] at the end of this chapter.

4.1 − Adiabatic Theorem and Approximation

The adiabatic theorem states that a quantum system whose Hamiltonian $\hat{H}$ depends on parameters that change in time stays in its instantaneous energy eigenstate for the whole time evolution if the parameter change during that time is slow enough [61–63]. In its original form, the theorem has been stated for the case of nondegenerate eigenstates and a discrete spectrum of $\hat{H}$ [61] but has since been generalised to different scenarios [62,63].

The adiabatic theorem justifies the adiabatic approximation, where, for all times t, the time-dependent state of a quantum system, which depends on parameters with a dynamics much slower than the other degrees of freedom, is equal to an instantaneous energy eigenstate for the given parameter configuration [90]. The instantaneous eigenstate is typically chosen to be the ground state and the adiabatic approximation usually leads to a significant simplification in the computation of observables.

For the quantum-classical spin systems of chapter 3 the strict adiabatic approximation reads

$$|\Psi(t)\rangle = |\Psi_0(\boldsymbol{S}(t))\rangle \ \forall t, \tag{4.1}$$

where the parameters are the classical spins and $|\Psi_0(\boldsymbol{S}(t))\rangle$ denotes the ground state of the system at time t with respect to the classical spin configuration $\boldsymbol{S}(t)$. The physical justification is that the timescale governing the dynamics of localised magnetic moments, here modelled by the classical spins, is typically much longer compared to the timescale of the dynamics of itinerant electrons such that the electrons almost instantaneously follow the motion of the spins. In a quantum-classical spin model with an interaction term $\propto J\hat{\boldsymbol{s}}\boldsymbol{S}(t)$, the timescale of the classical spins is mainly determined by the quantum-classical exchange coupling J, which thus has to be sufficiently small for the adiabatic approximation (4.1) to be valid. Quantum-classical hybrid systems often exhibit timescale separation between a fast quantum subsystem and a slow classical part [59].

4.2 – Berry Phase, Connection, and Curvature

A concept that is closely related to the adiabatic approximation is that of the geometric and Berry phase [64, 90]. Considering a Hamiltonian depending on parameters $\boldsymbol{\lambda}(t) = (\boldsymbol{\lambda}_1(t), \ldots, \boldsymbol{\lambda}_M(t))$, the adiabatic time evolution of a state $|\Psi_n(\boldsymbol{\lambda}(t))\rangle$ is associated with a path on the parameter manifold $\mathcal{M}$. Apart from the usual dynamical phase factor $e^{-i\int_0^t dt' E_n(t')}$, the state acquires a second phase factor given by

$$e^{i\gamma_n} = e^{i\int_0^t dt' \langle \Psi_n(\boldsymbol{\lambda}(t))|\frac{d}{dt}|\Psi_n(\boldsymbol{\lambda}(t))\rangle}, \tag{4.2}$$

where γ_n is the so-called geometric phase. It can also be written in the form

$$
\begin{aligned}
\gamma_n &= i \int_0^t dt' \langle \Psi_n(\boldsymbol{\lambda}(t))| \frac{d}{dt} |\Psi_n(\boldsymbol{\lambda}(t))\rangle \\
&= i \sum_m \int_{\boldsymbol{\lambda}_m(0)}^{\boldsymbol{\lambda}_m(t)} d\boldsymbol{\lambda}_m \langle \Psi_n(\boldsymbol{\lambda}(t))| \nabla_{\boldsymbol{\lambda}_m} |\Psi_n(\boldsymbol{\lambda}(t))\rangle \\
&=: \sum_m \int_{\boldsymbol{\lambda}_m(0)}^{\boldsymbol{\lambda}_m(t)} d\boldsymbol{\lambda}_m \boldsymbol{C}_m^n(\boldsymbol{\lambda})
\end{aligned}
\tag{4.3}
$$

with the Berry connection $\boldsymbol{C}_m^n(\boldsymbol{\lambda})$ that describes parallel transport of $|\Psi_n(\boldsymbol{\lambda}(t))\rangle$ on the manifold $\mathcal{M}$. One feature of the geometric phase is that, in contrast to the dynamical phase factor, it cannot be removed by gauge transformations if the path in parameter space is closed, i.e., if $\boldsymbol{\lambda}(0) = \boldsymbol{\lambda}(t)$. It is then also known as Berry phase. A third quantity related to both γ_n and $\boldsymbol{C}_m^n(\boldsymbol{\lambda})$ is the (Abelian) Berry curvature

$$\Omega_{m\alpha,m'\alpha'}^n(\boldsymbol{\lambda}) := \frac{\partial}{\partial \lambda_{m\alpha}} C_{m'\alpha'}^n(\boldsymbol{\lambda}) - \frac{\partial}{\partial \lambda_{m'\alpha'}} C_{m\alpha}^n(\boldsymbol{\lambda}), \tag{4.4}$$

which is the exterior derivative of the Berry connection. From the definition it is immediately obvious that the Berry curvature is antisymmetric, i.e., $\Omega_{m\alpha,m'\alpha'}^n = -\Omega_{m'\alpha',m\alpha}^n$. Importantly,

the Berry curvature is invariant under local gauge transformations of the ground states $|\Psi_0(\boldsymbol{\lambda})\rangle \rightarrow |\Psi_0(\boldsymbol{\lambda})\rangle' = e^{i\phi(\boldsymbol{\lambda})} |\Psi_0(\boldsymbol{\lambda})\rangle$ with a single-valued function $\phi(\boldsymbol{\lambda})$. The connection changes as $\boldsymbol{C}_m^n(\boldsymbol{\lambda}) \rightarrow \boldsymbol{C}_m^{n\prime}(\boldsymbol{\lambda}) = i \langle \Psi_n(\boldsymbol{\lambda}(t))| \nabla_{\boldsymbol{\lambda}_m} |\Psi_n(\boldsymbol{\lambda}(t))\rangle - \frac{\partial \phi}{\partial \boldsymbol{\lambda}_m}$ and a direct calculation shows

$$
\begin{aligned}
\Omega_{m\alpha,m'\alpha'}^{n\prime}(\boldsymbol{\lambda}) &= \frac{\partial}{\partial \lambda_{m\alpha}} C_{m'\alpha'}^n(\boldsymbol{\lambda}) - \frac{\partial}{\partial \lambda_{m\alpha}} \frac{\partial \phi}{\partial \lambda_{m'\alpha'}} \\
&\quad - \frac{\partial}{\partial \lambda_{m'\alpha'}} C_{m\alpha}^n(\boldsymbol{\lambda}) + \frac{\partial}{\partial \lambda_{m'\alpha'}} \frac{\partial \phi}{\partial \lambda_{m\alpha}} \\
&= \Omega_{m\alpha,m'\alpha'}^n(\boldsymbol{\lambda})
\end{aligned}
\tag{4.5}
$$

with the derivatives of ϕ cancelling due to Schwarz's theorem.

Since the classical parameters considered here are spins, the corresponding quantities $\boldsymbol{C}_m^n(\boldsymbol{S})$ and $\Omega_{m\alpha,m'\alpha'}^n(\boldsymbol{S})$ will be referred to as spin-Berry connection and curvature. While concepts like the Berry curvature and connection can be defined for an arbitrary parameter dependence $\boldsymbol{\lambda}(t)$, the name spin-Berry curvature is used to emphasise that the underlying parameter space is different compared to the Berry curvatures usually found in physics, which are mainly defined with regard to reciprocal space. The parameter manifold $\mathcal{M}$ of the classical spin configuration is the M-fold Cartesian product of 2-spheres, i.e., $\mathcal{M} = S^2 \times \cdots \times S^2$. For the rest of the chapter the superscript n will be omitted and it is understood that all quantities are expressed via the ground state $|\Psi_0(\boldsymbol{S}(t))\rangle$.

4.3 – Adiabatic Equations of Motion

Equation (4.1) is an additional holonomic constraint on the system dynamics. The question is how to properly incorporate it into the EOM of the system. The most straightforward way would be to plug it directly into (3.8) resulting in

$$
\dot{\boldsymbol{S}}_m = \frac{\partial \langle \hat{H} \rangle_0}{\partial \boldsymbol{S}_m} \times \boldsymbol{S}_m
\tag{4.6}
$$

with $\langle \hat{H} \rangle_0 = \langle \Psi_0(\boldsymbol{S}(t))| \hat{H} |\Psi_0(\boldsymbol{S}(t))\rangle$. This equation will be called the naive adiabatic EOM. However, the naive adiabatic theory is often insufficient to correctly describe the adiabatic dynamics, as will be shown in section 4.6 when examining a toy model.

The most natural framework for incorporating constraints into a dynamical system is the Lagrange formalism. First, one has to define a Lagrangian from which the equations (3.3) and (3.8) can be derived as Euler-Lagrange equations. Here, it is given by

$$
\begin{aligned}
L &= L(\boldsymbol{S}, \dot{\boldsymbol{S}}, |\Psi\rangle, |\dot{\Psi}\rangle, \langle\Psi|, \langle\dot{\Psi}|) \\
&= \sum_m \boldsymbol{A}(\boldsymbol{S}_m)\dot{\boldsymbol{S}}_m + \langle\Psi(t)| i\partial_t - \hat{H} |\Psi(t)\rangle
\end{aligned}
\tag{4.7}
$$

with M classical spins $\boldsymbol{S} \equiv (\boldsymbol{S}_1, \ldots, \boldsymbol{S}_M)$. The term $\boldsymbol{A}(\boldsymbol{S})$ satisfies $\nabla \times \boldsymbol{A}(\boldsymbol{S}) = -\boldsymbol{S}/S^3$ and can therefore be interpreted as the vector potential of a magnetic monopole located at $\boldsymbol{S} = 0$.

One has

$$\boldsymbol{A}(\boldsymbol{S}) = -\frac{1}{S^3}\frac{\boldsymbol{e} \times \boldsymbol{S}}{1 + \boldsymbol{e}\boldsymbol{S}/S} \tag{4.8}$$

with a unit vector $\boldsymbol{e}$. Plugging the constraint (4.1) into (4.7) yields an effective Lagrangian that depends on the classical spins only

$$L_{\mathrm{eff}}(\boldsymbol{S}, \dot{\boldsymbol{S}}) = \sum_m \boldsymbol{A}(\boldsymbol{S}_m)\dot{\boldsymbol{S}}_m + \langle\Psi_0(\boldsymbol{S}(t))|\, i\partial_t - \hat{H}\,|\Psi_0(\boldsymbol{S}(t))\rangle - \sum_m \boldsymbol{\lambda}_m \boldsymbol{S}_m^2, \tag{4.9}$$

where the $\boldsymbol{\lambda}_m$ are additional Lagrange multipliers that ensure the normalisation of the spins, i.e., $S_m = |\boldsymbol{S}_m| = 1$. From this Lagrangian the correct adiabatic EOM can be derived via the Euler-Lagrange equations, which are given by

$$\frac{d}{dt}\frac{\partial L_{\mathrm{eff}}}{\partial \dot{\boldsymbol{S}}_m} = \frac{\partial L_{\mathrm{eff}}}{\partial \boldsymbol{S}_m}, \; m \in \{1, \ldots, M\}. \tag{4.10}$$

At first glance, it looks like the first term in (4.9) depends on both $\boldsymbol{S}$ and $\dot{\boldsymbol{S}}$, while the second terms depends on $\boldsymbol{S}$ only. However, this is not the case since

$$\partial_t\,|\Psi_0(\boldsymbol{S}(t))\rangle = \nabla_{\boldsymbol{S}}\,|\Psi_0(\boldsymbol{S}(t))\rangle\,\dot{\boldsymbol{S}}. \tag{4.11}$$

Computing the right hand side of the Euler-Lagrange equations yields

$$\begin{aligned}
\frac{\partial L_{\mathrm{eff}}}{\partial \boldsymbol{S}_m} &= \sum_{m'\alpha'\alpha} \frac{\partial A_{\alpha'}(\boldsymbol{S}_{m'})}{\partial S_{m\alpha}} \dot{S}_{m'\alpha'}\boldsymbol{e}_\alpha + \sum_\alpha \frac{\partial}{\partial S_{m\alpha}}\left(\langle\Psi_0|\,i\partial_t\,|\Psi_0\rangle - \langle\Psi_0|\,\hat{H}\,|\Psi_0\rangle\right)\boldsymbol{e}_\alpha - 2\boldsymbol{\lambda}_m\boldsymbol{S}_m \\
&= \sum_{\alpha'\alpha} \frac{\partial A_{\alpha'}(\boldsymbol{S}_m)}{\partial S_{m\alpha}} \dot{S}_{m\alpha'}\boldsymbol{e}_\alpha + i\sum_{m'\alpha'\alpha} \frac{\partial}{\partial S_{m\alpha}} \langle\Psi_0|\,\frac{\partial}{\partial S_{m'\alpha'}}\,|\Psi_0\rangle \dot{S}_{m'\alpha'}\boldsymbol{e}_\alpha \\
&\quad - \sum_\alpha \langle\Psi_0|\,\frac{\partial \hat{H}}{\partial S_{m\alpha}}\,|\Psi_0\rangle\,\boldsymbol{e}_\alpha - 2\boldsymbol{\lambda}_m\boldsymbol{S}_m,
\end{aligned} \tag{4.12}$$

where in the third term the Hellmann-Feynman theorem was used. For the derivative of L_{eff} with regard to $\dot{\boldsymbol{S}}_m$, one has

$$\frac{\partial L_{\mathrm{eff}}}{\partial \dot{\boldsymbol{S}}_m} = \boldsymbol{A}(\boldsymbol{S}_m) + i\sum_\alpha \langle\Psi_0|\,\frac{\partial}{\partial S_{m\alpha}}\,|\Psi_0\rangle\,\boldsymbol{e}_\alpha \tag{4.13}$$

and it immediately follows

$$\frac{d}{dt}\frac{\partial L_{\mathrm{eff}}}{\partial \dot{\boldsymbol{S}}_m} = \sum_{\alpha\alpha'} \frac{\partial A_{\alpha'}(\boldsymbol{S}_m)}{\partial S_{m\alpha}} \dot{S}_{m\alpha}\boldsymbol{e}_{\alpha'} + i\sum_{m'\alpha'\alpha} \frac{\partial}{\partial S_{m'\alpha'}} \langle\Psi_0|\,\frac{\partial}{\partial S_{m\alpha}}\,|\Psi_0\rangle \dot{S}_{m'\alpha'}\boldsymbol{e}_\alpha. \tag{4.14}$$

With the definitions of the spin-Berry connection and curvature from above, the Euler-

Lagrange equations can be written as

$$
\begin{aligned}
0 &= \sum_{\alpha\alpha'}\left(\frac{\partial A_{\alpha'}}{\partial S_{m\alpha}} - \frac{\partial A_{\alpha}}{\partial S_{m\alpha'}}\right)\dot{S}_{m\alpha}\boldsymbol{e}_{\alpha'} + \sum_{m'\alpha'\alpha}\Omega_{m'\alpha',m\alpha}\dot{S}_{m'\alpha'}\boldsymbol{e}_{\alpha} + \langle\Psi_0|\nabla_{\boldsymbol{S}_m}\hat{H}|\Psi_0\rangle - 2\boldsymbol{\lambda}_m\boldsymbol{S}_m \\
&= -\dot{\boldsymbol{S}}_m \times (\nabla_{\boldsymbol{S}_m} \times \boldsymbol{A}(\boldsymbol{S}_m)) + \sum_{m'\alpha'\alpha}\Omega_{m'\alpha',m\alpha}\dot{S}_{m'\alpha'}\boldsymbol{e}_{\alpha} + \langle\Psi_0|\nabla_{\boldsymbol{S}_m}\hat{H}|\Psi_0\rangle - 2\boldsymbol{\lambda}_m\boldsymbol{S}_m \\
&= \dot{\boldsymbol{S}}_m \times \boldsymbol{S}_m + \sum_{m'\alpha'\alpha}\Omega_{m'\alpha',m\alpha}\dot{S}_{m'\alpha'}\boldsymbol{e}_{\alpha} + \langle\Psi_0|\nabla_{\boldsymbol{S}_m}\hat{H}|\Psi_0\rangle - 2\boldsymbol{\lambda}_m\boldsymbol{S}_m.
\end{aligned}
\tag{4.15}
$$

Taking the scalar product with $\boldsymbol{S}_m$ from the right, yields an equation that determines the Lagrange multipliers

$$
\boldsymbol{\lambda}_m = \frac{1}{2}\left(\sum_{m'\alpha'\alpha}\Omega_{m'\alpha',m\alpha}\dot{S}_{m'\alpha'}\boldsymbol{e}_{\alpha} + \langle\Psi_0|\nabla_{\boldsymbol{S}_m}\hat{H}|\Psi_0\rangle\right)\boldsymbol{S}_m,
\tag{4.16}
$$

while taking the cross product gives the effective EOM

$$
\dot{\boldsymbol{S}}_m = \langle\Psi_0|\nabla_{\boldsymbol{S}_m}\hat{H}|\Psi_0\rangle \times \boldsymbol{S}_m + \boldsymbol{T}_m^{(\text{geo})} \times \boldsymbol{S}_m.
\tag{4.17}
$$

One can see that when treating the adiabatic constraint (4.1) via the Lagrange formalism the resulting effective equations of motion exhibit an additional geometrical spin torque $\boldsymbol{T}_m^{(\text{geo})} \times \boldsymbol{S}_m$ compared to the naive adiabatic dynamics. The geometrical spin torque is defined via

$$
\boldsymbol{T}_m^{(\text{geo})} = \boldsymbol{T}_m^{(\text{geo})}(\boldsymbol{S}_m, \dot{\boldsymbol{S}}_m) := \sum_{m'\alpha'\alpha}\Omega_{m'\alpha',m\alpha}\dot{S}_{m'\alpha'}\boldsymbol{e}_{\alpha}.
\tag{4.18}
$$

The name geometrical spin torque derives from the geometric nature of the spin-Berry curvature $\underline{\Omega}$. Note that (4.17) is an implicit equation for $\dot{\boldsymbol{S}}_m$ since the right hand side still depends on $\dot{\boldsymbol{S}}_m$ via the geometrical spin torque. An explicit equation can only be derived for $\dot{\boldsymbol{S}} = (\dot{\boldsymbol{S}}_1, \ldots, \dot{\boldsymbol{S}}_M)$ as a whole. The geometrical spin torque can be written as

$$
\begin{aligned}
\boldsymbol{T}_m^{(\text{geo})} \times \boldsymbol{S}_m &= \sum_{\beta\gamma\delta}\varepsilon_{\beta\gamma\delta}\sum_{m'\alpha'}\Omega_{m'\alpha',m\beta}\dot{S}_{m'\alpha'}S_{m\gamma}\boldsymbol{e}_{\delta} \\
&=: \sum_{\delta}\sum_{m'\alpha'}M_{m\delta,m'\alpha'}\dot{S}_{m'\alpha'}\boldsymbol{e}_{\delta} \\
&= \sum_{\delta}(\underline{M}\dot{\boldsymbol{S}})_{m\delta}\boldsymbol{e}_{\delta}
\end{aligned}
\tag{4.19}
$$

with the definition of $M_{m\alpha,m'\alpha'} := \sum_{\beta\gamma}\varepsilon_{\beta\gamma\alpha}\Omega_{m'\alpha',m\beta}S_{m\gamma}$. The first term in (4.17) can be expressed as a matrix-vector product, see (3.22). Thus, one defines a block-diagonal matrix $\underline{A}$, $A_{m\alpha,m'\alpha'} = \delta_{mm'}B_{\alpha\alpha'}^{(m)}$, with the mth block $\underline{B}^{(m)}$ given by

$$
\underline{B}^{(m)} := \begin{pmatrix} 0 & -v_{mz} & v_{my} \\ v_{mz} & 0 & -v_{mx} \\ -v_{my} & v_{mx} & 0 \end{pmatrix} \quad \text{with } \boldsymbol{v}_m := \langle\Psi_0|\nabla_{\boldsymbol{S}_m}\hat{H}|\Psi_0\rangle.
\tag{4.20}
$$

Therewith, the explicit form of the $3M$-dimensional system of differential equations is

$$\dot{\boldsymbol{S}} = (\mathbb{1} - \underline{M})^{-1}\underline{A}\boldsymbol{S}. \tag{4.21}$$

Note that to compute $\dot{\boldsymbol{S}}$ at every time step the $3M$-dimensional matrix $\mathbb{1} - \underline{M}$ has to be inverted, which is numerically demanding for a large number of classical spins and/or long propagation times.

4.4 – Lehmann Representation of the Spin-Berry Curvature

It is useful to express the spin-Berry curvature in terms of energy eigenstates, as was done for the magnetic susceptibility above. A straightforward calculation yields

$$
\begin{aligned}
\Omega_{m\alpha,m'\alpha'} &= i\left\langle \partial_{S_{m\alpha}}\Psi_0 \middle| \partial_{S_{m'\alpha'}}\middle|\Psi_0\right\rangle - i\left\langle \partial_{S_{m'\alpha'}}\Psi_0 \middle| \partial_{S_{m\alpha}}\middle|\Psi_0\right\rangle \\
&= i\sum_{n\neq 0}\left[\left\langle \partial_{S_{m\alpha}}\Psi_0|n\right\rangle\left\langle n|\partial_{S_{m'\alpha'}}|\Psi_0\right\rangle - \left\langle \partial_{S_{m'\alpha'}}\Psi_0|n\right\rangle\left\langle n|\partial_{S_{m\alpha}}|\Psi_0\right\rangle\right],
\end{aligned} \tag{4.22}
$$

where $|n\rangle \equiv |\Psi_n\rangle$ denotes the nth eigenstate and for $n = 0$ both terms cancel. A further simplification can be achieved by using the identity

$$\left\langle n'\middle|\partial_{S_{m\alpha}}\middle|n\right\rangle = \frac{\langle n'|\frac{\partial\hat{H}}{\partial S_{m\alpha}}|n\rangle}{E_n - E_{n'}} \quad \text{for } E_n \neq E_{n'}, \tag{4.23}$$

which can be derived by differentiating the time-independent Schrödinger equation with respect to $S_{m\alpha}$

$$\partial_{S_{m\alpha}}(\hat{H}(\boldsymbol{S})|\Psi_n(\boldsymbol{S})\rangle) = \partial_{S_{m\alpha}}(E_n(\boldsymbol{S})|\Psi_n(\boldsymbol{S})\rangle)$$

$$\Leftrightarrow \langle\Psi_{n'}|(\partial_{S_{m\alpha}}\hat{H})|\Psi_n\rangle + E_{n'}\langle\Psi_{n'}|\partial_{S_{m\alpha}}|\Psi_n\rangle = (\partial_{S_{m\alpha}}E_n)\underbrace{\langle\Psi_{n'}|\Psi_n\rangle}_{=0 \text{ for } n\neq n'} + E_n\langle\Psi_{n'}|\partial_{S_{m\alpha}}|\Psi_n\rangle. \tag{4.24}$$

Plugging this into the spin-Berry curvature, one has

$$
\begin{aligned}
\Omega_{m\alpha,m'\alpha'} &= i\sum_{n\neq 0}\left[\frac{\langle 0|\frac{\partial\hat{H}}{\partial S_{m\alpha}}|n\rangle\langle n|\frac{\partial\hat{H}}{\partial S_{m'\alpha'}}|0\rangle}{(E_0 - E_n)^2} - \frac{\langle 0|\frac{\partial\hat{H}}{\partial S_{m'\alpha'}}|n\rangle\langle n|\frac{\partial\hat{H}}{\partial S_{m\alpha}}|0\rangle}{(E_0 - E_n)^2}\right] \\
&= -2\,\mathrm{Im}\left\{\sum_{n\neq 0}\frac{\langle 0|\frac{\partial\hat{H}}{\partial S_{m\alpha}}|n\rangle\langle n|\frac{\partial\hat{H}}{\partial S_{m'\alpha'}}|0\rangle}{(E_0 - E_n)^2}\right\}.
\end{aligned} \tag{4.25}
$$

Concretely, for a Hamiltonian of the form (3.1) and the interaction term (3.2) it is

$$\Omega_{m\alpha,m'\alpha'} = -2J^2\,\mathrm{Im}\left\{\sum_{n\neq 0}\frac{\langle 0|\hat{s}_{m\alpha}|n\rangle\langle n|\hat{s}_{m'\alpha'}|0\rangle}{(E_0 - E_n)^2}\right\}, \tag{4.26}$$

which is independent of H_{cl}. The eigenstates and eigenenergies can be expanded around the

eigenstates and eigenenergies of $\hat{H}_{\text{qu}}$, i.e., around $J = 0$,

$$|\Psi_n\rangle = \left|\Psi_n^{(0)}\right\rangle + \mathcal{O}(J) \tag{4.27}$$

$$E_n = E_n^{(0)} + \mathcal{O}(J). \tag{4.28}$$

Since the spin-Berry curvature itself is of order J^2, the corrections contribute only at $\mathcal{O}(J^3)$ such that one can write

$$\Omega_{m\alpha,m'\alpha'} = -2J^2 \operatorname{Im}\left\{\sum_{n\neq 0} \frac{\langle 0^{(0)}| \hat{s}_{m\alpha} |n^{(0)}\rangle \langle n^{(0)}| \hat{s}_{m'\alpha'} |0^{(0)}\rangle}{(E_0^{(0)} - E_n^{(0)})^2}\right\} + \mathcal{O}(J^3). \tag{4.29}$$

The first term in the expansion of $\underline{\Omega}$ is equivalent to $-iJ^2\partial_\omega\chi^A(0)$, compare (3.32), if one ignores the term $i0^+$ in the denominator. This is justified in the case of a nondegenerate ground state which is separated by a gap from the rest of the spectrum. In the weak-J regime one can, therefore, interpret the spin-Berry curvature as the linear response of the electron system, described by $\hat{H}_{\text{qu}}$, to a weak perturbation $\hat{H}_{\text{int}}$. Typically, this regime tends to be the most relevant for physics. However, there is a caveat when dealing with time-reversal invariant systems, for which the first term in (4.29) vanishes [57].

4.5 – The Role of Time-Reversal Symmetry

The time-reversal transformation $\mathbf{T}$ is a discrete transformation [91] that acts as

$$\hat{\boldsymbol{r}} \mapsto \hat{\boldsymbol{r}}, \quad \hat{\boldsymbol{p}} \mapsto -\hat{\boldsymbol{p}}, \quad \hat{\boldsymbol{s}} \mapsto -\hat{\boldsymbol{s}} \tag{4.30}$$

on position, momentum and spin operators. In contrast to most other transformations in quantum mechanics, it has to be represented as an antiunitary, i.e., a unitary and antilinear, transformation on Hilbert space. Let $\hat{\Theta}$ be the operator representing time-reversal transformation. A system is said to be time-reversal symmetric if $\hat{\Theta}$ commutes with the Hamiltonian $\hat{H}$. For a time-reversal symmetric system, it can be shown that it is either $\hat{\Theta}^2 = 1$ or $\hat{\Theta}^2 = -1$. In the former case, one can find an orthonormal basis of time-reversal-invariant energy eigenstates $|\Psi_n\rangle = \hat{\Theta}|\Psi_n\rangle$. In the latter case, a state and its time-reversal partner are orthogonal and energy-degenerate such that each energy is at least two-fold degenerate. These two-state pairs are called Kramer's pairs and the resulting degeneracy Kramer's degeneracy.

The action of the time-reversal operator $\hat{\Theta}$ on the fermionic field operators is defined by

$$\hat{\Theta}c_{i\uparrow}^\dagger\hat{\Theta}^\dagger = c_{i\downarrow}^\dagger, \ \hat{\Theta}c_{i\downarrow}^\dagger\hat{\Theta}^\dagger = -c_{i\uparrow}^\dagger. \tag{4.31}$$

For the local spin operator $\hat{s}_{i\alpha}$, this means

$$\hat{\Theta}\hat{s}_{i\alpha}\hat{\Theta}^\dagger = \frac{1}{2}\sum_{\sigma\sigma'} \hat{\Theta}c_{i\sigma}^\dagger\hat{\Theta}^\dagger\hat{\Theta}c_{i\sigma'}\hat{\Theta}^\dagger\tau_{\sigma\sigma'}^{(\alpha)\,*} = -\hat{s}_{i\alpha}. \tag{4.32}$$

Considering a time-reversal symmetric system with a nondegenerate ground state, we have $\hat{\Theta}^2 = 1$ since there is no Kramer's degeneracy. The matrix elements of the local spin operator

can then be calculated to be

$$
\begin{aligned}
\langle \Psi_{n'} | \, \hat{s}_{i\alpha} \, | \Psi_n \rangle &= \left\langle \hat{\Theta} \Psi_{n'} \middle| \, \hat{s}_{i\alpha} \hat{\Theta} \, | \Psi_n \right\rangle \\
&= \langle \Psi_{n'} | \, \hat{\Theta}^\dagger \hat{s}_{i\alpha} \hat{\Theta} \, | \Psi_n \rangle^* \\
&= -\langle \Psi_{n'} | \, \hat{s}_{i\alpha} \, | \Psi_n \rangle^* ,
\end{aligned}
\tag{4.33}
$$

where the second equality results from the antilinearity of $\hat{\Theta}$. Equation (4.33) shows that the matrix elements of $\hat{s}_{i\alpha}$ are imaginary and thus a product of two such matrix elements is real. Consequently, the spin-Berry curvature vanishes since it is the imaginary part of such a product, see (4.26).

If the quantum system $\hat{H}_{\mathrm{qu}}$ in our general setup (3.1) is time-reversal symmetric, we find that the first term of the J expansion of Ω is zero. On the other hand, higher order terms are finite since the quantum-classical interaction $\hat{H}_{\mathrm{int}}$ itself breaks time-reversal symmetry. Accordingly, there are two ways to obtain a finite spin-Berry curvature. Either work in the regime of intermediate to high J or with a quantum system that explicitly breaks time-reversal symmetry, e.g., a system with spontaneous magnetic order, see chapter 5 and publication [II].

4.6 − Minimal Model

This section introduces the minimal model discussed in [56] to show how ASD is applied in practice and closely follows the exposition therein. The same model is also used to illustrate the non-Abelian extension of the theory in publication [I].

The minimal model consists of a chain of noninteracting itinerant electrons with a classical impurity spin coupled to a single site. The Hamiltonian is given by

$$
\hat{H} = -T \sum_{\langle ii' \rangle \sigma} c_{i\sigma}^\dagger c_{i'\sigma} + J \hat{\boldsymbol{s}}_{i_0} \boldsymbol{S} - \boldsymbol{B} \boldsymbol{S}
\tag{4.34}
$$

with nearest-neighbour hopping amplitude T and an external magnetic field $\boldsymbol{B}$ that is used mainly to initiate dynamics of the classical spin. Concretely, the state of the system is prepared as an eigenstate for a magnetic field pointing in a certain direction, say the z direction. The magnetic field is then instantaneously switched to a different direction, say the x direction, initiating dynamics of the classical spin. The effective EOM (4.17) becomes

$$
\dot{\boldsymbol{S}} = J \langle \Psi_0 | \, \hat{\boldsymbol{s}}_{i_0} \, | \Psi_0 \rangle \times \boldsymbol{S} - \boldsymbol{B} \times \boldsymbol{S} + \boldsymbol{T}^{(\mathrm{geo})} \times \boldsymbol{S}
\tag{4.35}
$$

with $\boldsymbol{T}^{(\mathrm{geo})} = \sum_{\alpha\alpha'} \Omega_{\alpha'\alpha} \dot{S}_{\alpha'} \boldsymbol{e}_\alpha$. The spin-Berry curvature is a rank-2 antisymmetric tensor and can also be written as a pseudovector $\boldsymbol{\Omega}$ with components Ω_α. The pseudovector and the rank-2 tensor are related by

$$
\Omega_\alpha = \frac{1}{2} \sum_{\beta\gamma} \varepsilon_{\alpha\beta\gamma} \Omega_{\beta\gamma} \Leftrightarrow \Omega_{\alpha\beta} = \sum_\gamma \varepsilon_{\alpha\beta\gamma} \Omega_\gamma.
\tag{4.36}
$$

Therewith, the geometrical spin torque can be rewritten as

$$\sum_{\alpha\alpha'} \Omega_{\alpha'\alpha} \dot{S}_{\alpha'} \boldsymbol{e}_\alpha \times \boldsymbol{S} = \sum_{\alpha\alpha'\gamma} \varepsilon_{\gamma\alpha'\alpha} \Omega_\gamma \dot{S}_{\alpha'} \boldsymbol{e}_\alpha \times \boldsymbol{S}$$

$$= (\boldsymbol{\Omega} \times \dot{\boldsymbol{S}}) \times \boldsymbol{S}$$

$$= (\boldsymbol{\Omega}\boldsymbol{S})\dot{\boldsymbol{S}} - (\underbrace{\boldsymbol{S}\dot{\boldsymbol{S}}}_{=0})\boldsymbol{\Omega}, \tag{4.37}$$

where the last equality follows from the Graßmann identity of the double cross product and $\boldsymbol{S}\dot{\boldsymbol{S}} = 0$ since the spins are of fixed length. The effective EOM takes the explicit form

$$\dot{\boldsymbol{S}} = \frac{J\langle \hat{\boldsymbol{s}}_{i_0} \rangle_0 \times \boldsymbol{S} - \boldsymbol{B} \times \boldsymbol{S}}{1 - \boldsymbol{\Omega}\boldsymbol{S}}$$

$$= -\frac{\boldsymbol{B} \times \boldsymbol{S}}{1 \pm \Omega S} \tag{4.38}$$

with $\Omega = |\boldsymbol{\Omega}|$ and $S = |\boldsymbol{S}|$. The last equality follows since the classical spin $\boldsymbol{S}$ acts as a local magnetic field such that the system exhibits a rotational symmetry around the axis $\boldsymbol{e_S}$. Hence, the ground state expectation value of the local spin $\langle \boldsymbol{s}_{i_0} \rangle_0$ is parallel to $\boldsymbol{S}$ and we find $\boldsymbol{\Omega}(\boldsymbol{S}) = \pm\Omega(S)\boldsymbol{e_S}$. The effective EOM (4.38) describes a precession of the classical spin $\boldsymbol{S}$ around the axis given by the magnetic field $\boldsymbol{B}$ and one can read off the precession frequency as

$$\omega_p = \frac{\omega_L}{1 \pm \Omega S}, \tag{4.39}$$

where $\omega_L = |\boldsymbol{B}|$ denotes the classical Larmor frequency. Equation (4.39) shows clearly that the geometrical spin torque results in a renormalised precession frequency. It can be shown that for an even number of electrons one has $\Omega = 0$ and therefore no renormalisation, while for an odd number $\Omega = s/S^2$. In the present case, it is $s = 1/2$ and $S = 1$ which implies that in the strict adiabatic limit the precession frequency is twice as large compared to the Larmor frequency.

The predictions of ASD can be compared to numerical results of the full theory. Here the dynamics is computed according to (3.6) and can be used to calculate the precession frequency of the classical spin. In [56] this was done for different values of the nearest-neighbour hopping amplitude T and the quantum-classical exchange coupling J for a chain at half-filling. In the case of an odd number of electrons ($N = L = 11$ in [56]), the results are consistent with ASD and show that the precession frequency can be up to two times the Larmor frequency as predicted by (4.39). However, in the even case that kind of increase is found as well, although in a smaller parameter range. This is inconsistent with ASD, which predicts $\Omega = 0$ and thus no renormalisation of the precession. An extension of ASD that rectifies this and predicts the correct precession frequency for both an odd and an even number of electrons is NA-SD. NA-SD is developed in publication [I] presented in the next section. Nevertheless, the minimal model demonstrates that the effects of the geometrical spin torque on the classical spin dynamics can be substantial and ASD has a significant advantage over the naive adiabatic theory in which the renormalisation of the precession is completely absent.

Emergent non-Abelian gauge theory in coupled spin-electron dynamics

Nicolas Lenzing ![],[1] Alexander I. Lichtenstein,[1,2] and Michael Potthoff ![][1,2]

[1]*I. Institute of Theoretical Physics, Department of Physics, University of Hamburg, Notkestraße 9-11, 22607 Hamburg, Germany*
[2]*The Hamburg Centre for Ultrafast Imaging, Luruper Chaussee 149, 22761 Hamburg, Germany*

A clear separation of the timescales governing the dynamics of "slow" and "fast" degrees of freedom often serves as a prerequisite for the emergence of an independent low-energy theory. Here, we consider (slow) classical spins exchange coupled to a tight-binding system of (fast) conduction electrons. The effective equations of motion are derived under the constraint that the quantum state of the electron system at any instant of time t lies in the n-dimensional low-energy subspace for the corresponding spin configuration at t. The effective low-energy theory unfolds itself straightforwardly and takes the form of a non-Abelian gauge theory with the gauge freedom given by the arbitrariness of the basis spanning the instantaneous low-energy sector. The holonomic constraint generates a gauge-covariant spin-Berry curvature tensor in the equations of motion for the classical spins. In the non-Abelian theory for $n > 1$, opposed to the $n = 1$ adiabatic spin dynamics theory, the spin-Berry curvature is generically nonzero, even for time-reversal-symmetric systems. Its expectation value with the representation of the electron state is gauge invariant and gives rise to an additional *geometrical* spin torque. Aside from anomalous precession, the $n \geqslant 2$ theory also captures the spin nutational motion, which is usually considered as a retardation effect. This is demonstrated by proof-of-principle numerical calculations for a minimal model with a single classical spin. Already for $n = 2$ and in parameter regimes where the $n = 1$ adiabatic theory breaks down, we find good agreement with results obtained from the full (unconstrained) theory.

I. INTRODUCTION

Classical-spin models [1,2] are a highly useful and widely employed tool to understand the nonequilibrium dynamics of magnetic materials. At the expense of disregarding the quantum nature of the magnetic moments and related phenomena, such as the Kondo effect [3,4], they provide a numerically tractable framework for spin dynamics on an atomistic length scale [5–8]. Typically, classical-spin models may comprise a short-range isotropic Heisenberg-type exchange, various anisotropic couplings, and long-range, e.g., dipole interactions. The classical equations of motion are usually supplemented by Gilbert-damping terms to account for dissipation effects.

Spin-only models can actually be seen as effective low-energy theories emerging from a more fundamental level of modeling, where the local magnetic moments (classical spins S_i) at sites i of a lattice are coupled to the local spins s_i of a system of conduction electrons via a local exchange coupling J. Such quantum-classical spin-electron hybrid models are necessary to explain various phenomena, including indirect spin-exchange interactions, like the Ruderman-Kittel-Kasuya-Yoshida (RKKY) interaction [9], Gilbert spin damping due to coupling to electronic degrees of freedom [10], spin-inertia effects (nutation) [11,12], and other more strongly retarded effective spin-spin interactions mediated by the conduction-electron system.

The standard formal approach [13–17] that achieves the derivation of the effective spin-only theory is based on the (usually realistic) assumption that the local exchange coupling J is weak as compared to the typical energy scales of the electron system. Consider the s-d model [18] with Hamiltonian $H = H_{\rm el} + J \sum_i s_i S_i$ as a prototype. The torque on the classical spin at site i is given by $J \langle s_i \rangle_t \times S_i$, where the expectation value of the local electron spin s_i at site i is obtained from the many-body state $|\Psi(t)\rangle$ of the electron system (Hamiltonian $H_{\rm el}$) at time t. Since the electron state itself must be computed in the presence of the local exchange interaction term $\propto J$ for the (time-dependent) classical-spin configuration $\{S\}$, there is a retarded mutual effective interaction emerging. This is uncovered, for example, by linear-response theory, i.e., by lowest-order time-dependent perturbation theory in J. This leads to an integrodifferential equation of motion for S_i,

$$\dot{S}_i(t) = J^2 \sum_{i'} \int_0^t dt' \underline{\chi}_{ii'}(t - t') S_{i'}(t') \times S_i(t) \qquad (1)$$

which involves the retarded magnetic susceptibility tensor with elements $\chi_{ii'}^{(\alpha\alpha')}(t - t')$ of the electron ground state as the integral kernel ($\alpha, \alpha' = x, y, z$). The resulting spin dynamics is nonconservative, as Eq. (1) describes an open quantum system and is known from Redfield theory [19].

Assuming that $\underline{\chi}_{ii'}(t - t')$ is strongly peaked at $t' = t$, we can replace $S_{i'}(t')$ by the first few terms in its Taylor

expansion around $t' = t$, i.e., $\mathbf{S}_{i'}(t') \approx \mathbf{S}_{i'}(t) + \dot{\mathbf{S}}_{i'}(t)(t' - t) + \ddot{\mathbf{S}}_{i'}(t)(t' - t)^2/2$. Keeping the first term on the right-hand side only and extending the integration over t' to infinity, one obtains an effective Hamiltonian equation of motion for the spins $\mathbf{S}_i$, which involves the instantaneous spin-spin interaction mediated by the RKKY coupling $J_{ii'}^{(\mathrm{RKKY})} = J^2 \chi_{ii'}(\omega = 0)$. Including the second term, in addition, gives rise to a (nonlocal) Gilbert-damping tensor $\underline{\alpha}_{ii'} = -iJ^2 \partial_\omega \underline{\chi}_{ij}(\omega)|_{\omega=0}$, while the third term leads to spin-inertia effects, i.e., additional nutation of the spins. This derivation has been put forward in Refs. [15,16] and can be employed in the context of strongly correlated electron models [20] or, when combined with band-structure theory, for an *ab initio* computation of the Gilbert damping [21–24]. Nutation effects, as have been discussed in Refs. [25–27], for example, find a natural explanation in the same framework set by Eq. (1). Furthermore, at least in principle, systematic extensions of the resulting low-energy spin-only theory can be achieved by taking into account terms of higher order in the expansion. One may also drop the approximation on the t'-integration range. This leads to a time-dependent RKKY coupling $J_{ii'}^{(\mathrm{RKKY})}(t)$ and a time-dependent Gilbert damping $\underline{\alpha}_{ii'}(t)$, as has been mentioned in Refs. [16,17].

The above-sketched standard theory misses, however, an important effect pointed out recently [28]: The slow dynamics of the classical spins results in a nontrivial Berry curvature of the electronic quantum system as is well known since long [29,30]. Quite generally, however, this Berry curvature in turn has a feedback on the classical-spin dynamics [28,31–34]. Namely, there is a geometrical spin torque which comes with the same prefactor J^2 as the RKKY coupling and the Gilbert damping. This torque can give rise to unconventional spin dynamics as has been demonstrated [28,35] not only for a quantum-classical system as is considered here as well, but also for slow classical spins locally exchange coupled to a system of fast classical spins [36,37] and even for the dynamics of a quantum spin in a Kondo model [28].

This geometrical spin torque emerges in an effective low-energy spin-only theory that is derived by starting from the full theory of classical spins coupled to conduction electrons and by imposing the constraint that, at any instant of time t, the electron system is in its ground state, i.e., $|\Psi(t)\rangle = |\Psi_0(\{\mathbf{S}(t)\})\rangle$, for the spin configuration $\{\mathbf{S}(t)\}$ at time t. This is analogous to molecular dynamics approaches [33,38,39] where the slow nuclear coordinates are treated classically. If the exchange coupling J is weak, the classical-spin dynamics is slow compared to typical energy scales of the electron systems. The adiabatic spin dynamics (ASD) thus addresses the same parameter regime as the standard perturbative linear-response approach discussed above.

With this paper we explore a systematic extension of the ASD by relaxing the adiabatic constraint. The impact of electronic low-energy excitations from the instantaneous ground state $|\Psi_0(\{\mathbf{S}(t)\})\rangle$ on the classical-spin dynamics can be taken into account by imposing, as a weaker constraint, that the electron state $|\Psi(t)\rangle$ be at time t in the subspace of the Fock space spanned by the first $n > 1$ eigenstates of the Hamiltonian for the spin configuration $\{\mathbf{S}(t)\}$ at t. This beyond-adiabatic constraint leads to a non-Abelian Berry connection and curvature [30,40]. Here, we will work out the general formalism

of the non-Abelian gauge theory that emerges as the effective low-energy theory. The formally correct incorporation of the constraint is achieved within conventional Lagrange formalism. A simple toy model will be considered and solved numerically to study the effect of the geometric torque on the classical-spin dynamics in the non-Abelian case. We discuss the anomalies in the precessional spin dynamics and demonstrate that spin nutation arises naturally in our framework. The previously developed ASD represents the $n = 1$ limit of our non-Abelian spin-dynamics (NA-SD) theory. In the ASD for a single classical spin, the presence of an anomalous precession frequency has been found [28] for an odd number of conduction electrons only, while the full solution of the coupled equations of motion for spin and electron dynamics yields an anomalous frequency for both odd and even electron numbers. In the broader framework of NA-SD we can resolve this open issue.

The paper is organized as follows: Section II presents the general Hamiltonian and Lagrangian formulation of the theory. The equations of motion of the non-Abelian gauge theory in the instantaneous low-energy sector are worked out in Sec. III, and various formal aspects of the theory are discussed in Sec. IV. Sections V and VI are particularly devoted to a discussion of the impact of time-reversal symmetry and of gauge transformations, respectively. A minimal model, suitable for proof-of-principle studies, is introduced in Sec. VII. In Sec. VIII we present and discuss the results of numerical calculations. Conclusions are given in Sec. IX.

II. GENERAL THEORY

Geometric forces or torques originate in the adiabatic limit of hybrid systems consisting of quantum degrees of freedom interacting with classical degrees of freedom. Here, we consider a quantum lattice model of N conduction electrons interacting with M classical "spins" $\mathbf{S}_m$ of unit length $|\mathbf{S}_m| = 1$. The system dynamics is governed by a quantum-classical Hamiltonian of the form

$$\hat{H}(\{\mathbf{S}\}) = \hat{H}_{\mathrm{qu}} + H_{\mathrm{cl}}(\{\mathbf{S}\}) + \hat{H}_{\mathrm{int}}(\{\mathbf{S}\}). \quad (2)$$

The quantum Hamiltonian $\hat{H}_{\mathrm{qu}}$ is constructed in terms of fermion creation and annihilation operators $c_{\mathbf{r}\sigma}^\dagger$ and $c_{\mathbf{r}\sigma}$, where $\mathbf{r}$ refers to the sites of the lattice and $\sigma = \uparrow, \downarrow$ is the spin projection. Additional orbital degrees of freedom may be considered as well. The formulation of the theory is largely independent of $\hat{H}_{\mathrm{qu}}$ but requires a well-defined local quantum spin $\mathbf{s}_{\mathbf{r}}$ at lattice site $\mathbf{r}$:

$$\mathbf{s}_{\mathbf{r}} = \frac{1}{2} \sum_{\sigma\sigma'} c_{\mathbf{r}\sigma}^\dagger \boldsymbol{\sigma}_{\sigma\sigma'} c_{\mathbf{r}\sigma'}. \quad (3)$$

Here, $\boldsymbol{\sigma}$ is the vector of 2×2 Pauli matrices (and $\hbar \equiv 1$).

The dynamics of the subsystem of M classical spins $\{\mathbf{S}\} \equiv \{\mathbf{S}_1, \ldots, \mathbf{S}_M\}$ derives from a classical Hamilton function $H_{\mathrm{cl}}(\{\mathbf{S}\})$ and may comprise an external magnetic field and isotropic or anisotropic spin-exchange couplings. The third term in (2) represents a quantum-classical interaction term.

Here, we choose an isotropic local exchange interaction

$$\hat{H}_{\text{int}}(\{\boldsymbol{S}\}) = J \sum_{m=1}^{M} \boldsymbol{S}_m \boldsymbol{s}_{\boldsymbol{r}_m} , \qquad (4)$$

between the mth classical spin $\boldsymbol{S}_m$ and the local spin $\boldsymbol{s}_{\boldsymbol{r}_m}$ of the conduction-electron system at the site $\boldsymbol{r}_m$. The coupling strength is $J > 0$. The theory is developed for an arbitrary number of classical spins M, but we will later focus on a single classical-spin Kondo model ($M = 1$) for the sake of simplicity.

If the classical spins $\{\boldsymbol{S}\}$ were replaced by quantum spins, (2) would represent the Hamiltonian of the multi-impurity or lattice Kondo model. With the classical-spin approximation we disregard typical correlation effects, such as Kondo screening and heavy-fermion behavior, and hence we are essentially working on a mean-field-type level. The approximation may be justified in cases where there are well-formed spin moments which are stable on timescales exceeding all remaining timescales of the problem, e.g., in cases, where the Kondo effect is suppressed by magnetism or in case of quantum spins with large spin quantum numbers. An example has been given in Ref. [28], where anomalous quantum-classical dynamics due to a geometrical torque has also been found in the corresponding full quantum system. A consistent theory for a system that is entirely quantum with a least two largely different timescales has yet to be developed. This means that the presence of slow classical degrees of freedom is necessarily required for the very concept of geometrical forces and torques. The classical degrees of freedom are required to define the smooth manifold onto which the quantum dynamics is restricted in the adiabatic limit.

A pure state of the quantum-classical hybrid system at time t is specified by a Hilbert-space vector $|\Psi(t)\rangle$ and by the classical-spin configuration $\{\boldsymbol{S}(t)\}$ (see Refs. [41–43] for a general discussion of hybrid dynamics). The trajectory of the system state is obtained as the solution of a system of coupled ordinary differential equations. These consist of the Schrödinger equation, involving the quantum Hamiltonian and the interaction term, which depends on the classical-spin configuration

$$i\partial_t |\Psi(t)\rangle = [\hat{H}_{\text{qu}} + \hat{H}_{\text{int}}(\{\boldsymbol{S}(t)\})]|\Psi(t)\rangle , \qquad (5)$$

and the Hamilton equations of motion for the classical-spin configuration, involving the classical Hamilton function and the expectation value of the interaction term in the quantum state $|\Psi(t)\rangle$:

$$\dot{\boldsymbol{S}}_m(t) = \{\boldsymbol{S}_m(t), H_{\text{cl}}(\{\boldsymbol{S}(t)\}) + \langle \hat{H}_{\text{int}}(\{\boldsymbol{S}(t)\})\rangle\}_S . \qquad (6)$$

Here, the overdot denotes the time derivative, and $\{\cdot, \cdot\}_S$ is the Poisson bracket. In case of spin systems, the latter is defined for two arbitrary functions $A(\{\boldsymbol{S}\})$ and $B(\{\boldsymbol{S}\})$ as [44]

$$\{A, B\}_S = \sum_m \frac{\partial A}{\partial \boldsymbol{S}_m} \times \frac{\partial B}{\partial \boldsymbol{S}_m} \cdot \boldsymbol{S}_m. \qquad (7)$$

The coupled equations of motion (5) and (6) are generated as Euler-Lagrange equations by requiring stationarity of an action functional $\mathcal{S} = \int L \, dt$ with the Lagrangian

$L = L(\{\boldsymbol{S}\}, \{\dot{\boldsymbol{S}}\}, |\Psi\rangle, |\dot{\Psi}\rangle, \langle\Psi|, \langle\dot{\Psi}|)$:

$$L = \sum_m \boldsymbol{A}(\boldsymbol{S}_m)\dot{\boldsymbol{S}}_m + \langle\Psi(t)|i\partial_t - \hat{H}|\Psi(t)\rangle. \qquad (8)$$

Here, $\boldsymbol{A}(\boldsymbol{S})$ is a function satisfying $\nabla \times \boldsymbol{A}(\boldsymbol{S}) = -\boldsymbol{S}/S^3$, which can thus be interpreted as the vector potential of a unit magnetic monopole located at $\boldsymbol{S} = 0$. We have

$$\boldsymbol{A}(\boldsymbol{S}) = -\frac{1}{S^2}\frac{\boldsymbol{e} \times \boldsymbol{S}}{1 + \boldsymbol{e}\boldsymbol{S}/S}, \qquad (9)$$

with a unit vector $\boldsymbol{e}$. In the standard gauge [45] this is chosen as $\boldsymbol{e} = \boldsymbol{e}_z$. In this gauge, another representation is $\boldsymbol{A}(\boldsymbol{S}) = -(1/S)\tan(\vartheta/2)\boldsymbol{e}_\varphi$, using spherical coordinates (S, ϑ, φ). For details of deriving Eqs. (5) and (6) from $\delta\mathcal{S} = 0$, see Ref. [36] (Supplemental Material).

We will address the parameter regime of the Hamiltonian, where the system dynamics is characterized by two strongly different timescales, a slow spin dynamics and a fast dynamics of the electron state, which almost instantaneously follows the motion of the spins. In the extreme adiabatic limit, the quantum many-body state $|\Psi(t)\rangle$ of the electron system at time t is given by the ground state $|\Psi_0(\{\boldsymbol{S}(t)\})\rangle$ of $\hat{H}_{\text{qu}} + \hat{H}_{\text{int}}(\{\boldsymbol{S}(t)\})$, for the spin configuration $\{\boldsymbol{S}(t)\}$ at time t. When approaching the adiabatic limit in parameter space, the fast electron dynamics will be more and more constrained to the ground manifold $\{|\Psi_0(\{\boldsymbol{S}(t)\})\rangle\}$. Adiabatic spin-dynamics (ASD) theory [28,36,37] assumes that the dynamics is *perfectly* constrained to the ground-state manifold and employs

$$|\Psi(t)\rangle = |\Psi_0(\{\boldsymbol{S}(t)\})\rangle \qquad (10)$$

as a holonomic constraint to completely eliminate the electron degrees of freedom from the Lagrangian (8). In this way, one arrives at a spin-only effective Lagrangian $L_{\text{eff}}(\{\boldsymbol{S}\}, \{\dot{\boldsymbol{S}}\})$, and the resulting effective equations of motion include the geometrical spin torque as a holonomy effect [28]. The unconventional spin dynamics originating from the corresponding geometrical spin torque is missed by other approaches, such as the standard linear-response approach to a spin-only theory that has been discussed in the Introduction. On the other hand, retardation effects, e.g., nutational motion, are excluded within ASD by the very construction.

The validity of the basic assumption (10) strongly depends on the specific system considered and on the considered parameter range. Even for gapped systems, however, the strict adiabatic approximation is never perfectly satisfied, and the true slow spin dynamics will be affected to some degree by admixtures from (low-energy) excited electron states. As a systematic generalization of ASD, we therefore propose to relax the constraint (10) and to replace it by the weaker constraint

$$|\Psi(t)\rangle = \sum_{i=0}^{n-1} \alpha_i(t)|\Psi_i(\{\boldsymbol{S}(t)\})\rangle . \qquad (11)$$

Here, $|\Psi_i(\{\boldsymbol{S}(t)\})\rangle$ is the ith excited state of $\hat{H}_{\text{qu}} + \hat{H}_{\text{int}}(\{\boldsymbol{S}(t)\})$, i.e., we assume that at any instant of time t the conduction-electron state $|\Psi(t)\rangle$ is contained in the low-energy subspace $\mathcal{E}_n(\{\boldsymbol{S}\})$ spanned by the instantaneous ground state and the

lowest $n - 1$ instantaneous eigenstates for the spin configuration $\{S\} = \{S(t)\}$ at time t. Choosing a fixed orthonormal basis

$$\{|\Psi_i(\{S\})\rangle \,|\, i = 0, \ldots, n - 1\} \tag{12}$$

of $\mathcal{E}_n(\{S\})$ for any spin configuration, the electron state at time t is fully specified by the set of expansion coefficients $\{\alpha(t)\} \equiv \{\alpha_0(t), \ldots, \alpha_{n-1}(t)\}$ via (11).

For $n = 1$, we recover conventional ASD, and thus obtain a true spin-only theory. For small $n > 1$, the effective Lagrangian is obtained from (8) by substituting $|\Psi\rangle$, $\partial_t|\Psi\rangle$, $\langle\Psi|$, $\partial_t\langle\Psi|$ using (11). It thereby becomes a function of $\{S\}$ and $\{\dot{S}\}$ and furthermore a function of the set of expansion coefficients $\{\alpha\}$, i.e., we get $L_{\text{eff}} = L_{\text{eff}}(\{S\}, \{\dot{S}\}, \{\alpha\}, \{\alpha^*\}, \{\dot{\alpha}\}, \{\dot{\alpha}^*\})$. Hence, aside from the spin degrees of freedom, the resulting low-energy theory contains a few electronic degrees of freedom as well.

We also define the eigenenergies $E_i = E_i(\{S\})$ of $\hat{H}_{\text{qu}} + \hat{H}_{\text{int}}(\{S(t)\})$ corresponding to the basis states $|\Psi_i(\{S\})\rangle$. $E_i(\{S\})$ is the analog of the ith potential-energy (Born-Oppenheimer) surface known from molecular-dynamics theory [33,38]. The spin configuration $\{S\}$ takes the role of the configuration of atomic nuclei. Note that the strict adiabatic approximation (10) becomes invalid, if the trajectory of the spin configuration $\{S(t)\}$ passes a configuration $\{S_{\text{cr}}\}$, at which there is a crossing of the ground state with the first excited state, i.e., $E_0(\{S_{\text{cr}}\}) = E_1(\{S_{\text{cr}}\})$, since this is in conflict with the adiabatic theorem [46–48].

For $n > 1$, the relaxed condition (11) corresponds to a generalized adiabatic theorem (see Ref. [46]) stating that the condition is respected, if the low-energy sector $\mathcal{E}_n(\{S\})$ and its orthogonal complement (the "high-energy sector") remain gapped for all $\{S(t)\}$) and, of course, if the electron dynamics is sufficiently slow. In other words, for a given n, NA-SD applies if there is no crossing $E_{n-1}(\{S_{\text{cr}}\}) = E_n(\{S_{\text{cr}}\})$, while crossings of states *within* the low-energy sector are irrelevant. One should note, however, that a crossing of two states belonging to the low- and the high-energy sector, respectively, is in fact unproblematic, if the expansion coefficient $\alpha_{n-1}(t) = 0$ for all t, since in this case the $(n-1)$th excited eigenstate would not contribute to $|\Psi(t)\rangle$ anyway. This argument can be extended to $k < n - 1$, as long as there are crossings between "unoccupied" states with $\alpha_i(t) = 0$ and $\alpha_j(t) = 0$ for $k \leqslant i, j \leqslant n$ only. We conclude that the relaxed condition (11) for $n > 1$ also implies a less severe, relaxed approximation.

III. EFFECTIVE EQUATIONS OF MOTION

The effective Lagrangian that is obtained by using the constraint (11) to eliminate $|\Psi(t)\rangle$ from the original Lagrangian (8) is given by

$$L_{\text{eff}} = L_{\text{eff}}(\{S\}, \{\dot{S}\}, \{\alpha\}, \{\alpha^*\}, \{\dot{\alpha}\}, \{\dot{\alpha}^*\})$$

$$= \sum_m \boldsymbol{A}_m(S_m)\dot{S}_m + i \sum_{ij} \alpha_i^* \langle\Psi_i|\partial_t(\alpha_j|\Psi_j\rangle)$$

$$- \sum_{ij} \alpha_i^* \alpha_j \langle\Psi_i|\hat{H}|\Psi_j\rangle, \tag{13}$$

where $|\Psi_i\rangle = |\Psi_i(\{S_m\})\rangle$, and where the $\{\dot{S}\}$ dependence, besides the first term, is due to $\langle\Psi_i|\partial_t|\Psi_j\rangle = \sum_m \langle\Psi_i|\partial_{S_m}|\Psi_j\rangle\dot{S}_m$. The Euler-Lagrange equation $\partial_t(\partial L_{\text{eff}}/\partial\dot{\alpha}_i^*) - \partial L_{\text{eff}}/\partial\alpha_i^* = 0$ for the "wave function" α_i is straightforwardly obtained as

$$i\partial_t\alpha_i = \sum_j \langle\Psi_i|(\hat{H}_{\text{qu}} + \hat{H}_{\text{int}})|\Psi_j\rangle\alpha_j$$

$$- i \sum_m \sum_j \alpha_j \langle\Psi_i|\partial_{S_m}|\Psi_j\rangle\dot{S}_m. \tag{14}$$

The complex conjugate of this equation is just the equation of motion that is obtained for α_i^*.

Note that the second term involves the non-Abelian spin-Berry connection $\underline{\boldsymbol{C}}_m = \underline{\boldsymbol{C}}_m(\{S\})$. Opposed to the (Abelian) spin-Berry connection $\boldsymbol{C}_m = i\langle\Psi_0|\partial_{S_m}|\Psi_0\rangle$ of the (Abelian) ASD, this is, for each m, a matrix-valued vector with elements

$$\boldsymbol{C}_m^{(ij)} = i\langle\Psi_i|\partial_{S_m}|\Psi_j\rangle = i \sum_\gamma \langle\Psi_i|\partial_{S_{m\gamma}}|\Psi_j\rangle\boldsymbol{e}_\gamma = \sum_\gamma C_{m\gamma}^{(ij)}\boldsymbol{e}_\gamma. \tag{15}$$

The matrix dimension is given by the dimension of the low-energy subspace $n = \dim \mathcal{E}_n(\{S\})$. It is easy to see that this is a real quantity. Its transformation behavior under gauge transformations will be discussed in Sec. VI.

We proceed by deriving the second set of equations of motion from the effective Lagrangian $\partial_t(\partial L_{\text{eff}}/\partial\dot{S}_m) - \partial L_{\text{eff}}/\partial S_m = 0$. With (13) we straightforwardly find

$$\frac{\partial L_{\text{eff}}}{\partial S_m} = \frac{\partial}{\partial S_m}(\boldsymbol{A}_m\dot{S}_m) + i \sum_k \sum_{ij} \alpha_i^*\alpha_j \frac{\partial}{\partial S_m}(\langle\Psi_i|\partial_{S_k}|\Psi_j\rangle\dot{S}_k)$$

$$- \sum_{ij} \alpha_i^*\alpha_j \frac{\partial}{\partial S_m}(\langle\Psi_i|\hat{H}|\Psi_j\rangle), \tag{16}$$

and with $\partial L_{\text{eff}}/\partial\dot{S}_m = \boldsymbol{A}_m + i \sum_{ij} \alpha_i^*\alpha_j\langle\Psi_i|\partial_{S_m}|\Psi_j\rangle$,

$$\frac{d}{dt}\frac{\partial L_{\text{eff}}}{\partial\dot{S}_m} = \sum_\gamma \frac{\partial\boldsymbol{A}_m}{\partial S_{m\gamma}}\dot{S}_{m\gamma} + i \sum_{ij} [(\partial_t\alpha_i^*)\alpha_j + \alpha_i^*(\partial_t\alpha_j)]$$

$$\times \langle\Psi_i|\partial_{S_m}|\Psi_j\rangle + i \sum_k \sum_{ij} \alpha_i^*\alpha_j$$

$$\times (\dot{S}_k\partial_{S_k})(\langle\Psi_i|\partial_{S_m}|\Psi_j\rangle). \tag{17}$$

Both Eqs. (16) and (17) involve the spin-Berry connection. The third term in (16) can be rewritten using the identity

$$\frac{\partial}{\partial S_m}(\langle\Psi_i|\hat{H}|\Psi_j\rangle) = \langle\Psi_i|(\partial_{S_m}\hat{H})|\Psi_j\rangle - (E_j - E_i)\langle\Psi_i|\partial_{S_m}|\Psi_j\rangle, \tag{18}$$

and for the second term in (17) it is convenient to get rid of the time derivatives by using

$$i[(\partial_t\alpha_i^*)\alpha_j + \alpha_i^*(\partial_t\alpha_j)]$$

$$= i \sum_k \sum_l [\alpha_l^*\alpha_j\langle\Psi_l|\partial_{S_k}|\Psi_i\rangle$$

$$- \alpha_i^*\alpha_l\langle\Psi_j|\partial_{S_k}|\Psi_l\rangle]\dot{S}_k + \alpha_i^*\alpha_j(E_j - E_i), \tag{19}$$

which directly follows from the equation of motion for the wave functions (14). Therewith, we arrive at

$$
\begin{aligned}
0 &= \frac{d}{dt}\frac{\partial L_{\text{eff}}}{\partial \dot{\boldsymbol{S}}_m} - \frac{\partial L_{\text{eff}}}{\partial \boldsymbol{S}_m} \\
&= \sum_{\beta\gamma}\left(\frac{\partial A_{m\beta}}{\partial S_{m\gamma}} - \frac{\partial A_{m\gamma}}{\partial S_{m\beta}}\right)\dot{S}_{m\gamma}\hat{e}_\beta + \sum_{ij}\alpha_i^*\alpha_j\langle\Psi_i|(\partial_{\boldsymbol{S}_m}\hat{H})|\Psi_j\rangle \\
&\quad + i\sum_k\sum_{ij}\sum_\gamma \alpha_i^*\alpha_j[\partial_{S_{k\gamma}}(\langle\Psi_i|\partial_{\boldsymbol{S}_m}|\Psi_j\rangle) - \partial_{\boldsymbol{S}_m}(\langle\Psi_i|\partial_{S_{k\gamma}}|\Psi_j\rangle)]\dot{S}_{k\gamma} \\
&\quad + i\sum_k\sum_{ijl}\sum_\gamma[\alpha_l^*\alpha_j\langle\Psi_l|\partial_{S_{k\gamma}}|\Psi_i\rangle - \alpha_i^*\alpha_l\langle\Psi_j|\partial_{S_{k\gamma}}|\Psi_l\rangle]\langle\Psi_i|\partial_{\boldsymbol{S}_m}|\Psi_j\rangle\dot{S}_{k\gamma}.
\end{aligned}
\tag{20}
$$

The first term on the right-hand side is a twofold cross product, $-\dot{\boldsymbol{S}}_m \times (\nabla_{\boldsymbol{S}_m} \times \boldsymbol{A}_m)$, and with (9) and with the normalization $|\boldsymbol{S}_m| = 1$, the curl can be written as $\nabla \times \boldsymbol{A}(\boldsymbol{S}) = -\boldsymbol{S}$. The second term is an expectation value $\langle\partial_{\boldsymbol{S}_m}H\rangle$ of the "effective field" $\partial_{\boldsymbol{S}_m}H$ in the state of the electron system $|\Psi\rangle$ [see Eq. (11)]. With (15), the third term reads as $\sum_k\sum_{ij}\sum_\gamma \alpha_i^*\alpha_j[\partial_{S_{k\gamma}}\boldsymbol{C}_m^{(ij)} - \partial_{\boldsymbol{S}_m}C_{k\gamma}^{(ij)}]\dot{S}_{k\gamma}$. Its βth component involves the "curl"

$$
\underline{\Omega}_{k\gamma,m\beta}^{(\text{A})} = \partial_{S_{k\gamma}}\underline{C}_{m\beta} - \partial_{S_{m\beta}}\underline{C}_{k\gamma}
\tag{21}
$$

of the spin-Berry connection. Here, the underlines indicate that the spin-Berry connection and its curl are matrices in the indices i, j labeling the basis of the low-energy subspace for given spin configuration. $\underline{\Omega}^{(\text{A})}$ has the form of the spin-Berry curvature in the Abelian ($n = 1$) theory. We refer to this as the "Abelian spin-Berry curvature." Again with (15), the βth component of the fourth term in (20) reads as $-i\sum_k\sum_{ijl}\sum_\gamma[\alpha_l^*\alpha_j C_{k\gamma}^{(li)} - \alpha_i^*\alpha_l C_{k\gamma}^{(jl)}]C_{m\beta}^{(ij)}\dot{S}_{k\gamma}$. This involves the commutator $[\underline{C}_{k\gamma}, \underline{C}_{m\beta}]$ of the spin-Berry connection.

We define the (non-Abelian) spin-Berry curvature

$$
\begin{aligned}
\underline{\Omega}_{k\gamma,m\beta} &= \partial_{S_{k\gamma}}\underline{C}_{m\beta} - \partial_{S_{m\beta}}\underline{C}_{k\gamma} - i[\underline{C}_{k\gamma}, \underline{C}_{m\beta}] \\
&= \underline{\Omega}_{k\gamma,m\beta}^{(\text{A})} - i[\underline{C}_{k\gamma}, \underline{C}_{m\beta}],
\end{aligned}
\tag{22}
$$

which differs from the Abelian one by the additional commutator. Furthermore, we define the "expectation value" of the spin-Berry curvature in the state given by the wave function $\{\alpha\}$ as

$$
\langle\Omega\rangle_{k\gamma,m\beta} = \sum_{ij}\alpha_i^*\Omega_{k\gamma,m\beta}^{(ij)}\alpha_j.
\tag{23}
$$

With this, the effective equation of motion (20) for the classical-spin configuration can be written in the compact form

$$
\begin{aligned}
0 &= \frac{d}{dt}\frac{\partial L_{\text{eff}}}{\partial \dot{\boldsymbol{S}}_m} - \frac{\partial L_{\text{eff}}}{\partial \boldsymbol{S}_m} = \dot{\boldsymbol{S}}_m \times \boldsymbol{S}_m \\
&\quad + \langle\partial_{\boldsymbol{S}_m}\hat{H}\rangle + \sum_k\sum_{\beta\gamma}\dot{S}_{k\gamma}\langle\Omega\rangle_{k\gamma,m\beta}\boldsymbol{e}_\beta
\end{aligned}
\tag{24}
$$

or, exploiting the structure of the quantum-classical Hamiltonian (2) and the normalization of the wave function

$$
\sum_i |\alpha_i|^2 = 1,
$$
$$
0 = \dot{\boldsymbol{S}}_m \times \boldsymbol{S}_m + \langle\partial_{\boldsymbol{S}_m}\hat{H}_{\text{int}}\rangle + \partial_{\boldsymbol{S}_m}H_{\text{cl}} + \sum_k\sum_{\beta\gamma}\dot{S}_{k\gamma}\langle\Omega\rangle_{k\gamma,m\beta}\boldsymbol{e}_\beta.
\tag{25}
$$

This equation is an implicit equation for $\dot{\boldsymbol{S}}_m$. An explicit form is derived in Appendix A. Finally, we rewrite (14) using the definition of the spin-Berry connection (15):

$$
i\partial_t\alpha_i = \sum_j \langle\Psi_i|(\hat{H}_{\text{qu}} + \hat{H}_{\text{int}})|\Psi_j\rangle\alpha_j - \sum_m\sum_j \dot{\boldsymbol{S}}_m\boldsymbol{C}_m^{(ij)}\alpha_j.
\tag{26}
$$

Equations (25) and (26) represent a closed coupled set of nonlinear first-order differential equations for the effective many-body wave function $\{\alpha\}$ and for the classical-spin configuration $\{\boldsymbol{S}\}$.

IV. DISCUSSION

The respective last terms in the equations of motion (25) and (26) originate from the strict treatment of the holonomic constraint (11). Although the first time derivative of the local spins is reminiscent of a dissipative Gilbert-type damping, the resulting dynamics is strictly conserving, i.e., the total energy given by the expectation value of the total Hamiltonian (2) with the quantum state of the conduction-electron system is a constant of motion. Unlike the standard approach discussed in the Introduction, the equations of motion thus describe the dynamics of a closed quantum system (at low energies).

For the derivation of the equations of motion, we have treated all components of the spins and of the wave function as independent and have thereby disregarded the normalization conditions for the length of the classical spin and for the norm of the wave function

$$
|\boldsymbol{S}_m(t)| = 1, \qquad \sum_i |\alpha_i(t)|^2 = 1,
\tag{27}
$$

which must hold at any instant of time t. One can easily check directly, however, that these are respected. The normalization condition for the wave function can also be derived by noting that the effective Lagrangian is invariant under global U(1) phase transformations. Noether's theorem yields $Q = \sum_i |\alpha_i(t)|^2$ as a conserved charge. Alternatively, the conditions can be treated as additional constraints via appropriate

Lagrange multipliers. As is shown in Appendix B, the resulting Euler-Lagrange equations are in fact unchanged.

Adiabatic spin-dynamics (ASD) theory [28] is recovered for $n = 1$, where the conduction-electron dynamics is constrained to the ground-state manifold $|\Psi(t)\rangle = |\Psi_0(\{S(t)\})\rangle$ and where the wave function is $\alpha_0 \equiv 1$ trivially [see Eq. (11)]. In this case, the spin-Berry connection $C_m^{(ij)} = i\langle \Psi_i | \partial_{S_m} | \Psi_j \rangle$ with $i, j = 0, \ldots, n-1$, reduces to a vector with scalar entries only, $C_m = i\langle \Psi_0 | \partial_{S_m} | \Psi_0 \rangle$. Hence, the commutator in (22) vanishes, and the spin-Berry curvature $\underline{\Omega}_{k\gamma, m\beta}$ reduces to the corresponding expression $\underline{\Omega}_{k\gamma, m\beta}^{(A)}$ [Eq. (21)] of (Abelian) ASD theory.

In the opposite extreme case, i.e., when n is chosen as the dimension of the full many-electron Fock space $\mathcal{H}$, Eq. (11) is actually no longer a constraint but rather represents the expansion of the electron state $|\Psi(t)\rangle$ with respect to a complete orthonormal system of time-dependent basis states $\{|\Psi_i(t)\rangle\}$ with $|\Psi_i(t)\rangle = |\Psi_i(\{S(t)\})\rangle$. In this case, it is straightforward to see that (26) is just Schrödinger's equation $i\partial_t|\Psi(t)\rangle = \hat{H}|\Psi(t)\rangle$, i.e., (5), but formulated for the coefficients $\alpha_i(t)$ of $|\Psi(t)\rangle$ in that basis. The spin-Berry connection merely takes care of the fact that the basis changes smoothly with the parameters $\{S\}$. Equation (25) trivializes as well in this case: We can rewrite the (non-Abelian) spin-Berry curvature in the form (see Appendix C)

$$\Omega_{k\gamma, m\beta}^{(ij)} = i[\langle \partial_{S_{k\gamma}} \Psi_i | \mathcal{Q}_n | \partial_{S_{m\beta}} \Psi_j \rangle - (k\gamma \leftrightarrow m\beta)], \quad (28)$$

where $\mathcal{Q}_n := \mathbb{1} - \sum_{i=0}^{n-1} |\Psi_i\rangle\langle\Psi_i|$ projects onto the orthogonal complement of the low-energy space $\mathcal{E}_n(\{S\})$. If $n = \dim \mathcal{H}$, the complement is zero, and the spin-Berry curvature vanishes identically, so that

$$0 = \dot{S}_m \times S_m + \langle \partial_{S_m} \hat{H}_{\text{int}} \rangle + \partial_{S_m} H_{\text{cl}}. \quad (29)$$

Taking the cross product with S_m from the right on both sides of (25) and exploiting the normalization condition for the spin length, we get

$$\dot{S}_m = \frac{\partial \hat{H}(\{S\})}{\partial S_m} \times S_m. \quad (30)$$

This is just the explicit form of (6).

Some general properties of the spin-Berry curvature can be derived from (28). One immediately notes the antisymmetry

$$\Omega_{k\gamma, m\beta}^{(ij)} = -\Omega_{m\beta, k\gamma}^{(ij)} \quad (31)$$

for fixed i, j. Furthermore, complex conjugation yields

$$\Omega_{k\gamma, m\beta}^{(ij)*} = -\Omega_{m\beta, k\gamma}^{(ji)}. \quad (32)$$

With these properties, one can immediately conclude that

$$\langle \Omega \rangle_{k\gamma, m\beta} = \sum_{ij} \alpha_i^* \Omega_{k\gamma, m\beta}^{(ij)} \alpha_j = \langle \Omega \rangle_{k\gamma, m\beta}^*, \quad (33)$$

i.e., the expectation value, which enters the effective equation of motion (25), is real.

Quite generally, the (Abelian) Berry connection and Berry curvature arise in the adiabatic problem, where a quantum Hamiltonian $\hat{H} = \hat{H}(\lambda)$ depends on a family of slowly varying parameters λ and has a nondegenerate ground state for all λ. This gives rise to the famous Berry phase [29], which the ground state picks up during a closed loop in parameter

space and which can be computed, e.g., as an integral of the Berry curvature over the surface bounded by the loop. Mathematically, the phase is a holonomy, i.e., it results from a twist of the line bundle $\{(\lambda, |\Psi_0\rangle) | \hat{H}(\lambda)|\Psi_0\rangle = E_0(\{\lambda\})|\Psi_0\rangle\}$ [49]. The Berry phase is gauge invariant and thus observable and depends on the geometry of the closed loop only. Similarly, non-Abelian gauge fields arise in the adiabatic time evolution of an $(n > 1)$-fold degenerate ground state of a quantum system [40] and produce a nontrivial phase after completing a loop in parameter space.

Here, we consider a quantum system coupled to *dynamical* classical degrees of freedom (classical spins). In case of a clear timescale separation between the slow classical and the fast quantum dynamics, the classical spins induce a spin-Berry curvature in the quantum conduction-electron system. Generically, it is highly unlikely, however, that the classical state evolves along a closed path. The essential observation, however, is that there is an additional *feedback* of the Berry curvature on the classical-spin dynamics, seen in the last term in (25) for $\Omega = \Omega^{(A)}$. Already in the Abelian case $n = 1$, this leads to an anomalous geometrical spin torque [28]. This geometric feedback on slow classical dynamics has been pointed out [28,31–37] but has not yet been studied for spin dynamics in the non-Abelian case $1 < n = \dim \mathcal{E}_n\{S\} \ll \dim \mathcal{H}$.

V. TIME REVERSAL

Time-reversal symmetry plays an important role for the presence of a finite spin-Berry curvature in the adiabatic case ($n = 1$) [28]. For $n > 1$, however, this is entirely different: We assume that the electron system is time-reversal symmetric, i.e., that the Hamiltonian $\hat{H}_{\text{qu}}$ commutes with the antiunitary operator for time reversal Θ. The interaction term (4), on the other hand, is odd under time reversal, $\Theta\hat{H}_{\text{int}}\Theta^\dagger = -\hat{H}_{\text{int}}$, since $\Theta s_{r_m}\Theta^\dagger = -s_{r_m}$. The local spins S_m are classical degrees of freedom, which act as local magnetic fields and explicitly break time-reversal symmetry of the quantum system.

This effect, however, can be disregarded in the weak-J regime, where the spin-Berry curvature, in the spirit of linear-response theory, is a physical property of the electron system $\hat{H}_{\text{qu}}$ only. Namely, expanding $E_i = E_{i0} + O(J)$ and $|\Psi_l\rangle = |\Psi_l^0\rangle + O(J)$ and using the identity

$$\langle \Psi_l | \partial_{S_m} \Psi_j \rangle = \frac{\langle \Psi_l | \partial_{S_m} \hat{H}(\{S\})|\Psi_j \rangle}{E_j - E_l}, \quad (34)$$

which holds for $E_j \neq E_l$, Eq. (28) can be rewritten as

$$\Omega_{k\gamma, m\beta}^{(ij)} = i \sum_{l \geqslant n} \left[\frac{\langle \Psi_i^0 | \partial_{S_{k\gamma}} \hat{H} | \Psi_l^0 \rangle \langle \Psi_l^0 | \partial_{S_{m\beta}} \hat{H} | \Psi_j^0 \rangle}{E_{i0} - E_{l0}} \frac{}{E_{j0} - E_{l0}} \right.$$
$$\left. - (k\gamma \leftrightarrow m\beta) \right] + O(J^3) \quad (35)$$

since $\partial_{S_{k\gamma}} \hat{H}_{\text{int}} = Js_{\text{i}k\gamma} = O(J)$, so that the spin-Berry curvature is of order J^2 for weak J and expressed in terms of the eigenstates and eigenenergies of $\hat{H}_{\text{qu}}$ only. Note that $0 \leqslant i, j \leqslant n-1$ in (35).

For a system with an even number of spin-$\frac{1}{2}$ electrons, the time-reversal operator squares to unity, $\Theta^2 = +1$. In this

case, we can choose an orthonormal basis of time-reversal-symmetric energy eigenstates $|\Psi_i^0\rangle = \Theta|\Psi_i^0\rangle$. This implies that the matrix elements

$$
\begin{aligned}
\langle\Psi_i^0|\partial_{S_{k\gamma}}\hat{H}|\Psi_l^0\rangle &= -\langle\Psi_i^0|\Theta^\dagger\partial_{S_{k\gamma}}\hat{H}\Theta|\Psi_l^0\rangle \\
&= -\left(\langle\Theta\Psi_i^0|\partial_{S_{k\gamma}}\hat{H}|\Theta\Psi_l^0\rangle\right)^* \\
&= -\left(\langle\Psi_i^0|\partial_{S_{k\gamma}}\hat{H}|\Psi_l^0\rangle\right)^*
\end{aligned}
\tag{36}
$$

are purely imaginary. Note that only the (odd) interaction term $\hat{H}_{\text{int}}(\{\boldsymbol{S}\})$ contributes. Using this in (35) shows that $\Omega_{k\gamma,m\beta}^{(ij)}$ is purely imaginary. With (32) we can conclude that

$$
\Omega_{k\gamma,m\beta}^{(ij)} = \Omega_{m\beta,k\gamma}^{(ji)}.
\tag{37}
$$

In particular, Eqs. (31) and (37) imply that the $i = j$ elements of the spin-Berry curvature must vanish in the weak-J limit for $\Theta^2 = +1$. This is important for the Abelian case $n = 1$. For $i = j = 0$ we have $\Omega_{k\gamma,m\beta}^{(00)} = 0$ and, hence, there is no geometrical spin torque in the weak-J limit for a time-reversal-symmetric system with $\Theta^2 = +1$. In the general non-Abelian case, on the other hand, we find with (33) that

$$
\langle\Omega\rangle_{k\gamma,m\beta} = -\sum_{ij}\text{Im}(\alpha_i^*\alpha_j)\text{Im}\Omega_{k\gamma,m\beta}^{(ij)}
\tag{38}
$$

since $\Omega_{k\gamma,m\beta}^{(ij)}$ is imaginary. Generically, the coefficients $\alpha_i = \alpha_i(t)$ in the expansion (11) will be complex and oscillatory functions of time. The expression above thus shows that even in the weak-J limit and for a time-reversal-symmetric system, the geometrical spin torque in the equation of motion (25) is generally finite.

Let us briefly discuss the case of an odd electron number with $\Theta^2 = -1$. Here, the basis states can be grouped in orthogonal and energy-degenerate Kramers pairs $\{|\Psi_i^0\rangle, |\overline{\Psi}_i^0\rangle\}$ with $|\overline{\Psi}_i^0\rangle \equiv \Theta|\Psi_i^0\rangle$ for $i = 0,\ldots,(n/2) - 1$. An even number of states must be included in formulating the constraint (11). For the matrix elements, we have

$$
\begin{aligned}
\langle\Psi_i^0|\partial_{S_{k\gamma}}\hat{H}|\Psi_l^0\rangle &= -\langle\Psi_i^0|\Theta^\dagger\partial_{S_{k\gamma}}\hat{H}\Theta|\Psi_l^0\rangle \\
&= -\left(\langle\Theta\Psi_i^0|\partial_{S_{k\gamma}}\hat{H}|\Theta\Psi_l^0\rangle\right)^* \\
&= -\left(\langle\overline{\Psi}_i^0|\partial_{S_{k\gamma}}\hat{H}|\overline{\Psi}_l^0\rangle\right)^*.
\end{aligned}
\tag{39}
$$

This can be used in (35) since in the l sum with each term also the Kramers partner is included. We find

$$
\Omega_{k\gamma,m\beta}^{(ij)} = \Omega_{m\beta,k\gamma}^{(\overline{j}\,\overline{i})},
\tag{40}
$$

where the index $\overline{i}$ refers to the Kramers partner of $|\Psi_i^0\rangle$ and, furthermore, $(\Omega_{k\gamma,m\beta}^{(ij)})^* = -\Omega_{k\gamma,m\beta}^{(\overline{i}\,\overline{j})}$. As for the case $\Theta^2 = +1$, time-reversal symmetry does not lead to a vanishing spin-Berry curvature or a vanishing expectation value $\langle\Omega\rangle_{k\gamma,m\beta}$. Note that for $\Theta^2 = -1$ the adiabatic theory is not applicable anyway (for the weak-coupling limit) since the ground state is at least twofold Kramers degenerate.

VI. GAUGE TRANSFORMATIONS

The effective Lagrangian (13) can be written in a compact form as

$$
\begin{aligned}
L_{\text{eff}} = \sum_m \boldsymbol{A}_m(\boldsymbol{S}_m)\dot{\boldsymbol{S}}_m + i\boldsymbol{\alpha}^\dagger\partial_t\boldsymbol{\alpha} \\
+ \sum_m \boldsymbol{\alpha}^\dagger[\underline{\boldsymbol{C}}_m(\{\boldsymbol{S}\})\dot{\boldsymbol{S}}_m]\boldsymbol{\alpha} - \boldsymbol{\alpha}^\dagger\underline{H}(\{\boldsymbol{S}\})\boldsymbol{\alpha},
\end{aligned}
\tag{41}
$$

where $\boldsymbol{\alpha} = (\alpha_0,\ldots,\alpha_{n-1})^T$ and where $\underline{H}$ is the Hamilton matrix with elements $H_{ij} = \langle\Psi_i|\hat{H}|\Psi_j\rangle$ and the local basis states $|\Psi_j\rangle = |\Psi_j(\{\boldsymbol{S}\})\rangle$. We consider a gauge transformation

$$
\begin{aligned}
|\Psi_j(\{\boldsymbol{S}\})\rangle &\mapsto |\Psi_j'(\{\boldsymbol{S}\})\rangle = \sum_i U_{ij}^\dagger|\Psi_i(\{\boldsymbol{S}\})\rangle, \\
\boldsymbol{\alpha} &\mapsto \boldsymbol{\alpha}' = \underline{U}\boldsymbol{\alpha},
\end{aligned}
\tag{42}
$$

where $\underline{U}$ (with elements U_{ij}) is the defining matrix representation of SU(n) on the local low-energy subspace $\mathcal{E}_n(\{\boldsymbol{S}\})$ for given spin configuration $\{\boldsymbol{S}\}$. This transformation must leave observables invariant since (42) just means a rotation of the basis in $\mathcal{E}_n(\{\boldsymbol{S}\})$, which leaves the quantum state $|\Psi\rangle = \sum_{j=0}^{n-1}\alpha_j|\Psi_j(\{\boldsymbol{S}\})\rangle$, and thus the constraint (11) invariant when rotating the expansion coefficients (the wave function) accordingly. We distinguish between global SU(n) and local SU(n) transformations. For the latter, the transformation matrix $\underline{U} = \underline{U}(\{\boldsymbol{S}\})$ is an arbitrary but smooth function of the spin configuration $\{\boldsymbol{S}\}$. The effective Lagrangian is invariant under both global and local gauge transformations.

Note that the Hamilton matrix transforms in a covariant way,

$$
\underline{H} \mapsto \underline{H}' = \underline{U}\,\underline{H}\,\underline{U}^\dagger,
\tag{43}
$$

while the Berry connection transforms covariantly under a global gauge transformation only. For a local gauge transformation we rather have

$$
\underline{\boldsymbol{C}}_m \mapsto \underline{\boldsymbol{C}}_m' = \underline{U}\,\underline{\boldsymbol{C}}_m\,\underline{U}^\dagger + i\underline{U}\partial_{S_m}\underline{U}^\dagger.
\tag{44}
$$

The non-Abelian Berry curvature, opposed to its Abelian part (21), transforms covariantly:

$$
\underline{\Omega}_{k\gamma,m\beta} \mapsto \underline{\Omega}_{k\gamma,m\beta}' = \underline{U}\,\underline{\Omega}_{k\gamma,m\beta}\,\underline{U}^\dagger,
\tag{45}
$$

so that its expectation value in the state given by the wave function α_i is invariant: $\langle\Omega'\rangle_{k\gamma,m\beta}' = \langle\Omega\rangle_{k\gamma,m\beta}$. Hence, (25) is invariant under local gauge transformations. The Schrödinger-type equation (26), on the other hand, is form invariant under local transformations, i.e.,

$$
i\partial_t\alpha_i' = \sum_j\langle\Psi_i'|(\hat{H}_{\text{qu}} + \hat{H}_{\text{int}})|\Psi_j'\rangle\alpha_j' - \sum_{mj}\dot{\boldsymbol{S}}_m\boldsymbol{C}_m^{(ij)'}\alpha_j',
\tag{46}
$$

and the spin-Berry connection term on the right-hand side is necessary to compensate the extra term appearing on the left-hand side in case of an $\{\boldsymbol{S}\}$-dependent transformation.

Concluding, the effective Lagrangian emerging in the low-energy sector of hybrid spin-electron dynamics represents a non-Abelian SU(n) gauge theory. This is reminiscent of standard quantum field theories [50], where the Lagrangian is invariant under simultaneous transformations of coupled matter and gauge fields, and where these gauge transformations involve a gauge group, like SU(n), and are local in space-time.

There are a couple of differences though: Within non-Abelian spin-dynamics theory, space-time is not only replaced by a compact parameter manifold, namely, the Cartesian product of classical Bloch spheres representing the space of the spin configurations, but furthermore the spin configurations have their own dynamics. The theory is thus much more related to gauge theories that have been devised for molecular physics [33], where the state space of the nuclei, when treated classically, defines a dynamical parameter manifold, and where the role of the gauge field is played by the non-Abelian Berry connection.

Finally, it is worth mentioning that there is a second, less important, class of gauge freedom. This concerns the vector potential $A(S_m)$ [see the first term of L in (8)], i.e., already in the *full* Lagrangian. Any transformation of the unit vector $e \mapsto e'$ leads to a transformed potential $A(S_m) \mapsto A'(S_m)$ but leaves its curl invariant. This even includes "local" m-dependent transformations $A(S_m) \mapsto A'_m(S_m)$ resulting from $e \mapsto e'_m$. However, since only the curl $\nabla_S \times A(S_m)$ enters the equations of motion resulting from the full or from the effective Lagrangian [see Eq. (20) for instance], these are invariant.

VII. MINIMAL MODEL

For a further discussion of non-Abelian spin-dynamics theory, we will present numerical results for a minimal model, which includes a few degrees of freedom only but is sufficient to illustrate several key aspects. Our intention is to show by example that and how our theoretical approach can be evaluated in practice, how the numerical results compare with the full solution of the equations of motion, and what improvements the theory offers over the purely adiabatic (Abelian) version. This may also be seen as a preparation for future applications to more realistic but also more complicated physical systems, where various secondary issues become important.

The Hamiltonian of our toy model is given by

$$\hat{H} = -T \sum_{\langle i,j \rangle, \sigma} c_{i\sigma}^\dagger c_{j\sigma} + J s_{i_0} S - B S. \tag{47}$$

It describes a single classical spin ($M = 1$) locally exchange coupled (coupling constant $J > 0$) to a noninteracting tight-binding model in an open chain geometry with a small number of sites L hosting $N = L$ electrons, i.e., a half-filled conduction-electron system. The spin is coupled to the first site of the chain $i_0 = 1$. This is the *s-d* model [18] discussed in the Introduction and the same model as in Ref. [28]. Energy and time units are fixed by setting the nearest-neighbor hopping amplitude to $T = 1$. In addition, the Hamiltonian includes a local magnetic field of strength B coupling to the classical spin S. The model is visualized in Fig. 1.

The field term is employed to initiate the real-time dynamics: At time $t = 0$ the system is prepared in the ground state of $\hat{H}$ with the field in the x direction, i.e., the spin $S = S e_x$ is aligned to $B = B e_x$, and the conduction-electron state is the ground state $|\Psi(t = 0)\rangle = |\Psi_0(S)\rangle$. Time propagation for $t > 0$ is driven by the same Hamiltonian but with the field pointing in the z direction. Dynamics is thus initiated by a sudden change of the field direction from x to z direction.
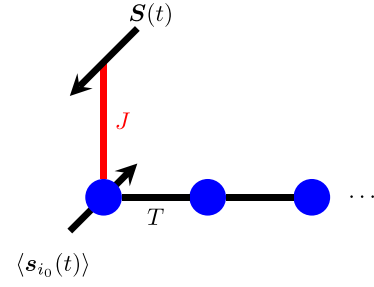

FIG. 1. Sketch of the minimal model studied numerically. A classical spin S of length $|S| = 1$ is antiferromagnetically exchange coupled with coupling strength $J > 0$ to the local spin moment s_{i_0} at the first site $i_0 = 1$ of a system of conduction electrons on a one-dimensional chain with open boundaries. T is the nearest-neighbor hopping. Real-time dynamics is initiated by a sudden change of the direction of a local magnetic field B coupled to S.

For $t > 0$ one expects that the spin starts precessing around the z axis. In the adiabatic approximation with $n = 1$, the electron system will follow the respective spin direction instantaneously, and its state at time t would be the instantaneous ground state $|\Psi_0(S(t))\rangle$. The timescale on which the precession takes place is given by the inverse of the Larmor frequency $\omega_L = B$. Depending on the field strength, this timescale $\tau_L = 1/\omega_L = 1/B$ can be much shorter than the inverse of the finite-size gap $\Delta = O(T/L)$. With $T = 1$ we thus expect that the adiabatic approximation breaks down for $B \gg T/L$ and that excited states $|\Psi_j(S)\rangle$ with $0 < j < n - 1$ will be populated. The number of states n included in the S-dependent basis controls the accuracy of the non-Abelian spin-dynamics approach.

For the single classical-spin model the effective equations of motion (25) and (26) are somewhat simplified. For $M = 1$ we can skip the m index and take the cross product with S on both sides of (25). Furthermore, we have $\langle \partial_S \hat{H}_{\text{int}} \rangle = J\langle s_{i_0} \rangle - B$ and $\partial_S H_{\text{cl}} = 0$. Therewith we get

$$\dot{S} = \frac{J\langle s_{i_0} \rangle \times S - B \times S}{1 - S\langle \Omega \rangle}, \tag{48}$$

where $\langle \Omega \rangle = \sum_{ij} \alpha_i^* \Omega^{(ij)} \alpha_j$ is the expectation value of the pseudovector $\Omega^{(ij)}$ with components $\Omega_\alpha^{(ij)} = \frac{1}{2} \sum_{\beta\gamma} \varepsilon_{\alpha\beta\gamma} \Omega_{\beta\gamma}^{(ij)}$ that can be constructed for $M = 1$ due to the antisymmetry of the Berry curvature tensor under $\beta \leftrightarrow \gamma$ for each pair (ij) [see Eq. (31)]. Furthermore, $\langle s_{i_0} \rangle = \langle s_{i_0} \rangle_t = \sum_{ij} \alpha_i^*(t) \langle \Psi_i(S(t)) | s_{i_0} | \Psi_j(S(t)) \rangle \alpha_j(t)$.

Remarkably, there is a renormalization of the precession frequency resulting from the geometrical spin torque, which has already been studied for the adiabatic case [28,35–37]. This manifests itself as an additional factor $1/(1 - S\langle \Omega \rangle)$ in (48). In the adiabatic case $n = 1$, the expectation value $\langle \Omega \rangle$ is strictly parallel or antiparallel to the classical-spin orientation due to symmetry reasons [28]. For $S \uparrow\uparrow \langle \Omega \rangle$ this results in a faster precessional dynamics, and its orientation is even reversed if $S\langle \Omega \rangle > 1$, while for $S \uparrow\downarrow \langle \Omega \rangle$ the precession is slowed down. Exactly at $S\langle \Omega \rangle = 1$ the right-hand side of (48) becomes singular. This is linked to a divergence of the precession frequency which, however, becomes relevant in an extreme case only: For the adiabatic case and $L = 1$, it was

found in Ref. [28] that singular dynamics can in principle be approached, if the length of the classical spin $|S| \rightarrow \frac{1}{2}$. At the same time, however, to stay in the adiabatic regime of the model, it was necessary to consider an ever-increasing coupling strength, i.e., $J \rightarrow \infty$.

Here, we see that the same type of singularity is in principle also present in the nonadiabatic case (for $M = 1$). Generally, however, we find $0 < S\langle \boldsymbol{\Omega} \rangle < 1$ (for antiferromagnetic exchange coupling $J > 0$): A possible singularity is regularized for $n > 1$ due to contributions from excited states and partly also due to the fact that $\langle \boldsymbol{\Omega} \rangle$ and S are no longer necessarily collinear.

The following NA-SD studies of the minimal model are based on a numerical solution of the coupled effective equations of motion (48) for the classical spin S and (26) for the wave function $\{\alpha\}$. For the computation of the expectation value of the spin-Berry curvature $\langle \boldsymbol{\Omega} \rangle$ we profit from simplifications, which hold in case of a noninteracting conduction-electron system. These are detailed in Appendix D.

We also compare the results of the NA-SD theory with the *full* solution of the fundamental equations of motion (5) and (6), which is obtained independently. More explicitly, Eq. (5) for the minimal model reads as

$$\dot{S} = J\langle \boldsymbol{s}_{i_0} \rangle_t \times S - B \times S. \tag{49}$$

Furthermore, in case of a noninteracting electron system, Eq. (6) can be replaced by the equation of motion

$$i\frac{d}{dt}\underline{\rho} = [\underline{T}^{(\text{eff})}, \underline{\rho}] \tag{50}$$

for the one-particle reduced density matrix $\underline{\rho}$ with elements $\rho_{ii'\sigma\sigma'}(t) = \langle c_{i'\sigma'}^{\dagger} c_{i\sigma} \rangle$, and where the elements of the effective hopping matrix $\underline{T}^{(\text{eff})}$ are given by

$$T_{ii'\sigma\sigma'}^{(\text{eff})} = T\delta_{\langle ii' \rangle}\delta_{\sigma\sigma'} + \frac{J}{2}\boldsymbol{\sigma}_{\sigma\sigma'} S \, \delta_{ii_0}\delta_{i'i_0}. \tag{51}$$

VIII. NUMERICAL RESULTS

A. Full theory

The precession around the z axis defined by the local magnetic field is expected to be the dominant effect in the classical-spin dynamics. In fact, this is the main phenomenon found by solving the full set of equations of motion (49) and (50). Figure 2 displays numerical results obtained with the full theory for a system with $L = 10$ sites at half-filling $N = L$, and for generic parameter values $J = 1$ and $B = 0.1$. The x component of the classical spin undergoes a quite regular oscillation with a period close to $2\pi/\omega_{\text{L}} = 2\pi/B \approx 62.8$. The y component exhibits the same but phase-shifted dynamics. We note that, for the selected parameter set, the geometrical spin torque is too small to produce a sizable renormalization of the precession frequency.

Damping of the spin dynamics and eventual alignment of the classical spin with the field $\boldsymbol{B} = B\boldsymbol{e}_z$ is typically a weaker effect, which takes place on a much longer timescale (see, e.g., the discussion in Refs. [10,15,16]). For a closed, finite and with $L = 10$ small system, as considered here, relaxation will be imperfect anyway, and even in the long-time limit, the
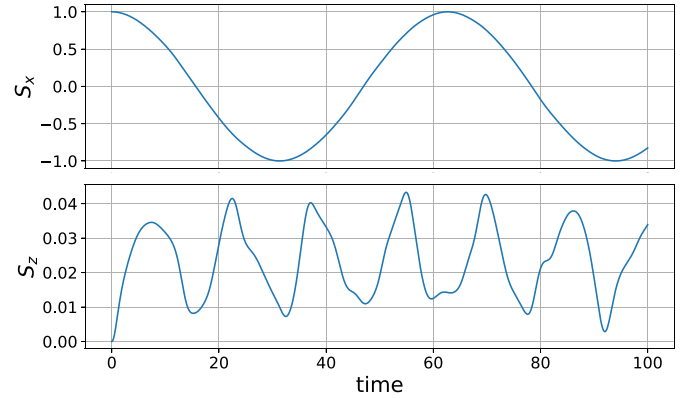

FIG. 2. Time evolution of the x and the z components of the classical spin as obtained from the full theory for a system with $L = 10$ sites at half-filling $N = L$. Parameters: $J = 1$, $B = 0.1$. The energy and time units are set by fixing the nearest-neighbor hopping at $T = 1$.

system cannot fully approach its ground state locally, in the vicinity of i_0. Uncovering this type of relaxation dynamics requires much larger systems, as discussed in Refs. [51,52], for example.

Figure 2 also displays the z component of the spin. In case of a perfect precessional motion, one would expect a constant S_z. As is seen in the figure, however, an almost oscillatory motion of S_z with some additional irregularities is found instead. This nutation of the spin is reminiscent of gyroscope theory [11,12], but is not understood easily. An explanation in terms of linear-response theory [see Eq. (1)], i.e., Redfield theory for open quantum systems, involves the second-order term in the Taylor expansion of the memory kernel [15,27]. For the parameters considered here, the nutation effect is at least an order of magnitude smaller as compared to the precessional dynamics (see Fig. 2). There are cases, however, where precessional and nutational oscillations can be of the same order of magnitude. The additional "irregularities" on top of the nutation are even more subtle. At this level of resolution at the latest, the complexity of the dynamics caused by the nonlinearity of the quantum-classical equations of motion appears to prohibit a simple explanation.

B. Anomalous precession

In the case of strong exchange coupling $J \gg T$, the classical spin S and the local magnetic moment $\langle \boldsymbol{s}_{i_0} \rangle$ at i_0 are tightly bound together. In this regime one would thus expect that $\langle \boldsymbol{s}_{i_0} \rangle$ follows the classical-spin direction almost instantaneously such that $\langle \boldsymbol{s}_{i_0} \rangle$ is almost perfectly aligned antiferromagnetically to S. The time evolution of the angle enclosed by S and $\langle \boldsymbol{s}_{i_0} \rangle$ is shown in Fig. 3. For $J = 1$ the mean deviation of the angle from $180°$ is in fact about $2°$ only, and it shrinks with increasing J (see the result for $J = 15$). On the other hand, the absolute value of the local moment $\langle \boldsymbol{s}_{i_0} \rangle$ of the conduction-electron systems that is induced by S, increases from $|\langle \boldsymbol{s}_{i_0} \rangle| \approx 0.18$ at $J = 1$ to $|\langle \boldsymbol{s}_{i_0} \rangle| \approx 0.49$ at $J = 15$. The net effect, however, is that the spin torque on S originating from the exchange term $J\langle \boldsymbol{s}_{i_0} \rangle \times S$ is weak compared to the torque due to the field $-\boldsymbol{B} \times S$. Following naive adiabatic
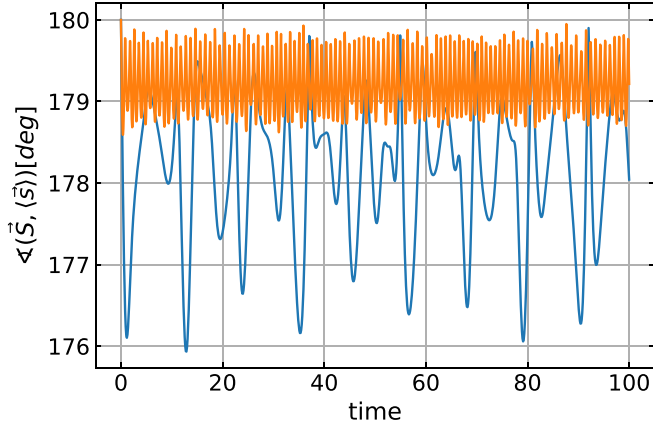
FIG. 3. Time evolution of the angle enclosed by the classical spin S and the expectation value of the local spin of the electron system at the impurity site $\langle s_{i_0} \rangle$. Results as obtained by the full theory for $J = 1$ (blue) and $J = 15$ (orange). Other parameters as in Fig. 2.

theory one would therefore expect a precessional motion of S in the x-y plane with a frequency ω_p close to the Larmor frequency $\omega_L = B$. However, this naive picture in principle disregards the effect due to the geometrical spin torque, which can be sizable. It is thus instructive to compare the naive expectation as well as adiabatic spin-dynamics (ASD) theory with the full solution of the fundamental equations of motion.

Numerical results for a strong coupling $J = 15$ are displayed in Fig. 4. The full theory (see red curve) does predict an oscillatory motion of S_x as expected for precessional dynamics. However, the precession is not perfect: Note, e.g., that S_x does not reach its minimum value $S_x = -1$, while $S_x \approx +1$ after a full period. In fact, the precession does not take place in the x-y plane but within a plane that is a somewhat tilted and, furthermore, the plane normal $n \propto S \times \dot{S}$ is slightly time dependent.

The most important effect seen in Fig. 4, however, is the strongly enhanced precession frequency $\omega_p \approx 0.19$, which is close to *twice* the Larmor frequency $\omega_L = B = 0.1$. This anomalous precession frequency ω_p is clearly at variance with the naive expectation and must therefore result from the
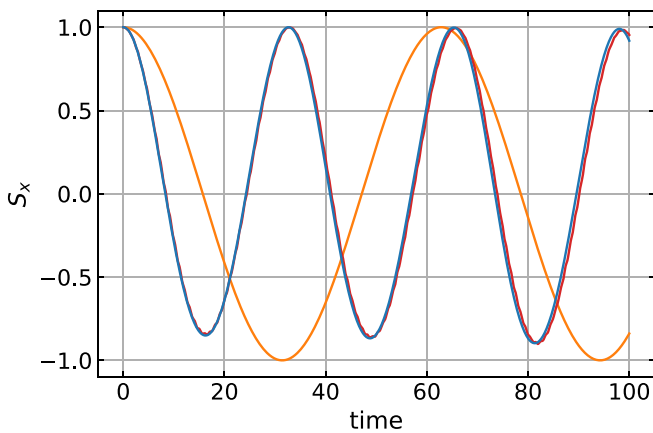

FIG. 4. Time dependence of the x component of the classical spin for $L = 10$, $J = 15$, $T = 1$, $B = 0.1$. Results as obtained from ASD ($n = 1$, orange), NA-SD with $n = 2$ (blue), and the full theory (red).
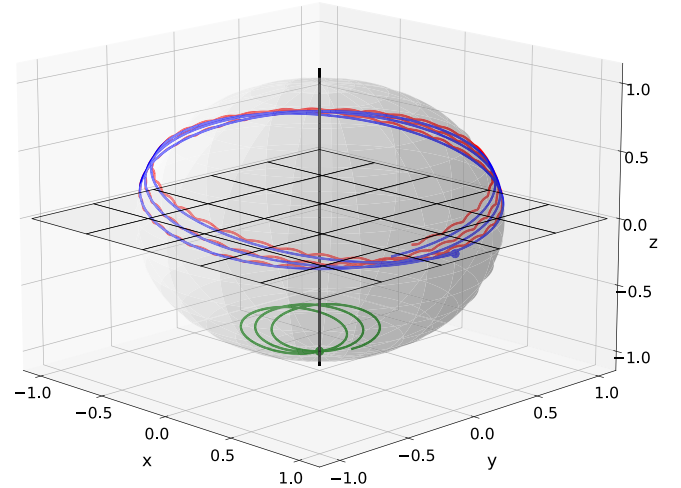

FIG. 5. The same as in Fig. 4 for the NA-SD (blue curve) and the full theory (red) but displayed on a classical Bloch sphere. The blue dot marks the spin position at time $t = 0$. Green curve: unit vector n normal to the instantaneous precession plane. The trajectories are shown for $0 \leqslant t \leqslant 100$.

renormalization factor $1/(1 - S\langle \mathbf{\Omega} \rangle)$ in (48). In fact, the full theory (red) almost perfectly agrees with the prediction of the non-Abelian spin-dynamics (NA-SD) theory (blue), when spanning the low-energy subspace $\mathcal{E}_n(\{S\})$ by the instantaneous ground and first excited states, i.e., for $n = 2$.

Figure 5 presents the same results of the NA-SD (blue curve) and the full theory (red) in a classical Bloch-sphere representation. At $t = 0$, the motion of S starts at $S = (1, 0, 0)$ (see blue dot) and completes about three full periods up to the maximum propagation time $t = 100$. The dynamics is close to a planar precession but the instantaneous plane normal n (green curve) exhibits a weak time dependence and precesses itself around an axis that is somewhat tilted against the z axis. The full theory exhibits some additional wiggles which can also be seen in Fig. 4 already and which are absent in the NA-SD. A low-energy subspace with more than $n = 2$ dimensions would be necessary to capture this effect. Apart from that, however, there is an almost perfect agreement of the NA-SD results with the results of the full theory.

While this is very satisfying and underpins the construction of the NA-SD, there is an interesting problem remaining: Comparing with the $n = 1$ theory, i.e., with ASD, there is strong discrepancy. ASD (see orange curve in Fig. 4) does in fact yield the same result as the naive adiabatic picture for the present setup since the ($n = 1$) spin-Berry curvature vanishes identically: $\mathbf{\Omega} = 0$. This has been noted in Ref. [28] already, and the anomalous precession frequency has been explained by referring to an effective two-spin model $H_{\text{two-spin}} = J s_{i_0} S - B S$ which disregards the presence of the sites $i \neq i_0$, which can be argued to be justified in the strong-J regime. The two-spin model indeed predicts $\mathbf{\Omega} = \frac{1}{2} S$, so that the renormalization factor $1/(1 - \mathbf{\Omega} S) = 2$, which is in reasonable agreement with the results of the full theory.

The remaining problem is to clarify why, for the full model (47), the $n = 1$ spin-Berry curvature vanishes. One should note that there is actually an odd-even effect. For an odd

number of sites L, the spin-Berry curvature is in fact finite, and the agreement with the full theory is satisfying already at the $n = 1$ level, while extending the effective theory to $n = 2$ yields smaller corrections only.

The odd-even effect can in fact be explained by a combination of time-reversal symmetry and the fact that a local spin-dependent perturbation applied to a nonmagnetic ground state cannot induce a finite spin polarization in one dimension. For $J = 0$, the ground state $|\Psi_0\rangle$ of a spin SU(2)-symmetric tight-binding model is a total-spin singlet. For $J > 0$, we have $|\Psi_0\rangle = |\Psi_0(\boldsymbol{S})\rangle$, where the $\boldsymbol{S}$ dependence is induced by the local perturbation $J\boldsymbol{S}\boldsymbol{s}_{i_0}$. Assuming, without loss of generality, that $\boldsymbol{S} = S\boldsymbol{e}_z$, it is given by a Slater determinant of the form $|\Psi_0(\boldsymbol{S})\rangle = \prod_k \prod_{k'} c_{k\uparrow}^\dagger c_{k'\downarrow}^\dagger |\mathrm{vac}\rangle$, where k, k' refer to the occupied spin-$\uparrow$ and spin-$\downarrow$ eigenstates of the full Hamiltonian, including the perturbation, with eigenenergies $\varepsilon_\uparrow(k)$ and $\varepsilon_\downarrow(k')$, respectively.

For a one-dimensional particle-hole-symmetric tight-binding model at half-filling, a local spin-dependent but spin-diagonal perturbation $J S_z s_{i_0 z}$ does not change the number of $\uparrow$ and of $\downarrow$ eigenstates with eigenenergies $\varepsilon_\uparrow(k)$, $\varepsilon_\downarrow(k) < 0$, for arbitrary coupling strength J [53]. This implies that for even L and at half-filling $N = L$, we must have $N_\uparrow = N_\downarrow = N/2$. Consequently, the number of factors in the Slater determinant, labeled by k and k', is the same, and thus $|\Psi_0(\boldsymbol{S})\rangle$ is still a total-spin singlet (constructed from $\boldsymbol{S}$-dependent one-particle states), irrespective of the strength of the perturbation J. This argument holds for any direction of $\boldsymbol{S}$ and thus implies that $\Theta|\Psi_0(\boldsymbol{S})\rangle = |\Psi_0(\boldsymbol{S})\rangle$, i.e., the ground state is invariant under time reversal Θ for all $\boldsymbol{S}$. Hence, the same holds for its $\boldsymbol{S}$ derivative: $\Theta|\partial_{\boldsymbol{S}}\Psi_0(\boldsymbol{S})\rangle = |\partial_{\boldsymbol{S}}\Psi_0(\boldsymbol{S})\rangle$. Some details on the invariance under time reversal are given in Appendix E.

Specializing (28) to the adiabatic case $n = 1$ we thus have $\boldsymbol{\Omega} = \frac{1}{2} \sum_{\alpha\beta\gamma} \varepsilon_{\alpha\beta\gamma} \boldsymbol{e}_\alpha \Omega_{\beta\gamma}$ with

$$
\begin{aligned}
\Omega_{\beta\gamma} &= i[\langle \partial_{S_\beta} \Psi_0 | | \partial_{S_\gamma} \Psi_0 \rangle - (\beta \leftrightarrow \gamma)] \\
&= -2\,\mathrm{Im}\langle \partial_{S_\beta} \Psi_0 | | \partial_{S_\gamma} \Psi_0 \rangle \\
&= -2\,\mathrm{Im}\langle \partial_{S_\beta} \Psi_0 | \Theta^\dagger \Theta | \partial_{S_\gamma} \Psi_0 \rangle^* \\
&= -2\,\mathrm{Im}\langle \partial_{S_\beta} \Psi_0 | | \partial_{S_\gamma} \Psi_0 \rangle^* = 0, \quad (52)
\end{aligned}
$$

where we have exploited the antiunitarity of Θ. In an extension of the discussion of Sec. V for the weak-J case, we can thus infer that the Abelian spin-Berry curvature must vanish for even L and arbitrary J in one dimension. Let us emphasize that the argument cannot be transferred to the non-Abelian case. For $n > 1$, we have $\langle \boldsymbol{\Omega} \rangle \neq 0$ in general.

C. Nutation

Apart from the precessional motion, the classical-spin dynamics also exhibits nutational oscillations with a frequency that is in general different from the precession frequency. The nutation is most easily seen in an oscillatory behavior of the z component of the classical spin: The field points into the z direction, $\boldsymbol{B} = B\boldsymbol{e}_z$, such that the z component of the torque on $\boldsymbol{S}$ due to the field must vanish $(\boldsymbol{B} \times \boldsymbol{S})_z = 0$. A nonzero time derivative $\dot{S}_z \neq 0$ is, therefore, solely due to the exchange coupling and directly proportional to $J(\langle \boldsymbol{s}_{i_0} \rangle \times \boldsymbol{S})_z$.

As such, a nutational motion cannot be captured by $n = 1$ adiabatic spin-dynamics (ASD) theory: The adiabatic con-
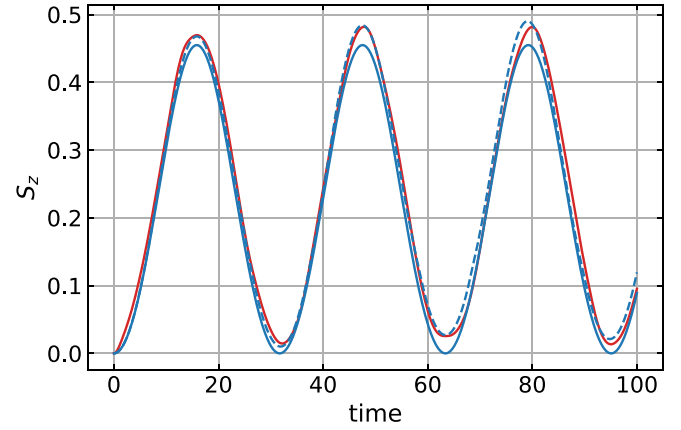

FIG. 6. Time dependence of the z component of the classical spin as obtained from $n = 2$ (solid blue curve) and from $n = 4$ (dashed blue curve) NA-SD, compared to the result (red curve) of the full theory. $L = 11$, $J = 1$, $B = 0.1$.

straint and a simple symmetry argument immediately imply that the ground-state local moment $\langle \boldsymbol{s}_{i_0} \rangle = \langle \Psi_0(\boldsymbol{S})|\boldsymbol{s}_{i_0}|\Psi_0(\boldsymbol{S})\rangle$ must be strictly antiparallel (for $J > 0$) to $\boldsymbol{S}$, which in turn implies that S_z is a constant of motion. The adiabatic spin dynamics is thus perfectly precessional albeit, opposed to naive adiabatic theory, with a renormalized precession frequency, as already discussed above.

Numerical results for $L = 11$ as obtained from non-Abelian spin-dynamics theory with $n = 2$ [see Fig. 6 (blue curve)] show that there can be a considerable variation of the amplitude of the z component of $\boldsymbol{S}$. The nutational oscillation is perfectly harmonic and S_z stays non-negative, when starting with $S_z = 0$ at $t = 0$. As compared with the S_z dynamics predicted by the full theory (red curve), the step from $n = 1$ (ASD) to $n = 2$ (most simple variant of NA-SD) is in fact the essential one, and the results for $n = 2$ are already close to those of the full theory. The latter, however, predicts a slight deviation from perfectly harmonic nutational motion, which is not reproduced with $n = 2$ but can be captured with an improved ($n = 4$) approximation within the NA-SD (dashed blue curve). A further increase of n becomes technically more and more involved and has also been found to improve the results in a nonmonotonic way only. It is thus very fortunate that the main improvement of the $n = 1$ ASD is already achieved with $n = 2$ NA-SD. For the rest of the discussion, we will therefore stick to the $n = 2$ case.

The physical cause of the nutation can be traced back to the time-dependent admixture of the first excited state $|\Psi_1(\boldsymbol{S}(t))\rangle$ to the instantaneous ground state $|\Psi_0(\boldsymbol{S}(t))\rangle$. Figure 7 for $J = 1$ (blue curve) displays the absolute square of the ground-state coefficient $|\alpha_0|^2$ as function of propagation time corresponding to the $n = 2$ NA-SD result for S_z in Fig. 6. Note that we have $|\alpha_1|^2 = 1 - |\alpha_0|^2$ for $n = 2$. As for $t = 0$ the conduction-electron system is prepared as the ground state of $\hat{H}$, the ground-state weight $|\alpha_0|^2 = 1$ initially. In the course of time, there is a weight transfer to the first excited state, which results in a significant reduction of the ground-state weight down to a minimal value of $|\alpha_0|^2 \approx 0.72$. Within the $n = 2$ NA-SD, the time-dependent weight transfer is
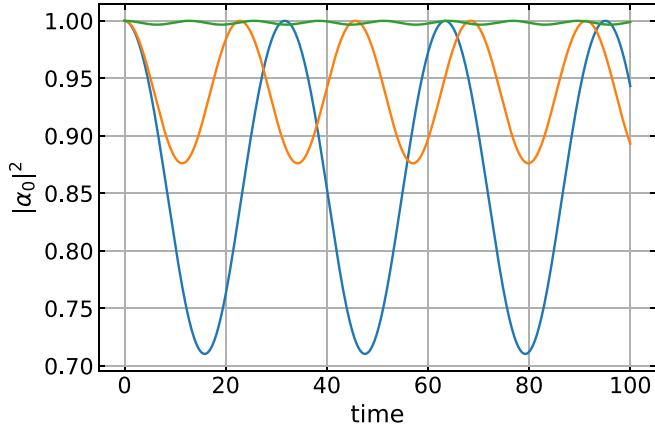
FIG. 7. Time dependence of the ground-state weight $|\alpha_0|^2$ as obtained from NA-SD with $n = 2$ for a system with $L = 11$, for $B = 0.1$, and for various coupling strengths $J = 1$ (blue), $J = 2$ (orange), and $J = 10$ (green).

FIG. 9. The same as Fig. 7 but for $L = 10$. Note that the same color coding is used. Coupling strengths: $J = 1$ (blue), $J = 2$ (orange), and $J = 10$ (green).

perfectly harmonic, and its frequency is exactly the same as the nutation frequency of S_z (see Fig. 6).

Increasing the coupling strength J results in a weaker admixture of the first excited state, as can be seen by the results for $J = 2$ (orange) and $J = 10$ (green) in Fig. 7. This is accompanied by an increasing frequency of the time-dependent weight transfer. Again, this frequency is precisely the nutation frequency that is observed in the time dependence of S_z, which is displayed in Fig. 8 for the different coupling strengths. We also note that this is unrelated with the precession frequency which is much less J dependent. Furthermore, also the J dependence of the minimal (maximal) amplitude shows the same trend for both the ground-state weight and for S_z, respectively.

Compared to the standard perturbative linear-response approach discussed in the Introduction, our approach thus provides an alternative explanation of nutational spin dynamics. As in the standard theory, nutation is the first phenomenon that is found in a systematic expansion starting around the adiabatic limit, namely, Taylor expansion in the retardation time on the one hand and expansion in the dimension of
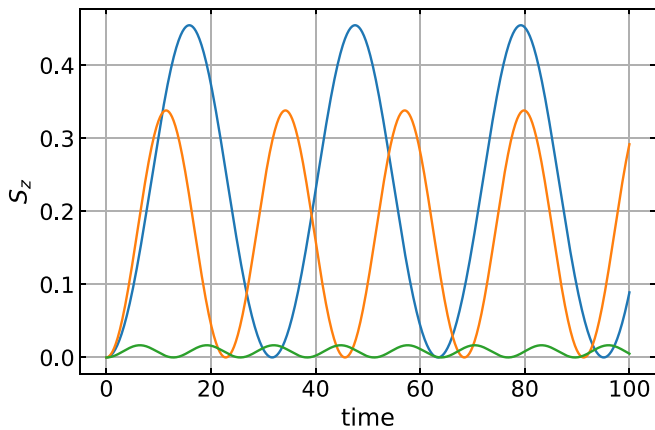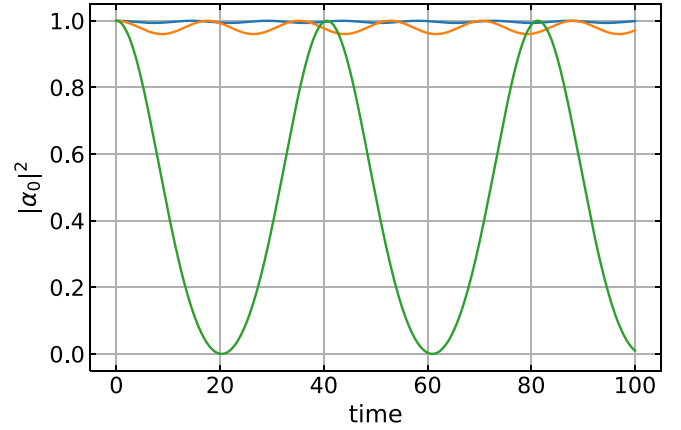
the instantaneous low-energy subspace on the other. Another important difference is that the NA-SD is formulated for a closed system while the standard theory relies on a formalism for open quantum systems. This also explains that the standard approach necessarily predicts nonconserving Gilbert damping accompanying the nutational motion.

The time dependence of the weight $|\alpha_0|^2$, as shown in Figs. 7 and 9, is reminiscent of the Rabi oscillations of the ground-state occupation in a simple two-level system driven by an oscillatory time-dependent external field. In our case the driving is due to the classical spin which is precessing around the axis of the magnetic field. However, the case is more complicated. Opposed to the standard Rabi setup [54], the "two-level system" emerging in the ($n = 2$) NA-SD is itself time dependent, has a feedback on the classical spin induced by the spin-Berry curvature via the geometrical torque, and **S** couples locally rather than globally to a time-dependent and in general only partially polarized local magnetic moment.

Let us return to the results for the ground-state weight for $L = 11$ shown in Fig. 7. It is tempting to interpret the decrease of the amplitude of the oscillations of $|\alpha_0|^2$ with

FIG. 8. The same as Fig. 7 but for the time dependence of S_z. Coupling strengths: $J = 1$ (blue), $J = 2$ (orange), and $J = 10$ (green).
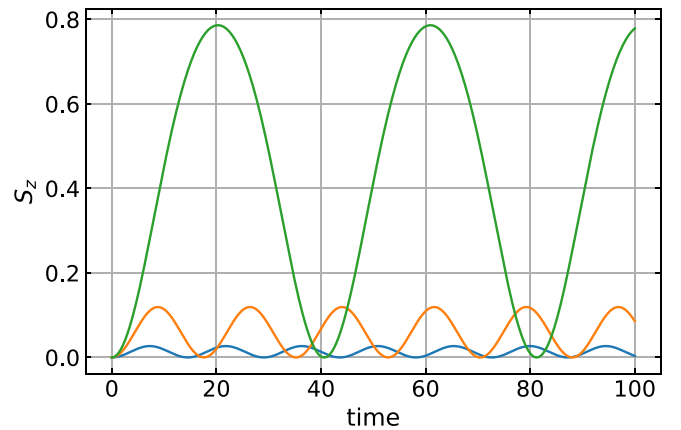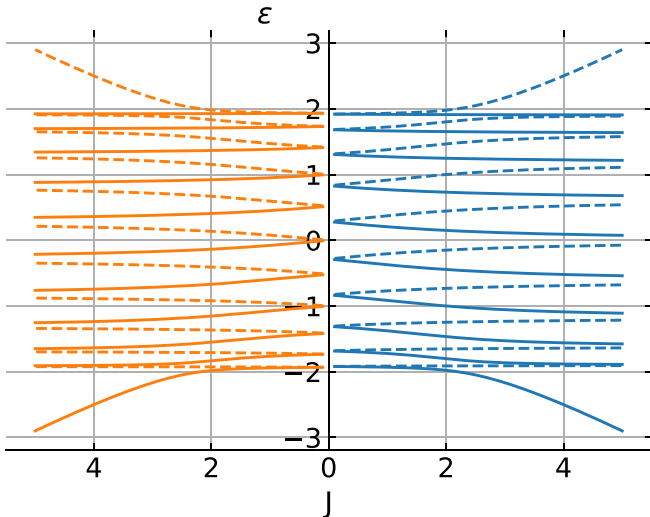

FIG. 10. The same as Fig. 9 but for the time dependence of S_z. Coupling strengths: $J = 1$ (blue), $J = 2$ (orange), and $J = 10$ (green).

FIG. 11. J dependence of the single-particle eigenenergies for $L = 10$ (right) and $L = 11$ (left). $B = 0.1$.

FIG. 12. The finite-size energy gap ΔE between the ground state and the first excited state as function of J for $L = 10$ (blue) and $L = 11$ (orange). $B = 0.1$.

increasing J as a consequence of approaching the adiabatic limit, where $|\alpha_0|^2 = 1$. In fact, this trend is consistent with the time-averaged angle enclosed by $\boldsymbol{S}$ and $\langle \boldsymbol{s}_{i_0} \rangle$ approaching $180°$ with increasing J (see Fig. 3). However, for a tight-binding chain with an even number of sites ($L = 10$), see the data in Fig. 9, we find that the oscillation amplitude of $|\alpha_0|^2$ grows with increasing J. We conclude that there is an odd-even effect not only with respect to the precessional, but also to the nutational dynamics. This odd-even effect is also obvious from the comparison of Figs. 8 and 10.

For an explanation of the effect, we consider the $2L$ single-particle eigenenergies ε_k of the minimal model (47). Their J dependence is shown in Fig. 11 for $L = 10$ (right, blue lines) and $L = 11$ (left, orange lines). Only at $J = 0$ are the eigenenergies spin degenerate, any finite $J > 0$ immediately lifts this degeneracy. Consistent with analytical results available for tridiagonal pseudo-Toeplitz matrices [53], we find that the $\varepsilon_k(J)$ curves do not intersect and that a finite "critical" coupling $J \approx 2$ is necessary to split off a pair of bound states, localized in the vicinity of i_0, from the "continuum" of delocalized states. Importantly, however, we note that the finite-size gap ΔE between the highest occupied and the lowest unoccupied eigenenergy, right below and right above $\varepsilon = 0$, respectively, shows opposite trends for $L = 10$ and 11.

The J dependence of the gap is displayed in Fig. 12. We note that ΔE monotonically shrinks with J for $L = 10$ (blue lines) and grows with J for $L = 11$. This is also characteristic in general, for systems with an even and odd number of sites, respectively. According to the adiabatic theorem [54], the real-time dynamics is close to adiabatic if the gap size is large compared to the inverse τ^{-1} of the typical timescale τ. Here, this can be estimated as given by $\tau^{-1} \sim B = 0.1$. For the case $L = 11$, this indeed implies that the adiabatic limit is approached with increasing J, while for $L = 10$ a decreasing J favors adiabatic dynamics. This also explains the different J dependence of the amplitudes of the nutational oscillations of S_z shown in Figs. 8 and 10, respectively.
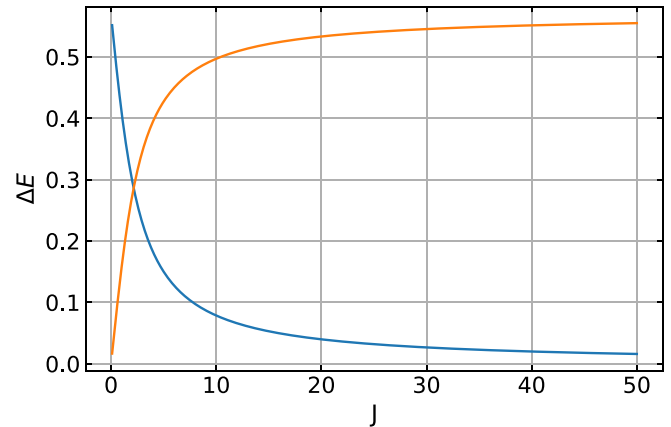
IX. CONCLUDING DISCUSSION

Systems of a single or a few quantum spins coupled to an extended lattice fermion model pose notoriously difficult quantum many-body problems. Here, by treating the impurity spins as classical objects with a dynamics that is slow as compared to the typical electronic timescales, we have concentrated on a simplified case with the ambition to exactly trace out the high-energy scales and to arrive at an effective low-energy theory that, apart from the classical spins, includes a minimal number of electronic degrees of freedom. Our approach in fact represents a systematic extension of the previously proposed adiabatic spin-dynamics (ASD) theory [28], where unconventional spin dynamics was observed to result from a geometrical spin torque.

For systems where the typical spin-dynamics timescale is much slower than the timescale of the electron dynamics, the adiabatic theorem, in case of gapped systems, tells us that the electron state at an instant of time t is the ground state of the electronic Hamiltonian for the given spin configuration at t. Alternatively and more generally, one may argue that adiabatic dynamics is due to fast electronic relaxation processes dissipating the excess energy to the bulk of the system or to external baths. These standard arguments and more explicit criteria, which typically motivate a purely adiabatic theory, are rarely controllable and hardly ever fully met in applications to realistic systems. In most practical cases, it is *a priori* extremely difficult to decide whether or not the dynamics is adiabatic. Our approach therefore aims at a straightforward way to improve the adiabatic spin-dynamics theory in an, at least in principle, systematic manner.

As the central and sole approximation we assume that the electronic state at any instant of time t lies in the n-dimensional low-energy sector spanned by the instantaneous ground state, realized for the classical-spin configuration at time t, and the corresponding lowest $n - 1$ instantaneous excited states of the electron system. The approximation is implemented as a holonomic constraint within a Lagrange formalism. We have seen that the effective low-energy theory unfolds itself straightforwardly and naturally takes the form of a non-Abelian gauge

theory, where the non-Abelian spin-Berry connection and spin-Berry curvature enter the resulting effective equations of motion for the electronic state and for the spins. The gauge freedom is given by the arbitrary choice of an orthonormal basis in the instantaneous low-energy subspace of the electron system. $SU(n)$ gauge transformations leave observables invariant. The number n of states considered in the non-Abelian spin dynamics (NA-SD) theory can be seen as a control parameter, so that comparing results for different n allows us to check the validity of the approach, at least in principle.

The physically interesting point of the emergent low-energy theory is that the spin dynamics is crucially affected by the gauge-invariant expectation value of the (gauge-covariant) spin-Berry curvature, i.e., by an additional geometrical spin torque. In the ASD ($n = 1$) a nonzero spin-Berry curvature is obtained for systems with broken time-reversal symmetry only. Opposed to ASD ($n = 1$), however, the non-Abelian spin dynamics (NA-SD) theory incorporates a spin-Berry curvature tensor, the elements of which are generically nonzero even in the more common time-reversal-symmetric case and both for the antiunitary time-reversal operator squaring to $+1$ and to -1. The NA-SD formalism also provides an elegant and straightforward explanation for the odd-even effect observed as function of the system size in the simpler ASD [28].

Applications of the NA-SD theory are promising in cases, where (i) the classical-spin approximation is reasonable, e.g., for magnetic atoms with high-spin quantum numbers or, more generally, with well-developed local magnetic moments, which are stable on timescales exceeding all other relevant timescales of the full system. This excludes, e.g., Kondo systems with a fast screening of the local moment. Strong magnetic anisotropies at surfaces or interfaces, on the other hand, can favor extremely stable magnetic moments with respect to both longitudinal and transversal spin fluctuations [55].

(ii) As regards the electron system, the amount of energy pumped in with the initial excitation must be small compared to the lowest electron excitation energies, such that a low-dimensional instantaneous low-energy subspace can fully capture the essential dynamics. Such situations could be realized in case of magnetic atoms coupled to tight-binding systems with essentially a finite number of orbitals, e.g., to metallic nanoislands supported by an insulating substrate [55] or in nanowires [35], for example. Correlated molecular magnetic systems are interesting as well, particularly in cases with a degenerate ground-state manifold (see Ref. [56] for an instructive example), which naturally defines the low-energy subspace. In case of formally infinite, e.g., condensed-matter systems, NA-SD may be applicable whenever there is a low-energy sector with a finite gap to excited states at higher energies, such as insulating systems with a symmetry-induced degenerate ground state. Topological insulators with gapless edge modes, e.g., Chern or Z_2 insulators, represent another class of systems which are worth to be considered, and the study of the relation between different Berry curvatures, the spin-Berry curvature considered here and the conventional

Berry curvature of topological band theory is expected to be particularly instructive. The real-time dynamics of classical spins coupled to the edge of a one-dimensional spinful Su-Schrieffer-Heger model [52] and to a two-dimensional spinful Kane-Mele model [57] have been discussed recently. In the former case, the low-energy subspace (at one edge) is spanned by two quantum states only. For the Z_2 Kane-Mele nanoribbon, the helical edge modes form a continuum but with an extremely small phase space for spin excitations, which suggests that considering a finite number of basis states for the low-energy sector could be a reasonably good approximation.

For classical spins coupled to gapless metallic bulk systems, any low-energy sector is formally infinite dimensional. While the adiabatic theorem does not apply to this case, one still expects that a low-energy subspace defined by a certain maximum excitation energy ΔE above the many-electron ground state could reliably capture the electron dynamics, depending on the initial excitation energy pumped into the system. If the electron system may be treated in the independent-electron approximation, the application of NA-SD is well conceivable since it merely involves diagonalization of the single-electron hopping matrix and computation of matrix elements of two-electron operators with two-electron and two-hole excited states above the Fermi sea (see Appendix D). By varying ΔE, the reliability of the approximation can be tested.

Here, as a proof of principle, we performed numerical calculations for a minimal but nontrivial model consisting of a single impurity spin coupled to the first site of a one-dimensional noninteracting tight-binding model with a small number of L sites. The real-time dynamics is initiated by a sudden change of the direction of a local magnetic field coupled to the impurity spin only. Results obtained from ASD ($n = 1$) and NA-SD (for $n = 2$ and 4) have been checked against results obtained from the numerical solution of the full, unconstrained set of equations of motion for the coupled spin-electron system. We find that the NA-SD reproduces the anomalous precession frequency that is already predicted by ASD for systems with an odd number of sites L. For even L, NA-SD correctly predicts anomalous precession, which is absent in the purely adiabatic approach. This deficiency of the ASD can be explained by a symmetry analysis. Depending on the coupling strength J, the dynamics of the impurity spin can exhibit a considerable nutational motion. As judged by comparison with the full theory, this more subtle effect is almost quantitatively covered with NA-SD for $n = 2$. NA-SD calculations for $n = 4$ show an even closer agreement with the full theory.

APPENDIX A: EXPLICIT FORM OF THE EQUATIONS OF MOTION FOR THE CLASSICAL SPINS

The equations of motion (25) for the classical spins derived in Sec. III are implicit differential equations. An explicit form, however, is more convenient for the numerical evaluation. Here, we briefly discuss a corresponding reformulation. We start with (25) and apply $\times \boldsymbol{S}_m$ from the right. This yields

$$\dot{\boldsymbol{S}}_m = \langle \partial_{\boldsymbol{S}_m} \hat{H}_{\text{int}} \rangle \times \boldsymbol{S}_m + \partial_{\boldsymbol{S}_m} H_{\text{cl}} \times \boldsymbol{S}_m + \sum_\delta \sum_{k\gamma} \left(\sum_{\alpha\beta} \varepsilon_{\alpha\beta\delta} S_{m\beta} \langle \Omega \rangle_{k\gamma,m\alpha} \right) \dot{S}_{k\gamma} \boldsymbol{e}_\delta. \tag{A1}$$

Next, we combine the components of all M spins in a single $3M$-dimensional column,

$$\boldsymbol{\mathcal{S}} := (\boldsymbol{S}_1, \boldsymbol{S}_2, \dots)^T = \sum_{m=1}^M \boldsymbol{e}_m^M \otimes \boldsymbol{S}_m. \tag{A2}$$

Here $\boldsymbol{e}_m^M$ is the mth canonical M-dimensional unit vector and $\otimes$ denotes the Kronecker product. Writing $\chi_{m\delta,k\gamma} = \sum_{\alpha\beta} \varepsilon_{\alpha\beta\delta} S_{m\beta} \langle \Omega \rangle_{k\gamma,m\alpha}$ for short, the last term on the right-hand side of (A1) can be written as $\sum_\delta (\underline{\chi} \dot{\boldsymbol{\mathcal{S}}})_{m\delta} \boldsymbol{e}_\delta$, and we find the explicit form of the $3M$-dimensional system of differential equations of motion:

$$\dot{\boldsymbol{\mathcal{S}}} = (\mathbb{1} - \underline{\chi})^{-1} \left(\sum_m \boldsymbol{e}_m^M \otimes \left(\langle \partial_{\boldsymbol{S}_m} \hat{H}_{\text{int}} \rangle \times \boldsymbol{S}_m + \partial_{\boldsymbol{S}_m} H_{\text{cl}} \times \boldsymbol{S}_m \right) \right). \tag{A3}$$

This involves an inversion of the $3M$-dimensional matrix $\mathbb{1} - \underline{\chi}$.

APPENDIX B: NORMALIZATION CONDITIONS

The equations of motion (25) and (26) respect the normalization conditions (27). We start with the wave-function normalization. Equation (26) implies

$$i \sum_i \alpha_i^* (\partial_t \alpha_i) = \sum_{ij} \alpha_i^* \alpha_j \langle \Psi_i | \hat{H} | \Psi_j \rangle - i \sum_{ij} \alpha_i^* \alpha_j \langle \Psi_i | \partial_t | \Psi_j \rangle = -i \sum_i (\partial_t \alpha_i^*) \alpha_i. \tag{B1}$$

This yields $\partial_t \sum_i |\alpha_i|^2 = 0$ as required. Conservation of the length of the classical spins can be verified directly from their equations of motion (25) or, more conveniently, by taking the scalar product of both sides of (A1) with $\boldsymbol{S}_m$. This yields $\boldsymbol{S}_m \dot{\boldsymbol{S}}_m = 0$ as required. However, conservation of the spin length has been exploited already in deriving (25), directly after (20).

Alternatively, we may thus explicitly take care of the normalization conditions $\boldsymbol{S}_m^2 = 1$ by treating them as additional constraints when deriving the equations of motion from the Lagrangian (13). This is done with M Lagrange multipliers λ_m, i.e., we replace the Lagrangian by

$$L'_{\text{eff}}(\{\boldsymbol{S}\}, \{\dot{\boldsymbol{S}}\}, \{\alpha\}, \{\alpha^*\}, \{\dot{\alpha}\}, \{\dot{\alpha}^*\}, \{\lambda\}) = L_{\text{eff}}(\{\boldsymbol{S}\}, \{\dot{\boldsymbol{S}}\}, \{\alpha\}, \{\alpha^*\}, \{\dot{\alpha}\}, \{\dot{\alpha}^*\}) - \sum_m \lambda_m (\boldsymbol{S}_m^2 - 1), \tag{B2}$$

such that the Euler-Lagrange equation for λ_m reads as $\boldsymbol{S}_m^2 = 1$. Further, the equation of motion for a classical spin $\boldsymbol{S}_m$ is modified as

$$0 = \frac{1}{|\boldsymbol{S}_m|^3} \dot{\boldsymbol{S}}_m \times \boldsymbol{S}_m + \langle \partial_{\boldsymbol{S}_m} \hat{H}_{\text{int}} \rangle + \partial_{\boldsymbol{S}_m} H_{\text{cl}} + \sum_k \sum_{\beta\gamma} \dot{S}_{k\gamma} \langle \Omega \rangle_{k\gamma,m\beta} \boldsymbol{e}_\beta + 2\lambda_m \boldsymbol{S}_m. \tag{B3}$$

Acting on both sides of the equation with $\times \boldsymbol{S}_m$ and with $\cdot \boldsymbol{S}_m$, respectively, gives a system of two equations, which is equivalent with (B3):

$$0 = (\dot{\boldsymbol{S}}_m \times \boldsymbol{S}_m) \times \frac{\boldsymbol{S}_m}{|\boldsymbol{S}_m|^3} + \langle \partial_{\boldsymbol{S}_m} \hat{H}_{\text{int}} \rangle \times \boldsymbol{S}_m + \partial_{\boldsymbol{S}_m} H_{\text{cl}} \times \boldsymbol{S}_m + \sum_k \sum_{\beta\gamma} \dot{S}_{k\gamma} \langle \Omega \rangle_{k\gamma,m\beta} \boldsymbol{e}_\beta \times \boldsymbol{S}_m,$$
$$0 = \langle \partial_{\boldsymbol{S}_m} \hat{H}_{\text{int}} \rangle \cdot \boldsymbol{S}_m + \partial_{\boldsymbol{S}_m} H_{\text{cl}} \cdot \boldsymbol{S}_m + \sum_k \sum_{\beta\gamma} \dot{S}_{k\gamma} \langle \Omega \rangle_{k\gamma,m\beta} \boldsymbol{e}_\beta \cdot \boldsymbol{S}_m + 2\lambda_m \boldsymbol{S}_m^2. \tag{B4}$$

Exploiting $\boldsymbol{S}_m^2 = 1$ in the second equation fixes the Lagrange multipliers as

$$\lambda_m = -\frac{1}{2} \left(\langle \partial_{\boldsymbol{S}_m} \hat{H}_{\text{int}} \rangle \cdot \boldsymbol{S}_m + \partial_{\boldsymbol{S}_m} H_{\text{cl}} \cdot \boldsymbol{S}_m + \sum_k \sum_{\beta\gamma} \dot{S}_{k\gamma} \langle \Omega \rangle_{k\gamma,m\beta} \boldsymbol{e}_\beta \cdot \boldsymbol{S}_m \right), \tag{B5}$$

while using it in the first equation reproduces the familiar equation of motion (25).

APPENDIX C: SPIN-BERRY CURVATURE IN TERMS OF A PROJECTION OPERATOR

To prove (28) we start from the definition (22) of the non-Abelian spin-Berry curvature and insert the definition for the spin-Berry connection (15). This gives

$$\Omega^{(ij)}_{k\gamma,m\beta} = i[\langle\partial_{S_{k\gamma}}\Psi_i|\partial_{S_{m\beta}}\Psi_j\rangle - \langle\partial_{S_{m\beta}}\Psi_i|\partial_{S_{k\gamma}}\Psi_j\rangle]$$
$$+ i\sum_{l=0}^{n-1}[\langle\Psi_i|\partial_{S_{k\gamma}}|\Psi_l\rangle\langle\Psi_l|\partial_{S_{m\beta}}|\Psi_j\rangle - \langle\Psi_i|\partial_{S_{m\beta}}|\Psi_l\rangle\langle\Psi_l|\partial_{S_{k\gamma}}|\Psi_j\rangle], \tag{C1}$$

where we have exploited the commutativity of the derivatives $\partial_{S_{k\gamma}}$ and $\partial_{S_{m\beta}}$. Using the completeness relation and inserting a unity,

$$\mathbb{1} = \mathcal{Q}_n + \sum_{l=0}^{n-1}|\Psi_l\rangle\langle\Psi_l|, \tag{C2}$$

where $Q_n = \sum_{i\geqslant n}|\Psi_i\rangle\langle\Psi_i|$ is the projector onto the orthogonal complement of the low-energy space $\mathcal{E}_n(\{\boldsymbol{S}\})$, we find

$$\Omega^{(ij)}_{k\gamma,m\beta} = i[\langle\partial_{S_{k\gamma}}\Psi_i|\mathcal{Q}_n|\partial_{S_{m\beta}}\Psi_j\rangle - \langle\partial_{S_{m\beta}}\Psi_i|\mathcal{Q}_n|\partial_{S_{k\gamma}}\Psi_j\rangle]$$
$$+ i\sum_{l=0}^{n-1}[\langle\partial_{S_{k\gamma}}\Psi_i|\Psi_l\rangle\langle\Psi_l|\partial_{S_{m\beta}}\Psi_j\rangle - \langle\partial_{S_{m\beta}}\Psi_i|\Psi_l\rangle\langle\Psi_l|\partial_{S_{k\gamma}}\Psi_j\rangle]$$
$$+ i\sum_{l=0}^{n-1}[\langle\Psi_i|\partial_{S_{k\gamma}}|\Psi_l\rangle\langle\Psi_l|\partial_{S_{m\beta}}|\Psi_j\rangle - \langle\Psi_i|\partial_{S_{m\beta}}|\Psi_l\rangle\langle\Psi_l|\partial_{S_{k\gamma}}|\Psi_j\rangle]. \tag{C3}$$

Noting that $\langle\partial_{S_{m\beta}}\Psi_i||\Psi_j\rangle = -\langle\Psi_i|\partial_{S_{m\beta}}|\Psi_j\rangle$, we see that the last two terms on the right-hand side cancel, and thus

$$\Omega^{(ij)}_{k\gamma,m\beta} = i[\langle\partial_{S_{k\gamma}}\Psi_i|\mathcal{Q}_n|\partial_{S_{m\beta}}\Psi_j\rangle - \langle\partial_{S_{m\beta}}\Psi_i|\mathcal{Q}_n|\partial_{S_{k\gamma}}\Psi_j\rangle]. \tag{C4}$$

APPENDIX D: NUMERICAL COMPUTATION OF SPIN-BERRY CURVATURE AND CONNECTION

The equations of motion (25) and (26) form a coupled, nonlinear set of ordinary differential equations, which can be solved numerically by standard techniques. Making use of the fact that the conduction-electron system is noninteracting, however, is essential for an efficient computation of the key quantities of the electron system, namely, the spin-Berry curvature and connection.

We start by specializing Eqs. (23) and (28) to the single-spin case $M = 1$,

$$\langle\Omega\rangle_{\beta\gamma} = i\sum_{i,j=0}^{n-1}\alpha_i^*\alpha_j(\langle\partial_\beta\Psi_i|\mathcal{Q}_n|\partial_\gamma\Psi_j\rangle - \langle\partial_\gamma\Psi_i|\mathcal{Q}_n|\partial_\beta\Psi_j\rangle) = 2\sum_{i,j=0}^{n-1}\sum_{l\geqslant n}\mathrm{Im}\,\alpha_i^*\alpha_j\langle\Psi_i|\partial_\beta|\Psi_l\rangle\langle\Psi_l|\partial_\gamma|\Psi_j\rangle, \tag{D1}$$

and use the identity

$$\langle\Psi_i|\partial_\beta|\Psi_l\rangle = \frac{\langle\Psi_i|\frac{\partial\hat{H}}{\partial S_\beta}|\Psi_l\rangle}{E_l - E_i} \qquad (E_i \neq E_l) \tag{D2}$$

to express $\langle\boldsymbol{\Omega}\rangle$ in the form

$$\langle\Omega\rangle_{\beta\gamma} = -2\,\mathrm{Im}\sum_{ij}\sum_l^{E_l\neq E_i,E_j}\alpha_i^*\alpha_j\frac{\langle\Psi_i|\frac{\partial\hat{H}}{\partial S_\beta}|\Psi_l\rangle\langle\Psi_l|\frac{\partial\hat{H}}{\partial S_\gamma}|\Psi_j\rangle}{(E_i - E_l)(E_j - E_l)} = -2\,\mathrm{Im}J^2\sum_{ij}\sum_l^{E_l\neq E_i,E_j}\frac{\alpha_i^*\alpha_j\langle\Psi_i|s_{i_0\beta}|\Psi_l\rangle\langle\Psi_l|s_{i_0\gamma}|\Psi_j\rangle}{(E_i - E_l)(E_j - E_l)}. \tag{D3}$$

The matrix elements can be computed by plugging in the definition of the local spin $\boldsymbol{s}_i = \frac{1}{2}\sum_{\sigma\sigma'}c_{i\sigma}^\dagger\boldsymbol{\sigma}_{\sigma\sigma'}c_{i\sigma'}$ and by transforming to the eigenstates of the effective hopping matrix:

$$c_{i\sigma}^\dagger = \sum_{k\tilde{\sigma}}U_{k\tilde{\sigma},i\sigma}^\dagger c_{k\tilde{\sigma}}^\dagger, \qquad c_{i\sigma} = \sum_{k\tilde{\sigma}}U_{i\sigma,k\tilde{\sigma}}c_{k\tilde{\sigma}}. \tag{D4}$$

This yields

$$\sum_{l}^{E_l \neq E_i, E_j} \frac{\langle \Psi_i | s_{i_0\beta} | \Psi_l \rangle \langle \Psi_l | s_{i_0\gamma} | \Psi_j \rangle}{(E_i - E_l)(E_j - E_l)} = \frac{1}{4} \sum_{\sigma\sigma'\tau\tau'} \sum_{\tilde{\sigma}\tilde{\sigma}'\tilde{\tau}\tilde{\tau}'}^{kk'qq'} U_{k\tilde{\sigma},i_0\sigma}^{\dagger} \sigma_{\sigma\sigma'}^{(\beta)} U_{i_0\sigma',k'\tilde{\sigma}'} U_{q\tilde{\tau},i_0\tau}^{\dagger} \sigma_{\tau\tau'}^{(\gamma)} U_{i_0\tau',q'\tilde{\tau}'}$$

$$\times \frac{\langle \Psi_i | c_{k\tilde{\sigma}}^{\dagger} c_{k'\tilde{\sigma}'} c_{q\tilde{\tau}}^{\dagger} c_{q'\tilde{\tau}'} | \Psi_j \rangle}{(E_i - E_j + \varepsilon_{q'\tilde{\tau}'} - \varepsilon_{q\tilde{\tau}})(\varepsilon_{q'\tilde{\tau}'} - \varepsilon_{q\tilde{\tau}})}, \quad \text{(D5)}$$

where $\sum''$ means that the indices $k, k', q, q', \tilde{\sigma}, \tilde{\sigma}', \tilde{\tau}, \tilde{\tau}'$ can only take values such that $c_{k'\tilde{\sigma}'}^{\dagger} c_{k\tilde{\sigma}} |i\rangle$ and $c_{q\tilde{\tau}}^{\dagger} c_{q'\tilde{\tau}'} |j\rangle$ are not contained in the low-energy subspace. For the summation indices it is required that

$$(k, \tilde{\sigma}) \neq (k', \tilde{\sigma}') \quad \text{and} \quad (q, \tilde{\tau}) \neq (q', \tilde{\tau}') \quad \text{(D6)}$$

since $i \neq l$ and $j \neq l$. Plugging this into (D3) gives an expression that can be evaluated straightforwardly by numerical means.

We also have to compute the Berry connection, i.e., the matrix elements $\langle \Psi_i | \partial_\beta | \Psi_j \rangle$ in (26) [see also (15)]. For $i \neq j$ we can again use (D2) since the single-particle energies are generically nondegenerate for finite J and since this implies that states $|\Psi_i\rangle$ and $|\Psi_j\rangle$ with $E_i = E_j$ must differ in more than one single-particle eigenstate. For $i = j$, on the other hand, $\langle \Psi_i | \partial_\beta | \Psi_i \rangle$ must be computed differently. We exploit that the many-particle state $|\Psi_i\rangle$ is a Slater determinant:

$$|\Psi_i\rangle = c_{n_1}^{\dagger} c_{n_2}^{\dagger} \dots c_{n_N}^{\dagger} |\text{vac}\rangle. \quad \text{(D7)}$$

Therewith, we get

$$\partial_{S_\beta} |\Psi_i\rangle = \sum_{i=1}^{N} c_{n_1}^{\dagger} \dots (\partial_{S_\beta} c_{n_i}^{\dagger}) \dots c_{n_N}^{\dagger} |\text{vac}\rangle \quad \text{(D8)}$$

with

$$\partial_{S_\beta} c_{n_i}^{\dagger} = \partial_{S_\beta} \sum_{j\sigma} U_{j\sigma,n_i} c_{j\sigma}^{\dagger} = \sum_{j\sigma} (\partial_{S_\beta} U_{j\sigma,n_i}) c_{j\sigma}^{\dagger} = \sum_{j\sigma} \sum_{m} (\partial_{S_\beta} U_{j\sigma,n_i}) U_{m,j\sigma}^{\dagger} c_m^{\dagger} = \sum_{m} (U^{\dagger} \partial_{S_\beta} U)_{mn_i} c_m^{\dagger}. \quad \text{(D9)}$$

Multiplying (D8) with $\langle \Psi_i |$ from the left yields

$$\langle \Psi_i | \partial_\beta | \Psi_i \rangle = \sum_{i=1}^{N} \sum_{m} (U^{\dagger} \partial_{S_\beta} U)_{mn_i} \underbrace{\langle \text{vac} | c_{n_N} \dots c_{n_i} \dots c_{n_1} c_{n_1}^{\dagger} \dots c_m^{\dagger} \dots c_{n_N}^{\dagger} | \text{vac} \rangle}_{\delta_{n_i m}}$$

$$= \sum_{i=1}^{N} (U^{\dagger} \partial_{S_\beta} U)_{n_i n_i} = \sum_{n}' (U^{\dagger} \partial_{S_\beta} U)_{nn} = \sum_{n} (U^{\dagger} \partial_{S_\beta} U)_{nn} \langle \Psi_i | \hat{n}_n | \Psi_i \rangle, \quad \text{(D10)}$$

where $\sum_n'$ indicates that the sum only contains those single-particle states that are occupied in the many-particle state $|\Psi_i\rangle$. The derivative of the U matrix can be computed by standard numerical means.

APPENDIX E: TIME-REVERSAL-SYMMETRIC GROUND STATE

We consider the minimal model with Hamiltonian H given by (47). For $J = 0$ the (electronic part of the) model is invariant under SU(2) spin rotations. For a given direction of the classical spin, say $\boldsymbol{S} = S\boldsymbol{e}_z$, and for $J > 0$ the symmetry breaks down to a U(1) symmetry under spin rotations around the z axis. As argued in the main text, the local spin-dependent perturbation is not strong enough to spin polarize the system, irrespective of the coupling strength J. In this case the ground state of H is invariant under time reversal, as is shown in the following.

The antiunitary operator Θ representing time reversal in Fock space is defined via its action on the creation and annihilation operators as

$$\Theta c_{i\uparrow}^{\dagger} \Theta^{\dagger} = c_{i\downarrow}^{\dagger}, \quad \Theta c_{i\downarrow}^{\dagger} \Theta^{\dagger} = -c_{i\uparrow}^{\dagger}, \quad \text{(E1)}$$

where i refers to lattice sites and $\sigma = \uparrow, \downarrow$ to the spin projection with respect to the z axis. Due to the remaining U(1)

symmetry, the Hamiltonian can be diagonalized in the spin-$\uparrow$ and spin-$\downarrow$ sectors separately, i.e., the single-particle eigenstates $c_{k\sigma}^{\dagger} |\text{vac}\rangle$ of H are obtained via a spin-diagonal and spin-independent unitary transformation:

$$c_{k\sigma}^{\dagger} = \sum_{i} U_{ik} c_{i\sigma}^{\dagger}. \quad \text{(E2)}$$

For the model (47) with $\boldsymbol{S} = S\boldsymbol{e}_z$, the effective hopping matrix (51) is real and symmetric, and we can thus assume a real and orthogonal transformation matrix U. The creation operators referring to the eigenbasis of H in the one-particle subspace thus transform as

$$\Theta c_{k\uparrow}^{\dagger} \Theta^{\dagger} = c_{k\downarrow}^{\dagger}, \quad \Theta c_{k\downarrow}^{\dagger} \Theta^{\dagger} = -c_{k\uparrow}^{\dagger} \quad \text{(E3)}$$

under time reversal.

For even N, the ground state of H is the Slater determinant

$$|\Psi_0\rangle = \prod_{k}^{\text{occ}} c_{k\uparrow}^{\dagger} \prod_{k'}^{\text{occ}} c_{k'\downarrow}^{\dagger} |\text{vac}\rangle, \quad \text{(E4)}$$

where $|\text{vac}\rangle$ is the time-reversal-invariant vacuum, $k = 1, \ldots, N_\uparrow$, and $k' = 1, \ldots, N_\downarrow$ with $N_\uparrow = N_\downarrow = N/2$, as the ground state is unpolarized. Applying Θ yields

$$\Theta|\Psi_0\rangle = (-1)^{N_\downarrow} \prod_k^{\text{occ}} c_{k\downarrow}^\dagger \prod_{k'}^{\text{occ}} c_{k'\uparrow}^\dagger |\text{vac}\rangle, \qquad \text{(E5)}$$

and, after reordering,

$$\Theta|\Psi_0\rangle = (-1)^{N_\uparrow N_\downarrow}(-1)^{N_\downarrow} \prod_{k'}^{\text{occ}} c_{k'\uparrow}^\dagger \prod_k^{\text{occ}} c_{k\downarrow}^\dagger |\text{vac}\rangle. \qquad \text{(E6)}$$

For $N_\uparrow = N_\downarrow = N/2$, however, the total sign is $+1$, and hence the ground state is time-reversal symmetric

$$\Theta|\Psi_0\rangle = |\Psi_0\rangle. \qquad \text{(E7)}$$

[1] U. Nowak, Classical spin models, in *Handbook of Magnetism and Advanced Magnetic Materials* (Wiley, Hoboken, NJ, 2007).

[2] G. Bertotti, I. D. Mayergoyz, and C. Serpico, *Nonlinear Magnetization Dynamics in Nanosystemes* (Elsevier, Amsterdam, 2009).

[3] J. Kondo, Prog. Theor. Phys. **32**, 37 (1964).

[4] A. C. Hewson, *The Kondo Problem to Heavy Fermions* (Cambridge University Press, Cambridge, 1993).

[5] G. Tatara, H. Kohno, and J. Shibata, Phys. Rep. **468**, 213 (2008).

[6] B. Skubic, J. Hellsvik, L. Nordström, and O. Eriksson, J. Phys.: Condens. Matter **20**, 315203 (2008).

[7] M. Fähnle and C. Illg, J. Phys.: Condens. Matter **23**, 493201 (2011).

[8] R. F. L. Evans, W. J. Fan, P. Chureemart, T. A. Ostler, M. O. A. Ellis, and R. W. Chantrell, J. Phys.: Condens. Matter **26**, 103202 (2014).

[9] M. A. Ruderman and C. Kittel, Phys. Rev. **96**, 99 (1954); T. Kasuya, Prog. Theor. Phys. **16**, 45 (1956); K. Yosida, Phys. Rev. **106**, 893 (1957).

[10] L. D. Landau and E. M. Lifshitz, Phys. Z. Sowjetunion 8, **153** (1935); T. Gilbert, Phys. Rev. **100**, 1243 (1955); IEEE Trans. Magn. **40**, 3443 (2004).

[11] E. Butikov, Eur. J. Phys. **27**, 1071 (2006).

[12] J.-E. Wegrowe and M.-C. Ciornei, Am. J. Phys. **80**, 607 (2012).

[13] M. Onoda and N. Nagaosa, Phys. Rev. Lett. **96**, 066603 (2006).

[14] N. Umetsu, D. Miura, and A. Sakuma, J. Appl. Phys. **111**, 07D117 (2012).

[15] S. Bhattacharjee, L. Nordström, and J. Fransson, Phys. Rev. Lett. **108**, 057204 (2012).

[16] M. Sayad and M. Potthoff, New J. Phys. **17**, 113058 (2015).

[17] U. Bajpai and B. K. Nikolic, Phys. Rev. B **99**, 134409 (2019).

[18] S. V. Vonsovsky, Zh. Éksp. Teor. Fiz. **16**, 981 (1946); C. Zener, Phys. Rev. **81**, 440 (1951); S. V. Vonsovsky and E. A. Turov, Zh. Éksp. Teor. Fiz. **24**, 419 (1953).

[19] H. Breuer and F. Petruccione, *The Theory of Open Quantum Systems* (Oxford University Press, New York, 2002).

[20] M. Sayad, R. Rausch, and M. Potthoff, Phys. Rev. Lett. **117**, 127201 (2016).

[21] V. P. Antropov, M. I. Katsnelson, M. van Schilfgaarde, and B. N. Harmon, Phys. Rev. Lett. **75**, 729 (1995).

[22] J. Kuneš and V. Kamberský, Phys. Rev. B **65**, 212411 (2002).

[23] K. Capelle and B. L. Gyorffy, Europhys. Lett. **61**, 354 (2003).

[24] H. Ebert, S. Mankovsky, D. Ködderitzsch, and P. J. Kelly, Phys. Rev. Lett. **107**, 066603 (2011).

[25] M. Fähnle, D. Steiauf, and C. Illg, Phys. Rev. B **84**, 172403 (2011).

[26] T. Kikuchi and G. Tatara, Phys. Rev. B **92**, 184410 (2015).

[27] M. Sayad, R. Rausch, and M. Potthoff, Europhys. Lett. **116**, 17001 (2016).

[28] C. Stahl and M. Potthoff, Phys. Rev. Lett. **119**, 227203 (2017).

[29] M. V. Berry, Proc. R. Soc. London A **392**, 45 (1984).

[30] D. Xiao, M.-C. Chang, and Q. Niu, Rev. Mod. Phys. **82**, 1959 (2010).

[31] X. G. Wen and A. Zee, Phys. Rev. Lett. **61**, 1025 (1988).

[32] Q. Niu and L. Kleinman, Phys. Rev. Lett. **80**, 2205 (1998).

[33] A. Bohm, A. Mostafazadeh, H. Koizumi, Q. Niu, and J. Zwanziger, *The Geometric Phase in Quantum Systems* (Springer, Berlin, 2003).

[34] Q. Niu, X. Wang, L. Kleinman, W.-M. Liu, D. M. C. Nicholson, and G. M. Stocks, Phys. Rev. Lett. **83**, 207 (1999).

[35] U. Bajpai and B. K. Nikolić, Phys. Rev. Lett. **125**, 187202 (2020).

[36] M. Elbracht, S. Michel, and M. Potthoff, Phys. Rev. Lett. **124**, 197202 (2020).

[37] S. Michel and M. Potthoff, Phys. Rev. B **103**, 024449 (2021).

[38] D. Marx and J. Hutter, *Ab initio molecular dynamics: Theory and Implementation, in Modern Methods and Algorithms of Quantum Chemistry*, NIC Series Vol. 1, edited by J. Grotendorst (John von Neumann Institute for Computing, Jülich, 2000), p. 301.

[39] Q. Zhang and B. Wu, Phys. Rev. Lett. **97**, 190401 (2006).

[40] F. Wilczek and A. Zee, Phys. Rev. Lett. **52**, 2111 (1984).

[41] A. Heslot, Phys. Rev. D **31**, 1341 (1985).

[42] M. J. W. Hall, Phys. Rev. A **78**, 042104 (2008).

[43] H. Elze, Phys. Rev. A **85**, 052109 (2012).

[44] A. Bulgac and D. Kusnezov, Ann. Phys. (NY) **199**, 187 (1990).

[45] P. A. M. Dirac, Proc. R. Soc. London A **133**, 60 (1931).

[46] T. Kato, J. Phys. Soc. Jpn. **5**, 435 (1950).

[47] J. E. Avron and A. Elgart, Commun. Math. Phys. **203**, 445 (1999).

[48] D. Comparat, Phys. Rev. A **80**, 012106 (2009).

[49] B. Simon, Phys. Rev. Lett. **51**, 2167 (1983).

[50] M. E. Peskin and D. V. Schroeder, in *An Introduction to Quantum Field Theory*, 3rd ed., edited by Array, Graduate Texts in Mathematics (Addison-Wesley, Reading, PA, 1996).

[51] M. Elbracht and M. Potthoff, Phys. Rev. B **102**, 115434 (2020).

[52] M. Elbracht and M. Potthoff, Phys. Rev. B **103**, 024301 (2021).

[53] D. Kulkarni, D. Schmidt, and S.-K. Tsui, *Eigenvalues of Tridiagonal Pseudo-Toeplitz Matrices*, Linear Algebra and its Applications Vol. 297 (Elsevier, Amsterdam, 1999).

[54] M. L. Bellac, *Quantum Physics* (Cambridge University Press, Cambridge, 2006).

[55] R. Wiesendanger, Rev. Mod. Phys. **81**, 1495 (2009).

[56] C. P. R. Rausch, M. Peschke, and C. Karrasch, Sci. Post Phys. **12**, 143 (2022).

[57] R. Quade and M. Potthoff, Phys. Rev. B **105**, 035406 (2022).

5 – Geometrical Spin Torque in a Magnet

Magnetic materials are an ideal platform for the geometrical spin torque arising in ASD and NA-SD because they exhibit two key features. First of all, they break time-reversal symmetry, which makes it possible to conduct the analysis in the weak-J limit using expressions from linear response theory. Secondly, they spontaneously break a continuous symmetry, namely, SU(2) spin-rotation symmetry, such that Goldstone's theorem [92, 93] predicts the existence of massless excitations in the energy spectrum. This can strongly boost the geometrical spin torque, which is demonstrated for the Heisenberg model in the following. It is found that there is a strong dependence on the type of interaction, i.e., if the coupling is ferro- or antiferromagnetic, as well as the presence of anisotropies. Furthermore, the dimension of the lattice plays a crucial role that is reminiscent of the Mermin-Wagner theorem [94–96].

5.1 – Ferromagnetic Heisenberg Model

The quantum Heisenberg model is one of the best known models to describe magnetic phenomena on a microscopic scale. It is suitable for models with permanent, localised magnetic moments whose interaction can be modelled by an exchange interaction. The Hamiltonian of the model reads

$$H = \sum_{ij} J_{ij} \left[\frac{1}{2}(s_i^+ s_j^- + s_i^- s_j^+) + \Delta s_i^z s_j^z \right] \tag{5.1}$$

with exchange couplings J_{ij} and an anisotropy parameter Δ. In the following, it is assumed that every quantum spin has the same spin quantum number s. For a negative exchange coupling, the ground states of the model are the fully polarised states, i.e., $|0\rangle = |\uparrow, \uparrow, \ldots\rangle$, in which all spins are aligned parallelly. As is commonly done, we choose the spontaneously-symmetry-broken ground state to be aligned with our quantisation axis. In general, the eigenstates of H are given by product states

$$|s, m_1\rangle_1 \otimes |s, m_2\rangle_2 \otimes \cdots \otimes |s, m_L\rangle_L \equiv |m_1, m_2, \ldots, m_L\rangle , \tag{5.2}$$

which constitute a basis of the Hilbert space. Assuming nearest-neighbour interaction only, we get

$$J_{ij} = \begin{cases} J_H & \text{for } \boldsymbol{R}_i - \boldsymbol{R}_j \in \boldsymbol{\delta} \\ 0 & \text{otherwise,} \end{cases} \tag{5.3}$$

where $\boldsymbol{R}_i$ is the position vector of the ith site and $\boldsymbol{\delta}$ is the set of nearest-neighbour translation vectors. For a hypercubic lattice in d dimensions with lattice constant $a = 1$, one has

$$\boldsymbol{\delta} = \{\boldsymbol{e}_{x_1}, -\boldsymbol{e}_{x_1}, \ldots, \boldsymbol{e}_{x_d}, -\boldsymbol{e}_{x_d}\} \tag{5.4}$$

with the canonical unit vector in the ith spatial direction $\boldsymbol{e}_{x_i}$. The Hamiltonian becomes

$$H = \sum_{<ij>} J_H(s_i^- s_j^+ + \Delta s_i^z s_j^z) \tag{5.5}$$

since for nearest-neighbour sites i and j it is $\left[s_i^+, s_j^-\right] = 0$. To describe the low-energy excitations of the ferromagnetic Heisenberg model, it is convenient to introduce the Holstein-Primakoff transformation [97]. This maps the spin operators onto bosonic operators a_i

$$\frac{1}{\hbar}s_i^z = s - n_i \tag{5.6}$$

$$\frac{1}{\hbar}s_i^+ = \sqrt{2s}\sqrt{1 - \frac{n_i}{2s}}a_i \tag{5.7}$$

$$\frac{1}{\hbar}s_i^- = \sqrt{2s}a_i^\dagger\sqrt{1 - \frac{n_i}{2s}} \tag{5.8}$$

with $n_i = a_i^\dagger a_i$. The bosonic operators fulfil the usual bosonic commutation relations and it can be shown that the transformed spin operators still satisfy $[s_{i\alpha}, s_{i\beta}] = \varepsilon_{\alpha\beta\gamma}s_{i\gamma}$. A Taylor expansion in $\frac{1}{s}$ of the Holstein-Primakoff expressions gives

$$\sqrt{1 - \frac{n_i}{2s}} = 1 - \frac{n_i}{4s} + \mathcal{O}\left(\frac{1}{s^2}\right) \tag{5.9}$$

such that for large spin quantum numbers it is sufficient to only consider the zeroth order, i.e., make the approximation

$$\sqrt{1 - \frac{n_i}{2s}} \approx 1. \tag{5.10}$$

For the approximation to be valid, one has to argue that $2s$ is much larger than $\langle n_i \rangle$. If $s = \frac{1}{2}$, one needs $n_i \ll 1$, which is typically true for small temperatures. The Hamiltonian takes the form

$$H = J_H \sum_{<ij>} (2s\hbar^2 a_i^\dagger a_j + \Delta\hbar^2(s^2 - sa_i^\dagger a_i - sa_j^\dagger a_j + n_i n_j))$$

$$= 2J_H\hbar^2 s \sum_{<ij>} \left(a_i^\dagger a_j - \Delta\left(a_i^\dagger a_i + \frac{1}{s}n_i n_j\right)\right) + J_H\Delta\hbar^2 s^2 Lz, \tag{5.11}$$

where z is the coordination number. Since we assumed $n_i \ll 1$, it makes sense to also discard the term $\propto n_i n_j$. The terms of the resulting Hamiltonian are then at most bilinear in the a-operators

$$H = 2J_H\hbar^2 s \sum_{<ij>} (a_i^\dagger a_j - \Delta a_i^\dagger a_i) + J_H\Delta\hbar^2 s^2 Lz. \tag{5.12}$$

This Hamiltonian can be diagonalised by Fourier transformation of the bosonic operators

$$a_i = \frac{1}{\sqrt{L}} \sum_{\boldsymbol{k}} e^{-i\boldsymbol{k}\boldsymbol{R}_i} a_{\boldsymbol{k}}, \quad a_{\boldsymbol{k}} = \frac{1}{\sqrt{L}} \sum_{i} e^{i\boldsymbol{k}\boldsymbol{R}_i} a_i \tag{5.13}$$

$$a_i^\dagger = \frac{1}{\sqrt{L}} \sum_{\boldsymbol{k}} e^{i\boldsymbol{k}\boldsymbol{R}_i} a_{\boldsymbol{k}}^\dagger, \quad a_{\boldsymbol{k}}^\dagger = \frac{1}{\sqrt{L}} \sum_{i} e^{-i\boldsymbol{k}\boldsymbol{R}_i} a_i^\dagger \tag{5.14}$$

with $\boldsymbol{k} \in$ BZ. Inserting this into (5.12), the first term transforms as

$$\begin{aligned}
\sum_{<ij>} a_i^\dagger a_j &= \sum_i \sum_{\boldsymbol{\delta}} a_i^\dagger a_{i+\boldsymbol{\delta}} \\
&= \frac{1}{L} \sum_i \sum_{\boldsymbol{\delta}} \sum_{\boldsymbol{k},\boldsymbol{k}'} e^{i\boldsymbol{k}\boldsymbol{R}_i} e^{-i\boldsymbol{k}'(\boldsymbol{R}_i+\boldsymbol{\delta})} a_{\boldsymbol{k}}^\dagger a_{\boldsymbol{k}'} \\
&= \sum_{\boldsymbol{k},\boldsymbol{k}'} \left(\frac{1}{L} \sum_i e^{i(\boldsymbol{k}-\boldsymbol{k}')\boldsymbol{R}_i} \right) \sum_{\boldsymbol{\delta}} e^{-i\boldsymbol{k}'\boldsymbol{\delta}} a_{\boldsymbol{k}}^\dagger a_{\boldsymbol{k}'} \\
&= \sum_{\boldsymbol{k}} \sum_{\boldsymbol{\delta}} e^{-i\boldsymbol{k}\boldsymbol{\delta}} a_{\boldsymbol{k}}^\dagger a_{\boldsymbol{k}} \\
&= \sum_{\boldsymbol{k}} \frac{1}{2} \sum_{\boldsymbol{\delta}} \left(e^{i\boldsymbol{k}\boldsymbol{\delta}} + e^{-i\boldsymbol{k}\boldsymbol{\delta}} \right) a_{\boldsymbol{k}}^\dagger a_{\boldsymbol{k}} \\
&= \sum_{\boldsymbol{k}} \sum_{\boldsymbol{\delta}} \cos(\boldsymbol{k}\boldsymbol{\delta}) a_{\boldsymbol{k}}^\dagger a_{\boldsymbol{k}},
\end{aligned} \tag{5.15}$$

where it was used that $\frac{1}{L} \sum_i e^{-i(\boldsymbol{k}-\boldsymbol{k}')\boldsymbol{R}_i} = \delta_{\boldsymbol{k}\boldsymbol{k}'}$ and the second to last equality holds because $\sum_{\boldsymbol{\delta}} f(\boldsymbol{\delta}) = \sum_{\boldsymbol{\delta}} f(-\boldsymbol{\delta})$. For the second term, one finds

$$\begin{aligned}
\sum_{<ij>} a_i^\dagger a_i &= z \sum_i a_i^\dagger a_i \\
&= \frac{z}{L} \sum_i \sum_{\boldsymbol{k},\boldsymbol{k}'} e^{i(\boldsymbol{k}-\boldsymbol{k}')\boldsymbol{R}_i} a_{\boldsymbol{k}}^\dagger a_{\boldsymbol{k}'} \\
&= z \sum_{\boldsymbol{k}} a_{\boldsymbol{k}}^\dagger a_{\boldsymbol{k}}.
\end{aligned} \tag{5.16}$$

The Fourier transformed Hamiltonian is diagonal and reads

$$H = 2J_H \hbar^2 s \sum_{\boldsymbol{k}} \omega(\boldsymbol{k}) a_{\boldsymbol{k}}^\dagger a_{\boldsymbol{k}} + E_0 \tag{5.17}$$

with the dispersion $\omega(\boldsymbol{k}) := \sum_{\boldsymbol{\delta}} \cos(\boldsymbol{k}\boldsymbol{\delta}) - \Delta z$ and ground state energy $E_0 = J_H \Delta \hbar^2 s^2 L z$. In the thermodynamic limit, $\boldsymbol{k}$ is continuous and the spectrum of low-energy excitations is gapless. This is predicted by Goldstone's theorem since the ferromagnetic Heisenberg model exhibits spontaneous symmetry breaking. Concretely, the Hamiltonian is invariant under SU(2) spin rotations. In principle, this is true for the ground state as well since it is only necessary for all spin moments to be parallel aligned, while the direction of alignment is irrelevant. Thus, there is an infinite number of ground states connected by SU(2) transformations. However, as mentioned above, a single one of those states is picked as the true ground state consequently breaking the SU(2) spin-rotation symmetry [98]. From the form

of the diagonalised Hamiltonian (5.17), it is sensible to interpret the low energy excitations as bosonic quasiparticles of momentum $\boldsymbol{k}$. The quasiparticles are called magnons and represent small deviations from the complete alignment of the spins. From a classical point of view, these excitations are also known as spin waves. The magnons are then the quanta of spin waves in complete analogy to phonons as the quanta of lattice vibrations [84]. Taking only the first term in the Taylor expansion of the Holstein-Primakoff expressions (5.9) into account, is, hence, also referred to as linear spin wave theory [99].

To compute the spin-Berry curvature of a single classical impurity spin coupled to the ferromagnetic Heisenberg model at zero temperature and for small quantum-classical coupling J, one has to evaluate

$$\Omega_{m\alpha,m'\alpha'} = -\frac{2J^2}{L}\,\mathrm{Im}\left\{\sum_{\boldsymbol{k}}\frac{\langle 0|\,s_{m\alpha}\,|\boldsymbol{k}\rangle\,\langle\boldsymbol{k}|\,s_{m'\alpha'}\,|0\rangle}{(E_0 - E_{\boldsymbol{k}})^2}\right\},\tag{5.18}$$

where $|\boldsymbol{k}\rangle$ denotes a single-magnon state of momentum $\boldsymbol{k}$ and $E_{\boldsymbol{k}} = 2J_H\hbar^2 s\omega(\boldsymbol{k}) + E_0$ the corresponding energy. A single-magnon state, without normalisation, is given by

$$|\boldsymbol{k}\rangle = s^-(\boldsymbol{k})\,|0\rangle\,,\quad \langle\boldsymbol{k}| = \langle 0|\,s^+(-\boldsymbol{k})\tag{5.19}$$

with $s^-(\boldsymbol{k}) = \frac{1}{\sqrt{L}}\sum_i e^{-i\boldsymbol{k}\boldsymbol{R}_i}s_i^-$ and $s^-(\boldsymbol{k})^\dagger = s^+(-\boldsymbol{k})$. The normalisation can be straightforwardly computed as

$$\langle 0|\,s^+(-\boldsymbol{k})s^-(\boldsymbol{k})\,|0\rangle = \langle 0|\,(s^-(\boldsymbol{k})s^+(-\boldsymbol{k}) + \frac{2\hbar}{L}\sum_i s_i^z(0))\,|0\rangle = 2\hbar^2 s\tag{5.20}$$

assuming that the ground state $|0\rangle$ is already normalised. To compute the matrix elements $\langle 0|\,s_{m\alpha}\,|\boldsymbol{k}\rangle$ the normalisation will be ignored for now and only included in the final expression for $\Omega_{m\alpha,m'\alpha'}$. This yields

$$\langle 0|\,s_i^x\,|\boldsymbol{k}\rangle = \langle 0|\,s_i^x s^-(\boldsymbol{k})\,|0\rangle = \frac{1}{2}e^{-i\boldsymbol{k}\boldsymbol{R}_i}\,\langle 0|\,s_i^+ s_i^-\,|0\rangle$$

$$\langle 0|\,s_i^y\,|\boldsymbol{k}\rangle = \langle 0|\,s_i^y s^-(\boldsymbol{k})\,|0\rangle = -\frac{i}{2}e^{-i\boldsymbol{k}\boldsymbol{R}_i}\,\langle 0|\,s_i^+ s_i^-\,|0\rangle$$

$$\langle 0|\,s_i^z\,|\boldsymbol{k}\rangle = 0.\tag{5.21}$$

The spin-Berry curvature is proportional to the imaginary part of the product of two such matrix elements. Therefore, the only nonzero contributions come from $\alpha,\alpha' \neq z$

$$\langle 0|\,s_i^x\,|\boldsymbol{k}\rangle\,\langle\boldsymbol{k}|\,s_j^y\,|0\rangle = \frac{i}{4}e^{-i\boldsymbol{k}(\boldsymbol{R}_i-\boldsymbol{R}_j)}\,\langle 0|\,s_i^+ s_i^-\,|0\rangle\,\langle 0|\,s_j^+ s_j^-\,|0\rangle$$

$$\langle 0|\,s_i^y\,|\boldsymbol{k}\rangle\,\langle\boldsymbol{k}|\,s_j^x\,|0\rangle = -\frac{i}{4}e^{-i\boldsymbol{k}(\boldsymbol{R}_i-\boldsymbol{R}_j)}\,\langle 0|\,s_i^+ s_i^-\,|0\rangle\,\langle 0|\,s_j^+ s_j^-\,|0\rangle$$

$$\langle 0|\,s_i^x\,|\boldsymbol{k}\rangle\,\langle\boldsymbol{k}|\,s_j^x\,|0\rangle = \langle 0|\,s_i^y\,|\boldsymbol{k}\rangle\,\langle\boldsymbol{k}|\,s_j^y\,|0\rangle = \frac{1}{4}e^{-i\boldsymbol{k}(\boldsymbol{R}_i-\boldsymbol{R}_j)}\,\langle 0|\,s_i^+ s_i^-\,|0\rangle\,\langle 0|\,s_j^+ s_j^-\,|0\rangle.\tag{5.22}$$

In the case $s = \frac{1}{2}$ with $|\uparrow\rangle = (1,0)^\mathsf{T}$ the matrix representation of s_i^+ and s_i^- is given by

$$s^+ = \hbar \begin{pmatrix} 0 & 1 \\ 0 & 0 \end{pmatrix}, \ s^- = \hbar \begin{pmatrix} 0 & 0 \\ 1 & 0 \end{pmatrix}$$

$$\Rightarrow s^+ s^- |\uparrow\rangle = \hbar^2 |\uparrow\rangle, \ s^+ s^- |\downarrow\rangle = 0$$

$$s^- s^+ |\downarrow\rangle = \hbar^2 |\downarrow\rangle, \ s^- s^+ |\uparrow\rangle = 0. \tag{5.23}$$

All in all, one has

$$\mathrm{Im}\Big\{ \langle 0| \, s_i^x \, |\boldsymbol{k}\rangle \, \langle \boldsymbol{k}| \, s_j^y \, |0\rangle \Big\} = \frac{\hbar^4}{4} \cos(\boldsymbol{k}(\boldsymbol{R}_i - \boldsymbol{R}_j))$$

$$\mathrm{Im}\Big\{ \langle 0| \, s_i^y \, |\boldsymbol{k}\rangle \, \langle \boldsymbol{k}| \, s_j^x \, |0\rangle \Big\} = -\frac{\hbar^4}{4} \cos(\boldsymbol{k}(\boldsymbol{R}_i - \boldsymbol{R}_j))$$

$$\mathrm{Im}\Big\{ \langle 0| \, s_i^x \, |\boldsymbol{k}\rangle \, \langle \boldsymbol{k}| \, s_j^x \, |0\rangle \Big\} = \mathrm{Im}\Big\{ \langle 0| \, s_i^y \, |\boldsymbol{k}\rangle \, \langle \boldsymbol{k}| \, s_j^y \, |0\rangle \Big\} = -\frac{\hbar^4}{4} \sin(\boldsymbol{k}(\boldsymbol{R}_i - \boldsymbol{R}_j)). \tag{5.24}$$

To include the normalisation, a factor of $\frac{1}{\sqrt{2\hbar^2 s}}$ has to be added per matrix element involving $|\boldsymbol{k}\rangle$ such that the final expression is

$$\Omega_{ixjx} = \Omega_{iyjy} = \frac{J^2}{2\hbar^2 J_H^2 L} \sum_{\boldsymbol{k}} \frac{\sin(\boldsymbol{k}(\boldsymbol{R}_i - \boldsymbol{R}_j))}{\omega(\boldsymbol{k})^2} = 0 \tag{5.25}$$

$$\Omega_{ixjy} = -\Omega_{jyix} = -\frac{J^2}{2\hbar^2 J_H^2 L} \sum_{\boldsymbol{k}} \frac{\cos(\boldsymbol{k}(\boldsymbol{R}_i - \boldsymbol{R}_j))}{\omega(\boldsymbol{k})^2}. \tag{5.26}$$

Here, the xx and yy components vanish since the sum over $\boldsymbol{k}$ contains both $\boldsymbol{k}$ and $-\boldsymbol{k}$ and sine is antisymmetric. For a hypercubic lattice in d dimensions, it is $z = 2d$ and thus $\omega(\boldsymbol{k}) = \sum_{\boldsymbol{\delta}} \cos(\boldsymbol{k}\boldsymbol{\delta}) - \Delta 2d = 2(\sum_{i=1}^{d} \cos(k_i)) - 2\Delta d$.
In the isotropic case, i.e. $\Delta = 1$, the denominator becomes zero if $k_i = 0$, $\forall i \in \{1, \ldots, d\}$. The elements of the vector $\boldsymbol{R}_{ij} := \boldsymbol{R}_i - \boldsymbol{R}_j$ are all integers for a hypercubic lattice with lattice constant set to one, such that at the points where the denominator vanishes $\cos(\boldsymbol{k}(\boldsymbol{R}_i - \boldsymbol{R}_j))$ is nonzero. At the point where $\boldsymbol{k} = \boldsymbol{0}$, one finds by Taylor expansion $\frac{\cos(\boldsymbol{k}(\boldsymbol{R}_i - \boldsymbol{R}_j))}{\omega(\boldsymbol{k})^2} \propto \frac{1}{|\boldsymbol{k}|^4}$. If we are in the thermodynamic limit and in d dimensions, one has

$$\frac{1}{L} \sum_{\boldsymbol{k}} \longrightarrow \frac{V_{\mathrm{WS}}}{(2\pi)^d} \int d^d \boldsymbol{k} \propto \int dk |\boldsymbol{k}|^{d-1}, \tag{5.27}$$

where V_{WS} is the volume of the Wigner-Seitz cell, which is a^d for a hypercubic lattice. For the transition from a sum to an integral, it was used that

$$V_{\mathrm{WS}} V_{\mathrm{BZ}} = (2\pi)^d, \ \frac{V}{V_{\mathrm{WS}}} = L, \ \Delta \boldsymbol{k} = \frac{V_{\mathrm{BZ}}}{L} \tag{5.28}$$

with $\Delta \boldsymbol{k}$ the spacing between $\boldsymbol{k}$ points. This means that Ω_{ixjy} and Ω_{jyix} diverge as $\frac{1}{|\boldsymbol{k}|}$ in

three dimensions. For arbitrary dimensions, one has

$$\int dk |\boldsymbol{k}|^{d-1} \frac{\cos(\boldsymbol{k}\boldsymbol{R})}{\omega(\boldsymbol{k})^2} \propto \begin{cases} |\boldsymbol{k}|^{d-4}, & \text{for } d \geq 5 \\ \ln |\boldsymbol{k}|, & \text{for } d = 4 \\ |\boldsymbol{k}|^{d-4}, & \text{for } d \leq 3 \end{cases} . \tag{5.29}$$

The lowest dimension for which the spin-Berry curvature does not diverge is five. In all lower dimension, including the physical relevant $d = 3$, it is ill-defined and linear spin wave theory breaks down. This is analogous to the so-called lower critical dimension in the context of the Mermin-Wagner theorem. The theorem states that thermal fluctuations can prevent spontaneous symmetry breaking in dimensions lower than two, which manifests itself by a divergence of the variance of the order parameter [100]. The lower critical dimension is the highest dimension for which this divergence occurs. Since for the ferromagnet the spin-Berry curvature diverges for all dimensions $d \leq 4$, the theory cannot be applied to spin dynamics in a sensible way. However, it seems useful to apply the same considerations as above to the antiferromagnetic version of the Heisenberg model. The reason is that there the magnon dispersion is $\propto \boldsymbol{k}$ at low energies such that the spin-Berry curvature is expected to be finite already for dimensions lower than five. This is investigated in publication [II] below.

Geometrical torque on magnetic moments coupled to a correlated antiferromagnet

Nicolas Lenzing,[1] David Krüger [●],[1] and Michael Potthoff [●][1,2]

[1]*University of Hamburg, Department of Physics, Notkestraße 9-11, 22607 Hamburg, Germany*
[2]*The Hamburg Centre for Ultrafast Imaging, Luruper Chaussee 149, 22761 Hamburg, Germany*

The geometrical spin torque mediates an indirect interaction of magnetic moments, which are weakly exchange coupled to a system of itinerant electrons. It originates from a finite spin-Berry curvature and leads to a non-Hamiltonian magnetic-moment dynamics. We demonstrate that there is an unprecedentedly strong geometrical spin torque in the case of an electron system, where correlations cause antiferromagnetic long-range order. The key observation is that the anomalous torque is strongly boosted by low-energy magnon modes emerging in the two-electron spin-excitation spectrum due to spontaneous breaking of SU(2) spin-rotation symmetry. As long as single-electron excitations are gapped out, the effect is largely universal, i.e., essentially independent of the details of the electronic structure, but decisively dependent on the lattice dimension and spatial and spin anisotropies. Analogous to the reasoning that leads to the Mermin-Wagner theorem, there is a lower critical dimension at and below which the spin-Berry curvature diverges.

I. INTRODUCTION

A magnetic moment coupled to a system of itinerant electrons via a local exchange interaction of strength J experiences a spin torque which leads to precession dynamics. For several magnetic moments S_m (with $m = 1, \ldots, M$), usually described as classical fixed-length spins, there are further torques caused by, e.g., indirect exchange interactions mediated by the electron system. These *Hamiltonian* spin torques, well known in micromagnetics [1] and in the theory of coupled spin-electron dynamics [2–8], all derive from interaction terms in the quantum-classical Hamiltonian [9] for the spin and electron degrees of freedom. In addition, there is a non-Hamiltonian spin torque that has a purely *geometric* nature. This geometrical spin torque represents the feedback of the Berry physics [10] on the classical magnetic-moment dynamics.

Generally, such feedback effects have been pointed out early [11–13] but have not been studied in spin dynamics theory until recently [14]. For weak J compared to the typical energy scales of the electron system, the classical spin dynamics is slow, such that the electron system accumulates a geometrical phase which is gauge independent in the case of a cyclic motion [10,15,16]. This Berry phase is closely related to the Berry curvature, a two-form which, when integrated in classical parameter space over a two-dimensional surface bounded by a closed path $\mathcal{C}$, yields the Berry phase associated with $\mathcal{C}$. For example, in molecular physics [17] and when treating the coordinates of the nuclei classically, the feedback

of the Berry physics produces an additional geometrical force, where the Berry curvature plays the role of a magnetic field in the nuclei equations of motion. This effect is known as "geometrical magnetism" [18,19].

The geometrical spin torque resulting from the spin-Berry curvature (SBC) [14] is the analogous concept in the field of atomistic spin dynamics [4,20]. As opposed to the closely related geometrical friction term [18,19], i.e., Gilbert damping [21], it is energy conserving. But, importantly, the SBC is non-Hamiltonian and emerges for weak J, i.e., in the limit of slow classical spin dynamics. However, the effects are typically weak [22] for a solid [23], such that it appears difficult to disentangle the effect of the geometrical spin torque from other contributions [24].

In this Letter we study the geometrical spin torque for magnetic moments coupled to a magnetic solid: a correlated D-dimensional antiferromagnetic (AF) insulator. This is a generic situation realized, e.g., by magnetic impurities in the bulk or by magnetic adatoms on the surface of the antiferromagnet. We demonstrate that the magnitude of the SBC is governed by the magnon-excitation spectrum. This has very general consequences: the SBC must diverge for $D = 1$ but is regular for $D \geqslant 3$, see Table I. For $D = 2$ the SBC generically exhibits a logarithmic divergence as a function of any perturbation causing a gap in the magnon dispersion, such as magnetic anisotropies or external magnetic fields. The magnitude of the SBC and thus the impact on the magnetic-moment dynamics is studied for the Hubbard model at half-filling and zero temperature as a prototype of a correlation-induced insulator.

II. TIME-REVERSAL SYMMETRY

Within adiabatic spin-dynamics theory [14,22], geometrical spin torque is obtained from the SBC of the electron

TABLE I. Spin-Berry curvature of a spontaneously symmetry-broken antiferromagnetic state with gapped single-particle excitations. $\boldsymbol{k}$: wave vector. See text for discussion.

Lattice dimension	SBC	Distance dependence	Magnetic ground state
1	Divergent	–	–
2	Log. divergent	–	Stable
3	Regular	$1/R$	Stable
$D \geqslant 4$	$\sim \int_0^{\Lambda_{\text{cutoff}}} dk\, k^{D-3}$	$1/R^{D-2}$	Stable

system, see Eq. (2) below. Importantly, a finite SBC generally requires time-reversal symmetry (TRS) breaking in the electron system [22]. If J is strong, as assumed in Ref. [14], TRS is broken by the classical spin moment itself, as this acts like a local symmetry-breaking field. TRS breaking can be waived only at the cost of working with a non-Abelian extension of the theory well beyond the adiabatic limit [25], where the dynamics is governed by the generically finite non-Abelian spin-Berry curvature. Another approach is to replace the electron system with an entirely classical model composed of "slow" and "fast" spin moments [26,27]. This circumvents the necessity of TRS breaking altogether but still exhibits the feedback of holonomy effects in purely classical systems [28]. For magnetic moments coupled to *quantum* systems and in the physically relevant weak-J regime, a finite SBC can be achieved with an external magnetic field, or with a (staggered) orbital field as considered recently [22] with the Haldane model [29] as a prototype of a TRS-breaking Chern insulator [30]. However, fine tuning of the parameters is required to achieve considerable effects [22]. Here we consider an electron system in which correlations induce a TRS-breaking AF state. The AF order not only enables a finite SBC but also strongly boosts its magnitude due to magnon modes in the spin-excitation spectrum.

III. DYNAMICS OF MAGNETIC MOMENTS

We are interested in the slow dynamics of M magnetic moments, described as classical spins $\boldsymbol{S}_m$ of unit length, which are coupled to a correlated electron system with Hamiltonian H_{el} via a local exchange interaction $H_{\text{int}} = J \sum_{m=1}^{M} \boldsymbol{s}_{i_m} \boldsymbol{S}_m$. Here, i_m is the site the mth moment is coupled to, and $\boldsymbol{s}_i = 1/2 \sum_{\sigma\sigma'} c_{i\sigma}^{\dagger} \boldsymbol{\tau}_{\sigma\sigma'} c_{i\sigma'}$ is the local spin moment at site i of the electron system. The total Hamiltonian is $H = H(\boldsymbol{S}) = H_{\text{el}} + H_{\text{int}}(\boldsymbol{S})$ and depends on the configuration $\boldsymbol{S} = (\boldsymbol{S}_1, \ldots, \boldsymbol{S}_M)$ of the magnetic moments.

Assuming that the electron system at any instant of time t is in its instantaneous ground state for the spin configuration $\boldsymbol{S}(t)$, i.e., $|\Psi(t)\rangle = |\Psi_0(\boldsymbol{S}(t))\rangle$, the equation of motion of adiabatic spin dynamics is given by [14,22]

$$\dot{\boldsymbol{S}}_m = \left(\boldsymbol{T}_m^{(\text{H})} + \boldsymbol{T}_m^{(\text{geo})} \right) \times \boldsymbol{S}_m . \tag{1}$$

Here $\boldsymbol{T}_m^{(\text{H})} \times \boldsymbol{S}_m$ with $\boldsymbol{T}_m^{(\text{H})} = \partial \langle H(\boldsymbol{S}) \rangle / \partial \boldsymbol{S}_m = J \langle \boldsymbol{s}_{i_m} \rangle$ is the conventional (Hamiltonian) spin torque, where $\langle \cdots \rangle$ is the instantaneous ground-state expectation value.

IV. GEOMETRICAL SPIN TORQUE

The second term, the geometrical spin torque $\boldsymbol{T}_m^{(\text{geo})} \times \boldsymbol{S}_m$, is necessary to enforce the constraint $|\Psi(t)\rangle = |\Psi_0(\boldsymbol{S}(t))\rangle$ and has been derived within a quantum-classical Lagrange formalism in Refs. [14] and [22]. This assumes that the ground state is nondegenerate (otherwise non-Abelian spin-dynamics theory [25] must be used) and that J is sufficiently weak so that the classical spin dynamics is much slower than typical relaxation time scales of the quantum system H_{el}. Alternatively, the term may be derived within adiabatic response theory [18,19,31] as the first nontrivial correction in a systematic expansion of the response of a driven system with respect to the driving speed, when applied to spin dynamics [32]. It is given by

$$\boldsymbol{T}_m^{(\text{geo})} = \sum_{\alpha} \sum_{m'\alpha'} \Omega_{m'm,\alpha'\alpha}(\boldsymbol{S}) \dot{S}_{m'\alpha'} \boldsymbol{e}_{\alpha}, \tag{2}$$

with $\alpha = x, y, z$ and the αth unit vector $\boldsymbol{e}_{\alpha}$, and where

$$\Omega_{mm',\alpha\alpha'}(\boldsymbol{S}) = \frac{\partial}{\partial S_{m\alpha}} A_{m'\alpha'}(\boldsymbol{S}) - \frac{\partial}{\partial S_{m'\alpha'}} A_{m\alpha}(\boldsymbol{S}) \tag{3}$$

is the spin-Berry curvature. At each spin configuration $\boldsymbol{S}$, this is a real antisymmetric tensor ($\Omega_{m'm,\alpha'\alpha} = -\Omega_{mm',\alpha\alpha'}$), which is invariant under local gauge transformations of the ground states $|\Psi_0(\boldsymbol{S})\rangle \mapsto e^{i\phi(\boldsymbol{S})}|\Psi_0(\boldsymbol{S})\rangle$. It is the exterior derivative of the spin-Berry connection $\boldsymbol{A}_m = i\langle \Psi_0 | \frac{\partial}{\partial S_m} | \Psi_0 \rangle$, which describes parallel transport of the ground state $|\Psi_0(\boldsymbol{S})\rangle$ on the manifold of spin configurations $\mathcal{M}$. For M classical spins $\boldsymbol{S}_m \in S^2$, this is given by the M-fold Cartesian product of 2-spheres $\mathcal{M} \equiv S^2 \times \cdots \times S^2$.

V. SPONTANEOUS ANTIFERROMAGNETIC ORDER

We consider a coupling of the magnetic spin moments to the single-band Hubbard model [33,34] on a D-dimensional hypercubic lattice as a prototypical model for itinerant magnetic order. Its Hamiltonian is $H_{\text{el}} = -t \sum_{ij}^{\text{n.n.}} \sum_{\sigma=\uparrow,\downarrow} c_{i\sigma}^{\dagger} c_{j\sigma} + U \sum_i n_{i\uparrow} n_{i\downarrow}$, where the nearest-neighbor hopping $t = 1$ fixes the energy and (with $\hbar \equiv 1$) the time scales. $c_{i\sigma}$ annihilates an electron at site i with spin projection σ, and $n_{i\sigma} = c_{i\sigma}^{\dagger} c_{i\sigma}$. The sums over i, j are restricted to nearest neighbors, and L is the total number of sites. It is well known [35–39] that at half-filling, repulsive Hubbard-U and for $D \geqslant 2$, the ground state of the system in the thermodynamical limit $L \to \infty$ develops long-range AF correlations. SU(2) spin-rotation symmetry and therewith TRS are spontaneously broken, and the ordered state is characterized by a finite staggered magnetization $\boldsymbol{m} = m\boldsymbol{e}_z$ with $m = L^{-1} \sum_i z_i \langle n_{i\uparrow} - n_{i\downarrow} \rangle$ and $z_i = \pm 1$ for i in sublattice A or B, respectively. We assume $m > 0$ for sublattice A.

At weak U, AF order is driven by the Slater mechanism and perturbatively accessible [36,38]. Within self-consistent Hartree-Fock theory [40], the one-electron excitation spectrum displays a gap $\Delta = Um$ at wave vector $\boldsymbol{Q} = (\pi, \pi, \ldots)$ in the conventional Brillouin zone. The two-electron spin-excitation spectrum is well described by standard random-phase approximation (RPA) but for the symmetry-broken AF state [41–44].

In the strong-U limit, the one-electron spectrum is dominated by a large Hubbard gap $\Delta \sim U$ and well-developed local spin moments, coupled via Anderson's superexchange [35,38]. Here, the model maps onto the Heisenberg spin-1/2 Hamiltonian with AF exchange $J_H = 4t^2/U$ and AF long-range order, see Refs. [37], [45], and [46], for example. To compute the low-energy magnon dispersion and states, we can apply spin-wave theory (SWT) [47] to the AF Heisenberg model and use the Holstein-Primakoff transformation [48] at linear order. Linear SWT is motivated by the fact that single-magnon decay requires overlap with the two-magnon continuum, so that the picture of a stable magnon gas is protected by kinematic restrictions at low energies [49–52].

VI. SPIN-BERRY CURVATURE OF AN ANTIFERROMAGNET

To compute the geometrical spin torque, we make use of a Lehmann-type representation of the SBC starting from Eq. (3). This is straightforwardly derived [22] using a resolution of the unity, $\mathbf{1} = \sum_n |\Psi_n(\mathbf{S})\rangle\langle\Psi_n(\mathbf{S})|$, with an orthonormal basis of instantaneous eigenstates of $H_{el} + H_{int}(\mathbf{S})$:

$$\Omega_{mm',\alpha\alpha'} = -2J^2 \mathrm{Im} \sum_{n\neq 0} \frac{\langle\Psi_0|s_{i_m}^\alpha|\Psi_n\rangle\langle\Psi_n|s_{i_{m'}}^{\alpha'}|\Psi_0\rangle}{(E_n - E_0)^2} . \quad (4)$$

Note that, due to the J^2 prefactor, the $\mathbf{S}$ dependence of the eigenenergies and eigenstates will provide corrections to Eq. (4) only at order J^3. As we refer to the weak-J limit, these will be neglected in the following.

In the AF phase and assuming that the order parameter is aligned to the z axis, $\langle s_i \rangle = (-1)^i m e_z$, there is a remaining SO(2) symmetry of the energy eigenstates under spin rotations around e_z. This unbroken spin-rotation symmetry, together with the spatial inversion and translation symmetries of H_{el}, and the antisymmetry $\Omega_{mm',\alpha\alpha'} = -\Omega_{m'm,\alpha'\alpha}$ [see Eq. (3)] imply that the spin-Berry curvature tensor is entirely fixed by a single real number $\Omega \equiv \Omega_{mm',xy} = -\Omega_{mm',yx}$ for each fixed pair of sites i_m, $i_{m'}$. All other elements must vanish, as is detailed by the symmetry analysis in Sections A and B of the Supplemental Material (SM) [53].

In a first step, for weak U, we compute the SBC via

$$\Omega_{mm'} = -iJ^2 \frac{\partial}{\partial\omega} \chi_{i_m i_{m'},xy}(\omega)\Big|_{\omega=0} + \mathcal{O}(J^3), \quad (5)$$

where $\chi_{ii',\alpha\alpha'}(\omega) = L^{-1}\sum_{\mathbf{k}} e^{i\mathbf{k}(\mathbf{R}_i - \mathbf{R}_{i'})}\chi_{\alpha\alpha'}(\mathbf{k},\omega)$ is the real-space retarded susceptibility, obtained by the RPA (see SM, Sec. C [53]). The relation Eq. (5) is easily derived by comparing the representation Eq. (4) of the SBC with the Lehmann representation of the susceptibility (SM, Secs. A and B [53]). Therewith, the susceptibility in the symmetry-broken AF state is seen to play a dual role for the spin dynamics: (i) via Eq. (5) and Eq. (2) its frequency derivative at $\omega = 0$ yields the geometrical spin torque $\mathbf{T}_m^{(\mathrm{geo})} \times \mathbf{S}_m$, and (ii) the static susceptibility yields, in the weak-J regime, the conventional RKKY spin torque $\mathbf{T}_m^{(H)} \times \mathbf{S}_m$ with $\mathbf{T}_m^{(H)} = \partial H_{\mathrm{RKKY}}/\partial \mathbf{S}_m$, where $H_{\mathrm{RKKY}} = J^2 \sum \chi_{i_m i_{m'},\alpha\alpha'}(\omega=0)S_{m\alpha}S_{m'\alpha'}$ is the perturbative RKKY Hamiltonian of the AF state.
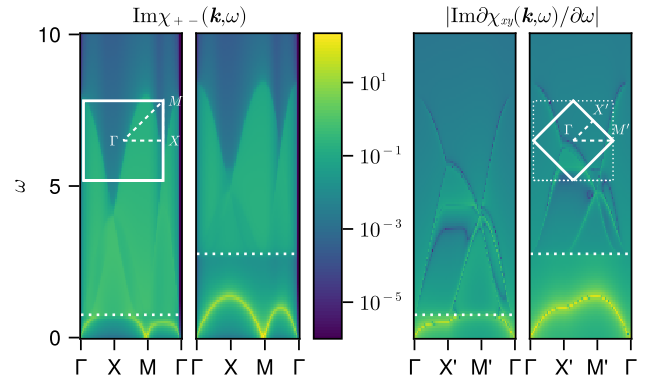

FIG. 1. Left: Transversal retarded ground-state spin susceptibility $\mathrm{Im}\,\chi_{+-}(\mathbf{k},\omega)$ for $U = 2$ and $U = 4$ along high-symmetry directions in the conventional $D = 2$ Brillouin zone, as obtained by RPA. Right: Frequency derivative $\mathrm{Im}\,\partial_\omega\chi_{xy}(\mathbf{k},\omega)$ (absolute values) in the mBz, related to the SBC at $\omega = 0$. White dotted lines: Slater gap $\Delta = Um$ (onset of the continuum). Lorentzian broadening $\omega \to \omega + i\eta$ with $\eta = 0.045$. Energy scale: $t = 1$.

For the Hubbard model on the $D = 2$ square lattice the spin-excitation spectrum $\chi_{+-}(\mathbf{k},\omega)$, see Fig. 1 (left) for $U = 2$ and $U = 4$, consists of a continuum at high frequencies $\omega > \Delta = Um$ ($\Delta \approx 0.75$ for $U = 2$, $\Delta \approx 2.76$ for $U = 4$) and, furthermore, within the gap an undamped transversal and doubly degenerate magnon mode. This mode takes most of the spectral weight. The magnon contribution to the derivative $\partial_\omega\chi_{xy}(\mathbf{k},\omega)$ on sublattice A (Fig. 1, right) is even more pronounced, especially for $\omega = 0$, where it is related to the SBC by Eq. (5).

VII. GOLDSTONE THEOREM, IMPLICATIONS

In our second step, we exploit the fact that the spin-excitation spectrum of an AF insulator has a universal structure at low frequencies. This is due to Goldstone's theorem, which enforces the presence of gapless magnon modes [54–56]. In the collinear AF state and corresponding to the two broken generators of the spin SU(2) symmetry, there are two degenerate modes with a linear and isotropic dispersion in the vicinity of the Γ point in the magnetic Brillouin zone (mBz). Linear SWT applied to the Heisenberg model that emerges in the strong-U limit captures this physics, i.e., the dispersion close to Γ is given by $\frac{1}{2}J_H\omega(\mathbf{k}) = c_s k + \mathcal{O}(k^2)$, where c_s is the spin-wave velocity. Using the magnon energies and eigenstates, we can compute the SBC in this limit from Eq. (4) directly (SM, Secs. D and E [53]), ending up with

$$\Omega_{mm'} = \mp \frac{2J^2}{J_H^2}\frac{1}{(2\pi)^D}\int_{\mathrm{mBz}} d^D k \frac{\cos[\mathbf{k}(\mathbf{R}_{i_m} - \mathbf{R}_{i_{m'}})]}{\omega(\mathbf{k})^2}, \quad (6)$$

if both i_m, $i_{m'}$ belong to sublattice A ($-$ sign) or B ($+$ sign), and $\Omega_{mm'} = 0$ else.

For $D = 2$, the linear dispersion close to Γ then implies a $1/k^2$ singularity of the integrand and thus a logarithmic infrared divergence. For $D \geqslant 3$, the local ($m = m'$) SBC is finite. We note that the same arguments as invoked for the Mermin-Wagner theorem [47,57], i.e., a divergence due to the low-energy spin excitations, here lead to a lower
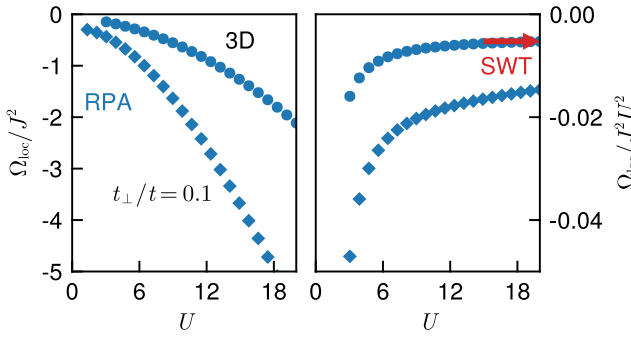
FIG. 2. Local SBC as function of U for $D = 3$, as obtained from RPA. Left: Ω_{loc}/J^2. Right: $\Omega_{\text{loc}}/J^2U^2$. Diamonds: $t_\perp/t = 0.1$, see also Fig. 3 (left). Red arrow: $D = 3$ SWT ($U \to \infty$) result. $\eta = 0.035$.

critical dimension ($D_c = 3$) that is shifted by one, see Table I. The numerical value for the $D = 3$ local SBC is $\Omega_{\text{loc}} \approx -0.084\, J^2/J_H^2 = -0.084\, J^2U^2/16t^4$. When scaling the hopping as $t = t^*/\sqrt{D}$ with $t^* = \text{const}$ [58,59], the modulus of the SBC decreases monotonically with D, and the SBC approaches a finite mean-field value $|\Omega_{\text{loc}}| \to J^2U^2/32t^{*4}$ for $D \to \infty$ (SM, Sec. F [53]).

VIII. MAGNITUDE OF THE SBC

SWT predicts a U^2 dependence of the SBC in the Heisenberg limit for strong U. For $U = 0$, on the other hand, TRS of the resulting paramagnetic state implies that it must vanish. For $U \to 0$, there is an intricate competition between the exponential suppression of the order parameter $m \propto e^{-1/U}$, i.e., of the "strength" of TRS breaking and thus of the SBC and, on the other hand, the exponential closure of the single-electron Slater gap $\Delta = Um$ and thus of the onset of the continuum in the spin-excitation spectrum resulting in continuum contributions that favor a large SBC. Our numerical results for the local SBC in $D = 3$, as obtained from weak-coupling RPA and strong-coupling SWT, are displayed in Fig. 2. With increasing U we find a smooth crossover from the Slater to the Heisenberg limit with a monotonically increasing $|\Omega_{\text{loc}}|$.

The nonlocal SBC at large distances $R \equiv \|\boldsymbol{R}_{i_m} - \boldsymbol{R}_{i_{m'}}\|$ is again governed by the linear dispersion at low frequencies. Carrying out the integration in Eq. (6) for $R \to \infty$ we find $\Omega(R) \propto 1/R^{D-2}$ (see Table I and SM, Sec. F [53]). For $D = 3$ this implies that the geometrical spin torque mediates a long-range coupling in the spin dynamics.

Compared to previous studies [14,22,24–27] the $D = 3$ value of the local SBC $|\Omega_{\text{loc}}| \approx 0.084\, J^2/J_H^2$ is several orders of magnitude larger for realistic parameters $J, J_H \ll t, U$. Renormalization of $c_s \to c_s' \approx 1.1 c_s$ due to magnon interaction [60] leads to a slightly smaller SBC, $|\Omega_{\text{loc}}| \to (c_s/c_s')^2 |\Omega_{\text{loc}}|$.

There are at least two routes that lead to an even larger $|\Omega_{\text{loc}}|$: namely, we can take advantage of the formally infinite SBC in $D = 2$ and regularize the theory (i) by dimensional crossover to $D = 3$ [61–63], i.e., by switching on a small hopping $t_\perp$ in the third dimension (Fig. 2), implying $J_H^\perp \ll J_{H,x} = J_{H,y} = J_H$, see Fig. 3 (left), or (ii) by switching on a magnetic anisotropy to open a small gap in the magnon
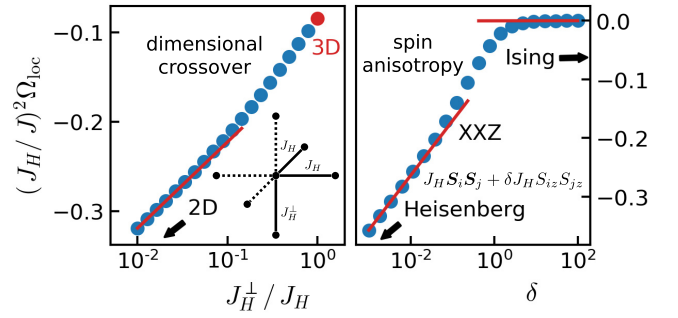

FIG. 3. SWT results (dots) for anisotropic systems. Left, dimensional crossover: local SBC for $D = 3$ but with a spatially anisotropic nearest-neighbor Heisenberg exchange $J_H^\perp \leqslant J_H$. Right, spin anisotropy: SBC as function of the coupling anisotropy parameter δ.

spectrum (Fig. 3, right), i.e., by adding an Ising term $\delta\, J_H S_{iz} S_{jz}$ to the standard Heisenberg coupling $J_H \boldsymbol{S}_i \boldsymbol{S}_j$. A moderate $J_H^\perp/J_H = 0.1$ yields a SBC $|\Omega_{\text{loc}}| \approx 0.22 J^2/J_H^2$. About the same enhancement is obtained for an anisotropy parameter $\delta \sim 10^{-2}$.

IX. GEOMETRICAL SPIN DYNAMICS

For the AF ordered phase, Eq. (1) tells us that the dominating effect in the magnetic-moment dynamics is a precession around the staggered magnetization $\boldsymbol{m}$ on a time scale $1/J$. This effect dominates the weaker (and slower) anisotropic RKKY-type exchange on the scale J^2. Importantly, the SBC $\Omega \sim J^2$ enters the equations of motion as a renormalization factor (for $M > 1$ classical spins as a matrix factor) rather than a summand and thus does not compete with the stronger direct exchange of order J (SM, Sec. G [53]). For $M = 1$ this factor amounts to $1/(1 - \Omega_{\text{loc}} S_z)$, such that the most pronounced effects are found for a SBC of intermediate strength, $\Omega_{\text{loc}} = \mathcal{O}(1)$. This holds true for $M = 2$ as well, as is detailed in the SM, Sec. G [53]. Note that a singular renormalization indicates a breakdown of the theory as this is the point where the condition for nearly adiabatic spin dynamics is invalidated. Note further that the precession comes with an inverted orientation beyond the singular point.

X. CONCLUSIONS AND OUTLOOK

A hitherto unknown but generic interplay of electron correlations, spontaneous symmetry breaking, gapless Goldstone bosons, and a holonomy on the configuration space of classical spin degrees of freedom leads to non-Hamiltonian effects, such as renormalization of precession frequencies, inverted orientation of the precessional motion, or long-range interactions, in the spin dynamics. This is due to a geometrical spin torque which is finite for correlated AF ground states in lattice models with dimension $D \geqslant 3$ and diverges for $D \leqslant 2$, caused by the same mechanism that leads to the Mermin-Wagner theorem, however, shifted by one dimension. With a SBC $\Omega_{\text{loc}} = \mathcal{O}(1)$ for typical parameters, the effect is unexpectedly large. It is boosted by electron correlations and further enhanced by spatial and spin anisotropies.

We expect a strong overall impact on the phenomenology of atomistic spin dynamics, in particular on the field of

antiferromagnetic spintronics [64–66], e.g., on spin-transfer torques in antiferromagnets (see Ref. [67], for example). An according concretization of the theory, however, has yet to be worked out. Anisotropic one- and two-dimensional magnetic-moment arrays, engineered atom by atom [68], or two-dimensional (anti)ferromagnetic materials [69] represent promising platforms for applications and comparison with experiments.

Treating the magnetic moments S_m as classical vectors, especially in the antiferromagnetic case [70], must be seen as an approximation that avoids a full quantum many-body setup but disregards correlation effects such as Kondo screening or heavy-fermion behavior. The approximation may be justified for high spin quantum numbers, see, e.g., Refs. [70,71], or generally in cases where there are well-formed spin moments that remain unscreened on timescales exceeding the remaining timescales of the problem. The very presence of the geometrical spin torque for the quantum-spin case, however, has been demonstrated using time-dependent density-matrix renormalization [14]. While this method and also exact time propagation (TDSE) are limited to one-dimensional or small systems and to very short femtosecond timescales, insightful results for nonclassical spin-transfer effects [72] and quantum spin transfer torque [73] were obtained recently. A consistent effective low-energy theory for a system that is entirely quantum mechanical with at least two largely different timescales has yet to be developed.

[1] G. Bertotti, I. D. Mayergoyz, and C. Serpico, *Nonlinear Magnetization Dynamics in Nanosystemes* (Elsevier, Amsterdam, 2009).

[2] W. Koshibae, N. Furukawa, and N. Nagaosa, Real-Time Quantum Dynamics of Interacting Electrons: Self-Organized Nanoscale Structure in a Spin-Electron Coupled System, Phys. Rev. Lett. **103**, 266402 (2009).

[3] S. Bhattacharjee, L. Nordström, and J. Fransson, Atomistic Spin Dynamic Method with both Damping and Moment of Inertia Effects Included from First Principles, Phys. Rev. Lett. **108**, 057204 (2012).

[4] R. F. L. Evans, W. J. Fan, P. Chureemart, T. A. Ostler, M. O. A. Ellis, and R. W. Chantrell, Atomistic spin model simulations of magnetic nanomaterials, J. Phys.: Condens. Matter **26**, 103202 (2014).

[5] M. Sayad and M. Potthoff, Spin dynamics and relaxation in the classical-spin Kondo-impurity model beyond the Landau-Lifschitz-Gilbert equation, New J. Phys. **17**, 113058 (2015).

[6] M. Sayad, R. Rausch, and M. Potthoff, Relaxation of a Classical Spin Coupled to a Strongly Correlated Electron System, Phys. Rev. Lett. **117**, 127201 (2016).

[7] G.-W. Chern, K. Barros, Z. Wang, H. Suwa, and C. D. Batista, Semiclassical dynamics of spin density waves, Phys. Rev. B **97**, 035120 (2018).

[8] U. Bajpai and B. K. Nikolic, Time-retarded damping and magnetic inertia in the Landau-Lifshitz-Gilbert equation self-consistently coupled to electronic time-dependent nonequilibrium green functions, Phys. Rev. B **99**, 134409 (2019).

[9] H. Elze, Linear dynamics of quantum-classical hybrids, Phys. Rev. A **85**, 052109 (2012).

[10] M. V. Berry, Quantal phase factors accompanying adiabatic changes, Proc. R. Soc. London A **392**, 45 (1984).

[11] H. Kuratsuji and S. Iida, Effective action for adiabatic process: Dynamical meaning of Berry and Simon's phase, Prog. Theor. Phys. **74**, 439 (1985).

[12] J. Moody, A. Shapere, and F. Wilczek, Realizations of Magnetic-Monopole Gauge Fields: Diatoms and Spin Precession, Phys. Rev. Lett. **56**, 893 (1986).

[13] B. Zygelman, Appearance of gauge potentials in atomic collision physics, Phys. Lett. A **125**, 476 (1987).

[14] C. Stahl and M. Potthoff, Anomalous Spin Precession under a Geometrical Torque, Phys. Rev. Lett. **119**, 227203 (2017).

[15] B. Simon, Holonomy, the Quantum Adiabatic Theorem, and Berry's Phase, Phys. Rev. Lett. **51**, 2167 (1983).

[16] F. Wilczek and A. Zee, Appearance of Gauge Structure in Simple Dynamical Systems, Phys. Rev. Lett. **52**, 2111 (1984).

[17] A. Bohm, A. Mostafazadeh, H. Koizumi, Q. Niu, and J. Zwanziger, *The Geometric Phase in Quantum Systems* (Springer, Berlin, 2003).

[18] M. Berry and J. Robbins, Chaotic classical and half-classical adiabatic reactions: Geometric magnetism and deterministic friction, Proc. R. Soc. London A **442**, 659 (1993).

[19] M. Campisi, S. Denisov, and P. Hänggi, Geometric magnetism in open quantum systems, Phys. Rev. A **86**, 032114 (2012).

[20] B. Skubic, J. Hellsvik, L. Nordström, and O. Eriksson, A method for atomistic spin dynamics simulations: Implementation and examples, J. Phys.: Condens. Matter **20**, 315203 (2008).

[21] L. D. Landau and E. M. Lifshitz, A Lagrangian formulation of the gyromagnetic equation of the magnetization field, Physik. Zeits. Sowjetunion **8**, 153 (1935); T. Gilbert, On the theory of the dispersion of magnetic permeability in ferromagnetic bodies, Phys. Rev. **100**, 1243 (1955); A phenomenological theory of damping in ferromagnetic materials, IEEE Trans. Magn. **40**, 3443 (2004).

[22] S. Michel and M. Potthoff, Spin Berry curvature of the Haldane model, Phys. Rev. B **106**, 235423 (2022).

[23] J. Ihm, Berry's Phase Originated from the Broken Time-Reversal Symmetry: Theory and Application to Anyon Superconductivity, Phys. Rev. Lett. **67**, 251 (1991).

[24] U. Bajpai and B. K. Nikolić, Spintronics Meets Nonadiabatic Molecular Dynamics: Geometric Spin Torque and Damping on Dynamical Classical Magnetic Texture due to an Electronic Open Quantum System, Phys. Rev. Lett. **125**, 187202 (2020).

[25] N. Lenzing, A. I. Lichtenstein, and M. Potthoff, Emergent non-Abelian gauge theory in coupled spin-electron dynamics, Phys. Rev. B **106**, 094433 (2022).

[26] M. Elbracht, S. Michel, and M. Potthoff, Topological Spin Torque Emerging in Classical Spin Systems with Different Timescales, Phys. Rev. Lett. **124**, 197202 (2020).

[27] S. Michel and M. Potthoff, Non-Hamiltonian dynamics of indirectly coupled classical impurity spins, Phys. Rev. B **103**, 024449 (2021).

[28] J. H. Hannay, Angle variable holonomy in adiabatic excursion of an integrable Hamiltonian, J. Phys. A: Math. Gen. **18**, 221 (1985).

[29] F. D. M. Haldane, Model for a Quantum Hall Effect without Landau Levels: Condensed-Matter Realization of the "Parity Anomaly," Phys. Rev. Lett. **61**, 2015 (1988).

[30] B. A. Bernevig, *Topological Insulators and Topological Superconductors* (Princeton University Press, Princeton, 2013).

[31] M. Berry and J. Robbins, The geometric phase for chaotic systems, Proc. R. Soc. London A **436**, 631 (1992).

[32] N. Lenzing and M. Potthoff (unpublished).

[33] F. Gebhard, *The Mott Metal-Insulator Transition* (Springer, Berlin, 1997).

[34] F. H. L. Essler, H. Frahm, F. Göhmann, A. Klümper, and V. Korepin, *The One-Dimensional Hubbard Model* (Cambridge University Press, Cambridge, 2005).

[35] P. W. Anderson, Antiferromagnetism. Theory of superexchange interaction, Phys. Rev. **79**, 350 (1950).

[36] J. R. Schrieffer, X. G. Wen, and S. C. Zhang, Dynamic spin fluctuations and the bag mechanism of high-T_c superconductivity, Phys. Rev. B **39**, 11663 (1989).

[37] E. Manousakis, The spin-1/2 Heisenberg antiferromagnet on a square lattice and its application to the cuprate oxides, Rev. Mod. Phys. **63**, 1 (1991).

[38] A. Auerbach, *Interacting Electrons and Quantum Magnetism* (Springer, New York, 1994).

[39] T. Schäfer, F. Geles, D. Rost, G. Rohringer, E. Arrigoni, K. Held, N. Blümer, M. Aichhorn, and A. Toschi, Fate of the false Mott-Hubbard transition in two dimensions, Phys. Rev. B **91**, 125109 (2015).

[40] T. Moriya, *Spin Fluctuations in Itinerant Electron Magnetism*, Springer Series in Solid-State Sciences (Springer, Berlin, 1985), Vol. 56.

[41] W. Rowe, J. Knolle, I. Eremin, and P. J. Hirschfeld, Spin excitations in layered antiferromagnetic metals and superconductors, Phys. Rev. B **86**, 134513 (2012).

[42] L. Del Re and A. Toschi, Dynamical vertex approximation for many-electron systems with spontaneously broken SU(2) symmetry, Phys. Rev. B **104**, 085120 (2021).

[43] J. M. Luttinger and J. C. Ward, Ground-state energy of a many-fermion system II, Phys. Rev. **118**, 1417 (1960).

[44] G. Rohringer, H. Hafermann, A. Toschi, A. A. Katanin, A. E. Antipov, M. I. Katsnelson, A. I. Lichtenstein, A. N. Rubtsov, and K. Held, Diagrammatic routes to nonlocal correlations beyond dynamical mean-field theory, Rev. Mod. Phys. **90**, 025003 (2018).

[45] S. Chakravarty, B. I. Halperin, and D. R. Nelson, Two-dimensional quantum Heisenberg antiferromagnet at low temperatures, Phys. Rev. B **39**, 2344 (1989).

[46] A. W. Sandvik, Finite-size scaling of the ground-state parameters of the two-dimensional Heisenberg model, Phys. Rev. B **56**, 11678 (1997).

[47] P. W. Anderson, An approximate quantum theory of the antiferromagnetic ground state, Phys. Rev. **86**, 694 (1952).

[48] J. Holstein and N. Primakoff, Field dependence of the intrinsic domain magnetization of a ferromagnet, Phys. Rev. **58**, 1098 (1940).

[49] C. J. Hamer, Z. Weihong, and P. Arndt, Third-order spin-wave theory for the Heisenberg antiferromagnet, Phys. Rev. B **46**, 6276 (1992).

[50] A. L. Chernyshev and P. A. Maksimov, Damped Topological Magnons in the Kagome-Lattice Ferromagnets, Phys. Rev. Lett. **117**, 187203 (2016).

[51] P. A. McClarty, X.-Y. Dong, M. Gohlke, J. G. Rau, F. Pollmann, R. Moessner, and K. Penc, Topological magnons in Kitaev magnets at high fields, Phys. Rev. B **98**, 060404(R) (2018).

[52] P. McClarty, Topological magnons: A review, Annu. Rev. Condens. Matter Phys. **13**, 171 (2022).

[53] See Supplemental Material at http://link.aps.org/supplemental/10.1103/PhysRevResearch.5.L032012 for various technical details and supplemental analytical results.

[54] J. Goldstone, Field theories with superconductor solutions, Nuovo Cim. **19**, 154 (1961).

[55] Y. Nambu and G. Jona-Lasinio, Dynamical model of elementary particles based on an analogy with superconductivity. I, Phys. Rev. **122**, 345 (1961).

[56] T. Brauner, Spontaneous symmetry breaking and Nambu-Goldstone bosons in quantum many-body systems, Symmetry **2**, 609 (2010).

[57] N. D. Mermin and H. Wagner, Absence of Ferromagnetism or Antiferromagnetism in One- or Two-Dimensional Isotropic Heisenberg Models, Phys. Rev. Lett. **17**, 1133 (1966).

[58] W. Metzner and D. Vollhardt, Correlated Lattice Fermions in $d = \infty$ Dimensions, Phys. Rev. Lett. **62**, 324 (1989).

[59] E. Müller-Hartmann, Correlated fermions on a lattice in high dimensions, Z. Phys. B **74**, 507 (1989).

[60] T. Oguchi, Theory of spin-wave interactions in ferro- and antiferromagnetism, Phys. Rev. **117**, 117 (1960).

[61] B.-G. Liu, Low-temperature properties of the quasi-two-dimensional antiferromagnetic Heisenberg model, Phys. Rev. B **41**, 9563 (1990).

[62] N. Majlis, S. Selzer, and G. C. Strinati, Dimensional crossover in the magnetic properties of highly anisotropic antiferromagnets, Phys. Rev. B **45**, 7872 (1992).

[63] N. Majlis, S. Selzer, and G. C. Strinati, Dimensional crossover in the magnetic properties of highly anisotropic antiferromagnets. II. Paramagnetic phase, Phys. Rev. B **48**, 957 (1993).

[64] A. A. Khajetoorians, J. Wiebe, B. Chilian, and R. Wiesendanger, Realizing all-spin-based logic operations atom by atom, Science **332**, 1062 (2011).

[65] T. Jungwirth, X. Marti, P. Wadley, and J. Wunderlich, Antiferromagnetic spintronics, Nat. Nanotechnol. **11**, 231 (2016).

[66] V. Baltz, A. Manchon, M. Tsoi, T. Moriyama, T. Ono, and Y. Tserkovnyak, Antiferromagnetic spintronics, Rev. Mod. Phys. **90**, 015005 (2018).

[67] R. Cheng, J. Xiao, Q. Niu, and A. Brataas, Spin Pumping and Spin-Transfer Torques in Antiferromagnets, Phys. Rev. Lett. **113**, 057601 (2014).

[68] R. Wiesendanger, Spin mapping at the nanoscale and atomic scale, Rev. Mod. Phys. **81**, 1495 (2009).

[69] M. Gibertini, M. Koperski, A. F. Morpurgo, and K. S. Novoselov, Magnetic 2D materials and heterostructures, Nat. Nanotechnol. **14**, 408 (2019).

[70] F. Garcia-Gaitan and B. K. Nikolić, Fate of entanglement in magnetism under Lindbladian or non-Markovian dynamics and conditions for their transition to Landau-Lifshitz-Gilbert classical dynamics, arXiv:2303.17596.

[71] M. Sayad, R. Rausch, and M. Potthoff, Inertia effects in the real-time dynamics of a quantum spin coupled to a Fermi sea, Europhys. Lett. **116**, 17001 (2016).

[72] A. Mitrofanov and S. Urazhdin, Nonclassical Spin Transfer Effects in an Antiferromagnet, Phys. Rev. Lett. **126**, 037203 (2021).

[73] M. D. Petrović, P. Mondal, A. E. Feiguin, and B. K. Nikolić, Quantum Spin Torque Driven Transmutation of an Antiferromagnetic Mott Insulator, Phys. Rev. Lett. **126**, 197202 (2021).

Geometrical torque on magnetic moments coupled to a correlated antiferromagnet

— Supplemental Material —

Nicolas Lenzing,[1] David Krüger,[1] and Michael Potthoff[1,2]

[1] *University of Hamburg, Department of Physics, Notkestraße 9-11, 22607 Hamburg, Germany*

[2] *The Hamburg Centre for Ultrafast Imaging, Luruper Chaussee 149, 22761 Hamburg, Germany*

Section A: SO(2) symmetry analysis. The retarded spin susceptibility is defined as

$$\chi_{ii',\alpha\alpha'}(t) = -i\Theta(t)\langle[s_{i\alpha}(t), s_{i'\alpha'}(0)]\rangle, \qquad (7)$$

where Θ is the step function, $s_{i\alpha}(t) = e^{iH_{el}t}s_{i\alpha}e^{-iH_{el}t}$, and $\langle\cdots\rangle$ is the ground-state expectation value. Fourier transformation to frequency space yields the Lehmann representation in terms of an energy eigenbasis $\{|\Psi_n\rangle\}$:

$$\chi_{ii',\alpha\alpha'}(\omega) = \sum_n \left(\frac{\langle\Psi_0|s_{i\alpha}|\Psi_n\rangle\langle\Psi_n|s_{i'\alpha'}|\Psi_0\rangle}{\omega + i\eta - (E_n - E_0)}\right.$$
$$\left. - \frac{\langle\Psi_0|s_{i'\alpha'}|\Psi_n\rangle\langle\Psi_n|s_{i\alpha}|\Psi_0\rangle}{\omega + i\eta - (E_0 - E_n)}\right). \qquad (8)$$

We have the relation $\chi_{ii',\alpha\alpha'}(\omega)^* = \chi_{ii',\alpha\alpha'}(-\omega)$. The spectral density $-(1/\pi)\text{Im}\chi_{ii',\alpha\alpha'}(\omega) = \chi_{ii',\alpha\alpha'}(\omega) - \chi_{ii',\alpha\alpha'}(-\omega)/2i$ is an antisymmetric function of ω.

In the AF phase with order parameter $\boldsymbol{m} = m\boldsymbol{e}_z$, there is a remaining SO(2) symmetry of the nondegenerate energy eigenstates under spin rotations around $\boldsymbol{e}_z$, which is unitarily represented by $U_R = e^{-is_{\text{tot},z}\varphi}$ on the Fock space with the z-component of the total spin $\boldsymbol{s}_{\text{tot}} = \sum_i \boldsymbol{s}_i$ as the unbroken generator and the rotation angle φ. We have $U_R^\dagger|\Psi_n\rangle = e^{i\phi_n}|\Psi_n\rangle$ with phases ϕ_n. Since $\boldsymbol{s}_i$ is a vector operator, we have $U_R^\dagger s_{i\alpha}U_R = \sum_\beta R_{\alpha\beta}s_{i\beta}$, where $\underline{R} = \underline{R}(\varphi)$ is the standard real 3×3 matrix representation of SO(2) rotations around $\boldsymbol{e}_z$. Hence, the first matrix element in Eq. (4) can be written as $\langle\Psi_0|U_R U_R^\dagger s_{i\alpha}U_R U_R^\dagger|\Psi_n\rangle = \sum_\beta R_{\alpha\beta}(\varphi)e^{i\phi_0}\langle\Psi_0|s_{i\beta}|\Psi_n\rangle e^{-i\phi_n}$. The phase factors cancel with those from the second matrix element, and we thus find: $\chi_{ii',\alpha\alpha'}(\omega) = \sum_{\beta\beta'} R_{\alpha\beta}(\varphi)\chi_{ii',\beta\beta'}(\omega)R_{\beta'\alpha'}^T(\varphi)$, i.e., $[\underline{\chi}_{ii'}(\omega), \underline{R}(\varphi)] = 0$ for all i, i' and φ. It is easily verified directly that this implies

$$\underline{\chi}_{ii'}(\omega) = \begin{pmatrix} \chi_{ii',xx}(\omega) & \chi_{ii',xy}(\omega) & 0 \\ -\chi_{ii',xy}(\omega) & \chi_{ii',xx}(\omega) & 0 \\ 0 & 0 & \chi_{ii',zz}(\omega) \end{pmatrix}, \quad (9)$$

i.e., there are only 3 independent entries for each pair i, i' (note that R is reducible, and furthermore Schur's lemma does not apply to representations over $\mathbb{R}$).

Section B: Spatial symmetries. With Eq. (8), we immediately see that the spin-Berry curvature is related to the spin susceptibility via

$$\Omega_{mm',\alpha\alpha'} = -iJ^2\frac{\partial}{\partial\omega}\chi_{i_m i_{m'},\alpha\alpha'}(\omega)\Big|_{\omega=0} \qquad (10)$$

up to correction terms of order J^3, see Eq. (5). Therefore, the same reasoning as above can be applied to the spin-Berry curvature tensor and yields the same result for its structure:

$$\underline{\Omega}_{mm'} = \begin{pmatrix} \Omega_{mm',xx} & \Omega_{mm',xy} & 0 \\ -\Omega_{mm',xy} & \Omega_{mm',xx} & 0 \\ 0 & 0 & \Omega_{mm',zz} \end{pmatrix}. \qquad (11)$$

In addition, for a given pair of sites i_m and $i_{m'}$, we may consider a combined transformation $T \circ I$, composed of the space inversion $\boldsymbol{R}_i \mapsto \boldsymbol{R}_{i_m} - \boldsymbol{R}_i$ with respect to i_m followed by the translation $\boldsymbol{R}_i \mapsto \boldsymbol{R}_i + (\boldsymbol{R}_{i_m} - \boldsymbol{R}_{i_{m'}})$ with the translation vector $\boldsymbol{R}_{i_m} - \boldsymbol{R}_{i_{m'}}$. $T \circ I$ is a discrete symmetry of the hypercubic lattice and interchanges i_m with $i_{m'}$. This implies that the Hamiltonian commutes with the standard unitary (and also Hermitian) representation U_{TI} of $T \circ I$.

For i_m and $i_{m'}$ in the same sublattice, the symmetry-broken ground state is an eigenstate of U_{TI} as well. Analogously to the SO(2) spin-rotation symmetry discussed above, we can thus immediately see from the analysis of the matrix elements in Eq. (4) that $\Omega_{mm',\alpha\alpha'} = \Omega_{m'm,\alpha\alpha'}$. For the spin-Berry curvature we have the additional antisymmetry, $\Omega_{mm',\alpha\alpha'} = -\Omega_{m'm,\alpha'\alpha}$, which follows from Eq. (3). With this we get $\Omega_{mm',\alpha\alpha'} = -\Omega_{mm',\alpha'\alpha}$, i.e., for each pair m, m', the spin-Berry curvature tensor is antisymmetric in the indices α, α' separately. Hence, with Eq. (11), we see that only the elements $\Omega_{mm',xy} = -\Omega_{mm',yx}$ can be nonzero. Analogously, for the spin susceptibility, the $T \circ I$ symmetry of the Hamiltonian implies $\chi_{ii',\alpha\alpha'}(\omega) = \chi_{i'i,\alpha\alpha'}(\omega)$. With the additional symmetry, $\chi_{ii',\alpha\alpha'}(0) = \chi_{i'i,\alpha'\alpha}(0)$, which follows from Eq. (8), this implies that the susceptibility matrix Eq. (9) is diagonal for $\omega = 0$.

For i_m and $i_{m'}$ in different sublattices, we concatenate the transformation $T \circ I$ with a flip F of the z-component of all spins. This is unitarily represented by U_F, which is

defined via $U_{\rm F}^\dagger c_{i\uparrow} U_{\rm F} = c_{i\downarrow}$ and $U_{\rm F}^\dagger c_{i\downarrow} U_{\rm F} = c_{i\uparrow}$. We have $[U_{\rm F}, U_{\rm TI}] = 0$ and $[U_{\rm F}, H_{\rm el}] = 0$. The symmetry-broken ground state and the corresponding excited states are eigenstates of $U \equiv U_{\rm TI} U_{\rm F}$. Hence, we find for the $\alpha = \alpha'$ matrix elements

$$
\begin{aligned}
&\langle \Psi_0 | s_{i_m \alpha} | \Psi_n \rangle \langle \Psi_n | s_{i_{m'} \alpha} | \Psi_0 \rangle \\
&= \langle \Psi_0 | U^\dagger s_{i_m \alpha} U | \Psi_n \rangle \langle \Psi_n | U^\dagger s_{i_{m'} \alpha} U | \Psi_0 \rangle \\
&= \langle \Psi_0 | s_{i_{m'} \alpha} | \Psi_n \rangle \langle \Psi_n | s_{i_m \alpha} | \Psi_0 \rangle \,,
\end{aligned}
\tag{12}
$$

and thus $\Omega_{mm',\alpha\alpha} = \Omega_{m'm,\alpha\alpha}$. With the antisymmetry of the full tensor, $\Omega_{mm',\alpha\alpha'} = -\Omega_{m'm,\alpha'\alpha}$, we thus find $\Omega_{mm',\alpha\alpha} = 0$. On the other hand,

$$
\begin{aligned}
&\langle \Psi_0 | s_{i_m x} | \Psi_n \rangle \langle \Psi_n | s_{i_{m'} y} | \Psi_0 \rangle \\
&= \langle \Psi_0 | U^\dagger s_{i_m x} U | \Psi_n \rangle \langle \Psi_n | U^\dagger s_{i_{m'} y} U | \Psi_0 \rangle \\
&= -\langle \Psi_0 | s_{i_{m'} x} | \Psi_n \rangle \langle \Psi_n | s_{i_m y} | \Psi_0 \rangle \,,
\end{aligned}
\tag{13}
$$

since $U_{\rm F}^\dagger s_{ix} U_{\rm F} = s_{ix}$ but $U_{\rm F}^\dagger s_{iy} U_{\rm F} = -s_{iy}$. This implies $\Omega_{mm',xy} = -\Omega_{m'm,xy}$, and with the antisymmetry of the full tensor we find $\Omega_{mm',xy} = \Omega_{mm',yx}$. Together with Eq. (11), we see that $\Omega_{mm',xy} = 0$, and hence the matrix $\underline{\Omega}_{mm'} = 0$ in Eq. (11).

Summing up, for arbitrary sites i_m and $i_{m'}$ we have

$$
\underline{\Omega}_{mm'} = \begin{pmatrix} 0 & \Omega & 0 \\ -\Omega & 0 & 0 \\ 0 & 0 & 0 \end{pmatrix} \,,
\tag{14}
$$

and hence the spin-Berry curvature is fixed by a single real number $\Omega \equiv \Omega_{mm',xy} = \Omega_{m'm,xy}$. Furthermore, $\Omega = 0$ if $i_m, i_{m'}$ belong to different sublattices.

Section C: Random phase approximation. The random phase approximation (RPA) represents a standard weak-coupling approach to the magnetic susceptibility, see, e.g., Refs. 41, 42. It can be motivated in various ways, for example, via a partial diagrammatic summation. In general, the RPA Luttinger-Ward functional $\Phi[\bm{G}]$ [43, 44] is given as the sum of the two closed and self-consistently renormalized first-order diagrams, i.e., by the Hartree and the Fock diagram. For the Hubbard model the Fock diagram vanishes such that we are left with

$$
\Phi[\bm{G}] = U \sum_i \frac{1}{\beta^2} \sum_{n,n'} G_{ii,\uparrow}(i\omega_n) G_{ii,\downarrow}(i\omega_{n'}) \,.
\tag{15}
$$

Here, i runs over the sites of the hypercubic lattice, $\sigma = \uparrow, \downarrow$ refers to the spin projection relative to the z axis, n labels the fermionic Matsubara frequencies $i\omega_n$, and β is the inverse temperature. Computations are done in the zero-temperature limit $1/\beta \to 0$, which is taken at the end. Furthermore, $G_{ii,\sigma}$ denotes the local one-particle Green's function at site i in the symmetry-broken AF state, as obtained within the self-consistent

Hartree-Fock approximation. The Hartree-Fock self-energy is generated by the Luttinger-Ward functional: $\Sigma_{ii,\sigma}(i\omega_n) = \beta \delta\Phi/\delta G_{ii\sigma}(i\omega_n) = U\beta^{-1} \sum_n G_{ii,-\sigma}(i\omega_n) = U \langle c_{i-\sigma}^\dagger c_{i-\sigma} \rangle$.

On the two-particle level, the RPA yields a local and frequency-independent irreducible vertex

$$
\Gamma_{\sigma,-\sigma}^{\rm (loc)}(i\omega_n, i\omega_{n'}) = \beta^2 \frac{\delta^2 \Phi}{\delta G_{ii,-\sigma}(i\omega_n) \delta G_{ii,\sigma}(i\omega_{n'})} = U \,.
\tag{16}
$$

This means that there is no feedback of two-particle correlations on the single-particle Green's function. The structureless vertex allows us to easily get the transversal magnetic susceptibility $\chi_{rs,+-}(\bm{k}, \omega) = \langle\langle s_{r,\bm{k}}^+ ; s_{s,\bm{k}}^- \rangle\rangle_\omega$ as the solution of a strongly simplified Bethe-Salpether equation in the particle-hole channel:

$$
\underline{\chi}_{+-}(\bm{k}, i\nu_n) = \underline{\chi}_{+-}^{(0)}(\bm{k}, i\nu_n) + \underline{\chi}_{+-}^{(0)}(\bm{k}, i\nu_n) U \underline{\chi}_{+-}(\bm{k}, i\nu_n) \,.
\tag{17}
$$

Here, $\underline{\chi}_{+-}$ is a 2×2 matrix in the sublattice degrees of freedom, and $\underline{\chi}_{+-}^{(0)}$ the bare susceptibility matrix, which is computed with the Hartree-Fock one-particle propagators. The equation is diagonal in the wave vectors $\bm{k}$ of the first magnetic Brillouin zone and in the bosonic Matsubara frequencies $i\nu_n$. The transversal susceptibility χ_{+-} is related to the susceptibility tensor $\chi_{\alpha\alpha'}$ introduced in Eqs. (7) and (8), via $\chi_{+-} = 2(\chi_{xx} - i\chi_{xy})$. From the renormalized zeroth-order diagram, we get the Hartree-Fock susceptibility in Eq. (17) as

$$
\begin{aligned}
\chi_{rs,+-}^{(0)}(\bm{k}, i\nu_n) =\ & \frac{-1}{L} \frac{1}{\beta} \sum_{\bm{q},n'} G_{sr,\uparrow}(\bm{q}, i\omega_{n'}) \\
& \times\ G_{rs,\downarrow}(\bm{q}+\bm{k}, i\nu_n + i\omega_{n'}) \,.
\end{aligned}
\tag{18}
$$

After performing the summation over the fermionic frequencies $i\omega_n$ analytically, we can replace $i\nu_n \mapsto \nu + i\eta$ to find the retarded susceptibility on the real-frequency axis. The frequency derivative in Eq. (10) is done numerically. In the thermodynamical limit, the $\bm{q}$ sum over the magnetic Brillouin zone in Eq. (18) can be converted into a $\bm{q}$-space integration. The latter is computed in two or three dimensions via a standard adaptive $\bm{q}$-space integration technique for arbitrary $\nu \in \mathbb{R}$ and for each allowed wave vector $\bm{k}$ in the magnetic Brillouin zone of a finite lattice with L sites and periodic boundary conditions. Practical computations are performed at a finite Lorentzian broadening parameter $\eta > 0$ replacing the infinitesimal η, and convergence with respect to L is controlled by runs for different system sizes L. The main numerical error is due to extrapolation of the data for $\eta \to 0$.

Section D: Magnon spectrum of an antiferromagnet. In the strong-U limit of the Hubbard model, the low-

energy physics is captured by the $s = 1/2$ antiferromagnetic Heisenberg model

$$H = J_{\mathrm{H}} \sum_{\langle ij \rangle} \left(\frac{1}{2}(s_i^+ s_j^- + s_i^- s_j^+) + \Delta s_i^z s_j^z \right) \quad (19)$$

with $J_{\mathrm{H}} = 4t^2/U$ and $\Delta = 1$. An anisotropy parameter $\Delta > 1$ can be used to discuss the effect of opening a gap in the dispersion. The sum runs over all nearest-neighbor pairs $\langle ij \rangle$.

We apply the standard Holstein-Primakoff transfomation for the model on the bipartite hypercubic lattice with dimension D. For sites i in sublattice A, the spin operators are expressed in terms of bosonic annihilators and creators, i.e.,

$$
\begin{aligned}
s_i^z &= s - a_i^\dagger a_i \,, \\
s_i^+ &= \sqrt{2s}\sqrt{1 - \frac{\hat{n}_i}{2s}} a_i \,, \\
s_i^- &= \sqrt{2s}\, a_i^\dagger \sqrt{1 - \frac{\hat{n}_i}{2s}} \,,
\end{aligned}
\quad (20)
$$

while for sites $j \in B$

$$
\begin{aligned}
s_j^z &= -s + b_j^\dagger b_j \,, \\
s_j^+ &= \sqrt{2s}\, b_j^\dagger \sqrt{1 - \frac{\hat{n}_j}{2s}} \,, \\
s_j^- &= \sqrt{2s}\sqrt{1 - \frac{\hat{n}_j}{2s}} b_j \,.
\end{aligned}
\quad (21)
$$

The transformed Hamiltonian reads

$$H = J_{\mathrm{H}} s \sum_{\langle ij \rangle} [(a_i b_j + a_i^\dagger b_j^\dagger) + \Delta(a_i^\dagger a_i + b_j^\dagger b_j)] - \frac{L}{2} z J_{\mathrm{H}} \Delta s^2 \,, \quad (22)$$

where $z = 2D$ is the coordination number, and L is the number of lattice sites. Quartic and higher-order magnon interaction terms resulting for the expansion of the square root have been disregarded.

We drop the additive energy constant and block-diagonalize H via Fourier transformation:

$$a_i = \frac{1}{\sqrt{L/2}} \sum_{\boldsymbol{k}} e^{-i\boldsymbol{k}\boldsymbol{R}_i} a_{\boldsymbol{k}} \,, \quad b_j = \frac{1}{\sqrt{L/2}} \sum_{\boldsymbol{k}} e^{i\boldsymbol{k}\boldsymbol{R}_j} b_{\boldsymbol{k}} \,. \quad (23)$$

Here, $\boldsymbol{R}_i$ are the translation vectors of the magnetic A sublattice (the same for $\boldsymbol{R}_j$ and the B sublattice), consisting of $L/2$ unit cells, and $\boldsymbol{k}$ is an allowed wave vector of the first magnetic Brillouin zone (mBz). Defining $\gamma_{\boldsymbol{k}} \equiv \sum_{\boldsymbol{\delta}} \cos(\boldsymbol{k}\boldsymbol{\delta})$ with nearest-neighbor vectors $\boldsymbol{\delta}$, the Fourier-transformed model reads as

$$H = J_{\mathrm{H}} s \sum_{\boldsymbol{k}} [\gamma_{\boldsymbol{k}}(a_{\boldsymbol{k}} b_{\boldsymbol{k}} + b_{\boldsymbol{k}}^\dagger a_{\boldsymbol{k}}^\dagger) + z\Delta(a_{\boldsymbol{k}} a_{\boldsymbol{k}}^\dagger + b_{\boldsymbol{k}}^\dagger b_{\boldsymbol{k}})] \quad (24)$$

and can be diagonalized by Bogoliubov transformation

$$a_{\boldsymbol{k}} = u_{\boldsymbol{k}} \alpha_{\boldsymbol{k}} + v_{\boldsymbol{k}} \beta_{\boldsymbol{k}}^\dagger \,, \quad b_{\boldsymbol{k}} = u_{\boldsymbol{k}} \beta_{\boldsymbol{k}} + v_{\boldsymbol{k}} \alpha_{\boldsymbol{k}}^\dagger \quad (25)$$

with real coefficients $u_{\boldsymbol{k}}$ and $v_{\boldsymbol{k}}$. We require

$$u_{\boldsymbol{k}}^2 - v_{\boldsymbol{k}}^2 = 1 \,, \quad (26)$$

to ensure that $\alpha_{\boldsymbol{k}}$ and $\beta_{\boldsymbol{k}}$ satisfy bosonic commutation relations, as well as

$$2z\Delta u_{\boldsymbol{k}} v_{\boldsymbol{k}} + \gamma_{\boldsymbol{k}}(u_{\boldsymbol{k}}^2 + v_{\boldsymbol{k}}^2) \overset{!}{=} 0 \,, \quad (27)$$

as usual, to get the Hamiltonian to the form

$$H = J_{\mathrm{H}} s \sum_{\boldsymbol{k}} \omega(\boldsymbol{k})(\alpha_{\boldsymbol{k}}^\dagger \alpha_{\boldsymbol{k}} + \beta_{\boldsymbol{k}}^\dagger \beta_{\boldsymbol{k}}) \,, \quad (28)$$

where we again dropped an unimportant constant energy term. The magnon spectrum consists of two degenerate branches with dispersion $J_{\mathrm{H}} s\, \omega(\boldsymbol{k})$ given by

$$\omega(\boldsymbol{k}) = \sqrt{(z\Delta)^2 - \gamma_{\boldsymbol{k}}^2} = \sqrt{z^2\Delta^2 - \left(\sum_{\boldsymbol{\delta}} \cos(\boldsymbol{k}\boldsymbol{\delta})\right)^2} \,. \quad (29)$$

Close to $\boldsymbol{k} = 0$ and in the isotropic case $\Delta = 1$, the dispersion $J_{\mathrm{H}} s\, \omega(\boldsymbol{k})$ is linear,

$$\omega(\boldsymbol{k}) = 2\sqrt{D}k + \mathcal{O}(k^3) \,, \quad (30)$$

while for $\Delta > 1$ the spectrum is gapped, and $\omega(\boldsymbol{k}) = 2S\sqrt{\Delta^2 - 1} + \mathcal{O}(k^2)$.

From the conditions Eq. (26) and Eq. (27), we can deduce the well-known results

$$
\begin{aligned}
u_{\boldsymbol{k}}^2 &= \frac{1}{2}\left(\frac{z\Delta}{\sqrt{(z\Delta)^2 - \gamma_{\boldsymbol{k}}^2}} + 1\right) = \frac{1}{2}\left(\frac{z\Delta}{\omega(\boldsymbol{k})} + 1\right) \,, \\
v_{\boldsymbol{k}}^2 &= \frac{1}{2}\left(\frac{z\Delta}{\sqrt{(z\Delta)^2 - \gamma_{\boldsymbol{k}}^2}} - 1\right) = \frac{1}{2}\left(\frac{z\Delta}{\omega(\boldsymbol{k})} - 1\right)
\end{aligned}
\quad (31)
$$

and

$$u_{\boldsymbol{k}} v_{\boldsymbol{k}} = -\frac{\gamma_{\boldsymbol{k}}}{2\sqrt{(z\Delta)^2 - \gamma_{\boldsymbol{k}}^2}} = -\frac{\gamma_{\boldsymbol{k}}}{2\omega(\boldsymbol{k})} \,, \quad (32)$$

see Refs. [47], [48].

Section E: Computing the spin-Berry curvature from the magnon Hamiltonian. The contribution of the magnon excitations to the spin-Berry curvature is obtained from

$$\Omega_{mm',\alpha\alpha'} = -2J^2 \mathrm{Im} \sum_{\boldsymbol{k},\eta=1,2} \frac{\langle 0|s_{i_m}^\alpha|\boldsymbol{k},\eta\rangle\langle\boldsymbol{k},\eta|s_{i_{m'}}^{\alpha'}|0\rangle}{(E_0 - E_{\boldsymbol{k}})^2} \,, \quad (33)$$

where $|\boldsymbol{k},1\rangle \equiv \alpha_{\boldsymbol{k}}^{\dagger}|0\rangle$ and $|\boldsymbol{k},2\rangle \equiv \beta_{\boldsymbol{k}}^{\dagger}|0\rangle$ are the single-magnon states. Following Eq. (14), it is sufficient to compute $\Omega_{mm'} = \Omega_{mm',xy} = -\Omega_{mm',yx}$. Furthermore, $\Omega_{mm'} \neq 0$ only for i_m and $i_{m'}$ in the same sublattice, as also argued in section B. Expressing the spin components in terms of the Bogoliubov operators,

$$
\begin{aligned}
s_i^+ &= \sqrt{2s}\frac{1}{\sqrt{L/2}}\sum_{\boldsymbol{k}} e^{-i\boldsymbol{k}\boldsymbol{R}_i}(u_{\boldsymbol{k}}\alpha_{\boldsymbol{k}} + v_{\boldsymbol{k}}\beta_{\boldsymbol{k}}^{\dagger}) \\
s_i^- &= \sqrt{2s}\frac{1}{\sqrt{L/2}}\sum_{\boldsymbol{k}} e^{i\boldsymbol{k}\boldsymbol{R}_i}(u_{\boldsymbol{k}}\alpha_{\boldsymbol{k}}^{\dagger} + v_{\boldsymbol{k}}\beta_{\boldsymbol{k}}) \\
s_j^+ &= \sqrt{2s}\frac{1}{\sqrt{L/2}}\sum_{\boldsymbol{k}} e^{-i\boldsymbol{k}\boldsymbol{R}_j}(u_{\boldsymbol{k}}\beta_{\boldsymbol{k}}^{\dagger} + v_{\boldsymbol{k}}\alpha_{\boldsymbol{k}}) \\
s_j^- &= \sqrt{2s}\frac{1}{\sqrt{L/2}}\sum_{\boldsymbol{k}} e^{i\boldsymbol{k}\boldsymbol{R}_j}(u_{\boldsymbol{k}}\beta_{\boldsymbol{k}} + v_{\boldsymbol{k}}\alpha_{\boldsymbol{k}}^{\dagger}), \quad (34)
\end{aligned}
$$

we find

$$
\begin{aligned}
\langle 0|s_i^x|\boldsymbol{k},1\rangle\langle \boldsymbol{k},1|s_{i'}^y|0\rangle &= i\frac{s}{L}u_{\boldsymbol{k}}^2 e^{-i\boldsymbol{k}(\boldsymbol{R}_i-\boldsymbol{R}_{i'})}, \\
\langle 0|s_i^x|\boldsymbol{k},2\rangle\langle \boldsymbol{k},2|s_{i'}^y|0\rangle &= -i\frac{s}{L}v_{\boldsymbol{k}}^2 e^{i\boldsymbol{k}(\boldsymbol{R}_i-\boldsymbol{R}_{i'})} \quad (35)
\end{aligned}
$$

for i, i' in sublattice A, and

$$
\begin{aligned}
\langle 0|s_j^x|\boldsymbol{k},1\rangle\langle \boldsymbol{k},1|s_{j'}^y|0\rangle &= i\frac{s}{L}v_{\boldsymbol{k}}^2 e^{-i\boldsymbol{k}(\boldsymbol{R}_j-\boldsymbol{R}_{j'})}, \\
\langle 0|s_j^x|\boldsymbol{k},2\rangle\langle \boldsymbol{k},2|s_{j'}^y|0\rangle &= -i\frac{s}{L}u_{\boldsymbol{k}}^2 e^{i\boldsymbol{k}(\boldsymbol{R}_j-\boldsymbol{R}_{j'})} \quad (36)
\end{aligned}
$$

for j, j' in sublattice B. This implies

$$
\begin{aligned}
\mathrm{Im}\sum_{\eta=1,2}\langle 0|s_i^x|\boldsymbol{k},\eta\rangle\langle \boldsymbol{k},\eta|s_{i'}^y|0\rangle &= \frac{s}{L}\cos(\boldsymbol{k}(\boldsymbol{R}_i-\boldsymbol{R}_{i'})) \\
\mathrm{Im}\sum_{\eta=1,2}\langle 0|s_j^x|\boldsymbol{k},\eta\rangle\langle \boldsymbol{k},\eta|s_{j'}^y|0\rangle &= -\frac{s}{L}\cos(\boldsymbol{k}(\boldsymbol{R}_j-\boldsymbol{R}_{j'})),
\end{aligned}
$$
$$(37)$$

and finally we get

$$
\Omega_{mm'} = \mp\frac{1}{s}\frac{J^2}{J_{\mathrm{H}}^2}\frac{2}{L}\sum_{\boldsymbol{k}}^{\mathrm{mBz}}\frac{\cos(\boldsymbol{k}(\boldsymbol{R}_{i_m}-\boldsymbol{R}_{i_{m'}}))}{\omega(\boldsymbol{k})^2}, \quad (38)
$$

where the upper sign refers to $i_m, i_{m'}$ in sublattice A and the lower for $i_m, i_{m'}$ in sublattice B. Recall that $\Omega_{mm'} = 0$ if $i_m, i_{m'}$ belong to different sublattices.

Eq. (38) can be evaluated numerically. For $D = 3$, for example, we find

$$
\Omega_{\mathrm{loc}} \approx -0.084\frac{J^2}{J_{\mathrm{H}}^2} \quad (39)
$$

for the local element of the SBC with $i_m = i_{m'}$ in sublattice A.

Section F: Different dimensions and distance dependence. In the thermodynamic limit $L \to \infty$ (and in the isotropic case $\Delta = 1$), the convergence of the resulting integral in Eq. (38) over the magnetic Brillouin zone decisively depends on the lattice dimension D. We consider the critical contribution of the long-wave-length magnons by integrating over a D-dimensional ball around $\boldsymbol{k} = 0$ with small cutoff radius k_c, such that we can make use of Eq. (30), i.e., of the linearity and isotropy of the magnon dispersion for $k \to 0$:

$$
\Omega_{mm'} \sim \lim_{\kappa \to 0}\int_{\kappa}^{k_c} dk\, k^{D-1}\frac{1}{\omega(\boldsymbol{k})^2} \propto \lim_{\kappa \to 0}\int_{\kappa}^{k_c} dk\, k^{D-1}\frac{1}{k^2}. \quad (40)
$$

This yields

$$
\Omega_{mm'} \sim \begin{cases} \kappa^{D-2} & \text{for } D \geq 3 \\ \ln\kappa & \text{for } D = 2 \\ 1/\kappa & \text{for } D = 1 \end{cases}. \quad (41)
$$

For $\kappa \to 0$, the spin-Berry curvature diverges for $D = 1$ and $D = 2$. We conclude that a meaningful theory is obtained in dimensions $D \geq 3$ only.

The magnitude of the spin-Berry curvature decreases with increasing distance $\boldsymbol{R} \equiv \boldsymbol{R}_{i_m} - \boldsymbol{R}_{i_{m'}}$. For $D \geq 3$ its dependence in the large-R limit is governed by long-wave-length magnon excitations, and we have:

$$
\Omega(R) \propto \int_0^{k_c} dk\, k^{D-1}\int d\Omega \frac{\cos(kR\cos\theta)}{k^2}, \quad (42)
$$

where $\int d\Omega$ denotes the surface integral over the $(D-1)$-dimensional unit sphere, and θ the angle between $\boldsymbol{k}$ and $\boldsymbol{R}$. Furthermore, we made use of Eq. (30) for k smaller than the cutoff k_c. We note that the distance dependence at large R is isotropic. Substituting $kR \to k$ in the one-dimensional k integral immediately yields

$$
\Omega(R) \propto \frac{1}{R^{D-2}}. \quad (43)
$$

For $D = 3$, we have $\Omega(R) \propto 1/R$. In the infinite-D limit, we expect a local spin-Berry curvature

To compute the local element $m = m'$ of the spin-Berry curvature Eq. (38) in this limit, we start from the representation

$$
\Omega_{\mathrm{loc}} = -\frac{1}{s}\frac{J^2}{J_{\mathrm{H}}^2}\int_{-\infty}^{\infty} dx\, \rho_D(x)\frac{1}{z^2\Delta^2 - Dx^2}, \quad (44)
$$

where, for dimension D, we have defined the density function

$$
\rho_D(x) = \frac{2}{L}\sum_{\boldsymbol{k}}^{\mathrm{mBz}}\delta(x - \gamma_{\boldsymbol{k}}/\sqrt{D}), \quad (45)
$$

and where we have used Eq. (29). We have $z = 2D$ for the D-dimensional hypercubic lattice and, in the Heisenberg

limit of the Hubbard model, $J_{\rm H} = 4t^2/U = 4t^{*2}/DU$, when using the scaling $t = t^*/\sqrt{D}$ with $t^* = $ const. In the limit $D \to \infty$, this scaling of the hopping ensures that the kinetic energy of the Hubbard model remains nontrivial and balances the interaction term [59]. Moreover, the density function converges to a Gaussian [59]:

$$\rho_D(x) \to \rho_\infty(x) = \frac{1}{2\sqrt{\pi}} \exp\left(-\frac{x^2}{4}\right) . \qquad (46)$$

In the Heisenberg limit and with the scaled hopping, we thus have

$$\Omega_{\rm loc}(D) = -\frac{1}{s} \frac{J^2 U^2}{16t^{*4}} \int_{-\infty}^{\infty} \frac{dx \rho_D(x)}{4\Delta^2 - x^2/D} , \qquad (47)$$

which for $D \to \infty$, and assuming $s = 1/2$ and $\Delta = 1$ converges to

$$\Omega_{\rm loc}(\infty) = -\frac{1}{32t^{*4}} J^2 U^2 . \qquad (48)$$

This represents the mean-field value of the (lcoal) spin-Berry curvature in the antiferromagnetic state at large U.

To compare with the result obtained for $D = 3$, we must use the same scaling of the hopping. This yields

$$\Omega_{\rm loc}(3) \approx -0.084 \frac{J^2 U^2}{16t^{*4}} D^2 \bigg|_{D=3} \approx 1.51 \cdot \Omega(\infty). \qquad (49)$$

For lattice dimensions $D > 3$ we find: $\Omega_{\rm loc}(4) \approx 1.22\,\Omega(\infty)$, $\Omega_{\rm loc}(5) \approx 1.16\,\Omega(\infty)$, $\Omega_{\rm loc}(6) \approx 1.12\,\Omega(\infty)$. Hence, given the standard scaling of the hopping with D, the absolute value of $\Omega_{\rm loc}(D)$ increases with decreasing D and finally, for $D = 2$ diverges.

Finally, when addressing the dimensional crossover [61–63], we consider the Heisenberg model given by Eq. (19) again, but with spatially anisotropic nearest-neighbor exchange couplings $J_{\rm H} \equiv J_{\rm H,x} = J_{\rm H,y} \geq J_{\rm H,z}$. Proceeding analogously to Sec. C, one ends up with a modified magnon dispersion only:

$$\omega(\boldsymbol{k}) = \sqrt{(z_{\rm eff}\Delta)^2 - \gamma_{\boldsymbol{k}}'^2} . \qquad (50)$$

Here, we have defined an effective coordination number $z_{\rm eff} = 2(J_{\rm H,x} + J_{\rm H,y} + J_{\rm H,z})/J_{\rm H,x}$. Furthermore, $\gamma_{\boldsymbol{k}}' := 2(J_{\rm H,x} \cos k_x + J_{\rm H,y} \cos k_y + J_{\rm H,z} \cos k_z)/J_{\rm H,x}$.

Section G: Spin dynamics. The equations of motion Eq. (1) for the classical spins comprise the conventional (Hamiltonian) and the geometrical spin torque, see Eq. (2). In the weak-J limit, the former results from the local direct exchange J as well as from the indirect RKKY-type exchange. We have:

$$\dot{\boldsymbol{S}}_m = J\langle \boldsymbol{s}_{i_m}\rangle^{(0)} \times \boldsymbol{S}_m + J^2 \sum_{m'} \underline{\chi}_{i_m i_{m'}}(0)\boldsymbol{S}_{m'} \times \boldsymbol{S}_m + \sum_{\alpha} \sum_{m'\alpha'} \Omega_{m'm,\alpha'\alpha}(\boldsymbol{S})\dot{S}_{m'\alpha'}\boldsymbol{e}_\alpha \times \boldsymbol{S}_m , \qquad (51)$$

where $\langle \ldots \rangle^{(0)}$ denotes the expectation value at $J = 0$. For the non-vanishing components of the spin susceptibility and of the spin-Berry curvature on sublattice A we have

$$\chi_{ii'} \equiv \chi_{ii',xx}(0) = \chi_{ii',yy}(0) = -\frac{z\Delta}{J_{\rm H}} \frac{2}{L} \sum_{\boldsymbol{k}}^{\rm mBz} \frac{\cos \boldsymbol{k}(\boldsymbol{R}_i - \boldsymbol{R}_{i'})}{\omega(\boldsymbol{k})^2} \qquad (52)$$

and

$$\Omega_{mm'} \equiv \Omega_{mm',xy} = -\Omega_{mm',yx} = -\frac{1}{s} \frac{J^2}{J_{\rm H}^2} \frac{2}{L} \sum_{\boldsymbol{k}}^{\rm mBz} \frac{\cos(\boldsymbol{k}(\boldsymbol{R}_{i_m} - \boldsymbol{R}_{i_{m'}}))}{\omega(\boldsymbol{k})^2} . \qquad (53)$$

Specializing Eq. (51) for $M = 1$, i.e., for a single classical spin, we get

$$\dot{\boldsymbol{S}}_1 = \boldsymbol{T}_1^{(\rm H)} \times \boldsymbol{S}_1 + \Omega_{11}(\boldsymbol{e}_z \times \dot{\boldsymbol{S}}_1) \times \boldsymbol{S}_1 , \qquad (54)$$

where

$$\boldsymbol{T}_1^{(\rm H)} = J\langle \boldsymbol{s}_{i_1}\rangle^{(0)} + J^2 \chi_{i_1 i_1}(\boldsymbol{e}_z \times \boldsymbol{S}_m) \times \boldsymbol{e}_z . \qquad (55)$$

With

$$\underline{T}_1^{(\rm H)} = \begin{pmatrix} 0 & -T_{1,z}^{(\rm H)} & T_{1,y}^{(\rm H)} \\ T_{1,z}^{(\rm H)} & 0 & -T_{1,x}^{(\rm H)} \\ -T_{1,y}^{(\rm H)} & T_{1,x}^{(\rm H)} & 0 \end{pmatrix} \qquad (56)$$

the cross product can be written as a matrix-vector product, $\boldsymbol{T}_1^{(\mathrm{H})} \times \boldsymbol{S}_1 = \underline{\boldsymbol{T}}_1^{(\mathrm{H})} \boldsymbol{S}_1$, and the equation of motion reads:

$$\dot{\boldsymbol{S}}_1 = \frac{1}{1 - \Omega_{11} S_{1z}} \underline{\boldsymbol{T}}_1^{(\mathrm{H})} \boldsymbol{S}_1 . \tag{57}$$

The classical spin undergoes a purely precessional dynamics around the z axis, but with a renormalized precession frequency. The renormalization is due to the local spin-Berry curvature $\Omega_{\mathrm{loc}} = \Omega_{11}$ and is the strongest for $\Omega_{\mathrm{loc}} = \mathcal{O}(1)$. Right at $\Omega_{\mathrm{loc}} = 1/S_{1z}$, the precession frequency diverges. This implies that the spin dynamics is no longer adiabatic and the theory breaks down.

In case of two classical spins, $M = 2$, the equations of motion (51) can be cast into the form

$$\begin{aligned}
\dot{\boldsymbol{S}}_1 &= \boldsymbol{T}_1^{(\mathrm{H})} \times \boldsymbol{S}_1 + \boldsymbol{T}_1^{(\mathrm{geo})} \times \boldsymbol{S}_1 , \\
\dot{\boldsymbol{S}}_2 &= \boldsymbol{T}_2^{(\mathrm{H})} \times \boldsymbol{S}_2 + \boldsymbol{T}_2^{(\mathrm{geo})} \times \boldsymbol{S}_2 ,
\end{aligned} \tag{58}$$

where

$$\begin{aligned}
\boldsymbol{T}_1^{(\mathrm{H})} &= J\langle \boldsymbol{s}_{i_1}\rangle^{(0)} + J^2 \chi_{i_1 i_1}(\boldsymbol{e}_z \times \boldsymbol{S}_1) \times \boldsymbol{e}_z + J^2 \chi_{i_1 i_2}(\boldsymbol{e}_z \times \boldsymbol{S}_2) \times \boldsymbol{e}_z , \\
\boldsymbol{T}_2^{(\mathrm{H})} &= J\langle \boldsymbol{s}_{i_2}\rangle^{(0)} + J^2 \chi_{i_2 i_2}(\boldsymbol{e}_z \times \boldsymbol{S}_2) \times \boldsymbol{e}_z + J^2 \chi_{i_2 i_1}(\boldsymbol{e}_z \times \boldsymbol{S}_1) \times \boldsymbol{e}_z .
\end{aligned} \tag{59}$$

and

$$\begin{aligned}
\boldsymbol{T}_1^{(\mathrm{geo})} &= \Omega_{11}(\boldsymbol{e}_z \times \dot{\boldsymbol{S}}_1) \times \boldsymbol{S}_1 + \Omega_{12}(\boldsymbol{e}_z \times \dot{\boldsymbol{S}}_2) \times \boldsymbol{S}_1 \\
\boldsymbol{T}_2^{(\mathrm{geo})} &= \Omega_{22}(\boldsymbol{e}_z \times \dot{\boldsymbol{S}}_2) \times \boldsymbol{S}_2 + \Omega_{12}(\boldsymbol{e}_z \times \dot{\boldsymbol{S}}_1) \times \boldsymbol{S}_2 .
\end{aligned} \tag{60}$$

Here, we have assumed that the two spins couple to sites in the same sublattice, as otherwise the spin-Berry curvature vanishes. The local spin-Berry curvature term can be treated in the same way as in the $M = 1$ case, while the nonlocal term can be written as a matrix-vector product:

$$\begin{aligned}
(1 - \Omega_{11} S_{1z})\dot{\boldsymbol{S}}_1 &= \boldsymbol{T}_1^{(\mathrm{H})} \times \boldsymbol{S}_1 - \Omega_{12}\underline{\mathcal{A}}_1^{(z)} \dot{\boldsymbol{S}}_2 , \\
(1 - \Omega_{22} S_{2z})\dot{\boldsymbol{S}}_2 &= \boldsymbol{T}_2^{(\mathrm{H})} \times \boldsymbol{S}_2 - \Omega_{12}\underline{\mathcal{A}}_2^{(z)} \dot{\boldsymbol{S}}_1 ,
\end{aligned} \tag{61}$$

with

$$\underline{\mathcal{A}}_m^{(z)} = \begin{pmatrix} -S_{mz} & 0 & 0 \\ 0 & -S_{mz} & 0 \\ S_{mx} & S_{my} & 0 \end{pmatrix} . \tag{62}$$

This allows us to cast the equations of motion into an explicit system of ordinary differential equations:

$$\begin{pmatrix} \dot{\boldsymbol{S}}_1 \\ \dot{\boldsymbol{S}}_2 \end{pmatrix} = \mathcal{M}^{-1} \begin{pmatrix} \boldsymbol{T}_1^{(\mathrm{H})} \times \boldsymbol{S}_1 \\ \boldsymbol{T}_2^{(\mathrm{H})} \times \boldsymbol{S}_2 \end{pmatrix} . \tag{63}$$

Here, the 6×6 matrix

$$\mathcal{M} = \begin{pmatrix} (1 - \Omega_{11} S_{1z})\mathbf{1} & \Omega_{12}\underline{\mathcal{A}}_1^{(z)} \\ \Omega_{12}\underline{\mathcal{A}}_2^{(z)} & (1 - \Omega_{22} S_{2z})\mathbf{1} \end{pmatrix} \tag{64}$$

is given in terms of the components of the spin-Berry curvature tensor. Eq. (63) demonstrates that the effect of the geometrical spin torque is not simply additive and hence does not directly compete with the conventional spin torque, but enters the spin dynamics as a multiplicative (matrix) factor.

The determinant of $\mathcal{M}$ can be computed analytically:

$$\det \mathcal{M} = (1 - \Omega_{11} S_{1z})(1 - \Omega_{11} S_{2z})\left[(1 - \Omega_{11} S_{1z})(1 - \Omega_{22} S_{2z}) - \Omega_{12}^2 S_{1z} S_{2z}\right]^2 . \tag{65}$$

The theory breaks down if $\det \mathcal{M} = 0$. We consider $\det \mathcal{M}$ as a function of the local elements $\Omega_{\mathrm{loc}} = \Omega_{11} = \Omega_{22}$ and assume that the nonlocal elements are small, $\Omega_{\mathrm{nonloc}} = |\Omega_{12}| \ll \Omega_{\mathrm{loc}}$. We immediately see that the zeros of $\det \mathcal{M}$ are of the order of unity. This implies that anomalous spin dynamics, which is substantially affected by the geometrical spin torque, is expected if $\Omega_{\mathrm{loc}} = \mathcal{O}(1)$ and thus close to, but yet different from the zeros of $\mathcal{M}$.

5.3 − Linearisation of the Effective EOM

Above, the derivation of effective equations of motion for classical impurity spins coupled to an antiferromagnet was limited to cases with one and two impurity spins. More generally one can consider a setup where there is one classical spin at every lattice site. For an antiferromagnetic quantum-classical exchange interaction, the classical spins order antiferromagnetically as well and exhibit collective excitations, namely, spin wave excitations. Here, linearisation is used in an attempt to derive the corresponding dispersion relation and analyse the impact of the geometrical spin torque.

Linearisation can be an effective way to analyse the dynamics of a (nonlinear) differential equation around an equilibrium point. A typical procedure is to determine an equilibrium configuration as a starting point and then Taylor expand the differential equation up to linear order in the deviation from that point. Here the differential equation of interest is the effective equation of motion for the classical spins

$$\frac{d\boldsymbol{S}}{dt} = f(\boldsymbol{S}), \tag{5.30}$$

where $f(\boldsymbol{S}) = (\mathbb{1} - \underline{M}(\boldsymbol{S}))^{-1}\underline{A}(\boldsymbol{S})\boldsymbol{S}$ is a nonlinear function of the complete classical spin configuration $\boldsymbol{S} = (\boldsymbol{S}_1, \ldots, \boldsymbol{S}_M)$. The Taylor expansion up to linear order is given by

$$\frac{d\boldsymbol{S}}{dt} = f(\boldsymbol{S}^*) + \left.\frac{\partial f}{\partial \boldsymbol{S}}\right|_{\boldsymbol{S}^*} \delta\boldsymbol{S} + \mathcal{O}(\delta\boldsymbol{S}^2) \tag{5.31}$$

with the equilibrium configuration $\boldsymbol{S}^*$ and $\delta\boldsymbol{S} := (\boldsymbol{S} - \boldsymbol{S}^*)$. Of course, ignoring everything beyond linear order requires $\delta\boldsymbol{S}$, i.e., the deviation from the equilibrium configuration, to be small. Since $\boldsymbol{S}^*$ is an equilibrium configuration, its time derivative is zero and thus $\dot{\boldsymbol{S}} = \delta\dot{\boldsymbol{S}}$. The quantum-classical coupling considered here is positive such that in the ground state local quantum spins and classical spins are ordered antiferromagnetically. On the other hand, this also means that the classical spins are ordered antiferromagnetically among themselves, with the classical spins in sublattice A (B) pointing in negative (positive) z direction. Expanding the factor $(\mathbb{1} - \underline{M}(\boldsymbol{S}))^{-1}$ yields

$$(\mathbb{1} - \underline{M}(\boldsymbol{S}))^{-1} = (\mathbb{1} - \underline{M}(\boldsymbol{S}^*))^{-1} + \sum_m (\partial_{\boldsymbol{S}_m}(\mathbb{1} - \underline{M}(\boldsymbol{S}))^{-1})|_{\boldsymbol{S}=\boldsymbol{S}^*}\delta\boldsymbol{S}_m + \mathcal{O}(\delta\boldsymbol{S}^2). \tag{5.32}$$

The derivative can be evaluated by the rule

$$\partial_x \underline{U}^{-1}(x) = -\underline{U}^{-1}(\partial_x \underline{U})\underline{U}^{-1}$$
$$\Rightarrow \partial_{\boldsymbol{S}_m}(\mathbb{1} - \underline{M}(\boldsymbol{S}))^{-1} = (\mathbb{1} - \underline{M}(\boldsymbol{S}))^{-1}(\partial_{\boldsymbol{S}_m}\underline{M}(\boldsymbol{S}))(\mathbb{1} - \underline{M}(\boldsymbol{S}))^{-1}. \tag{5.33}$$

For the other factor, one gets

$$\underline{A}(\boldsymbol{S}) = \underline{A}(\boldsymbol{S}^*) + \sum_m \partial_{\boldsymbol{S}_m}\underline{A}(\boldsymbol{S})|_{\boldsymbol{S}=\boldsymbol{S}^*}\delta\boldsymbol{S}_m + \mathcal{O}(\delta\boldsymbol{S}^2). \tag{5.34}$$

Plugging both expressions into the EOM and ignoring terms of order $\delta \boldsymbol{S}^2$, it is

$$
\begin{aligned}
\delta \dot{\boldsymbol{S}} &= \left[(\mathbb{1} - \underline{M}^*)^{-1} \underline{A}^* + (\mathbb{1} - \underline{M}^*)^{-1} \sum_m \partial_{\boldsymbol{S}_m} \underline{A}|_{\boldsymbol{S}^*} \delta \boldsymbol{S}_m + \sum_m (\partial_{\boldsymbol{S}_m} (\mathbb{1} - \underline{M})^{-1})|_{\boldsymbol{S}^*} \delta \boldsymbol{S}_m \underline{A}^* \right] \boldsymbol{S} \\
&= (\mathbb{1} - \underline{M}^*)^{-1} \underline{A}^* \delta \boldsymbol{S} + \left[(\mathbb{1} - \underline{M}^*)^{-1} \sum_m \partial_{\boldsymbol{S}_m} \underline{A}|_{\boldsymbol{S}^*} \delta \boldsymbol{S}_m + \sum_m (\partial_{\boldsymbol{S}_m} (\mathbb{1} - \underline{M})^{-1})|_{\boldsymbol{S}^*} \delta \boldsymbol{S}_m \underline{A}^* \right] \boldsymbol{S}^* \\
&= (\mathbb{1} - \underline{M}^*)^{-1} \left[\underline{A}^* \delta \boldsymbol{S} + \sum_m \partial_{\boldsymbol{S}_m} \underline{A}|_{\boldsymbol{S}^*} \delta \boldsymbol{S}_m \boldsymbol{S}^* + \sum_m (\partial_{\boldsymbol{S}_m} \underline{M})|_{\boldsymbol{S}^*} (\mathbb{1} - \underline{M}^*)^{-1} \delta \boldsymbol{S}_m \underline{A}^* \boldsymbol{S}^* \right] \\
&= (\mathbb{1} - \underline{M}^*)^{-1} \left[\underline{A}(\boldsymbol{S}^*) \delta \boldsymbol{S} + \sum_m \partial_{\boldsymbol{S}_m} \underline{A}|_{\boldsymbol{S}^*} \delta \boldsymbol{S}_m \boldsymbol{S}^* \right] ,
\end{aligned}
\tag{5.35}
$$

where $\underline{M}^* \equiv \underline{M}(\boldsymbol{S}^*)$, $\underline{A}^* \equiv \underline{A}(\boldsymbol{S}^*)$, and in the last equality it was used that $\underline{A}(\boldsymbol{S}^*) \boldsymbol{S}^*$ vanishes since $\boldsymbol{v}_m(\boldsymbol{S}^*)$ points into the z direction for all m. In the next step, one can calculate the equilibrium quantities $\underline{M}^*$ and $\underline{A}^*$. Starting from the definition, this gives

$$
\begin{aligned}
M^*_{m\alpha,m'\alpha'} &= \sum_{\beta\gamma} \varepsilon_{\beta\gamma\alpha} S^*_{m\gamma} \Omega_{m'\alpha',m\beta} \\
&= \sum_{\beta} \varepsilon_{\beta z\alpha} S^*_{mz} \Omega_{m'\alpha',m\beta} \\
&= \mp |S| \sum_{\beta} \delta_{\alpha\alpha'} \varepsilon_{\beta z\alpha} \Omega_{m'\alpha',m\beta},
\end{aligned}
\tag{5.36}
$$

where sign $\mp$ signifies whether m is from sublattice A (-) or from sublattice B (+). However, for the spin-Berry curvature computed in publication [II] this sign does not matter, since $\Omega_{m'\alpha',m\beta}$ is nonzero only when m and m' are from the same sublattice and picks up a minus sign when changing the sublattice. Also note that $\underline{M}^*$ is symmetric under the exchange $m, \alpha \leftrightarrow m', \alpha'$. The matrix $\underline{A}$ can be written as

$$
\begin{aligned}
A_{m\alpha,m'\alpha'} &= \delta_{mm'} B^{(m)}_{\alpha\alpha'} = \delta_{mm'} \sum_{\beta} \varepsilon_{\alpha'\alpha\beta} v_{m\beta} \\
&= \delta_{mm'} \sum_{\beta} \varepsilon_{\alpha'\alpha\beta} (J \langle s_{i_m,\beta} \rangle + J^2 \sum_{m''\gamma} \chi_{mm'',\beta\gamma}(0) S_{m''\gamma}).
\end{aligned}
\tag{5.37}
$$

In this section, $\langle \boldsymbol{s}_{i_m} \rangle$ denotes the expectation value at $J = 0$, dropping the superscript (0) used in [II]. Here both $\langle \boldsymbol{s}_{i_m} \rangle$ and $\underline{\chi}_{mm'}(0)$ are independent of the $\boldsymbol{S}_m$'s. This means that

$$
\begin{aligned}
(\partial_{S_{m\alpha}} \underline{A}(\boldsymbol{S}))_{m'\alpha',m''\alpha''} &= \delta_{m'm''} J^2 \partial_{S_{m\alpha}} \sum_{\tilde{m}\beta\gamma} \varepsilon_{\alpha''\alpha'\beta} \chi_{m'\tilde{m},\beta\gamma}(0) S_{\tilde{m}\gamma} \\
&= \delta_{m'm''} J^2 \sum_{\beta} \varepsilon_{\alpha''\alpha'\beta} \chi_{m'm,\beta\alpha}(0) \\
&= \delta_{m'm''} J^2 \varepsilon_{\alpha''\alpha'\alpha} \chi_{m'm,\alpha\alpha}(0)
\end{aligned}
\tag{5.38}
$$

since in the antiferromagnetic model it is $\chi_{m'm,\beta\alpha}(0) = \chi_{m'm,\alpha\alpha}(0)\delta_{\beta\alpha}$. The derivatives of $\underline{A}$

are actually independent of the classical spins. Furthermore, one has

$$
\begin{aligned}
A_{m\alpha,m'\alpha'}(\boldsymbol{S}^*) &= \delta_{mm'} \sum_{\beta} \varepsilon_{\alpha'\alpha\beta}(J \langle s_{i_m,\beta} \rangle + J^2 \sum_{m''} \chi_{mm'',\beta z}(0) S^*_{m''z}) \\
&= \delta_{mm'}\varepsilon_{\alpha'\alpha z} J \langle s_{i_m,z} \rangle ,
\end{aligned}
\tag{5.39}
$$

which is antisymmetric under the exchange $m, \alpha \leftrightarrow m', \alpha'$. Therefore, the first term of the linearised EOM can be written as $\underline{X}\delta\boldsymbol{S}$ with an antisymmetric matrix

$$
\begin{aligned}
X_{m\alpha m'\alpha'} &= \sum_{m''\alpha''} (\mathbb{1} - \underline{M}(\boldsymbol{S}^*))^{-1}_{m\alpha m''\alpha''} A(\boldsymbol{S}^*)_{m''\alpha''m'\alpha'} \\
&= J \sum_{m''\alpha''} (\mathbb{1} - \underline{M}(\boldsymbol{S}^*))^{-1}_{m\alpha m''\alpha''} \delta_{m''m'} \langle s_{i_{m''},z} \rangle \varepsilon_{\alpha'\alpha''z}.
\end{aligned}
\tag{5.40}
$$

Similarly, one can formulate the second term in the form $\underline{\widetilde{X}}\delta\boldsymbol{S}$. Writing everything in components, yields

$$
\begin{aligned}
(\mathbb{1} - \underline{M}^*)^{-1} \sum_{m\alpha} \partial_{S_{m\alpha}}\underline{A}\delta S_{m\alpha}\boldsymbol{S}^* &= \sum_{m\alpha} \left[\left((\mathbb{1} - \underline{M}^*)^{-1}\partial_{S_{m\alpha}}\underline{A} \right) \boldsymbol{S}^* \right] \delta S_{m\alpha} \\
&= \sum_{m\alpha} \sum_{\substack{m'\alpha' \\ m''\alpha''}} \left[\left((\mathbb{1} - \underline{M}^*)^{-1}\partial_{S_{m\alpha}}\underline{A} \right)_{m'\alpha',m''\alpha''} S^*_{m''\alpha''}\boldsymbol{e}_{m'\alpha'} \right] \delta S_{m\alpha} \\
&=: \sum_{m'\alpha'} \sum_{m\alpha} \widetilde{X}_{m'\alpha',m\alpha}\delta S_{m\alpha}\boldsymbol{e}_{m'\alpha'},
\end{aligned}
\tag{5.41}
$$

where $\underline{\widetilde{X}}$ is defined as

$$
\begin{aligned}
\widetilde{X}_{m'\alpha',m\alpha} &= \sum_{m''\alpha''} \left((\mathbb{1} - \underline{M}^*)^{-1}\partial_{S_{m\alpha}}\underline{A} \right)_{m'\alpha',m''\alpha''} S^*_{m''\alpha''} \\
&= J^2 \sum_{\tilde{m}\tilde{\alpha}} (\mathbb{1} - \underline{M}^*)^{-1}_{m'\alpha',\tilde{m}\tilde{\alpha}} \varepsilon_{z\tilde{\alpha}\alpha}\chi_{\tilde{m}m,\alpha\alpha}(0) S^*_{\tilde{m}z}.
\end{aligned}
\tag{5.42}
$$

All in all, the linearised EOM can be written as $\delta\dot{\boldsymbol{S}} = \underline{\widetilde{M}}\delta\boldsymbol{S}$ with $\underline{\widetilde{M}} := \underline{X} + \underline{\widetilde{X}}$. In components one has

$$
\widetilde{M}_{m\alpha m'\alpha'} = \sum_{\tilde{m}} (\mathbb{1} - \underline{M}^*)^{-1}_{m,\tilde{m}}\varepsilon_{\alpha'\alpha z} \left(J\delta_{\tilde{m}m'} \langle s_{i_{\tilde{m}},z} \rangle - J^2\chi_{\tilde{m}m',\alpha'\alpha'}(0) S^*_{\tilde{m}z} \right),
\tag{5.43}
$$

where it was used that $(\mathbb{1} - \underline{M}^*)^{-1}_{m\alpha,\tilde{m}\tilde{\alpha}} = (\mathbb{1} - \underline{M}^*)^{-1}_{m,\tilde{m}}\delta_{\alpha\tilde{\alpha}}$. The linearised EOM can be formally solved by

$$
\delta\boldsymbol{S}(t) = \exp\left(\underline{\widetilde{M}}t \right)\delta\boldsymbol{S}_0.
\tag{5.44}
$$

To get a sensible solution, it is important for the eigenvalues λ_i of $\underline{\widetilde{M}}$ to have a real part $\text{Re}\{\lambda_i\} \leq 0$. Otherwise, there are unphysical modes that diverge exponentially over time. Imaginary eigenvalues, for instance, can be ensured if the matrix $\underline{\widetilde{M}}$ is antisymmetric. The first term

$$(\mathbb{1} - \underline{M}^*)^{-1}_{m,m'} \left\langle s_{i_{m'},z} \right\rangle J\varepsilon_{\alpha'\alpha z} \tag{5.45}$$

is indeed antisymmetric under exchange of $m, \alpha \leftrightarrow m', \alpha'$. This can be seen as follows: $(\mathbb{1} - \underline{M}^*)^{-1}$ is only nonzero for m and m' from the same sublattice and also symmetric under their exchange. If m and m' are from the same sublattice, then $\left\langle s_{i_m,z} \right\rangle = \left\langle s_{i_{m'},z} \right\rangle$, i.e., the term as a whole is symmetric under the exchange of m and m'. Under the exchange of α and α', it is obviously antisymmetric and thus antisymmetric under the simultaneous exchange. The second term is

$$\sum_{\tilde{m}}(\mathbb{1} - \underline{M}^*)^{-1}_{m,\tilde{m}}J^2\varepsilon_{z\alpha\alpha'}\chi_{\tilde{m}m',\alpha'\alpha'}(0)S^*_{\tilde{m}z} \tag{5.46}$$

and is antisymmetric under the exchange of α and α'. This is because the only nonzero terms have $\alpha \neq \alpha'$ and $\alpha, \alpha' \in \{x, y\}$ such that $\underline{\chi}$ is invariant under the exchange. Concerning the spatial indices, note that $(\mathbb{1} - \underline{M}^*)^{-1}$ and $\underline{\chi}$ are symmetric under their exchange and, due to $(\mathbb{1} - \underline{M}^*)^{-1}$ being nonzero only for spatial indices from the same sublattice, $\tilde{m}$ only takes on values from the same sublattice as m. When m and m' are from the same sublattice their exchange leaves the expression invariant, since $(\mathbb{1} - \underline{M}^*)^{-1}_{m\tilde{m}}$ and $\chi_{\tilde{m}m',\alpha'\alpha'}(0)$ have the sublattice translation invariance and $\tilde{m}$ does not change sublattices, such that $S^*_{\tilde{m}z}$ remains unchanged too. On the other hand, for m and m' from different sublattices, one has $\sum_{\tilde{m}}(\mathbb{1} - \underline{M}^*)^{-1}_{m,\tilde{m}} = \sum_{\tilde{m}}(\mathbb{1} - \underline{M}^*)^{-1}_{m',\tilde{m}}$ as $(\mathbb{1} - \underline{M}^*)^{-1}_{m,\tilde{m}}$ depends only on the distance between sites m and $\tilde{m}$, and has the same value on both sublattices. For $\underline{\chi}$ there is also no significant change since its spatial indices are from different sublattices before and after the exchange. Furthermore, it still has sublattice translational invariance. However, after the exchange of m and m' from different sublattices the sum in (5.46) filters $\tilde{m}$ for a different sublattice, such that $S^*_{\tilde{m}z}$ changes sign, and we have an overall sign change.

Therefore, (5.46) is antisymmetric under the simultaneous exchange of spatial and spin indices only if the spatial indices are from the same sublattice and symmetric otherwise. In conclusion, $\widetilde{\underline{M}}$ as a whole is not antisymmetric under said exchange in general. Although this does not exclude $\widetilde{\underline{M}}$ from only having eigenvalues with real part $\mathrm{Re}\{\lambda_i\} \leq 0$, it is found numerically that for the parameter configurations we are interested in $\widetilde{\underline{M}}$ typically does have some eigenvalues with $\mathrm{Re}\{\lambda_i\} > 0$. Thus, for our purposes the linearisation of the EOM is not beneficial.

6 – Dissipative Spin Dynamics

So far, in the derivation of spin-only theories for classical spins coupled to a quantum mechanical host system, the main focus was on the geometrical spin torque connected to the antisymmetric part of the magnetic susceptibility χ. In contrast, the contribution of the symmetric part of χ has been mentioned only briefly. This contribution gives rise to the Gilbert damping, which can be crucial for the spin dynamics. Above, it is was shown how this can be derived via linear response theory. This chapter introduces another kind of response theory called adiabatic response theory (ART) [71, 72], which focusses on an expansion around the adiabatic limit rather than the strength of the quantum-classical interaction. ART can be seen as a finite temperature generalisation of ASD. Its derivation and subsequent application to spin dynamics will take up the first part of this chapter. It will be shown that ART yields expressions for both, the spin-Berry curvature and the Gilbert damping. This will provide the theoretical foundation for the results of publication [III] found at the end of this chapter. There, the results for the Gilbert damping from ART and LRT will be compared at the example of a single impurity spin coupled to a one-dimensional host system of conduction electrons. The publication also deals with dissipative spin dynamics of multiple impurities in two dimensions. Overall, the nonlocalities of the Gilbert damping will play a decisive role.

6.1 – Adiabatic Response Theory

The question answered by adiabatic response theory is how a driven system responds to a slow perturbation. The connection to adiabaticity comes due to the perturbation being slow and the theory can be seen as a generalisation of concepts like adiabatic evolution and Berry's phase. Berry and Robbins [71] developed the first theory of this kind using the microcanonical ensemble from statistical mechanics. More recently, Campisi, Denisov and Hänggi [72] developed an adiabatic response theory for open quantum systems using a canonical ensemble. The important steps in the derivation of the latter theory will be reproduced here with the goal to apply it to quantum-classical spin systems. The starting point is a quantum-classical Hamiltonian of the form

$$\mathcal{H}(\boldsymbol{S}) = H_{\mathrm{B}} + H_{\mathrm{SB}} + H_{\mathrm{S}}(\boldsymbol{S}) \tag{6.1}$$

describing a system coupled to an ideal thermal bath of fixed temperature T modelled by the bath Hamiltonian H_{B}, the system bath coupling H_{SB}, and the system Hamiltonian H_{S} that depends on time-dependent classical parameters $\boldsymbol{S}(t) = (\boldsymbol{S}_1(t), \boldsymbol{S}_2(t), \dots)$, which in this thesis are classical spins. As usual, the system Hamiltonian can itself be separated in a similar fashion as $H_{\mathrm{S}}(\boldsymbol{S}) = H_{\mathrm{qu}} + H_{\mathrm{int}}(\boldsymbol{S}) + H_{\mathrm{cl}}(\boldsymbol{S})$. Further important quantities are the

instantaneous equilibrium density operator and the corresponding partition function [72]

$$\rho^{\mathrm{eq}}(\boldsymbol{S}(t)) = \frac{e^{-\beta \mathcal{H}(\boldsymbol{S}(t))}}{Z(\boldsymbol{S}(t))}, \quad Z(\boldsymbol{S}(t)) = \mathrm{tr}\left(e^{-\beta \mathcal{H}(\boldsymbol{S}(t))}\right). \tag{6.2}$$

Also recall the definition of a Heisenberg operator $O(t) = U^\dagger(t)OU(t)$, where $U(t)$ is the time evolution operator, and its expectation value as well as the equilibrium expectation defined by

$$\langle O(t) \rangle := \mathrm{tr}(\rho^{\mathrm{eq}}(\boldsymbol{S}(0))O(t)) = \mathrm{tr}(\rho(t)O), \quad \langle O \rangle_{\boldsymbol{S}(t)}^{\mathrm{eq}} := \mathrm{tr}(\rho^{\mathrm{eq}}(\boldsymbol{S}(t))O). \tag{6.3}$$

An important quantity that will be needed to develop the theory is the dissipated work W_{dis}, which is defined as the difference between the work performed when changing the external parameters and the adiabatic work. The adiabatic work is the work that is performed if the change of parameters is infinitely slow. The work due to parameter change is defined as [101]

$$W = \int_0^t dt' \dot{\boldsymbol{\lambda}} \nabla_{\boldsymbol{\lambda}} H_{\boldsymbol{\lambda}}, \tag{6.4}$$

where $\boldsymbol{\lambda}$ denotes the external parameters and $H_{\boldsymbol{\lambda}}$ the parameter dependent Hamiltonian. Note that in the quantum case W is represented by an operator but is not an observable [102, 103]. On the other hand, the adiabatic work is given by

$$\begin{aligned} W_{\mathrm{ad}} &= \int_{\boldsymbol{\lambda}_0}^{\boldsymbol{\lambda}_t} d\boldsymbol{\lambda} \, \langle \nabla_{\boldsymbol{\lambda}} H_{\boldsymbol{\lambda}} \rangle_{\boldsymbol{\lambda}}^{\mathrm{eq}} \\ &= \int_0^t dt' \dot{\boldsymbol{\lambda}} \, \langle \nabla_{\boldsymbol{\lambda}} H_{\boldsymbol{\lambda}} \rangle_{\boldsymbol{\lambda}}^{\mathrm{eq}}. \end{aligned} \tag{6.5}$$

For the dissipated work, one has

$$\begin{aligned} W_{\mathrm{dis}} &= W - W_{\mathrm{ad}} \\ &= \int_0^t dt' \dot{\boldsymbol{\lambda}} \left[\nabla_{\boldsymbol{\lambda}} H_{\boldsymbol{\lambda}} - \langle \nabla_{\boldsymbol{\lambda}} H_{\boldsymbol{\lambda}} \rangle_{\boldsymbol{\lambda}}^{\mathrm{eq}} \right]. \end{aligned} \tag{6.6}$$

The reason that the dissipated work is useful in adiabatic response theory is that it will be very small if the evolution of the system is near adiabatic. Concretely, its nonequilibrium expectation value in the adiabatic limit is zero [72]. Thus, the important physical quantities can be perturbatively expanded up to first order in W_{dis}, namely, the expectation values of observables. This will be shown using the example of quantum-classical spin systems. Here, the "external" parameters are the classical spins, i.e., $\boldsymbol{\lambda} = \boldsymbol{S}(t) = (\boldsymbol{S}_1(t), \boldsymbol{S}_2(t), \dots)$ and $W_{\mathrm{dis}} = \int_0^t dt' \sum_m \dot{\boldsymbol{S}}_m(t') \left[\nabla_{\boldsymbol{S}_m} H(t') - \langle \nabla_{\boldsymbol{S}_m} H \rangle_{\boldsymbol{S}_{t'}}^{\mathrm{eq}} \right]$. For an interaction term of the form

$H_{\text{int}} = J \sum_m \boldsymbol{s}_{i_m} \boldsymbol{S}_m$, it is

$$W_{\text{dis}} = J \int_0^t dt' \sum_m \dot{\boldsymbol{S}}_m(t') \left[\boldsymbol{s}_{i_m}(t') - \langle \boldsymbol{s}_{i_m} \rangle_{\boldsymbol{S}_{t'}}^{\text{eq}} \right]$$

$$= J \int_0^t dt' \sum_m \dot{\boldsymbol{S}}_m(t') \Delta \boldsymbol{s}_{i_m}(t'). \tag{6.7}$$

Writing the work as $W = \mathcal{H}(\boldsymbol{S}(t), t) - \mathcal{H}(\boldsymbol{S}_0)$, one can prove the important intermediate result

$$\begin{aligned}
\langle O(t) e^{-\beta \mathcal{H}(\boldsymbol{S}(t),t)} e^{\beta \mathcal{H}(\boldsymbol{S}_0)} \rangle_{\boldsymbol{S}_0}^{\text{eq}} &= \langle U^\dagger(t) O U(t) e^{-\beta \mathcal{H}(\boldsymbol{S}(t),t)} e^{\beta \mathcal{H}(\boldsymbol{S}_0)} \rangle_{\boldsymbol{S}_0}^{\text{eq}} \\
&= \text{tr}\left(\rho^{\text{eq}}(\boldsymbol{S}_0) U^\dagger(t) O U(t) e^{-\beta \mathcal{H}(\boldsymbol{S}(t),t)} e^{\beta \mathcal{H}(\boldsymbol{S}_0)} \right) \\
&\overset{(6.2)}{=} \frac{Z(\boldsymbol{S}(t))}{Z(\boldsymbol{S}_0)} \text{tr}\left(e^{-\beta \mathcal{H}(\boldsymbol{S}_0)} U^\dagger(t) O U(t) U^\dagger(t) \frac{e^{-\beta \mathcal{H}(\boldsymbol{S}(t))}}{Z(\boldsymbol{S}(t))} U(t) e^{\beta \mathcal{H}(\boldsymbol{S}_0)} \right) \\
&= e^{-\beta W_{\text{ad}}} \text{tr}(O \rho^{\text{eq}}(\boldsymbol{S}(t))) \\
&= e^{-\beta W_{\text{ad}}} \langle O \rangle_{\boldsymbol{S}(t)}^{\text{eq}}, \tag{6.8}
\end{aligned}$$

which can also be written in the form

$$\langle O(t) e^{-\beta \mathcal{H}(\boldsymbol{S}(t),t)} e^{\beta(\mathcal{H}(\boldsymbol{S}(t),t) - W_{\text{dis}})} \rangle_{\boldsymbol{S}_0}^{\text{eq}} = \langle O \rangle_{\boldsymbol{S}(t)}^{\text{eq}}. \tag{6.9}$$

Further, one needs the operator expansion formula [104]

$$\begin{aligned}
e^{\beta A} e^{-\beta(A-B)} &= \mathbb{1} + \int_0^\beta du\, e^{uA} B e^{-u(A-B)} \\
&= \mathbb{1} + \int_0^\beta du\, e^{uA} B e^{-uA} + \mathcal{O}(B^2), \tag{6.10}
\end{aligned}$$

where the first equality can be proven by differentiating both sides with respect to β and exploiting that it is true for $\beta = 0$. Using this, one gets for the difference between the expectation value of an operator $O(t)$ in the Heisenberg picture and the corresponding equilibrium expectation value in the Schrödinger picture:

$$\begin{aligned}
\langle \Delta O(t) \rangle &:= \langle O(t) \rangle - \langle O \rangle_{\boldsymbol{S}(t)}^{\text{eq}} \\
&= \langle O(t) \rangle - \left\langle O(t) e^{-\beta \mathcal{H}(\boldsymbol{S}(t),t)} e^{\beta(\mathcal{H}(\boldsymbol{S}(t),t) - W_{\text{dis}})} \right\rangle_{\boldsymbol{S}_0}^{\text{eq}} \\
&= \int_0^\beta du \left\langle O(t) e^{-u \mathcal{H}(\boldsymbol{S}(t),t)} W_{\text{dis}} e^{u \mathcal{H}(\boldsymbol{S}(t),t)} \right\rangle_{\boldsymbol{S}_0}^{\text{eq}} + \mathcal{O}(W_{\text{dis}}^2). \tag{6.11}
\end{aligned}$$

With the explicit expression of W_{dis} for our spin system and setting $O(t) = J s_{i_m}^{(\alpha)}(t)$, i.e., the αth component of the mth local spin, one has

$$J \langle \Delta s_{i_m}^{(\alpha)}(t) \rangle = J^2 \int_0^t dt' \int_0^\beta du \sum_{m'} \left\langle s_{i_m}^{(\alpha)}(t) e^{-u \mathcal{H}(\boldsymbol{S}(t),t)} \Delta \boldsymbol{s}_{i_{m'}}(t') e^{u \mathcal{H}(\boldsymbol{S}(t),t)} \right\rangle_{\boldsymbol{S}_0}^{\text{eq}} \dot{\boldsymbol{S}}_{m'}(t') - \mathcal{O}(W_{\text{dis}}^2),$$

$$\tag{6.12}$$

where the expectation value in the integrand can be written as

$$\text{tr}\left[\rho(t)s_{i_m}^{(\alpha)}e^{-u\mathcal{H}(\boldsymbol{S}(t))}U(t,t')\Delta\boldsymbol{s}_{i_{m'}}U^\dagger(t,t')e^{u\mathcal{H}(\boldsymbol{S}(t))}\right] \tag{6.13}$$

with $U(t,t') = U(t)U^\dagger(t')$. Up to first order in W_{dis}, one can replace $\rho(t)$ with $\rho^{\text{eq}}(\boldsymbol{S}(t))$. In order to develop adiabtaic response theory, one also has to make the assumption that the correlation function in (6.11) decays quickly compared to the variation of the classical spin, which is, therefore, frozen at $\boldsymbol{S} = \boldsymbol{S}(t)$. This is again justified by the timescale separation between the fast quantum and the slow classical degrees of freedom. Then one can write

$$U(t,t') \approx e^{-i\mathcal{H}(\boldsymbol{S}(t))(t'-t)} \tag{6.14}$$

and replace $\boldsymbol{S}(t')$ with $\boldsymbol{S}(t)$ everywhere. Put together, we can simplify (6.13) as

$$\text{tr}\left[\rho^{\text{eq}}(\boldsymbol{S}(t))s_{i_m}^{(\alpha)}(-iu)\Delta\boldsymbol{s}_{i_{m'}}(t'-t)\right] = \left\langle s_{i_m}^{(\alpha)}(-iu)\Delta\boldsymbol{s}_{i_{m'}}(t'-t)\right\rangle_{\boldsymbol{S}(t)}^{\text{eq}}, \tag{6.15}$$

where it is $s_{i_m}^{(\alpha)}(-iu) = e^{u\mathcal{H}(\boldsymbol{S}(t))}s_{i_m}^{(\alpha)}e^{-u\mathcal{H}(\boldsymbol{S}(t))}$ and we used that $\rho^{\text{eq}}(\boldsymbol{S}(t))$ and $e^{u\mathcal{H}(\boldsymbol{S}(t))}$ commute. All in all, one has the result

$$J\left\langle\Delta s_{i_m}^{(\alpha)}(t)\right\rangle = J^2\int_0^t dt'\int_0^\beta du\sum_{m'}\left\langle s_{i_m}^{(\alpha)}(-iu)\Delta\boldsymbol{s}_{i_{m'}}(t'-t)\right\rangle_{\boldsymbol{S}(t)}^{\text{eq}}\dot{\boldsymbol{S}}_{m'}(t)$$
$$= J^2\sum_{m'\alpha'}K_{i_m i_{m'}}^{(\alpha\alpha')}(\boldsymbol{S}(t))\dot{S}_{m'}^{(\alpha')}(t), \tag{6.16}$$

or in matrix-vector notation

$$J\left\langle\Delta\boldsymbol{s}_{i_m}(t)\right\rangle = J^2\sum_{m'}\underline{K}_{i_m i_{m'}}(\boldsymbol{S}(t))\dot{\boldsymbol{S}}_{m'}. \tag{6.17}$$

Here $\underline{K}$ is a matrix with elements given by

$$K_{i_m i_{m'}}^{(\alpha\alpha')}(\boldsymbol{S}(t)) = \int_0^t dt'\int_0^\beta du\left\langle s_{i_m}^{(\alpha)}(-iu)s_{i_{m'}}^{(\alpha')}(t'-t)\right\rangle_{\boldsymbol{S}(t)}^{\text{eq}}$$
$$-\int_0^t dt'\int_0^\beta du\left\langle s_{i_m}^{(\alpha)}(-iu)\right\rangle_{\boldsymbol{S}(t)}^{\text{eq}}\left\langle s_{i_{m'}}^{(\alpha')}(t'-t)\right\rangle_{\boldsymbol{S}(t)}^{\text{eq}}. \tag{6.18}$$

The single-operator expectation values appearing in the second term are actually time-independent as a straightforward calculation shows

$$\langle\boldsymbol{s}_{i_m}(-iu)\rangle_{\boldsymbol{S}(t)}^{\text{eq}} = \text{tr}\left[\rho^{\text{eq}}(\boldsymbol{S}(t))e^{u\mathcal{H}(\boldsymbol{S}(t))}\Delta\boldsymbol{s}_{i_m}e^{-u\mathcal{H}(\boldsymbol{S}(t))}\right]$$
$$= \text{tr}[\rho^{\text{eq}}(\boldsymbol{S}(t))\Delta\boldsymbol{s}_{i_m}]$$
$$= \langle\boldsymbol{s}_{i_m}\rangle_{\boldsymbol{S}(t)}^{\text{eq}}. \tag{6.19}$$

In the first term of (6.18), one can make the substitution $t' \mapsto \tau = t - t'$ and then rename

$\tau \to t'$. Thus, it is

$$K_{i_m i_{m'}}^{(\alpha\alpha')}(\boldsymbol{S}(t)) = \int_0^t dt' \int_0^\beta du \left\langle s_{i_m}^{(\alpha)}(-iu)s_{i_{m'}}^{(\alpha')}(-t') \right\rangle_{\boldsymbol{S}(t)}^{\text{eq}}$$
$$- \int_0^t dt' \int_0^\beta du \left\langle s_{i_m}^{(\alpha)} \right\rangle_{\boldsymbol{S}(t)}^{\text{eq}} \left\langle s_{i_{m'}}^{(\alpha')} \right\rangle_{\boldsymbol{S}(t)}^{\text{eq}}. \tag{6.20}$$

Like in the case of the magnetic susceptibility in linear response theory, it is useful to separate $\underline{K}$ into a symmetric and an antisymmetric contribution

$$K_{i_m i_{m'}}^{S(\alpha\alpha')} = \frac{1}{2} \int_0^t dt' \int_0^\beta du \left\langle s_{i_m}^{(\alpha)}(-iu)s_{i_{m'}}^{(\alpha')}(-t') + s_{i_{m'}}^{(\alpha')}(-iu)s_{i_m}^{(\alpha)}(-t') \right\rangle_{\boldsymbol{S}(t)}^{\text{eq}}$$
$$- \int_0^t dt' \int_0^\beta du \left\langle s_{i_m}^{(\alpha)} \right\rangle_{\boldsymbol{S}(t)}^{\text{eq}} \left\langle s_{i_{m'}}^{(\alpha')} \right\rangle_{\boldsymbol{S}(t)}^{\text{eq}} \tag{6.21}$$

$$K_{i_m i_{m'}}^{A(\alpha\alpha')} = \frac{1}{2} \int_0^t dt' \int_0^\beta du \left\langle s_{i_m}^{(\alpha)}(-iu)s_{i_{m'}}^{(\alpha')}(-t') - s_{i_{m'}}^{(\alpha')}(-iu)s_{i_m}^{(\alpha)}(-t') \right\rangle_{\boldsymbol{S}(t)}^{\text{eq}}. \tag{6.22}$$

In the literature [71, 72] the antisymmetric part is called geometric magnetism, while the symmetric part is known as geometric friction. The reason for these names is that in the EOM derived by adiabatic response theory the symmetric part has a damping effect, while the antisymmetric part appears in a way similar to the Lorentz force. The latter can be shown as follows. Locally $\underline{K}^A$ is a skew-symmetric 3×3 matrix. In three dimensions, its product with a column vector can be written as a vector product

$$\underline{K}^A = \begin{pmatrix} 0 & -K_3 & K_2 \\ K_3 & 0 & -K_1 \\ -K_2 & K_1 & 0 \end{pmatrix}$$

$$\Rightarrow \underline{K}^A \boldsymbol{A} = \boldsymbol{K}^A \times \boldsymbol{A} \text{ with } \boldsymbol{K}^A = (K_1, K_2, K_3)^\mathsf{T}, \text{ i.e., } K_i^A = -\frac{1}{2} \sum_{jk} \varepsilon_{ijk} K_{jk}^A. \tag{6.23}$$

In terms of spin operators, we have

$$\boldsymbol{K}_{i_m i_{m'}}^A := -\frac{1}{2} \int_0^t dt' \int_0^\beta du \left\langle \boldsymbol{s}_{i_m}(-iu) \times \boldsymbol{s}_{i_{m'}}(-t') \right\rangle. \tag{6.24}$$

Using the symmetric and the antisymmetric part, $\langle \Delta \boldsymbol{s}_{i_m}(t) \rangle$ can be expressed as

$$\langle \Delta \boldsymbol{s}_{i_m}(t) \rangle = J \sum_{m'} \underline{K}_{i_m i_{m'}}(\boldsymbol{S}(t))\dot{\boldsymbol{S}}_{m'}$$
$$= J \sum_{m'} (\underline{K}_{i_m i_{m'}}^S(\boldsymbol{S}(t)) + \underline{K}_{i_m i_{m'}}^A(\boldsymbol{S}(t)))\dot{\boldsymbol{S}}_{m'}. \tag{6.25}$$

In the effective EOM resulting from ART, the full expectation value of the local magnetic moment $\boldsymbol{s}_{i_m}$ is replaced by its equilibrium expectation and its first non-equilibrium correction $\langle \Delta \boldsymbol{s}_{i_m} \rangle$

$$\frac{d\boldsymbol{S}_m}{dt} = J \langle \boldsymbol{s}_{i_m} \rangle_{\boldsymbol{S}(t)}^{\text{eq}} \times \boldsymbol{S}_m + J \langle \Delta \boldsymbol{s}_{i_m} \rangle \times \boldsymbol{S}_m. \tag{6.26}$$

6.2 – Lehmann Representation

Similar to the magnetic susceptibility from linear response theory, it can be advantageous to express the symmetric and the antisymmetric part of the conductance matrix in the instantaneous energy eigenbasis of the system defined by

$$\mathcal{H}(\boldsymbol{S}(t))\,|m,\boldsymbol{S}(t)\rangle = E_m(\boldsymbol{S}(t))\,|m,\boldsymbol{S}(t)\rangle. \tag{6.27}$$

Applied to the integrand of the antisymmetric part of $\underline{K}$, which will be referred to as $I^A_{m\alpha,m'\alpha'}(-iu,-t')$ to save space, one finds

$$I^A_{m\alpha,m'\alpha'}(-iu,-t') = \mathrm{tr}\Big[\rho^{\mathrm{eq}}_{\boldsymbol{S}_t}\,e^{u\mathcal{H}}s^{(\alpha)}_{i_m}e^{-u\mathcal{H}}e^{-it'\mathcal{H}}s^{(\alpha')}_{i_{m'}}e^{it'\mathcal{H}} - \alpha,m \leftrightarrow \alpha',m'\Big]$$

$$= \frac{1}{Z}\sum_{n,n'}^{n\neq n'}e^{-\beta E_n}e^{(u+it')(E_n-E_{n'})}\Big(\langle n|\,s^{(\alpha)}_{i_m}\,|n'\rangle\,\langle n'|\,s^{(\alpha')}_{i_{m'}}\,|n\rangle - \mathrm{H.c.}\Big), \tag{6.28}$$

where all the Hamiltonians are given for the parameter configuration at time t, i.e. $\mathcal{H} = \mathcal{H}(\boldsymbol{S}_t)$. To do the t' integral in the limit $t \to \infty$, one needs to introduce a regularising factor of $e^{-\eta t'}$, cf. section 3.3, with an infinitesimal η. This yields

$$\int_0^\infty dt'\,e^{it'(E_n-E_{n'})}e^{-\eta t'} = \frac{i}{E_n - E_{n'} + i\eta}. \tag{6.29}$$

Remember that in the end η has to be taken to zero but only after taking the thermodynamic limit. For finite systems, calculations have to be carried out with a small but finite η, the specific value depending on the system size, see for example the discussion in [23]. Combined with the u-integral, which gives

$$\int_0^\beta du\,e^{u(E_n-E_{n'})} = \frac{e^{\beta(E_n-E_{n'})} - 1}{E_n - E_{n'}}, \tag{6.30}$$

one has for the antisymmetric part

$$K^{A(\alpha\alpha')}_{i_m i_{m'}} = \frac{i}{2Z}\sum_{n,n'}^{n\neq n'}(e^{-\beta E_{n'}} - e^{-\beta E_n})\left(\frac{\langle n|\,s^{(\alpha)}_{i_m}\,|n'\rangle\,\langle n'|\,s^{(\alpha')}_{i_{m'}}\,|n\rangle}{(E_n - E_{n'} + i\eta)(E_n - E_{n'})} - \frac{\langle n|\,s^{(\alpha')}_{i_{m'}}\,|n'\rangle\,\langle n'|\,s^{(\alpha)}_{i_m}\,|n\rangle}{(E_n - E_{n'} + i\eta)(E_n - E_{n'})}\right)$$

$$= -\frac{1}{Z}\sum_{n,n'}^{n\neq n'}\mathrm{Im}\Big\{\langle n|\,s^{(\alpha)}_{i_m}\,|n'\rangle\,\langle n'|\,s^{(\alpha')}_{i_{m'}}\,|n\rangle\Big\}\frac{e^{-\beta E_{n'}} - e^{-\beta E_n}}{(E_n - E_{n'} + i\eta)(E_n - E_{n'})}$$

$$= \frac{2i}{Z}\sum_{n,n'}^{n\neq n'}\mathrm{Im}\Big\{\langle n|\,s^{(\alpha)}_{i_m}\,|n'\rangle\,\langle n'|\,s^{(\alpha')}_{i_{m'}}\,|n\rangle\Big\}\mathrm{Im}\Big\{\frac{1}{(E_n - E_{n'} + i\eta)}\Big\}\frac{e^{-\beta E_n}}{E_n - E_{n'}}, \tag{6.31}$$

where going from the second to the third line one has to exchange $n \leftrightarrow n'$ in the first term. If nondegenerate states are assumed, one can discard the regularisation of $i\eta$ such that

$$K^{A(\alpha\alpha')}_{i_m i_{m'}} = \frac{2}{Z}\sum_{n,n'}^{n\neq n'}e^{-\beta E_n}\frac{\mathrm{Im}\Big\{\langle n|\,s^{(\alpha)}_{i_m}\,|n'\rangle\,\langle n'|\,s^{(\alpha')}_{i_{m'}}\,|n\rangle\Big\}}{(E_n - E_{n'})^2}. \tag{6.32}$$

In the case of weak J and weak coupling to the bath, the energy eigenstates and the corresponding eigenvalues might be expanded in both. The lowest-order quantities are then independent of J as well as the system-bath coupling. The conductance matrix becomes

$$K_{i_m i_{m'}}^{A(\alpha\alpha')}(J=0) = \frac{2}{Z} \sum_{n,n'}^{n \neq n'} e^{-\beta E_n^{(0)}} \frac{\text{Im}\left\{ \langle n^{(0)} | s_{i_m}^{(\alpha)} | n'^{(0)} \rangle \langle n'^{(0)} | s_{i_{m'}}^{(\alpha')} | n^{(0)} \rangle \right\}}{\left(E_n^{(0)} - E_{n'}^{(0)} \right)^2}, \qquad (6.33)$$

where $|n^{(0)}\rangle$ and $E_n^{(0)}$ are eigenstates and eigenenergies of $H_S(\boldsymbol{S})$. The zero temperature limit, i.e., $\beta \to \infty$, of (6.33) yields

$$K_{i_m i_{m'}}^{A(\alpha\alpha')} = 2 \sum_{n \neq 0} \frac{\text{Im}\left\{ \langle 0 | s_{i_m}^{(\alpha)} | n \rangle \langle n | s_{i_{m'}}^{(\alpha')} | 0 \rangle \right\}}{(E_0 - E_n)^2}, \qquad (6.34)$$

again dropping the superscript (0). This is the same as (3.32), i.e., in the weak-J limit the expressions for the geometrical spin torque in linear and adiabatic response theory coincide. In the symmetric part (6.21), the first term can be written as

$$\frac{1}{Z} \sum_{n,n'} e^{-\beta E_n} e^{u(E_n - E_{n'})} e^{it'(E_n - E_{n'})} \left(\langle n | s_{i_m}^{(\alpha)} | n' \rangle \langle n' | s_{i_{m'}}^{(\alpha')} | n \rangle + \text{H.c.} \right). \qquad (6.35)$$

For the single-operator expectation value, one gets

$$\left\langle s_{i_m}^{(\alpha)} \right\rangle_{\boldsymbol{S}_t}^{\text{eq}} = \text{tr}\left[\rho_{\boldsymbol{S}_t}^{\text{eq}} s_{i_m}^{(\alpha)} \right] = \frac{1}{Z} \sum_n e^{-\beta E_n} \langle n | s_{i_m}^{(\alpha)} | n \rangle, \qquad (6.36)$$

such that the second term is

$$\left\langle s_{i_m}^{(\alpha)} \right\rangle_{\boldsymbol{S}(t)}^{\text{eq}} \left\langle s_{i_{m'}}^{(\alpha')} \right\rangle_{\boldsymbol{S}(t)}^{\text{eq}} = \frac{1}{Z^2} \sum_{n,n'} e^{-\beta(E_n + E_{n'})} \langle n | s_{i_m}^{(\alpha)} | n \rangle \langle n' | s_{i_{m'}}^{(\alpha')} | n' \rangle. \qquad (6.37)$$

One ends up with

$$\begin{aligned}
K_{i_m i_{m'}}^{S(\alpha\alpha')} &= \frac{1}{2Z} \int_0^t dt' \int_0^\beta du \Bigg[\sum_{n,n'} e^{-\beta E_n} e^{u(E_n - E_{n'})} e^{it'(E_n - E_{n'})} \left(\langle n | s_{i_m}^{(\alpha)} | n' \rangle \langle n' | s_{i_{m'}}^{(\alpha')} | n \rangle + \text{H.c.} \right) \\
&\qquad - \frac{2}{Z^2} \sum_{n,n'} e^{-\beta(E_n + E_{n'})} \langle n | s_{i_m}^{(\alpha)} | n \rangle \langle n' | s_{i_{m'}}^{(\alpha')} | n' \rangle \Bigg] \\
&= \frac{1}{2Z} \int_0^t dt' \Bigg[\sum_{n,n'} e^{-\beta E_n} e^{it'(E_n - E_{n'})} \frac{e^{\beta(E_n - E_{n'})} - 1}{E_n - E_{n'}} \left(\langle n | s_{i_m}^{(\alpha)} | n' \rangle \langle n' | s_{i_{m'}}^{(\alpha')} | n \rangle + \text{H.c.} \right) \\
&\qquad - \frac{2\beta}{Z^2} \sum_{n,n'} e^{-\beta(E_n + E_{n'})} \langle n | s_{i_m}^{(\alpha)} | n \rangle \langle n' | s_{i_{m'}}^{(\alpha')} | n' \rangle \Bigg],
\end{aligned} \qquad (6.38)$$

where the first sum has a divergence at $n = n'$. In the thermodynamic limit, however, the spectrum of eigenenergies is continuous and one finds $\lim_{E_n \to E_{n'}} \frac{e^{\beta(E_n - E_{n'})} - 1}{E_n - E_{n'}} = \beta$ using L'Hospital's rule. For SU(2) spin-rotation invariant systems and in the absence of spontaneous magnetic order, the expectation value $\langle n | s_{i_m}^{(\alpha)} | n \rangle$ vanishes such that in the first sum the term $n = n'$ can be excluded, while the second sum is zero as a whole. This strongly simplifies the

expression for $\underline{K}^S$ and yields

$$
\begin{aligned}
K^{S(\alpha\alpha')}_{i_m i_{m'}} &= \frac{1}{2Z} \int_0^t dt' \sum_{n \neq n'} e^{it'(E_n - E_{n'})} \frac{e^{-\beta E_{n'}} - e^{-\beta E_n}}{E_n - E_{n'}} \left(\langle n| s^{(\alpha)}_{i_m} |n'\rangle \langle n'| s^{(\alpha')}_{i_{m'}} |n\rangle + \text{H.c.} \right) \\
&= \frac{1}{Z} \int_0^t dt' \sum_{n \neq n'} e^{it'(E_n - E_{n'})} \frac{e^{-\beta E_{n'}} - e^{-\beta E_n}}{E_n - E_{n'}} \text{Re}\Big\{ \langle n| s^{(\alpha)}_{i_m} |n'\rangle \langle n'| s^{(\alpha')}_{i_{m'}} |n\rangle \Big\} \\
&= -\frac{1}{Z} \int_0^t dt' \sum_{n \neq n'} e^{-\beta E_n} \text{Re}\Big\{ \langle n| s^{(\alpha)}_{i_m} |n'\rangle \langle n'| s^{(\alpha')}_{i_{m'}} |n\rangle \Big\} \frac{e^{it'(E_n - E_{n'})} + e^{-it'(E_n - E_{n'})}}{E_n - E_{n'}}.
\end{aligned} \tag{6.39}
$$

With the usual procedure of evaluating the t' integral in the limit $t \to \infty$, one gets

$$
K^{S(\alpha\alpha')}_{i_m i_{m'}} = \frac{2}{Z} \sum_{n \neq n'} e^{-\beta E_n} \text{Im}\left\{ \frac{\text{Re}\Big\{ \langle n| s^{(\alpha)}_{i_m} |n'\rangle \langle n'| s^{(\alpha')}_{i_{m'}} |n\rangle \Big\}}{(E_n - E_{n'})(E_n - E_{n'} + i\eta)} \right\}, \tag{6.40}
$$

which in the zero temperature limit $\beta \to \infty$ gives

$$
K^{S(\alpha\alpha')}_{i_m i_{m'}} = 2 \sum_{n \neq 0} \text{Im}\left\{ \frac{\text{Re}\Big\{ \langle 0| s^{(\alpha)}_{i_m} |n\rangle \langle n| s^{(\alpha')}_{i_{m'}} |0\rangle \Big\}}{(E_0 - E_n)(E_0 - E_n + i\eta)} \right\}. \tag{6.41}
$$

In the equations of motion, the symmetric part of the conductance matrix produces spin dissipation analogous to the Gilbert damping. This will be investigated in publication [III], found directly below, for a tight-binding model of conduction electrons. The setup of a single classical impurity spin will be used to compare the expression for the Gilbert damping derived via ART with the one from LRT derived in chapter 3.

Microscopic theory of spin friction and dissipative spin dynamics

Nicolas Lenzing [1], David Krüger [1], and Michael Potthoff [1,2]

[1]*I. Institute of Theoretical Physics, Department of Physics, University of Hamburg, Notkestraße 9-11, 22607 Hamburg, Germany*
[2]*The Hamburg Centre for Ultrafast Imaging, Luruper Chaussee 149, 22761 Hamburg, Germany*

The real-time dynamics of local magnetic moments exchange coupled to a metallic system of conduction electrons is subject to dissipative friction, even in the absence of spin-orbit coupling. Phenomenologically, this is usually described by a local Gilbert damping constant. Here, we use both linear response theory (LRT) and adiabatic response theory (ART) to derive the spin friction microscopically for a generic single-band tight-binding model of the electronic structure. The resulting Gilbert damping is time dependent and nonlocal. For a one-dimensional model, we compare the emergent relaxation dynamics as obtained from LRT and ART against each other and against the full solution of the microscopic equations of motion and demonstrate the importance of nonlocality, while the time dependence turns out to be irrelevant. In two dimensions and for a few magnetic moments in different geometries, it is found that the inclusion of nonlocal Gilbert damping can counterintuitively lead to longer relaxation times. Besides the distance dependence, the directional dependence of the nonlocal Gilbert damping turns out to be very important. Our results are based on an expression relating the nonlocal Gilbert damping to the nonlocal tight-binding density of states close to the Fermi energy. This is exact in the case of noninteracting electrons. Effects due to electronic correlations are studied within the random-phase approximation. For the Hubbard model at half filling and with increasing interaction strength, we find a strong enhancement of the nonlocality of spin friction.

I. INTRODUCTION

The understanding of the relaxation dynamics of local magnetic moments on an atomistic level represents an essential step for further progress in the field of nanospintronics [1–4]. A prototypical model within atomistic spin-dynamics theory [5–8] is given by the multi-impurity Kondo model with a few localized spins, replaced by classical vectors of unit length to represent the local magnetic moments. This is also known as the *s-d* exchange (Vonsovsky-Zener) model [9]. Its Hamiltonian has the form $\hat{H} = \hat{H}_{\rm el} + \hat{H}_{\rm int}$, where $\hat{H}_{\rm el}$ is a tight-binding model of the electronic structure on a D-dimensional lattice, and where $\hat{H}_{\rm int}$ is a generic local exchange interaction between the classical spins $\boldsymbol{S}_m$ (with $m = 1, \ldots, M$) and the local spin-moment operators $\hat{\boldsymbol{s}}_{i_m}$ at the sites i_m of the lattice. In its most simple form, assuming a single spin-degenerate orbital per site, one has

$$\hat{H} = \sum_{\langle ii' \rangle} \sum_{\sigma = \uparrow, \downarrow} T_{ii'} c_{i\sigma}^\dagger c_{i'\sigma} + J \sum_m \hat{\boldsymbol{s}}_{i_m} \boldsymbol{S}_m. \qquad (1)$$

Here, $T_{ii'}$ is the hopping amplitude between sites i and i', and $J > 0$ is the local exchange-coupling strength.

The time dependence of the electron and the classical-spin degrees of freedom follows the general rules for quantum-classical dynamics [10,11]. As the model is quadratic in the electron annihilators and creators, $c_{i\sigma}$ and $c_{i\sigma}^\dagger$ ($i = 1, \ldots, L$ sites, $\sigma = \uparrow, \downarrow$ spin projection), for each spin configuration $\boldsymbol{S} \equiv (\boldsymbol{S}_1, \ldots, \boldsymbol{S}_M)$, there is a closed system of equations of motions, for the one-particle reduced density matrix and for the classical spins. The dynamics of the latter is governed by classical Landau-Lifshitz equations $\dot{\boldsymbol{S}}_m = \partial \langle \hat{H} \rangle / \partial \boldsymbol{S}_m \times \boldsymbol{S}_m$.

Here, we are interested in the relaxation dynamics of systems with a few impurity spins, $M = 1, \ldots, 10$, for the single-orbital model given by Eq. (1) in the thermodynamical limit $L \to \infty$. The computational effort for solving the related coupled system of nonlinear ordinary differential equations roughly scales quadratically in the number of lattice sites $L = l^D$ and linearly in the propagation time t [11]. To avoid unwanted reflections (or interferences) of propagating excitations from the system boundaries (or due to periodic boundary conditions), however, systems with a linear extension $l \sim vt$ must be considered if v is the (ballistic) propagation speed. The Gaussian electronic part can be formally integrated out within a path-integral formalism, but at the cost of a highly time-nonlocal effective action for the classical spins, which, if treated exactly, does not improve the scaling.

For one-dimensional (1D) systems, absorbing boundary conditions, e.g., using a generalized Lindblad master-equation approach to couple the edge sites of the conduction-electron tight-binding model to an external bath, have turned out to be helpful [12,13]. It has been demonstrated that this allows one to exceed the characteristic femtosecond electronic scale set by the inverse nearest-neighbor hopping by more than five orders of magnitude. For $D \geqslant 2$, however, an exact time propagation of an initial state on the pico- or even nanosecond scale appears out of reach, but is quite relevant from general considerations of the timescales of magnetic processes [14]. Even at thermal equilibrium and using advanced Monte Carlo techniques, quantum-classical hybrid systems with a linear extension $l \lesssim 30$ in $D = 3$ are computationally challenging [15].

On the other hand, for physically relevant applications, the classical-spin dynamics takes place on a characteristic timescale $\tau_{\rm sp}$, which is more than an order of magnitude slower than the femtosecond ($\tau_{\rm el} \sim 1/T$) electron dynamics set by the nearest-neighbor hopping T. This implies that the electronic quantum state follows the classical dynamics almost instantly, i.e., the electron dynamics is almost adiabatic and characterized by a typical retardation time $\tau_{\rm ret}$ much shorter than $\tau_{\rm sp}$.

This situation has motivated theoretical efforts to approximately "integrate out" the fast electron degrees of freedom, using the interrelated assumptions of weak J and small $\tau_{\rm ret}$. These justify a double expansion, namely, (i) a perturbative treatment of the exchange coupling J, followed by (ii) an expansion in the retardation time as put forward in Refs. [16–19]. This results in an effective spin-only theory, given by a (generalized) Landau-Lifshitz-Gilbert (LLG) equation [20],

$$\dot{\boldsymbol{S}}_m = \sum_{m'} J_{mm'} \boldsymbol{S}_{m'} \times \boldsymbol{S}_m + \sum_{m'} \alpha_{mm'} \boldsymbol{S}_m \times \dot{\boldsymbol{S}}_{m'}, \qquad (2)$$

where both the Gilbert damping $\alpha_{mm'}$ and the indirect Ruderman–Kittel–Kasuya–Yosida (RKKY) exchange interaction $J_{mm'}$ [21–23] must be computed from the $J = 0$ ground state of the electron system.

It has been pointed out [11,24,25] that the Gilbert damping $\alpha_{mm'}$ is usually nonlocal, i.e., dependent on two spatial indices m, m' with $\alpha_{mm'} \neq 0$ for $m \neq m'$. In addition, and depending on the translational symmetries of the underlying system, the Gilbert damping can be inhomogeneous, i.e., α_{mm} can be m dependent or, more generally, $\alpha_{mm'}$ can depend nontrivially on both m and m'. Here, assuming a hopping matrix that fully respects the translational symmetries of the lattice, we consider the homogeneous case only and focus on the nonlocality of the damping. Moreover, the purely electronic part $\hat{H}_{\rm el}$ of the Hamiltonian (1) is invariant under SU(2) spin rotations. With this choice, we also disregard anisotropy effects and thus assume for a 3×3 Gilbert-damping tensor that $\alpha_{m\alpha,m'\alpha'} = \alpha_{mm'}\delta_{\alpha\alpha'}$ with $\alpha, \alpha' = x, y, z$.

Importantly, even for the conceptually simple model Hamiltonian given by Eq. (1), the local and the nonlocal elements of the Gilbert damping are nonzero and actually comparatively large. The physical mechanism is a retardation effect, as described in Refs. [11,26]: Although the impurity-spin dynamics is slow compared to the femtosecond timescale of the electron dynamics, the quantum state does not instantly follow the time-dependent impurity-spin configuration, i.e., the electron dynamics is slightly nonadiabatic. Already for the ($M = 1$) single impurity case, this implies that $\boldsymbol{S}$ and $\langle \hat{\boldsymbol{s}} \rangle$ are noncollinear, which in turn produces spin damping. This view should be contrasted with previous work, where the local damping α_{mm} is attributed to relativistic effects, i.e., to spin-orbit coupling [27–41]; see, also, the related discussion in Ref. [25].

In the quite common continuum (as opposed to the discrete tight-binding) approach, the nonlocality of the Gilbert damping is typically accounted for by additional gradient terms $\partial_\alpha \boldsymbol{S}(\boldsymbol{r}, t)$ [42–48]. This assumes a weak spatial variation of the damping on the atomic scale and that the leading correction beyond a fully local damping suffices. On the contrary, we

will demonstrate that $\alpha_{mm'}$ is typically even more nonlocal than, e.g., the RKKY interaction $J_{mm'}$, at least for the model studied here.

With the present paper, we focus on the generic, nonrelativistic model given by Eq. (1) on the $D = 1$ chain and on the $D = 2$ square lattice, and study the local and nonlocal elements of the Gilbert-damping matrix. To this end, we derive a compact expression for $\alpha_{mm'}$ based on the local and nonlocal tight-binding density of states.

Furthermore, we discuss the impact of the spin damping on the relaxation dynamics for systems with different number M of impurity spins coupled to the electron system in various geometries. For two classical spins ($M = 2$) coupled to next-nearest-neighbor sites of a one-dimensional tight-binding chain, it has been observed [49] that the local and the nonlocal elements of $\alpha_{mm'}$ are exactly identical, $\alpha_{11} = \alpha_{22} = \alpha_{12} = \alpha_{21}$, and that this results in a completely *undamped* spin dynamics. This counterintuitive effect actually represents a general feature of $D = 1$ classical, quantum, and quantum-classical bipartite multi-impurity models [25,49]. If and how this still manifests itself in higher dimensions is an obvious question to be answered.

The LLG equation (2) is rederived for the model given by Eq. (1) by invoking linear response theory and, subsequently, by an expansion in the retardation time and corresponding truncation, i.e., using the two above-mentioned approximations controlled by (i) weak local exchange J and (ii) short typical retardation times. We demonstrate that the result is essentially the same when interchanging the order of the approximations, i.e., when first starting from the completely different formalism of adiabatic response theory [50], adapted to the present case, and make use of a weak-J approximation thereafter. For $D = 1$, the impurity-spin relaxation dynamics from both approaches will be checked against the fully numerical solution of the exact equations of motion.

Both formalisms show that $\alpha_{mm'} = \alpha_{mm'}(t)$ is actually time dependent. However, very different time dependencies are obtained when evaluated numerically. This and the impact on the long-time dynamics and the relaxation time is studied for the $D = 1$ case, where the linear and the adiabatic response approaches can be checked against the full solution.

The paper is organized as follows: In the next section, we discuss the fundamental equations of motion for the coupled spin-electron dynamics. The linear response and the adiabatic response approaches are introduced in Secs. III and IV, respectively. Section V is devoted to computational details. Results are presented in Sec. VI, which address the time dependence and the nonlocality of the spin friction (Secs. VI A and VI B), the dynamics of a single spin driven by a magnetic field (Sec. VI C), and the breakdown of the effective theory if there is a van Hove singularity at the Fermi energy (Sec. VI D). The anomalous dynamics of two impurity spins in $D = 1$ is discussed in Sec. VI E. We then proceed with dimension $D = 2$ and analyze the local and nonlocal spin friction in Sec. VI F and the distance and directional dependencies of the Gilbert damping in Sec. VI G. The effects of spin friction on the dynamics of two impurity spins and of impurity-spin arrays are analyzed in Secs. VI H and VI I. Electron-correlation effects, on the level of the random-phase approximation,

are touched in Sec. VI J. Our concluding remarks are given in Sec. VII.

II. FULL SPIN DYNAMICS

Starting from the Hamiltonian, given by Eq. (1), the exact equations of motion for the classical spins $\boldsymbol{S}_m$, with $m = 1, \ldots, M$ and $|\boldsymbol{S}_m| = 1$, and of the one-particle reduced density matrix $\boldsymbol{\rho}(t)$ with elements

$$\rho_{i\sigma, i'\sigma'}(t) = \langle \Psi(t)| c_{i'\sigma'}^{\dagger} c_{i\sigma} |\Psi(t)\rangle, \qquad (3)$$

are readily derived (see, e.g., Ref. [11]). We find

$$\frac{d}{dt}\boldsymbol{S}_m(t) = J\langle \boldsymbol{s}_{i_m}\rangle_t \times \boldsymbol{S}_m(t) - \sum_m \boldsymbol{B}_m \times \boldsymbol{S}_m(t), \qquad (4)$$

where $\langle \boldsymbol{s}_{i_m}\rangle_t$ is the expectation value of the local spin at site i_m of the electron system in the N-electron state $|\Psi(t)\rangle$. If $\boldsymbol{\tau}$ denotes the vector of Pauli matrices, we have $\boldsymbol{s}_i = \frac{1}{2} \sum_{\sigma\sigma'} c_{i\sigma}^{\dagger} \boldsymbol{\tau}_{\sigma\sigma'} c_{i\sigma'}$. The last term on the right-hand side results from local magnetic fields $\boldsymbol{B}_m$ coupling to the impurity spins $\boldsymbol{S}_m$, i.e., we have replaced the Hamiltonian in Eq. (1) by $\hat{H} \mapsto \hat{H} - \sum_m \boldsymbol{B}_m \boldsymbol{S}_m$. This will be convenient in the following. The equation of motion for the density matrix is given by

$$i\frac{d}{dt}\boldsymbol{\rho}(t) = [\boldsymbol{T}^{(\mathrm{eff})}(t), \boldsymbol{\rho}(t)], \qquad (5)$$

where $\boldsymbol{T}^{(\mathrm{eff})}(t)$ is an effective hopping matrix with elements

$$T_{i\sigma, i'\sigma'}^{(\mathrm{eff})}(t) = \delta_{\sigma\sigma'} T_{ii'} + \frac{J}{2}\delta_{ii'} \sum_{m=1}^{M} \delta_{ii_m} \boldsymbol{\tau}_{\sigma\sigma'} \boldsymbol{S}_m(t). \qquad (6)$$

Initially, at time $t = 0$, we specify a certain start configuration $\boldsymbol{S}(0) = [\boldsymbol{S}_1(0), \ldots, \boldsymbol{S}_M(0)]$ for the impurity spins. Furthermore, we assume that the electron system, at time $t = 0$, is in its ground state for $J = 0$. The corresponding ground-state one-particle reduced density matrix,

$$\boldsymbol{\rho}(0) = \Theta(\mu\mathbf{1} - \boldsymbol{T}), \qquad (7)$$

is formally given in terms of the Heaviside step function $\Theta(\cdots)$ and can be computed by diagonalizing the hopping matrix $\boldsymbol{T}$.

In the multi-impurity-spin case ($M > 1$), real-time dynamics is initiated by suddenly switching on $\hat{H}_{\mathrm{int}}$. For $M = 1$, we suddenly switch the direction of a local magnetic field $\boldsymbol{B}$ that couples to the impurity spin $\boldsymbol{S}$.

Equations (4) and (5) form a closed set of nonlinear ordinary differential equations for the spin configuration $\boldsymbol{S} = (\boldsymbol{S}_1, \ldots, \boldsymbol{S}_M)$ and $\boldsymbol{\rho}$. This can be solved numerically by standard techniques for a D-dimensional lattice with a finite number of sites $L = l^D$. Accessible propagation times τ are limited by the requirement $\tau \lesssim l/v$, where v is the (ballistic) propagation speed.

III. LINEAR RESPONSE THEORY

The effective spin-only dynamics, determined by the LLG equation (2), is obtained in the limit of weak J and short retardation times. In the linear response approach, we start by treating J perturbatively. The corresponding

Kubo formula reads

$$\langle \boldsymbol{s}_{i_m}\rangle_t = J\sum_m \int_0^t d\tau\, \chi_{mm'}(\tau) \boldsymbol{S}_{m'}(t - \tau) + O(J^2). \qquad (8)$$

The integral kernel is given in terms of the unperturbed ($J = 0$), retarded, nonlocal, and time-homogeneous magnetic susceptibility,

$$\chi_{mm'}^{\alpha\alpha'}(t) = -i\Theta(t)e^{-\eta t}\langle [s_{i_m}^{\alpha}(t), s_{i_{m'}}^{\alpha'}(0)]\rangle^{(0)}. \qquad (9)$$

Here, $\langle \cdots \rangle^{(0)}$ denotes the expectation value with respect to the unperturbed system at $J = 0$. Furthermore, $\eta > 0$ is an infinitesimal, and $\alpha = x, y, z$. Since $\hat{H}_{\mathrm{el}}$ is invariant under SU(2) spin rotations, the susceptibility is diagonal with respect to the directional indices and also α independent: $\chi_{mm'}^{\alpha\alpha'}(t) = \delta^{\alpha\alpha'}\chi_{mm'}(t)$.

As a second approximation, we assume that the retardation time τ in Eq. (8) is small, i.e., that the integral kernel $\chi_{mm'}(\tau)$ is peaked at small τ, on the characteristic timescale $1/T$ of the electron system, as compared to the much slower timescale on which the classical spins evolve. This justifies a Taylor expansion $\boldsymbol{S}_{m'}(t - \tau) = \boldsymbol{S}_{m'}(t) - \tau\dot{\boldsymbol{S}}_{m'}(t) + \cdots$. Truncating the expansion after the first order and inserting into Eq. (8) yields

$$\langle \boldsymbol{s}_{i_m}\rangle_t = J\sum_{m'}\left[\int_0^t d\tau\, \chi_{mm'}(\tau)\right]\boldsymbol{S}_{m'}(t)$$
$$- J\sum_{m'}\left[\int_0^t d\tau\, \tau\chi_{mm'}(\tau)\right]\dot{\boldsymbol{S}}_{m'}(t). \qquad (10)$$

With Eq. (4), we then get

$$\frac{d}{dt}\boldsymbol{S}_m(t) = \sum_{m'} J_{mm'}(t)\boldsymbol{S}_{m'}(t) \times \boldsymbol{S}_m(t)$$
$$+ \sum_{m'} \alpha_{mm'}(t)\dot{\boldsymbol{S}}_{m'}(t) \times \boldsymbol{S}_m(t)$$
$$- \sum_m \boldsymbol{B}_m \times \boldsymbol{S}_m(t), \qquad (11)$$

where we have defined the time-dependent RKKY exchange interaction,

$$J_{mm'}(t) = J^2 \int_0^t d\tau\, \chi_{mm'}(\tau), \qquad (12)$$

and the time-dependent Gilbert damping,

$$\alpha_{mm'}(t) = -J^2 \int_0^t d\tau\, \tau\chi_{mm'}(\tau). \qquad (13)$$

Equation (11) should be compared with the LLG Eq. (2). Apart from the additional magnetic-field term, the main difference is the time dependence of the coupling constants.

The time-independent RKKY interaction, defined as $J_{mm'} = \lim_{t\to\infty} J_{mm'}(t)$, corresponds to an effective RKKY Hamiltonian, $H_{\mathrm{RKKY}} = \frac{1}{2}\sum_{mm'}^{m\neq m'} J_{mm'}\boldsymbol{S}_m\boldsymbol{S}_{m'}$. We furthermore define the time-independent Gilbert damping as $\alpha_{mm'} = \lim_{t\to\infty} \alpha_{mm'}(t)$. The sign in the definition (13) of the damping matrix is chosen such that $\alpha_{mm} > 0$. (This is opposite to the convention used in Refs. [11,49]). Through Fourier transformation of the susceptibility, $\chi_{mm'}(\omega) = \int d\tau\, e^{i\omega\tau}\chi_{mm'}(\tau)$, we

get the alternative representation,

$$\alpha_{mm'} = iJ^2 \frac{d}{d\omega} \chi_{mm'}(\omega = 0) = -J^2 \frac{d}{d\omega} \mathrm{Im}\chi_{mm'}(\omega = 0).$$
(14)

Most convenient for the numerical simulations, however, is the representation of the damping matrix,

$$\alpha_{mm'} = \frac{\pi}{2} J^2 A_{i_m i_{m'}}(\omega = 0)^2,$$
(15)

in terms of the local or nonlocal tight-binding density of states $A_{ii'}(\omega)$. In the context of a single impurity spin and local Gilbert damping ($m = m'$), a derivation of Eq. (15) is given in Refs. [51–54]. A general derivation is given in the Appendix; see, also, Refs. [11,18,55,56].

Assuming a translation-invariant system with lattice vectors $\boldsymbol{R}_i$ and periodic boundary conditions, we have

$$A_{ii'}(\omega) = \frac{1}{L} \sum_{\boldsymbol{k}} e^{i\boldsymbol{k}(\boldsymbol{R}_i - \boldsymbol{R}_{i'})} \delta[\omega + \mu - \varepsilon(\boldsymbol{k})],$$
(16)

where $\varepsilon(\boldsymbol{k}) = \varepsilon(-\boldsymbol{k})$ is the tight-binding dispersion and μ is the chemical potential, which fixes the average particle number $\langle N \rangle$.

According to the derivation given in the Appendix, the temperature dependence of the damping parameters can be obtained via

$$\alpha_{mm'} = -\frac{\pi}{2} J^2 \int dx \, f'(x) A_{i_m i_{m'}}(x)^2.$$
(17)

In the low-temperature ($\beta \to \infty$) or in the wide-band limit, we can replace the one-electron spectral density by a constant, $A_{i_m i_{m'}}(x) \to \rho_{mm'}$. This yields

$$\alpha_{mm'}^{(\infty)} = \frac{\pi}{2} J^2 \rho_{mm'}^2.$$
(18)

Hence, a nontrivial temperature dependence at low temperatures is due to the variation of the spectral density near $\omega = 0$. We can make use of the Sommerfeld expansion in powers of β^{-2} to make this explicit. A straightforward calculation yields

$$\alpha_{mm'} = \alpha_{mm'}^{(\infty)} + \frac{\pi^3}{6} \frac{J^2}{\beta^2} [(\rho_{mm'}')^2 + \rho_{mm'} \rho_{mm'}''] + O(\beta^{-4}),$$
(19)

where we have defined

$$\rho_{mm'}^{(n)} = \frac{d^n}{dx^n} A_{i_m i_{m'}}(x) \Big|_{x=0}.$$
(20)

IV. ADIABATIC RESPONSE THEORY

In the limit of weak J and short retardation times, the same effective spin-only dynamics, given by Eq. (2), is obtained when first assuming that the electron system almost adiabatically follows the spin dynamics, while the weak-J approximation is done at a later stage. This can be seen by starting with the adiabatic response theory as outlined in Ref. [50] and adapted to the case of spin dynamics.

The considered setup is that of an open quantum system, driven by external parameters $\boldsymbol{S} = (\boldsymbol{S}_1, \ldots, \boldsymbol{S}_M)$ and in contact with a large thermal bath at temperature $1/\beta$. The total

Hamiltonian is

$$\hat{H}_{\mathrm{total}} = \hat{H} + \hat{H}_{\mathrm{B}} + \hat{H}_{\mathrm{SB}},$$
(21)

where $\hat{H}$ is the Hamiltonian given by Eq. (1), $\hat{H}_{\mathrm{B}}$ denotes the Hamiltonian of the thermal bath, and $\hat{H}_{\mathrm{SB}}$ is the system-bath interaction. The latter terms, $\hat{H}_{\mathrm{B}}$ and $\hat{H}_{\mathrm{SB}}$, are introduced for formal reasons only and can be disregarded at the end of the consideration, assuming that the system-bath coupling is sufficiently weak. Finally, we will also take the zero-temperature limit $\beta \to \infty$.

The goal is to determine the expectation value $\langle s_{i_m} \rangle_t$ of the local spin of the electron system at site i_m in the many-electron quantum state, for a given trajectory of the classical spins $\boldsymbol{S}(t')$ with $t' \leqslant t$. This is needed for Eq. (4) to obtain a closed set of equations of motion for the classical spins $\boldsymbol{S}$ only. To this end, we start with the thermal (canonical) equilibrium value $\langle s_{i_m} \rangle_{S(t)}^{(\mathrm{eq})}$ for a fixed spin configuration $\boldsymbol{S}(t)$ at time t. In the adiabatic approximation, we would have $\langle s_{i_m} \rangle_t = \langle s_{i_m} \rangle_{S(t)}^{(\mathrm{eq})}$.

Within adiabatic response theory, the difference,

$$\langle \Delta s_{i_m}(t) \rangle = \langle s_{i_m} \rangle_t - \langle s_{i_m} \rangle_{S(t)}^{(\mathrm{eq})},$$
(22)

is computed perturbatively in the deviation from a strictly adiabatic, infinitely slow spin dynamics $\boldsymbol{S}(t)$. The "small parameter" is given by the dissipated work [50,57],

$$W = \int_0^t dt' \dot{\boldsymbol{S}}(t') \{\nabla_S \hat{H}[\boldsymbol{S}(t')] - \langle \nabla_S \hat{H}[\boldsymbol{S}(t')] \rangle_{S(t')}^{(\mathrm{eq})}\},$$
(23)

where $\hat{H}[\boldsymbol{S}(t)]$ is the total Hamiltonian (1) for a given spin configuration. Note that W is an operator, but not an observable [58,59]. The dissipated work can be interpreted as the difference between the work performed on the system along a certain trajectory $\boldsymbol{S}(t)$ in the spin-configuration space and the work along the same path but traversed adiabatically. For an isothermal process, the second contribution is given by the free-energy difference between the initial and the final state at $\boldsymbol{S}(0)$ and $\boldsymbol{S}(t)$, respectively.

As detailed in Ref. [50], one finds

$$\langle \Delta s_{i_m}(t) \rangle = J \sum_{m'} \boldsymbol{K}_{mm'}[t, \boldsymbol{S}(t)] \dot{\boldsymbol{S}}_{m'}(t),$$
(24)

up to first order in W. Here, $\boldsymbol{K}_{mm'}$ is a 3×3 matrix for each index pair m, m', which depends on t explicitly, and also implicitly via $\boldsymbol{S}(t)$. The elements of this matrix are given by

$$K_{mm'}^{\alpha\alpha'}[t, \boldsymbol{S}(t)] = \int_0^t dt' \int_0^\beta du \langle s_{i_m}^\alpha(-iu) s_{i_{m'}}^{\alpha'}(t'-t) \rangle_{S(t)}^{(\mathrm{eq})}$$

$$- \int_0^t dt' \int_0^\beta du \langle s_{i_m}^\alpha(-iu) \rangle_{S(t)}^{(\mathrm{eq})}$$

$$\times \langle s_{i_{m'}}^{\alpha'}(t'-t) \rangle_{S(t)}^{(\mathrm{eq})}.$$
(25)

Here, $\alpha, \alpha' = x, y, z$ and u refers to imaginary time. Inserting $\langle s_{i_m} \rangle_t$, as obtained from Eqs. (22) and (24), into Eq. (4), we get

$$\dot{\boldsymbol{S}}_m(t) = J \langle s_{i_m} \rangle_{S(t)}^{(\mathrm{eq})} \times \boldsymbol{S}_m(t) - \sum_m \boldsymbol{B}_m \times \boldsymbol{S}_m(t)$$

$$+ J^2 \sum_\alpha \sum_{m'\alpha'} K_{mm'}^{\alpha\alpha'}[t, \boldsymbol{S}(t)] \dot{S}_{m'\alpha'} \boldsymbol{e}_\alpha \times \boldsymbol{S}_m(t). \quad (26)$$

In the second step, we additionally assume that J is weak. For a fixed spin configuration $\boldsymbol{S}(t)$, the static, equilibrium expectation value $\langle \boldsymbol{s}_{i_m} \rangle^{(\text{eq})}_{\boldsymbol{S}(t)}$ in the first term on the right-hand side of Eq. (26) can be expanded in powers of J as

$$\langle \boldsymbol{s}_{i_m} \rangle^{(\text{eq})}_{\boldsymbol{S}(t)} = \langle \boldsymbol{s}_{i_m} \rangle^{(\text{eq})}_{J=0} + J \sum_{m'} \chi_{mm'} \boldsymbol{S}_{m'}(t) + O(J^2), \quad (27)$$

where $\chi_{mm'} \equiv \chi_{mm'}(\omega = 0)$ is the static and unperturbed ($J = 0$) magnetic susceptibility, i.e., the $\omega = 0$ Fourier component of $\chi^{\alpha\alpha'}_{mm'}(t) = \delta^{\alpha\alpha'} \chi_{mm'}(t)$ defined in Eq. (9). The first term, $\langle \boldsymbol{s}_{i_m} \rangle^{(\text{eq})}_{J=0}$, vanishes as there is no spontaneous magnetic order for a system of noninteracting conduction electrons and since the magnetic field $\boldsymbol{B}_m$ only couples to the impurity spin $\boldsymbol{S}_m$. With this, the first term on the right-hand side of Eq. (26) reduces to the RKKY term $\sum_{m'} J^2 \chi_{mm'} \boldsymbol{S}_{m'}(t) \times \boldsymbol{S}_m(t)$, if terms of the order of J^3 are neglected. Since the K matrix in Eq. (26) already carries a J^2 factor, we can then disregard its dependence on $\boldsymbol{S}(t)$ as this would produce terms of $O(J^3)$ as well. With the same argument and since the model is SU(2) symmetric and does not support spontaneous magnetic order, the second term on the right-hand side of Eq. (25) can be disregarded. We are left with

$$K^{\alpha\alpha'}_{mm'}(t) = \delta^{\alpha\alpha'} \int_0^t dt' \int_0^\beta du \, \langle s^\alpha_{i_m}(-iu) s^{\alpha'}_{i_{m'}}(t'-t) \rangle^{(0)}. \quad (28)$$

Inserting a resolution of the identity $\boldsymbol{1} = \sum |\Psi_n\rangle\langle\Psi_n|$ with energy eigenstates between the spin operators in Eq. (28) and expressing the expectation value as $Z^{-1} \sum e^{-\beta E_n} \langle\Psi_{n'}| \cdots |\Psi_{n'}\rangle$, one can derive a Lehmann-type representation. This involves matrix elements $\langle\Psi_n|s^\alpha_i|\Psi_{n'}\rangle$ with eigenstates of the $J = 0$ Hamiltonian $\hat{H}_{\text{el}}$. In the sector with even total particle number N, the latter is invariant under time reversal, $[\Theta, \hat{H}_{\text{el}}] = 0$, where the representation of time reversal is given by an antiunitary operator Θ with $\Theta^2 = \boldsymbol{1}$, $\Theta\Theta^\dagger = \boldsymbol{1}$, and $\Theta \boldsymbol{s}_i \Theta^\dagger = -\boldsymbol{s}_i$. A straightforward consequence is that the matrix elements $\langle\Psi_n|s^\alpha_i|\Psi_{n'}\rangle = \langle\Theta\Psi_n|s^\alpha_i|\Theta\Psi_{n'}\rangle = \langle\Psi_n|\Theta^\dagger s^\alpha_i \Theta|\Psi_{n'}\rangle^* = -\langle\Psi_n|s^\alpha_i|\Psi_{n'}\rangle^* \in i\mathbb{R}$ are purely imaginary (see, also, Ref. [60]). This immediately implies that K is symmetric, $K^{\alpha\alpha'}_{mm'}(t) = K^{\alpha'\alpha}_{m'm}(t)$.

It is important to see that there is a finite *antisymmetric* part for strong J, i.e., in the regime where the weak-J approximation does not apply, e.g., for systems directly coupled to an external magnetic field or systems where time-reversal symmetry is explicitly broken in the electronic sector, as in the case of the Haldane model [61]. In the equations of motion for the classical spins, this would lead to an additional geometrical spin torque,

$$\sum_\alpha \sum_{m'\alpha'} \Omega^{\alpha\alpha'}_{mm'}[\boldsymbol{S}(t)] \dot{S}_{m'\alpha'} \boldsymbol{e}_\alpha \times \boldsymbol{S}_m(t), \quad (29)$$

resulting from the spin-Berry curvature,

$$\Omega^{\alpha\alpha'}_{mm'}(\boldsymbol{S}(t)) = J^2 \tfrac{1}{2} \{ K^{\alpha\alpha'}_{mm'}[\boldsymbol{S}(t)] - K^{\alpha'\alpha}_{m'm}[\boldsymbol{S}(t)] \}. \quad (30)$$

Previously, this was derived within the framework of adiabatic spin dynamics [60,62–64]. The spin-Berry curvature represents the feedback [65] of the Berry-phase physics [66] in the electron system on the dynamics of the classical degrees of freedom. Here, we see that the same geometrical spin torque can be derived within the context of adiabatic response theory

[50] as well. Importantly, the spin-Berry curvature is a *geometrical* object and only depends on t via $\boldsymbol{S}(t)$, *if* the explicit t dependence of $K^{\alpha\alpha'}_{mm'}[t, \boldsymbol{S}(t)]$ in Eq. (25) can be disregarded, i.e., in the long-time limit.

Let us return to our main focus, namely, spin damping. Generally, we define

$$\overline{K}^{\alpha\alpha'}_{mm'}(t) = \tfrac{1}{2} \{ K^{\alpha\alpha'}_{mm'}[t, \boldsymbol{S}(t)] + K^{\alpha'\alpha}_{m'm}[t, \boldsymbol{S}(t)] \}. \quad (31)$$

Specifically, for the time-reversal and spin-SU(2) symmetric model $\hat{H}_{\text{el}}$ considered here and in the weak-J limit, the symmetrization is superfluous and, furthermore, the 3×3 tensor is actually isotropic, i.e., $\overline{K}^{\alpha\alpha'}_{mm'}(t) = \delta^{\alpha\alpha'} \overline{K}_{mm'}(t)$. Hence, the last term on the right-hand side of Eq. (26) reads

$$\sum_m \alpha_{mm'}(t) \dot{\boldsymbol{S}}_{m'}(t) \times \boldsymbol{S}_m(t), \quad (32)$$

when identifying

$$\alpha_{mm'}(t) = J^2 \overline{K}_{mm'}(t). \quad (33)$$

With the term Eq. (32) and with Eq. (27) inserted into Eq. (26), we find the same spin-only effective equation of motion (11) that was derived within linear response theory and the subsequent perturbative treatment of retardation effects, but with two exceptions: The RKKY coupling constants are time independent and the expression given by Eq. (32) for the damping constants differs from Eq. (13).

V. COMPUTATIONAL DETAILS

The fundamental equations of motion (4) and (5) as well as the effective equations of motion (2) can be solved using standard numerical techniques [67–69]. On timescales up to $\sim 10^9$ in units of the inverse nearest-neighbor hopping $1/T$, the achieved numerical accuracy is sufficient, i.e., the effects of numerical errors are invisible in all the spin-dynamics plots shown below.

We consider a tight-binding model of noninteracting electrons $\hat{H}_{\text{el}}$ on a D-dimensional lattice with periodic boundary conditions such that diagonalization of the hopping matrix $\boldsymbol{T} = \boldsymbol{U}\boldsymbol{\varepsilon}\boldsymbol{U}^\dagger$ is achieved analytically via Fourier transformation. Hence, the tight-binding dispersions are given by

$$\varepsilon(k) = -2T \cos(k) - 2T' \cos(2k), \quad (34)$$

for $D = 1$, where the nearest-neighbor hopping $T = 1$ fixes the energy (and with $\hbar \equiv 1$ the timescale) and where T' is the next-nearest-neighbor hopping. The lattice constant is set to unity as well. For $D = 2$, we have

$$\varepsilon(\boldsymbol{k}) = -2T[\cos(k_x) + \cos(k_y)] - 4T' \cos(k_x)\cos(k_y). \quad (35)$$

The necessary ingredients for the effective equations (2) or, more generally, for the effective equations of motion with time-dependent parameters, given by Eq. (11), can be computed numerically as follows.

We start with the RKKY interaction parameters $J_{mm'}(t)$. These are obtained from Eq. (12) by performing the τ integration numerically. For the integrand, we use the

representation

$$\chi_{mm'}(\tau) = \Theta(\tau)e^{-\eta\tau}\,\text{Im}\left[\left(\frac{e^{iT\tau}}{e^{\beta(T-\mu\mathbf{1})}+1}\right)_{i_{m'}i_m}\left(\frac{e^{-iT\tau}}{1+e^{-\beta(T-\mu\mathbf{1})}}\right)_{i_m i_{m'}}\right] \tag{36}$$

of the ($J=0$) retarded magnetic susceptibility, where we made use of the fact that the hopping matrix is diagonal in the spin indices σ, σ' and spin independent. With $U_{ik} = \frac{1}{\sqrt{L}}e^{-ikR_i}$, and in the zero-temperature limit $\beta \to \infty$, one gets

$$\chi_{mm'}(\tau) = \Theta(\tau)e^{-\eta\tau}\,\text{Im}\left[\frac{1}{L^2}\sum_k^{\text{occ}}e^{i\varepsilon(k)\tau}e^{ik(R_{i_{m'}}-R_{i_m})}\sum_{k'}^{\text{unocc}}e^{-ik'(R_{i_m}-R_{i_{m'}})}e^{-i\varepsilon(k')\tau}\right]. \tag{37}$$

We see that the susceptibility is symmetric with respect to m, m'. As argued above, this is a consequence of the time-reversal symmetry of $\hat{H}_{\text{el}}$.

Importantly, the wave-vector summations over the occupied or unoccupied points in the first Brillouin zone factorize. This allows us to address fairly large systems and to control the thermodynamic limit. The $L \to \infty$ limit should be taken with a finite $\eta > 0$ in the regularization factor $e^{-\eta\tau}$, which appears in the definition of the retarded susceptibility given by Eq. (9) and which ensures the convergence of the limit $t \to \infty$ in Eq. (12). The latter is necessary for the computation of the time-independent RKKY coupling, $J_{mm'} = \lim_{t\to\infty}J_{mm'}(t) = J^2\chi_{mm'}(\omega = 0)$. The limit $\eta \searrow 0$ should be taken in the end.

Within linear response theory, the time-dependent Gilbert-damping parameters $\alpha_{mm'}(t)$ are obtained from Eq. (13) via numerical integration. The time-independent parameters $\alpha_{mm'}$ are obtained from Eq. (A9).

Within adiabatic response theory and for weak J, the identification Eq. (33) leads us exactly to the same effective equations of motion (11) that were obtained within linear response theory, albeit with a different expression for $\alpha_{mm'}(t)$ as compared to Eq. (13). For its numerical evaluation, we first consider Eq. (28). Making use of isotropy and time-reversal symmetry, $K^{\alpha\alpha'}_{mm'}(t) = \overline{K}^{\alpha\alpha'}_{mm'}(t) = \delta^{\alpha\alpha'}K_{mm'}(t)$, inserting a resolution of the identity with an orthonormal basis of eigenstates of $\hat{H}_{\text{el}}$ as described below Eq. (28), and evaluating the corresponding matrix elements of $s^{\alpha}_{i_m}$ and $s^{\alpha'}_{i_{m'}}$ yields

$$K_{mm'}(t) = \frac{1}{2}\int_0^t dt'\int_0^\beta du\left(\frac{e^{T(it'+u)}}{e^{\beta(T-\mu\mathbf{1})}+1}\right)_{m'm}$$
$$\times\left(\frac{e^{-T(it'+u)}}{1+e^{-\beta(T-\mu\mathbf{1})}}\right)_{mm'}, \tag{38}$$

and, after diagonalization of the hopping matrix T,

$$K_{mm'}(t) = \frac{1}{2}\frac{1}{L^2}\sum_{kk'}f[\varepsilon(k)-\mu]f[\mu-\varepsilon(k')]e^{ik(R_{i_m}-R_{i_{m'}})}$$
$$\times e^{-ik'(R_{i_m}-R_{i_{m'}})}\int_0^t dt'\int_0^\beta du\,e^{[\varepsilon(k)-\varepsilon(k')](u+it')}. \tag{39}$$

Here, $f(x) = 1/(e^{\beta x}+1)$ is the Fermi function. We carry out the integration over imaginary time u with the case distinction (i) $\varepsilon(k) \neq \varepsilon(k')$ and (ii) $\varepsilon(k) = \varepsilon(k')$. Using the identity $(e^{\beta(x-x')}-1)f(x)f(-x') = f(-x)f(x') - f(x)f(-x')$ in

addition and carrying out the t' integration, we arrive at

$$K_{mm'}(t) = \frac{1}{L^2}\sum_{kk'}^{\varepsilon(k)\neq\varepsilon(k')}f[\varepsilon(k)-\mu]f(\mu-\varepsilon(k'))$$
$$\times\frac{\text{Im}[e^{i(k-k')(R_{i_m}-R_{i_{m'}})}(1-e^{i[\varepsilon(k)-\varepsilon(k')]t})]}{[\varepsilon(k)-\varepsilon(k')]^2}$$
$$+ K^{(\text{deg})}_{mm'}(t), \tag{40}$$

where the first term refers to case (i) and where the second term refers to case (ii), and is given by

$$K^{(\text{deg})}_{mm'}(t) = \frac{1}{2}\frac{\beta t}{L^2}\sum_{kk'}^{\varepsilon(k)=\varepsilon(k')}f[\varepsilon(k)-\mu]f(\mu-\varepsilon(k'))$$
$$\times e^{ik(R_{i_m}-R_{i_{m'}})}e^{-ik'(R_{i_m}-R_{i_{m'}})}. \tag{41}$$

In the thermodynamic limit $L \to \infty$, this second term vanishes, unless there is a macroscopic number of degeneracies in the tight-binding dispersion $\varepsilon(k)$. Assuming that this is not the case, taking the zero-temperature limit $\beta \to \infty$, and inserting into Eq. (33) we find

$$\alpha_{mm'}(t) = J^2\frac{1}{L^2}\sum_k^{\text{occ}}\sum_{k'}^{\text{unocc}}$$
$$\times\frac{\text{Im}[e^{i(k-k')(R_{i_m}-R_{i_{m'}})}(1-e^{i[\varepsilon(k)-\varepsilon(k')]t})]}{(\varepsilon(k)-\varepsilon(k'))^2}. \tag{42}$$

Unfortunately, the numerical evaluation is much more time consuming as compared to linear response theory, i.e., Eq. (13) and Eq. (37).

VI. RESULTS

A. Time-dependent spin friction

In the effective spin-only theory, the relaxation towards the ground-state spin configuration is determined by the Gilbert damping $\alpha_{mm'}(t)$. As shown above, there are at least three different ways to calculate this quantity, namely, (i) via linear response theory (LRT), resulting in Eq. (13); (ii) via adiabatic response theory (ART), resulting in Eq. (33), and, finally, (iii) one usually assumes time-independent damping constants $\alpha_{mm'} = \lim_{t\to\infty}\alpha_{mm'}(t)$. We start the discussion by a corresponding comparison. This is done for a one-dimensional tight-binding model with dispersion Eq. (34) at half filling. The next-nearest-neighbor hopping is set to $T' = 0$, for simplicity.
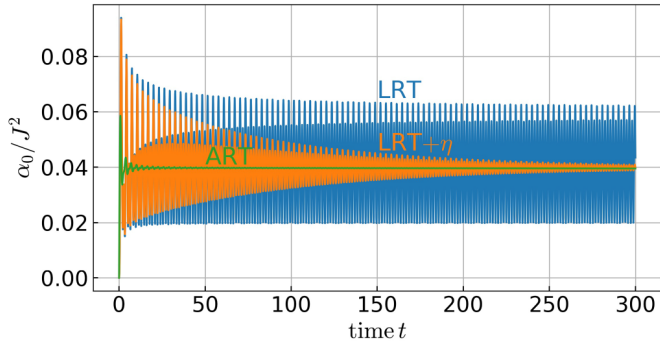
FIG. 1. Time-dependent local Gilbert damping $\alpha_0(t)/J^2$ as obtained from linear response theory (blue) and from adiabatic response theory (green) for the one-dimensional system at half filling. $T = 1$ sets the energy scale (and with $\hbar \equiv 1$ the timescale). Orange line: Linear response theory with $\eta = 0.01$. Calculations for $T' = 0$, $L = 10^5$, and periodic boundary conditions.

Figure 1 shows results for the local Gilbert damping for a system with $L = 10^5$ sites. Periodic boundary conditions are assumed such that $\alpha_{mm}(t) = \alpha_0(t)$ is m independent. Within LRT, we find that $\alpha_0(t)$ exhibits an undamped oscillation, after some initial decay at shorter times. Fourier analysis yields a dominating frequency $\omega_{\text{vH}} \approx 2.0$, which stems from the van Hove singularities at $\omega_{\text{vH}} = \pm 2$ in the local density of states, as already explained in Ref. [11]. Within ART, the same oscillation frequency is found, but there is a strong damping of the oscillation such that $\alpha_0(t)$ converges to an essentially constant value $\alpha_0 \approx 0.040J^2$ on a timescale of roughly $t = 50$.

For the nearest-neighbor Gilbert damping α_1, the same qualitative behavior is observed for both approaches, LRT and ART, as can be seen in Fig. 2. However, the time-independent nearest-neighbor damping constant vanishes, $\alpha_1 \approx 0$. The same values for the local and the nearest-neighbor damping, $\alpha_0 \approx 0.040J^2$ and $\alpha_1 \approx 0$, are obtained from LRT with a finite regularization parameter η. In Figs. 1 and 2, results are shown for $\eta = 0.01$ (orange lines). However, within numerical accuracy, the damping constants, α_0 and α_1, do not depend on the choice for η, as long as η is sufficiently small (but $\eta \gtrsim 1/L$, since the limit $\eta \searrow 0$ must be taken after the limit $L \to \infty$). This independence of η is expected; see the discussion in Refs. [11,49] and the discussion of the two-dimensional systems below. It is remarkable, however, that both approaches,
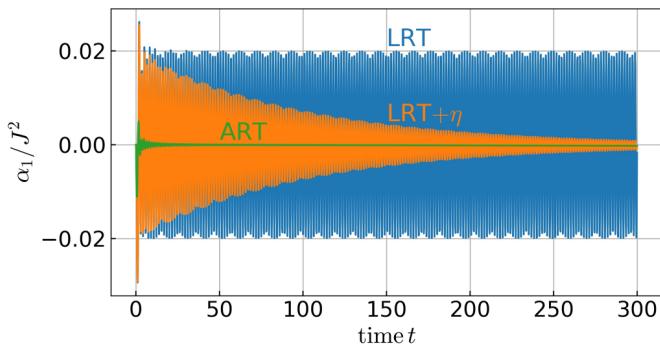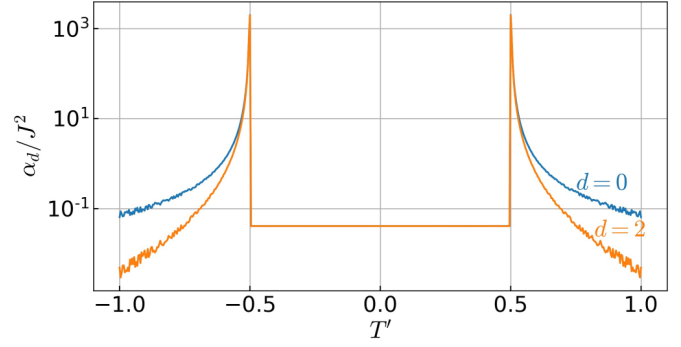

FIG. 3. Local and next-nearest-neighbor damping parameters, α_0 and α_2, for the $D = 1$ system at half filling as a function of the next-nearest-neighbor hopping T'. Calculations for $L = 10^6$.

LRT and ART, yield the same local and nonlocal damping constants.

B. Nonlocal spin friction

We have also calculated α_d for larger distances, $d = i_{m'} - i_m$. Both approaches precisely reproduce the finding of Refs. [25,49], namely, $\alpha_{d+2} = \alpha_d = \text{const} > 0$ for even distances $d = 0, 2, 4, \ldots$ and $\alpha_{d+2} = \alpha_d = \text{const} = 0$ for odd d. This distance (in)dependence of α_d is a characteristic feature for the $D = 1$ model at half filling.

Another, at first sight nonintuitive, numerical result is the T' dependence of the local and the next-nearest-neighbor Gilbert damping. This is shown in Fig. 3. We find that $\alpha_0(T') = \alpha_2(T') = \text{const}$ for all T' with $-T_c' < T' < T_c'$. The critical next-nearest-neighbor hopping is given by $T_c' = T/2$. Furthermore, $\alpha_1(T') = \alpha_3(T') = 0$ within the same T' range (not shown). For $|T'| > T_c'$, the T' dependence of $\alpha_d(T')$ is nontrivial. Again, this result is characteristic for $D = 1$ and half filling.

There is a simple proof for both the peculiar d and T' dependencies of $\alpha_d(T')$, which is based on the density-of-states formula given by Eq. (15). We first note that $T_c' = T/2$ is the critical value for a Lifshitz transition of the Fermi "surface." If $-T_c' < T' < T_c'$, the occupied k points lie in the range $-k_F < k < k_F$, with $k_F = \pi/2$ in the first Brillouin zone $[-\pi, \pi]$, i.e., k_F is independent of T' in this T' range. However, for $|T'| > T_c'$, the "Fermi-surface volume" splits into three disconnected parts. This is illustrated with Fig. 4.

For $D = 1$, $-T_c' < T' < T_c'$, and for $L \to \infty$, we can express the spectral density $A_d(0) \equiv A_{i_m i_{m'}}(\omega = 0)$ with $d = i_{m'} - i_m$ in the form

$$A_d(0) = \frac{1}{2\pi} \int_{-\pi}^{\pi} dk\, e^{ikd} \delta[\mu - \varepsilon(k)]$$

$$= \frac{1}{2\pi} \sum_{k_F} e^{ik_F d} \left(\frac{d\varepsilon(k)}{dk} \bigg|_{k=k_F} \right)^{-1}$$

$$= \frac{1}{\pi} \cos\left(\frac{\pi}{2} d \right) \frac{1}{2T}, \tag{43}$$

with Fermi wave vectors $k_F = \pm \pi/2$. With Eq. (15), this demonstrates that $\alpha_d(T')$ is independent of T' and oscillates

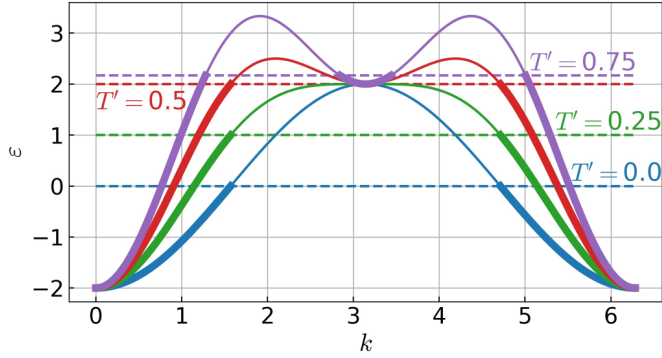FIG. 2. The same as Fig. 1, but for the nearest-neighbor damping $\alpha_1(t)/J^2$, i.e., $d = i_{m'} - i_m = 1$.

FIG. 4. Dispersion (34) for various T'. *Blue:* $T' = 0.0$ (no offset). *Green:* $T' = 0.25$, with vertical offset $\Delta \varepsilon = 0.5$. *Red:* $T' = 0.50$ ($\Delta \varepsilon = 1.0$). *Violet:* $T' = 0.75$ ($\Delta \varepsilon = 1.5$). Horizontal dashed lines: respective chemical potentials μ, corresponding to half filling. Thick lines indicate occupied states.

between 0 and $\alpha_0 = J^2/8\pi T^2 \approx 0.0398 J^2$ (with $T = 1$) for odd and even d, respectively.

C. Single-spin dynamics in $D = 1$

While LRT and ART yield the same Gilbert damping constant $\alpha_{mm'} = \lim_{t \to \infty} \alpha_{mm'}(t)$, the time dependence of the damping is very different, as discussed above (Figs. 1 and 2). The resulting spin dynamics, however, turns out to be essentially independent of the approach used, at least in the regime where the effective spin-only theory applies. In addition, the time dependence of the damping is practically irrelevant for the spin dynamics.

We start the related discussion with Fig. 5, which shows the time evolution of the x component of a single impurity spin coupled to a site of the one-dimensional model with $T' = 0$. Initially, the impurity spin points in the x direction, and the electron system is prepared in its ground state for
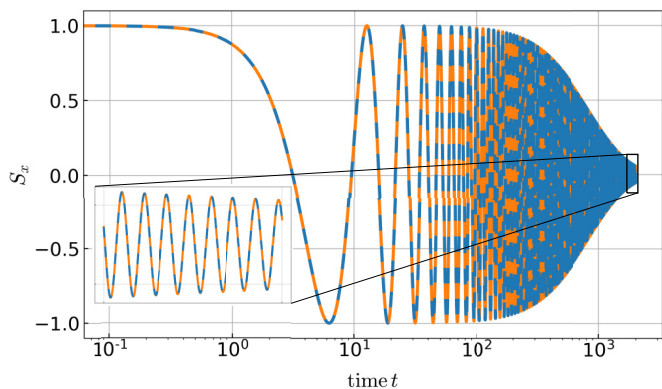

FIG. 5. Time dependence of the x component of a single impurity spin S coupled to a site of the $D = 1$ tight-binding model via a local exchange interaction J. At time $t = 0$, where J is suddenly switched on, the spin points in the x direction. For $t > 0$, the spin dynamics is driven by a finite local magnetic field $\boldsymbol{B} = (0, 0, B)$ in the z direction, which couples to S. Dashed blue line: LRT calculation with time-dependent damping. Solid orange line: LRT calculation with constant damping. Parameters: $L = 4000$, $T' = 0$, $J = 0.3$, $B = 0.5$, half filling.

$J = 0$. At time $t = 0$, we suddenly switch on the exchange coupling J and, in addition, a local and time-independent magnetic field $\boldsymbol{B} = (0, 0, B)$ in the z direction, which couples to the spin, i.e., $\hat{H} \mapsto \hat{H} - \boldsymbol{BS}$ (see, also, the discussion at the end of Sec. VI C). The purpose of the field is to drive the spin dynamics. In fact, for $t > 0$, the spin starts to precess around $\boldsymbol{B}$ with the Larmor frequency $\omega \approx B$, as seen in the oscillations of S_x and of S_y (not shown). On a timescale of a few thousand inverse hoppings, the spin finally aligns to the field, i.e., $S_z \to 1$ (not shown) and $S_x, S_y \to 0$. Importantly, Fig. 5 shows the prediction of LRT, as obtained from the equation of motion $\dot{\boldsymbol{S}}(t) = \alpha_0(t)\dot{\boldsymbol{S}}(t) \times \boldsymbol{S}(t) - \boldsymbol{B} \times \boldsymbol{S}(t)$ with time-dependent $\alpha_0(t)$ (dashed blue line) and for the same equation of motion but replacing $\alpha_0(t) \mapsto \alpha_0$, i.e., for time-independent α_0 (solid orange line).

There are no significant differences, either at early times or for times close to the relaxation time. Furthermore, inspection of the numerical data shows that the agreement becomes even better with decreasing field strength. The obvious interpretation is that the precession timescale $1/B$ set by the field strength B is long compared to the timescale for the oscillations of α_d that is set by the electronic band width, such that only the average over many α oscillations is actually relevant. This argument becomes increasingly pertinent with weaker (and thus more physical) field strengths B.

We have also calculated the spin dynamics within ART. The result perfectly agrees with that shown in Fig. 5. After the previous discussion, this was only to be expected since, within ART, $\alpha_0(t)$ oscillates with the same frequency as seen within LRT (cf. Fig. 1) and converges to the constant α_0 after a few oscillations anyway. We conclude that the time dependence of the Gilbert damping is practically irrelevant for the resulting spin dynamics within both approaches, LRT and ART. From this point on, we therefore use LRT with time-independent damping constants $\alpha_{mm'}$.

The predictions of the effective spin-only theory agree very well with the results obtained from the full theory, i.e., from Eqs. (4) and (5). For a numerical evaluation of the full theory up to a propagation time t_{prop} and avoiding unwanted finite-size effects, i.e., interferences due to excitations propagating back to the impurity spin (in the case of periodic boundary conditions), one must consider systems with $L \gtrsim v t_{\text{prop}}$, where $v = d\varepsilon(k_F)/dk$ is the Fermi velocity. At half filling and for $T' = 0$, we have $v_F = 2$. This implies that a system with $L = 1000$ sites is sufficiently large to see complete spin relaxation, if the relaxation time is $\tau \lesssim 500$.

As can be seen in Fig. 6, this is the case when choosing $J = 0.5$ and $B = 1.0$ (see top panel). While S_x (and S_y, not shown) oscillates with the Larmor frequency $\omega \approx B$, the z component of the spin monotonously increases from $S_z = 0$ for $t = 0$ to $S_z \approx 1$ for $t \approx 300$. The dynamical evolution is qualitatively the same for both the full theory and the effective spin-only theory. The agreement is even quantitative; there is merely a small difference of a few percent between the full and the effective theory visible in the z component of $\boldsymbol{S}(t)$ around $t = 100$, and the relaxation is somewhat faster in the full theory.

Physically relevant coupling strengths J and magnetic fields B (or effective "Weiss" fields produced via RKKY exchange in a multi-impurity-spin system) are generically
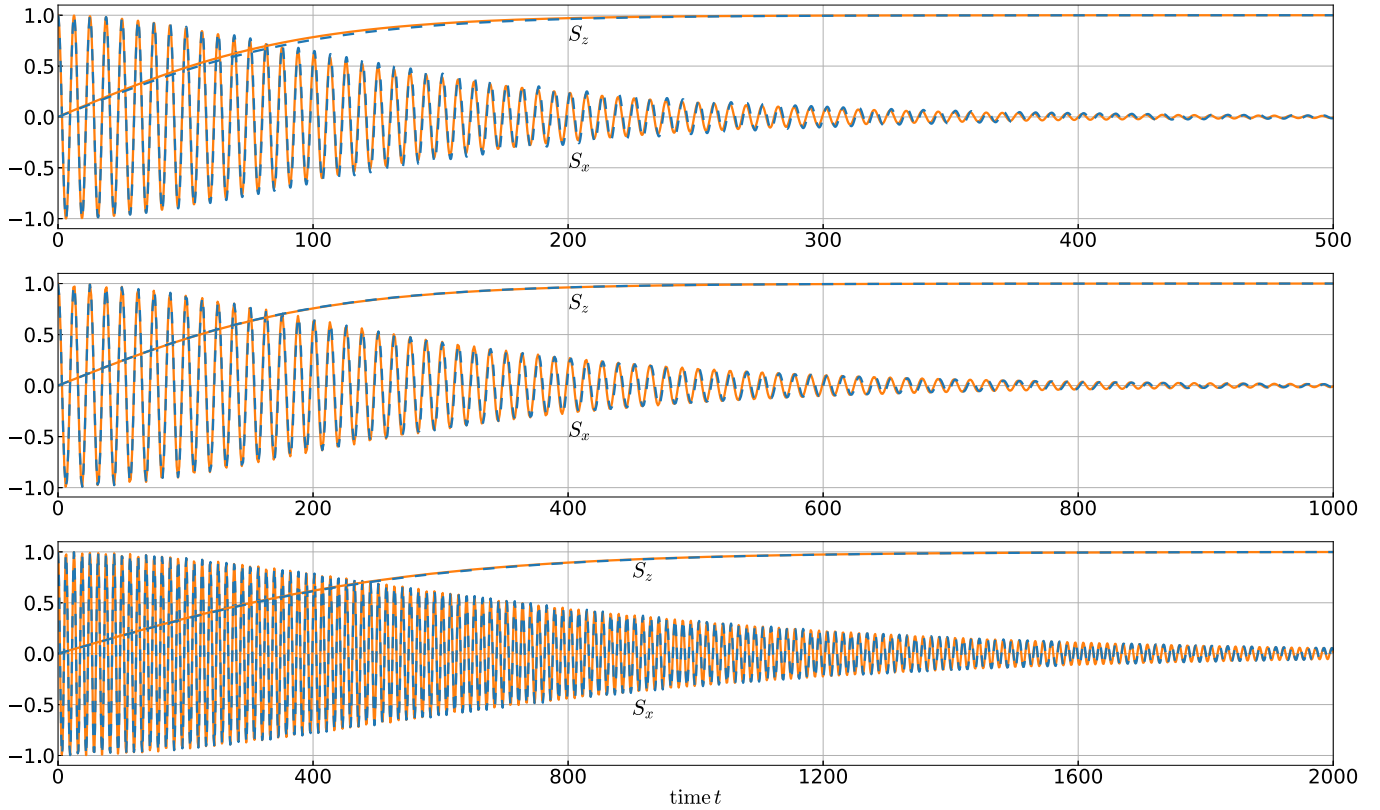
FIG. 6. Time dependence of S_x and of S_z as obtained from the full theory (solid orange line), Eqs. (4) and (5), compared to the effective theory (dashed blue). Top: Calculations with $J = 0.5$ and $B = 1.0$ for a chain of length $L = 1000$ with periodic boundaries; $T' = 0$. Middle: The same, but for $J = 0.5$ and $B = 0.5$. System size: $L = 2000$. Note the different timescale. Bottom: The same, but for $J = 0.3$ and $B = 0.5$. System size: $L = 4000$. Note the different timescale.

much weaker. A weaker field B implies a smaller precession frequency and thus a slower spin dynamics. Hence, this implies a more adiabatic motion and thus improves the short-retardation-time approximation. In fact, comparing the results at fixed $J = 0.5$, for $B = 1.0$ (Fig. 6, top panel) with those obtained for $B = 0.5$ (Fig. 6, middle panel), one finds an even better agreement between the full and the effective theory for the smaller field strength. Note that the relaxation time increases with decreasing B. We have thus extended the maximum propagation time to $t_{\text{prop}} = 1000$ and, accordingly, the system size to $L = 2000$.

Similarly, a weaker J, at fixed B, improves the weak-coupling approximation. In the bottom panel of Fig. 6, for $J = 0.3$ and $B = 0.5$, the agreement between the full and the effective theory is perfect on the scale of the figure. The relaxation time increases once more.

The results discussed so far have been obtained by simultaneously switching on the coupling J and the field B at time $t = 0$. This setup for initiating the dynamics is the one that is conceptually consistent with the linear response approach. Alternatively, we have tentatively initiated the dynamics by starting from the coupled system at finite J and switching on the field B only. Using this second setup and within the full theory, we did not find any significant differences in the spin dynamics. This is easily understood since, (i) for the considered coupling strengths, there is only a very weak polarization of the conduction-electron local magnetic moment $\langle s_{i_0} \rangle$ at $t = 0$. At $J = 0.5$, for example, its magnitude amounts

to $|\langle s_{i_0} \rangle| \approx 0.064$, i.e., almost an order of magnitude smaller that the saturation value, and hence its feedback effect on the spin dynamics is weak. (ii) While in the first setup $\langle s_{i_0} \rangle = 0$ at time $t = 0$, the moment very quickly polarizes *in the course of time* to the same value $|\langle s_{i_0} \rangle| \approx 0.064$ that is found at $t = 0$ in the second setup. In fact, the polarization takes place on the fast electronic timescale and is fully completed already after $t = 1/T = 1$. We can thus state that the spin dynamics practically does not depend on the preparation of the initial state.

D. Van Hove singularities

Besides J, the strength of the (local) Gilbert damping also depends on the density of states at the Fermi energy, as Eq. (15) demonstrates. A divergence of the density of states at the Fermi energy then implies a divergent damping constant α_0. The analysis of the effective equation of motion for a single spin [11,56,70],

$$\dot{\boldsymbol{S}}(t) = \alpha_0 \, \dot{\boldsymbol{S}}(t) \times \boldsymbol{S}(t) \ - \boldsymbol{B} \times \boldsymbol{S}(t),$$

gives the exact analytical result,

$$\tau \propto \frac{1 + \alpha_0^2}{\alpha_0} \frac{1}{B}, \tag{44}$$

for the relaxation time τ. The relaxation time diverges for $\alpha_0 \to \infty$.

We have checked this against the numerical evaluation of the full theory, given by Eqs. (4) and (5), for the half-filled
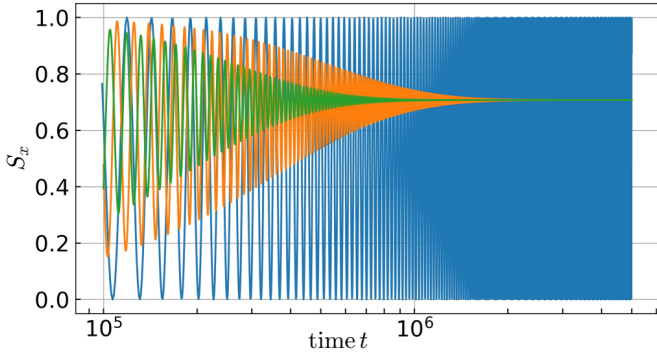
FIG. 7. Time evolution of the x component of $\boldsymbol{S}_1$ in a setup with two spins $\boldsymbol{S}_1$ and $\boldsymbol{S}_2$ at distance $d = 2$ and for $J = 0.1$. Results for $T' = 0$ (blue line), $T' = 0.6$ (orange). The green line is the result of a calculation for $T' = 0.6$, where α_2 is set to zero. Parameters: $L = 10^6$, $\eta = 10^{-5}$.
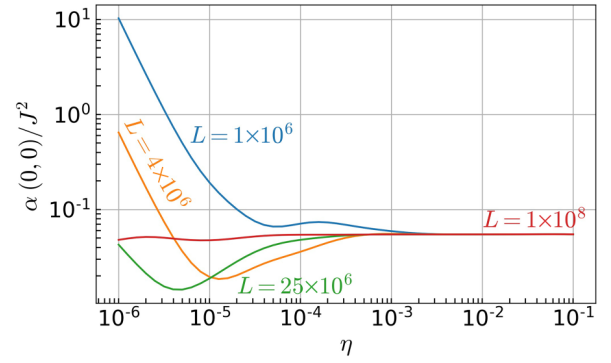

FIG. 8. Local Gilbert-damping parameter $\alpha(0, 0)/J^2$ as a function of the regularization parameter η for different system sizes L. Calculations for the $D = 2$ square lattice with next-nearest-neighbor hopping $T' = -0.3$.

system, $J = 0.5$, $B = 1.0$, and next-nearest-neighbor hopping $T' = -0.5$, where the density of states exhibits a strong $1/\sqrt{\omega}$ van Hove singularity at the Fermi energy (see Fig. 3). In addition, slightly smaller $T' \lesssim -0.5$ have been considered. Contrary to the prediction of the effective theory, we find a finite relaxation time of the order of $\tau = O(10^2)$. This shows that the effective theory fails if the (dimensionless) parameter, given by the product of J with the density of states at the Fermi energy, is large.

E. Two-spin dynamics in $D = 1$

In the case of two impurity spins at distance $d = i_{m'} - i_m$ and vanishing magnetic field, the effective equations of motion read

$$\dot{\boldsymbol{S}}_1 = J_d \boldsymbol{S}_2 \times \boldsymbol{S}_1 + \alpha_0 \boldsymbol{S}_1 \times \dot{\boldsymbol{S}}_1 + \alpha_d \boldsymbol{S}_1 \times \dot{\boldsymbol{S}}_2, \qquad (45)$$

$$\dot{\boldsymbol{S}}_2 = J_d \boldsymbol{S}_1 \times \boldsymbol{S}_2 + \alpha_0 \boldsymbol{S}_2 \times \dot{\boldsymbol{S}}_2 + \alpha_d \boldsymbol{S}_2 \times \dot{\boldsymbol{S}}_1. \qquad (46)$$

Here, we have disregarded the time dependence of $\alpha_d(t)$, as discussed above, but also of the RKKY coupling $J_d(t)$ [see Eq. (12)]. The latter shows an oscillatory time dependence with the same characteristic frequency $\omega_{\mathrm{vH}} = \pm 2$ that was found for $\alpha_d(t)$, but decays quickly on a timescale of a few tens of inverse hoppings. Using the same reasoning as for the damping, we can also ignore the t dependence of $J_d(t)$, if J is sufficiently small.

As discussed above, for half filling and if $-T_{\mathrm{c}}' < T' < T_{\mathrm{c}}'$, the damping parameters α_d for all even d are equal, while $\alpha_d = 0$ for arbitrary odd d. Hence, coupling the two impurity spins to neighboring lattice sites, the nonlocal damping vanishes and, independent of the initial spin configuration, one finds a relaxation of the spin system to its ground state that is driven by the local damping parameter α_0 only.

For distance $d = 2$, the situation is completely different (see, also, the discussion in Ref. [49]): Exploiting the fact that $\alpha_0 = \alpha_2$ and adding the two Eqs. (45) and (46) immediately implies that $\boldsymbol{S}_{\mathrm{tot}} = \boldsymbol{S}_1 + \boldsymbol{S}_2$ is a constant of motion and, consequently, $\boldsymbol{S}_1 \boldsymbol{S}_2$ is constant as well. We conclude that the spin system does not relax at all, if d is even.

This is demonstrated with Fig. 7, where the time dependence of the x component of $\boldsymbol{S}_1$ is shown for a system with

two impurity spins at distance $d = 2$, initially prepared as mutually orthogonal, $\boldsymbol{S}_1 \boldsymbol{S}_2 = 0$. In fact, there is no relaxation for $T' = 0$ and S_{1x} exhibits an undamped oscillation. This appears to be counterintuitive.

On the contrary, for $T' = 0.6 > T_{\mathrm{c}}' = 0.5$, the two-spin system relaxes to its (ferromagnetic) ground-state spin configuration. The rather long relaxation time $\tau \sim 10^6$ is due to the chosen weak coupling strength $J = 0.1$. The relaxation is due to the fact that $\alpha_0 = \alpha_2$ is no longer enforced by the arguments leading to Eq. (43): At $T' = 0.6$, we find $\alpha_0 = 1.169$ and $\alpha_2 = 0.581$.

Figure 7 also shows the time evolution of $S_{1x}(t)$ for the same $T' = 0.6$, but neglecting the nonlocal damping, i.e., the result of a calculation where we have *ad hoc* set $\alpha_2 = 0$. Intuitively, one would expect that switching off the nonlocal damping would lead to a longer relaxation time. However, as is seen in the figure, the opposite behavior is found and τ, in fact, *decreases* if one sets $\alpha_2 = 0$.

F. Local and nonlocal spin friction in $D = 2$

The numerical computation of the local and the nonlocal elements of the (time-independent) Gilbert damping $\alpha_{mm'}$ on the $D = 2$ square lattice proceeds along the lines described in Sec. V. As for $D = 1$, a proper choice of the regularization parameter η is decisive.

Due to translational symmetry, the damping parameters $\alpha_{mm'}$ only depend on the distance vector $\boldsymbol{R} = (R_x, R_y)$ between the two sites i_m and $i_{m'}$ in the square lattice. Figure 8 shows the local damping parameter $\alpha(0, 0)$, and Fig. 9 shows the nonlocal damping parameter $\alpha(9, 9)$, i.e., for two spins $\boldsymbol{S}_1$ and $\boldsymbol{S}_2$ along the diagonal with distance vector $\boldsymbol{R} = (9, 9)$, which is the maximum distance considered here.

Note that the limit $L \to \infty$ should be taken for a finite $\eta > 0$, and that the $\eta \searrow 0$ limit should be taken in the end. For $\boldsymbol{R} = (0, 0)$ (Fig. 8) and for $\eta = 10^{-3}$, the thermodynamic limit is reached with $L \gtrsim 4 \times 10^6$ in practice. The same result for $\alpha(0, 0)$ is obtained with larger parameters, e.g., with $\eta = 10^{-2}$, where the thermodynamical limit is reached even earlier ($L = 1 \times 10^6$ is sufficient). Computations with, e.g., $L = 10^6$ and $\eta = 10^{-2}$ are fully converged. A too small η requires larger system sizes, otherwise one only resolves finite-size
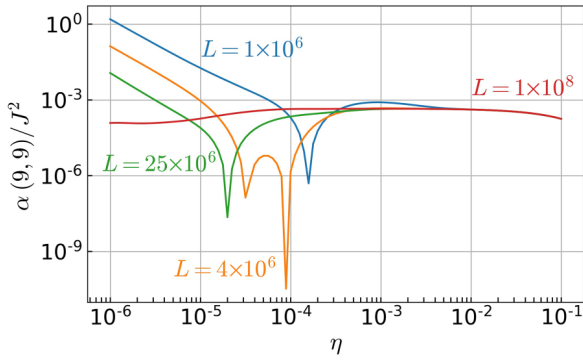
FIG. 9. The same as Fig. 8, but for the nonlocal Gilbert-damping parameter $\alpha(9,9)/J^2$ for sites linked by the distance vector $R = (9, 9)$.

artifacts. For a too large η, on the other hand, results start to get an unphysical η dependence (even for sufficiently large L).

Achieving convergence, i.e., $\lim_{\eta \searrow 0} \lim_{L \to \infty}(\cdots)$, is more difficult for longer distance vectors $\boldsymbol{R}$. At $\boldsymbol{R} = (9, 9)$ (see Fig. 9), there is an η-independent plateau for sufficiently large L (e.g., $L = 4 \times 10^6$) in a smaller η range, $\eta = 10^{-3}$–10^{-2} [note the logarithmic scale for $\alpha(\boldsymbol{R})/J^2$].

In the rest of the paper, we consider classical spins that are exchange coupled to a half-filled conduction-electron system with nearest-neighbor hopping $T = 1$ and finite next-nearest-neighbor hopping T' on the $D = 2$ square lattice. The tight-binding dispersion is given by Eq. (35). Considering a finite next-nearest-neighbor hopping is essential for $D = 2$ and at half filling since for $T' = 0$ the density of states exhibits a logarithmic van Hove singularity at the corresponding chemical potential.

This is also seen in Fig. 10, which shows the μ dependence of the local damping $\alpha(0, 0)$ for different T'. For $T' = 0$, the chemical potential corresponding to half filling is $\mu = 0$, i.e., the Gilbert damping diverges and the effective theory would break down, as discussed in Sec. VI D. With decreasing T', the location of the divergence shifts to lower chemical potentials. At $T' = -0.3$, the singularity is located at
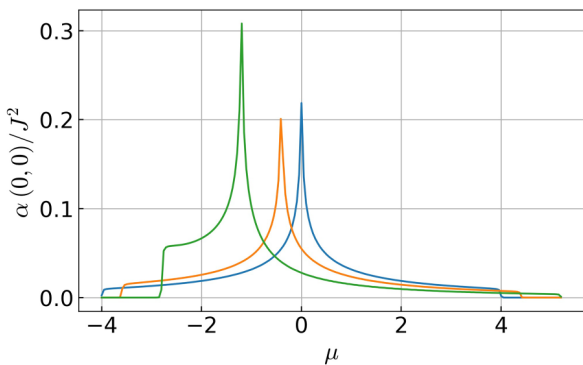

FIG. 10. Local Gilbert damping $\alpha(0, 0)$ for the $D = 2$ tight-binding model as a function of the chemical potential μ for different values of the next-nearest-neighbor hopping. Blue line: $T' = 0$. Orange: $T' = -0.1$. Green: $T' = -0.3$. Parameters: $L = 10^6$, $\eta = 10^{-2}$. At $T' = -0.3$, half filling is achieved with $\mu \approx -0.66$.
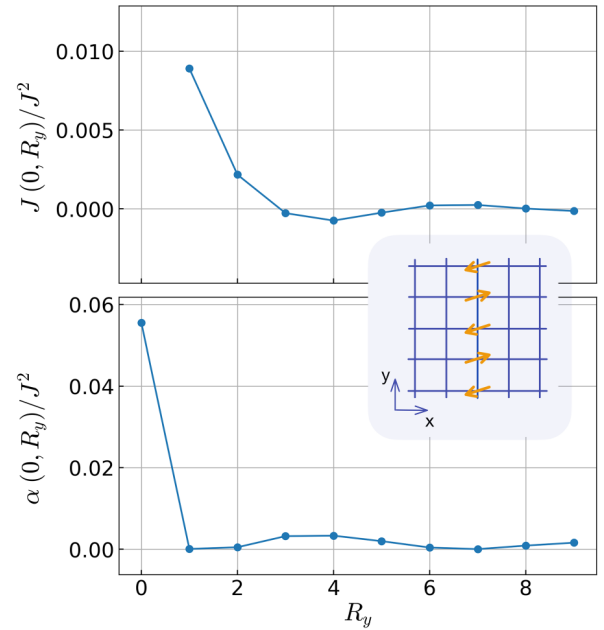

FIG. 11. Distance dependence of the RKKY interaction $J(\boldsymbol{R})$ (upper panel) and of the Gilbert damping $\alpha(\boldsymbol{R})$ (lower panel), both normalized to unit local exchange J, along the y axis of the square lattice, $\boldsymbol{R} = (0, R_y)$. $T = 1$, $T' = -0.3$, $L = 4 \times 10^6$, $\eta = 1 \times 10^{-3}$. Inset: A ground-state spin configuration.

$\mu \approx -1.19$, while half filling is achieved with $\mu \approx -0.66$, where $\alpha(0, 0) \approx 0.055$ is still small.

G. Distance and directional dependence

In the one-dimensional case and for T' with $-T'_c < T' < T'_c$, the counterintuitive relaxation dynamics of two spins at distance d results from the extremely nonlocal spin friction given by $\alpha_d = \frac{1}{2}[1 + (-1)^d]\alpha_0$, as has been discussed in Sec. VI B.

For higher-dimensional lattices, $D \geqslant 2$, the dependence of the Gilbert damping $\alpha(R)$ with $R = |\boldsymbol{R}|$ can be computed analytically, when assuming a free dispersion $\varepsilon(\boldsymbol{k}) = \frac{k^2}{2m}$. One easily finds

$$\alpha(R) \propto \frac{1}{R^{D-1}} \quad \text{for } R \to \infty. \tag{47}$$

This may be compared to the well-known distance dependence of the RKKY interaction,

$$J(R) \propto \frac{1}{R^D} \quad \text{for } R \to \infty, \tag{48}$$

which decays more rapidly with R. Analytical results for $\alpha(R)$ for all R and including the proportionality constants (but still assuming a free dispersion) can be found in Ref. [25].

Here, for the tight-binding dispersion and for not too large distances, we show that the distance dependencies are less regular and that the directional dependencies are much more important. Numerical results for the $D = 2$ tight-binding system and a generic value for the next-nearest-neighbor hopping $T' = -0.3$ are shown in Figs. 11 and 12. Along the y axis with $\boldsymbol{R} = (0, R_y)$ (see Fig. 11), we find an oscillatory dependence of $J(0, R_y)$ with decreasing amplitude as R_y increases.
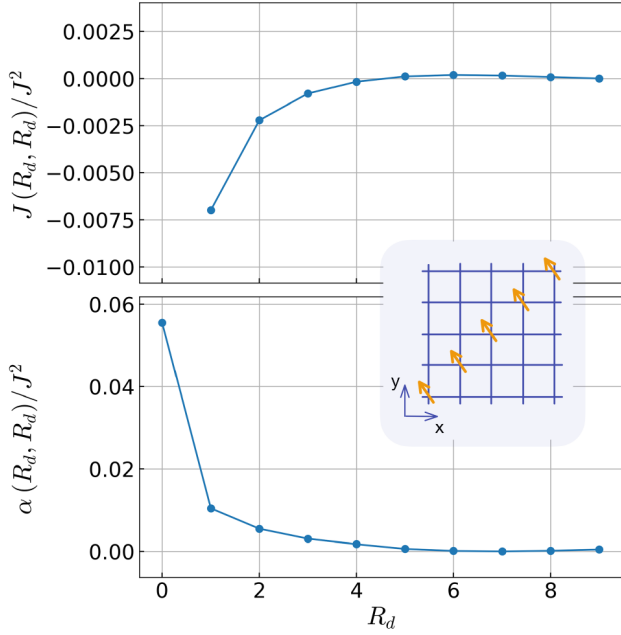
FIG. 12. The same as Fig. 11, but along the diagonal $\boldsymbol{R} = (R_d, R_d)$ with $R_x = R_y = R_d$. Inset: A ground-state spin configuration.

The nonlocal Gilbert damping $\alpha(0, R_y)$ is positive and shows slight oscillations with decreasing amplitude. Remarkably, all nonlocal elements $\alpha(0, R_y)$ with $R_y \geqslant 1$ are smaller by more than one order of magnitude as compared to the local Gilbert damping $\alpha(0, 0)$.

Along the diagonal of the square lattice (see Fig. 12), the RKKY coupling is negative (ferromagnetic) rather than oscillatory at short distances $R_x = R_y \leqslant 4$. Likewise, the Gilbert damping exhibits a strong directional dependence. For nearest and next-nearest neighbors along the diagonal, i.e., for $\boldsymbol{R} = (1, 1)$ and for $\boldsymbol{R} = (2, 2)$, it is much stronger as compared to nearest- and next-nearest-neighbor positions along the y axis, $\boldsymbol{R} = (0, 1)$ and $\boldsymbol{R} = (0, 2)$, for example.

H. Effect of nonlocal Gilbert damping in $D = 2$

To study the effect of the nonlocal Gilbert damping on the relaxation dynamics of impurity spins in two dimensions, we first consider a setup with two classical spins that are exchange coupled to next-nearest-neighbor sites, i.e., $\boldsymbol{R} = (1, 1)$. Figure 13 shows the relaxation time τ as a function of the next-nearest-neighbor hopping T', starting from an initial state where the two classical spins are orthogonal.

Of course, the definition of τ is somewhat arbitrary. As an operational criterion for (almost) full relaxation of R impurity spins, we employ the condition

$$\frac{1}{R-1} \sum_{r=1}^{R-1} |\boldsymbol{S}_r \boldsymbol{S}_{r+1} \mp 1| < \epsilon, \qquad (49)$$

with the $-$ sign in the case of a ferromagnetic alignment in the ground state and with the $+$ sign for antiferromagnetic alignment. Furthermore, we choose $\epsilon = 0.001$. We find that the criterion given by Eq. (49) is completely fulfilled for a sufficiently long time evolution so that we can define the
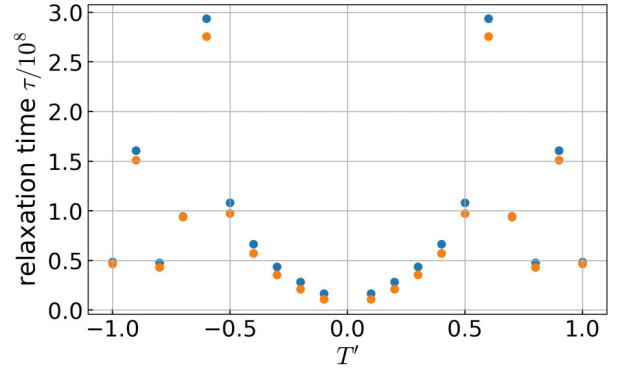

FIG. 13. Relaxation time τ as function of the next-nearest-neighbor hopping T' for a system with two classical spins that are locally exchange coupled with $J = 0.1$ to next-nearest-neighbor sites of the square lattice, $\boldsymbol{R} = (1, 1)$. In the initial state, the two impurity spins enclose the angle $\pi/2$. Blue: Computation including the non-local Gilbert damping. Orange: Computation with nonlocal Gilbert damping set to zero. The conduction-electron system is at half filling. Parameters: $L = 4 \times 10^6$, $\eta = 0.01$.

relaxation time τ as the latest time for which Eq. (49) no longer applies.

As can be seen in Fig. 13, τ monotonously increases with increasing $|T'|$ up to $|T'| = 0.6$, while for $|T'| \geqslant 0.7$, the τ dependence becomes more complicated. This is partly related to the T' dependence of the ground-state spin configuration, which is determined by the RKKY interaction. For $T' = 0$ and $\boldsymbol{R} = (1, 1)$, we have $J(\boldsymbol{R}) < 0$, i.e., ferromagnetic coupling. A finite (positive or negative) T' increases the tendency towards antiferromagnetic coupling. In fact, we find $J(\boldsymbol{R}) < 0$ (ferromagnetic) for the data points up to $T' = 0.6$, and for $T' = 0.8$, while $J(\boldsymbol{R}) > 0$ (antiferromagnetic) for $T' = 0.7, 0.9, 1.0$. This "irregularity" in the ground-state spin configuration and in the relaxation time is due to the nontrivial T' dependence of both the RKKY coupling and the Gilbert damping. In all cases, the impurity-spin configuration in the fully relaxed state is identical to the ground-state configuration.

The relaxation timescale crucially depends on J and is clearly unreachable in practice by *full* quantum-classical theory at a local exchange coupling $J = 0.1$. The numerical results of the effective spin-only theory (Fig. 13) show that roughly, the relaxation time is of the order of $\tau \sim 10^8$ (see blue symbols) and thus, at the same value for J, about two orders of magnitude larger than for the $D = 1$ case (see Sec. VI E).

Let us note here that the spin dynamics is numerically very stable and does not significantly change when sharpening the tolerances for numerical errors in the solution of the system of differential equations. Furthermore, slight deviations in the initial state, e.g., a small change of the angle enclosed by the two spins, only leads to small changes of τ.

Interestingly, a clearly *shorter* relaxation time is obtained when disregarding the nonlocal Gilbert damping. At $T' = \pm 0.3$, where the value for $\alpha(1, 1)$ is about 18% of the local damping (see Fig. 12), a decrease of τ by about 10% is found, when *ad hoc* switching off the nonlocal damping. The effect becomes stronger with decreasing $|T'|$.

Let us mention that for $T' = 0$, the relaxation time is infinite in the effective theory due to the van Hove singularity at the Fermi energy of the half-filled conduction-electron system (see the discussion in Sec. VI D). The equations of motion given by Eq. (2) are meaningless in this case since $\alpha(\mathbf{R})$ is divergent.

The finding that including nonlocal Gilbert damping leads to *longer* relaxation times is reminiscent of the results found for the $D = 1$ lattice. For the $D = 1$ case, the effect could be explained analytically as the result of an emergent conserved quantity that is not caused by a symmetry of the Hamiltonian; see Sec. VI E. The main point is that an infinite relaxation time is obtained if $\alpha_0 = \alpha_d$, which is exactly realized for impurity spins coupled to next-nearest-neighbor (distance $d = 2$) sites on the $D = 1$ lattice. For the $D = 2$ case, the ratio $\alpha(1, 1)/\alpha(0, 0)$ is clearly smaller than unity (see Fig. 12 for $T' = -0.3$) and, therefore, there is a weak reminiscence of the effect only, but still the relaxation time *increases* due to nonlocal damping. This is corroborated by the observation that the effect is practically absent if the impurity spins couple to nearest-neighbor sites along the y axis of the square lattice, where we find $\alpha(0, 1)/\alpha(0, 0) \approx 0.001$ (see Fig. 11 for $T' = -0.3$).

I. Relaxation of spin arrays

For the above-discussed setup with two impurity spins coupled to the square lattice, the *local* Gilbert damping dominates the relaxation dynamics. Considering more impurity spins introduces additional complexity: The spatial structure of the RKKY interaction might lead to magnetic frustration, and the growing number of nonlocal damping terms might result in a qualitatively different relaxation dynamics.

Here, we study systems in two different chain geometries: (i) nearest-neighbor chains of R impurity spins along, say, the y direction, as visualized with the inset in Fig. 11, and (ii) next-nearest-neighbor chains of length R along a diagonal of the square lattice; see the inset in Fig. 12. The respective relaxation times τ, defined via Eq. (49), are shown as a function of the chain length R in Figs. 14 and 15.

We start with the discussion of the chain along the y axis. Two different initial spin configurations have been considered. The filled circles in Fig. 14 refer to the first initial configuration, a $\pi/2$-spin spiral state at time $t = 0$, where each spin $\mathbf{S}_m$ is obtained from $\mathbf{S}_{m-1}$ by a $\pi/2$ rotation around an axis perpendicular to the first spin $\mathbf{S}_1$.

The computations have been performed for $T' = -0.3$, where we have a strongly positive RKKY coupling between nearest neighbors and a smaller but still positive RKKY coupling between next-nearest neighbors; see Fig. 11. While this implies significant magnetic frustration, we find that the ground-state spin configuration of the chain is antiferromagnetic for all $R = 2, \ldots, 10$. This ground-state configuration is, in fact, reached on *roughly* the same timescale $\tau \sim 10^8$ (at $J = 0.1$) for all chain lengths R. We find that the relaxation time is clearly shorter for chains with even R, opposed to chains with an odd number of spins. This implies a rather regular oscillation of τ with R and might be traced back to the choice of the initial state. Indeed, a less regular R dependence of τ is seen for the second initial spin configuration, where we have
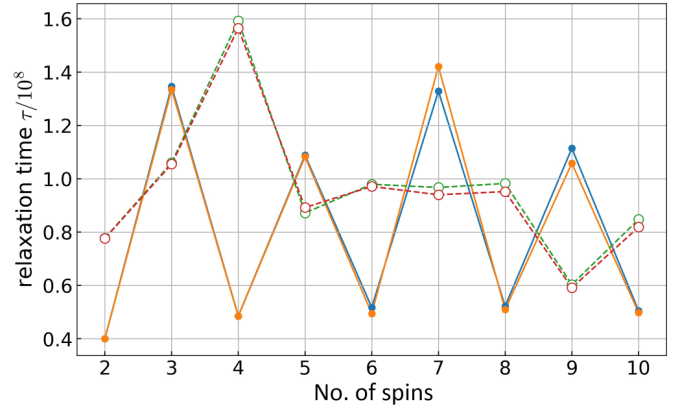

FIG. 14. Relaxation time τ as function of the number of spins, R, as determined via Eq. (49) for $\epsilon = 0.001$. Computations for a system of R impurity spins ($R = 2$–10) coupled to the sites $(0, 0), (0, 1), (0, 2), \ldots, (0, R - 1)$ of the square lattice; see inset of Fig. 11. Filled circles: data obtained for an initial spin configuration with $\mathbf{S}_m = O^{m-1}\mathbf{S}_1$ for $m = 2, \ldots, R$, where O is the orthogonal 3×3 matrix representing a $\pi/2$ rotation around a fixed axis perpendicular to $\mathbf{S}_1$ ($\pi/2$ spin spiral). Open circles: initial spin configuration given by $\mathbf{S}_m = (-1)^m \mathbf{S}_2$ for $m = 3, \ldots, R$ and $\mathbf{S}_1 = O\mathbf{S}_2$ (antiferromagnetic configuration with first spin rotated by $\pi/2$). $\mathbf{S}_1$ is kept fixed during the time evolution. Orange and red symbols: relaxation time as obtained from computations with all nonlocal Gilbert-damping parameters set to zero. Blue and green symbols: computations including the full nonlocal Gilbert damping. Parameters: $L = 4 \times 10^6$, $\eta = 10^{-3}$, $T' = -0.3$.

assumed all spins aligned antiferromagnetically, except for the first, which is rotated by $\pi/2$ around an axis perpendicular to the directions of the remaining spins and kept fixed during the subsequent dynamics.

For both types of initial states, there is no general *overall* increase or decrease of τ with increasing R, i.e., the relax-
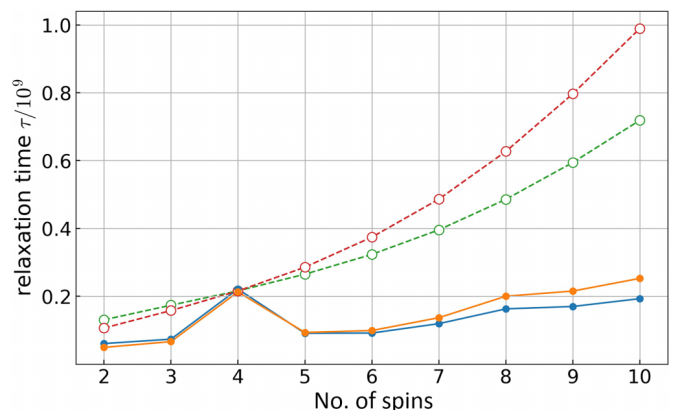
FIG. 15. The same as Fig. 14, but for impurity No. of spins coupled to the sites $(0, 0), (1, 1), (2, 2), \ldots, (R - 1, R - 1)$ along a diagonal on the square lattice; see inset of Fig. 12. As in Fig. 14, the first initial spin configuration (filled circles) is a $\pi/2$-spin spiral. Contrary to Fig. 14, however, the second configuration (open circles) is given by a *ferromagnetic* spin configuration, except for the first spin $\mathbf{S}_1$, which is rotated by $\pi/2$ (and kept fixed during the time evolution).

ation timescale $\tau \sim 10^8$ roughly remains constant. This hints towards a dominantly local relaxation mechanism, where the relaxation time is mainly dominated by the approach of the local ground state, while reaching the overall collinear spin structure is not very crucial.

This view is corroborated by the observation that the local Gilbert damping still dominates the relaxation dynamics: For both types of initial conditions, we have performed computations with all nonlocal damping switched off, i.e., $\alpha(\boldsymbol{R}) = 0$ for all $\boldsymbol{R}$ except for $\boldsymbol{R} = (0, 0)$. Results are displayed by orange and red circles in the figure. While there is some effect of the nonlocal damping, it is generally small. This is remarkable since the number of nonlocal damping terms grows as $R(R - 1)/2$ with R, i.e., quadratically for large R opposed to the number R of local damping terms. We also note that switching off the nonlocal damping counterintuitively leads to shorter relaxation times τ for *some R*, as discussed above for $R = 2$, but there seems to be no clear trend.

This is very much different for chains along the diagonal of the square lattice; see the results in Fig. 15. Here, the RKKY couplings $J(\boldsymbol{R})$ for the first three distance vectors $\boldsymbol{R} = (1, 1), (2, 2), (3, 3)$ are non-negligible and all negative (ferromagnetic); see Fig. 12. Hence, there is no significant magnetic frustration. In fact, the ground-state spin configuration turns out to be ferromagnetic for all $\boldsymbol{R}$ and is always reached as the final state of the relaxation dynamics.

For the diagonal spin chain, we find that the relaxation time τ increases with the number of spins, R, for both initial spin configurations, the global $\pi/2$-spin spiral (filled circles) and for an initial configuration (open circles) with only the first spin $\boldsymbol{S}_1$ rotated by $\pi/2$ out of the ferromagnetic ground-state configuration. The growth of τ with R is plausible in both cases since there is a total impurity-spin difference between the initial and the final configurations, which linearly grows with R. As the total spin of the full quantum-classical system (including the conduction electrons) is a constant of motion, this difference must be compensated in the course of time by a corresponding difference in the conduction-electron system. In other words, the necessary amount of spin dissipation grows with R and leads to a (superlinearly) growing relaxation time. Note that for the second type of initial conditions, only the component of the total spin along the direction of $\boldsymbol{S}_1$ is constant. This reasoning is also supported by the fact that overall the relaxation times are about an order of magnitude larger (of the order of $\tau \sim 10^9$) for the spin chain along the diagonal compared to the chain along the y axis ($\tau \sim 10^8$).

The data obtained for the initial $R = 4$ spin spiral represent an exception and, to a lesser extent, those for $R = 8$ as well; see the respective peaks of $\tau(R)$ in Fig. 15. As already discussed above (Fig. 14), this appears related to the period of the $\pi/2$-spin spiral, as for $R = 4, 8, 12, \ldots$ the total impurity spin is zero and thus the necessary spin dissipation is at a maximum. We have checked this by analogous computations for a $2\pi/3$-spin spiral. As expected, the corresponding relaxation times peak at $R = 3, 6, 9$ with strongly decreasing peak heights as R increases.

Finally, switching off all nonlocal Gilbert damping constants, $\alpha(\boldsymbol{R}) = 0$ for $\boldsymbol{R} \neq (0, 0)$, has a substantial impact on the relaxation time for the spin chain on the diagonal. Very consistently, the relaxation time slightly *decreases* for both

types of initial states, if $R = 1, 2, 3$—this is the counterintuitive effect observed and discussed earlier. For $R = 5, 6, \ldots$, on the other hand, we find an increasing relaxation time. We attribute this trend reversal to the fact that the overall larger nonlocal damping (see Figs. 11 and 12), in combination with the growing number of nonlocal terms as R increases, now substantially adds to the local damping mechanism.

J. Weakly interacting systems

The derivation (see the Appendix) of Eq. (15) is based on the application of Wick's theorem and thus cannot be used to compute the Gilbert damping in the case of a correlated electron system. Therefore, we compute $\alpha_{mm'}$ via the frequency derivative of the magnetic susceptibility at $\omega = 0$, i.e., via Eq. (14). Addressing weakly interacting systems, the random-phase approximation (RPA) [64,71–73] is employed here. We start from Eq. (37) for the noninteracting retarded magnetic susceptibility, denoted here as $\chi_{mm'}^{(0)}(t)$, to get $\chi^{(0)}(\boldsymbol{k}, \omega)$ via Fourier transformation from real to $\boldsymbol{k}$ space and from time to frequency representation. The interacting RPA susceptibility is then obtained as

$$\chi(\boldsymbol{k}, \omega) = \frac{\chi^{(0)}(\boldsymbol{k}, \omega)}{1 + U \chi^{(0)}(\boldsymbol{k}, \omega)}, \tag{50}$$

for the $D = 2$ Hubbard model on the square lattice,

$$\hat{H}_{\text{el}} = \sum_{\langle ii' \rangle} \sum_{\sigma = \uparrow, \downarrow} T_{ii'} c_{i\sigma}^{\dagger} c_{i'\sigma} + U \sum_{i} n_{i\uparrow} n_{i\downarrow}, \tag{51}$$

where U is the strength of the on-site Hubbard interaction.

On the level of one-particle excitations, the RPA corresponds to the Hartree-Fock approach. We consider the paramagnetic phase of the Hubbard model at weak U and finite next-nearest-neighbor hopping $T' \neq 0$. As has been found within Hartree-Fock theory [74], the paramagnetic state of the system becomes unstable towards an antiferromagnetic state at a finite critical interaction $U_c = U_c(T')$.

Our numerical calculations have been performed for lattices with $L = 512 \times 512$ sites, periodic boundary conditions, a large inverse temperature $\beta = 500$, and using a small regularization parameter $\eta = 0.015$. We have checked that the results do not significantly depend on these choices and are representative for the zero-temperature and the thermodynamical limit. In particular, we recover the known results for U_c [74]. At $T' = -0.3$, for instance, we find $U_c \approx 2.53$, which is straightforwardly obtained as the singularity of $\chi(\boldsymbol{k}, \omega)$ at $\boldsymbol{k} = (\pi, \pi)$ and $\omega = 0$.

In reciprocal space, the frequency derivative of the susceptibility can be computed analytically,

$$\frac{d}{d\omega} \chi(\boldsymbol{k}, \omega) = \frac{d\chi^{(0)}(\boldsymbol{k}, \omega)/d\omega}{[1 + U \chi^{(0)}(\boldsymbol{k}, \omega)]^2}. \tag{52}$$

Via Fourier transformation of $\chi(\boldsymbol{k}, 0)$ and of $d\chi(\boldsymbol{k}, 0)/d\omega$, we find the distance-dependent RKKY interaction $J(\boldsymbol{R})$ and the Gilbert damping $\alpha(\boldsymbol{R})$ in real space. Figure 16 shows the nearest-neighbor RKKY coupling $J(0, 1)/J^2$ as well as the local Gilbert damping $\alpha(0, 0)/J^2$ as functions of U for $T' = -0.3$. In reciprocal space, on approaching the phase transition via $U \to U_c \approx 2.53$, we have $\chi(\boldsymbol{k}, 0) \sim (U_c - U)^{-1}$ at $\boldsymbol{k} = (\pi, \pi)$, while $d\chi(\boldsymbol{k}, 0)/d\omega \sim (U_c - U)^{-2}$. The stronger
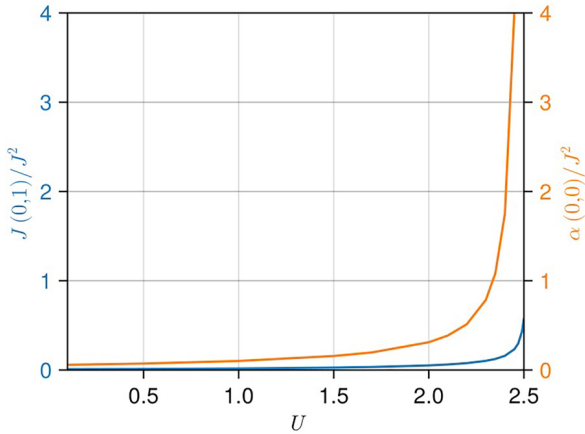
FIG. 16. U dependence of the RKKY interaction $J(\boldsymbol{R})/J^2$ between nearest neighbors $\boldsymbol{R} = (0, 1)$ (blue) and the local Gilbert damping $\alpha(\boldsymbol{R})$ with $\boldsymbol{R} = (0, 0)$, as obtained from RPA calculations for the half-filled Hubbard model with $T' = -0.3$ on the square lattice. Parameters: $L = 512 \times 512$, $\eta = 0.015$, $\beta = 500$.

divergence of $d\chi/d\omega$ compared to χ leads to the stronger enhancement of $\alpha(\boldsymbol{R})$, compared to $J(\boldsymbol{R})$, which can be seen in the figure.

Generally, the increase of the local Gilbert damping with increasing U for the square lattice is consistent with the results of a previous study performed for a single impurity spin coupled to the $D = 1$ Hubbard model [75], where a decreasing relaxation time with increasing U has been found in the weak-interaction regime.

More importantly, however, we find that the Hubbard interaction causes a strongly *nonlocal* Gilbert damping. This is demonstrated by the results shown in Fig. 17, where the full spatial dependence of the RKKY interaction $J(\boldsymbol{R})$ and of the Gilbert damping $\alpha(\boldsymbol{R})$ is plotted, after normalization to the respective local element. For $U = 0$ (left panels), one recovers the above-discussed directional dependence of the
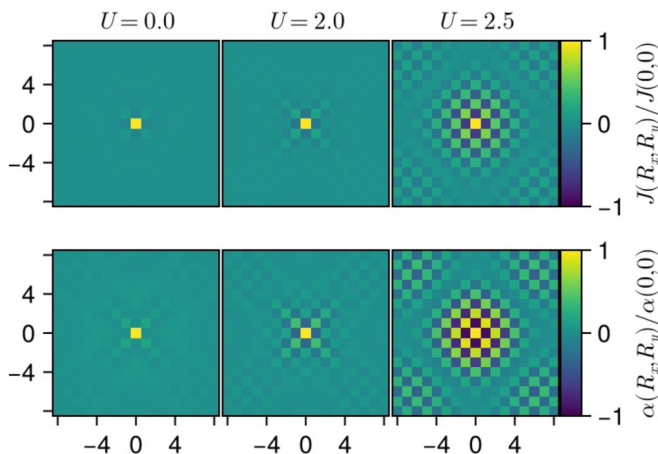

FIG. 17. Distance and directional dependence of the RKKY interaction $J(\boldsymbol{R})/J(\boldsymbol{0})$ and the Gilbert damping $\alpha(\boldsymbol{R})/\alpha(\boldsymbol{0})$, normalized to the local values (color scale) for $R_x, R_y = -8, -7, \dots, 7, 8$. RPA calculations for the half-filled Hubbard model at $T' = -0.3$ and for $U = 0$, $U = 2$, and $U = 2.5$, as indicated. Parameters: $L = 512 \times 512$, $\eta = 0.015$, $\beta = 500$.

Gilbert damping (bottom panels). As compared to the RKKY interaction (top panels), this is much more pronounced. With increasing U (see the middle panels for $U = 2.0$), the directional dependence of $\alpha(\boldsymbol{R})$ is strongly enhanced due to the strong increase of the nonlocal damping parameters, relative to $\alpha(0, 0)$.

At $U = 2.5$ (upper right panel of Fig. 17), the RKKY coupling exhibits a checkerboard pattern with $J(\boldsymbol{R})$ strongly oscillating between positive (antiferromagnetic) and negative (ferromagnetic) values. Comparing with $U = 2.0$, we see that this pattern extends spatially and is expected to eventually cover the entire lattice upon approaching the phase transition at $U_c \approx 2.53$. This is indicated by the closed nodal line of RKKY-coupling zeros extending spatially with increasing U.

Similarly, in the same spatial region enclosed by this line, the Gilbert damping at $U = 2.5$ (lower right panel) is found to oscillate. Eventually, for $U \to U_c$, the spatial structure of the Gilbert damping is expected to be given by $\alpha(R_x, R_y)/\alpha(0, 0) \to (-1)^{R_x+R_y}$. This is very reminiscent of the distance dependence of the Gilbert damping on the $D = 1$ chain, $\alpha_d/\alpha_0 = \frac{1}{2}[1 + (-1)^d]$, which has been discussed in Sec. VI B for the noninteracting case.

For a system with, e.g., two impurity spins coupled to next-nearest-neighbor sites with $\boldsymbol{R} = (1, 1)$, and if one trusted the effective theory right at the phase transition, the spatial structure of the (divergent) Gilbert damping would imply that the total spin $\boldsymbol{S}_1 + \boldsymbol{S}_2$ and the enclosed angle $\arccos(\boldsymbol{S}_1\boldsymbol{S}_2)$ are constants of motion and thus the system never relaxes to its ground-state spin configuration. However, it remains an open question as to what the relaxation dynamics would look like in $D = 2$ and for $U \to U_c$ since the absolute (unnormalized) Gilbert damping is divergent (Fig. 16) and, hence, the effective spin-only theory is likely to break down at the critical point.

VII. CONCLUSIONS

Local magnetic moments, modeled as classical spins and locally exchange coupled to an extended metallic system of conduction electrons at zero temperature, undergo a relaxation dynamics. To reduce the computational complexity, it is tempting to describe this dynamics within an effective spin-only theory. Actually, this is necessary to access the emergent relaxation timescale, which can be orders of magnitude longer than the fast femtosecond timescale of the conduction-electron dynamics.

This reduction to a spin-only theory is possible by invoking two mutually interrelated approximations: (i) The exchange-coupling strength J is small compared to, e.g., the nearest-neighbor hopping matrix element T. (ii) The electron dynamics follows the spin dynamics almost adiabatically, i.e., the retardation time of the electron system is short compared to the spin-dynamics timescale. Within the framework of linear response theory (LRT), one focuses on step (i) first, and adopts step (ii) in a subsequent step, while in the framework of adiabatic response theory (ART), one starts from step (ii) and later on adopts the weak-J approximation of step (i). Both approaches, LRT and ART, yield a system of nonlinear differential equations of motion involving the impurity-spin $\boldsymbol{S}_m$ only, as well as time-dependent and nonlocal parameters, namely,

the RKKY interaction strengths $J_{mm'}(t)$ and the Gilbert-damping parameters $\alpha_{mm'}(t)$, and possibly external magnetic fields coupling to the spins. The parameters $J_{mm'}(t)$ and $\alpha_{mm'}(t)$ are properties of the conduction-electron system only and are closely related to its retarded magnetic susceptibility.

The reliability of the effective spin-only theory has been tested against the numerical solution of the full coupled quantum-classical electron-spin dynamics for a single spin, driven by an external field **B**, coupled to a one-dimensional tight-binding electron system. The expressions for $J_{mm'}(t)$ and $\alpha_{mm'}(t)$, as obtained within LRT and ART, exhibit a quite different time dependence. It has been found, however, that the static RKKY interaction and the static Gilbert damping $J_{mm'} = \lim_{t \to \infty} J_{mm'}(t)$ and $\alpha_{mm'} = \lim_{t \to \infty} \alpha_{mm'}(t)$ perfectly agree. Furthermore, the strong temporal oscillations of $J_{mm'}(t)$ and $\alpha_{mm'}(t)$ seen within LRT are irrelevant for the spin dynamics as they take place on the fast electron timescale only. In fact, if J is sufficiently weak and if the spin-dynamics timescale $\sim 1/B$ is sufficiently slow, then almost perfect agreement is found when comparing the LRT and ART results against each other *and* against the results of the full theory.

To achieve computationally manageable relaxation times (within the full theory), this comparison was done for values of J and B of the order of T. Realistic values for J are very specific to the concrete system being considered, but will typically be an order of magnitude smaller than T: Assuming a nearest-neighbor RKKY exchange of the order of $J_{\text{RKKY}} \sim 0.01T$ (with $J_{\text{RKKY}} \sim 1$ meV) or smaller (see, e.g., Ref. [76]), we may deduce from $J_{\text{RKKY}} = J^2 \chi \sim J^2/T$ a typical value $J = 0.1T$ for the local exchange. Realistic values for B are even smaller. Hence, for computations addressing real systems, one may expect that the reliability of the effective theory is even better.

In the absence of an external driving field **B**, the timescale on which the spin dynamics takes place is governed by the RKKY coupling. Since $J_{mm'} \propto J^2$, one actually has to control the exchange-coupling strength J only. We have derived a simple expression for the Gilbert damping in the wide-band limit, $\alpha_{mm'} = \frac{\pi}{2} J^2 \rho_{mm'}^2$, which involves the (nonlocal) densities of states $\rho_{mm'}$ at the Fermi energy. This shows that the dimensionless parameter $J\rho_{mm}$ is a suitable control parameter for the reliability of the effective theory. In fact, if the local density of states ρ_{mm} diverges, as in the case of a van Hove singularity, the effective theory is found to break down.

The $D = 1$ case turns out to be critical in the sense that the Gilbert damping α_d does not decay as a function of the distance $d = i_m - i_{m'}$ but rather oscillates between the local value α_0 and zero for even and odd d, respectively. This causes an anomalous spin dynamics where relaxation is prohibited by an emergent conserved quantity that does not derive from a symmetry of the full Hamiltonian. This anomaly has already been discussed in Ref. [49] for $T' = 0$. Here, we could demonstrate that it occurs for the absolute value of the next-nearest-neighbor hoppings T' that are smaller than a critical value $T_c' = T/2$ and were able to relate the critical value to a Lifshitz transition of the Fermi "surface." Our analysis also explains why the relaxation time counterintuitively *decreases* when disregarding the nonlocal terms $m \neq m'$ in the matrix of Gilbert-damping parameters $\alpha_{mm'}$.

This is actually a recurring theme in the discussion of relaxation dynamics in $D = 2$ dimensions: For two, initially orthogonal impurity spins coupled to next-nearest-neighbor sites on the square lattice and for all values of T' ($|T'| < T$), we again find a decrease of the relaxation time when *ad hoc* switching off the nonlocal Gilbert damping. As compared to $D = 1$, however, the effect is much smaller such that even disregarding the nonlocality of the Gilbert damping might be a reasonable approximation, depending on the value for T'.

For the $D = 2$ square lattice and distances $R = |\mathbf{R}|$ up to $R \sim 10$ lattice constants, we did not see a universal simple power law $\alpha(R) \propto R^{-(D-1)}$, which is expected for large R (assuming a free, $\propto k^2$ dispersion). More importantly, the nonlocal Gilbert damping exhibits a strong directional dependence. This reflects itself, e.g., in the relaxation dynamics of one-dimensional spin chains coupled to the square lattice. For chains with 2–10 impurity spins coupled to nearest-neighboring sites along the x or, equivalently, the y direction, the relaxation time τ turns out to oscillate with the length of the chain without a significant overall increase of τ, independent of the initial spin configuration. On the contrary, for chains of spins coupled to next-nearest-neighboring sites along a diagonal direction, there is an overall superlinear increase of τ with the chain length. The same behavior is found for an initial $\pi/2$-spin-spiral configuration, as compared to an initial state, where all spins are in their ground-state (ferromagnetic) configuration, except for an edge spin rotated by $\pi/2$ that is kept fixed during the time evolution. The strong increase of τ with the chain length can be explained with the necessarily increasing amount of spin dissipation.

There are several main lines of relevant future research: (i) Our studies can straightforwardly be extended to more realistic models for the electronic structure and also combined with *ab initio* band-structure calculations. In particular, it would be interesting to consider multiorbital systems and to see the effect of band degeneracy on the nonlocality of the Gilbert damping.

(ii) The present study had focused on systems with a gapless metallic electronic structure and weak local exchange J, where Gilbert damping is the dominant leading-order effect. For gapped systems, on the other hand, the spin dynamics is additionally affected by the geometrical spin torque [60,62,64,77]. Semimetals, where one would expect a drastically reduced damping and a still well-defined geometrical spin torque [60], are worth studying. Furthermore, somewhat relaxing the almost adiabatic time evolution, by truncating at the next higher order in the expansion in the typical retardation time τ_{ret}, brings in additional effects such as nutation [63,78–80].

(iii) Modeling the impurity local magnetic moments as classical spins can only be a first step towards a theory of spin friction and dissipative dynamics of *quantum* spins. Clearly, this is a hard correlation problem as it essentially requires a conceptually and computationally feasible treatment of the long-time dynamics in a multi-impurity Kondo model.

More promising is (iv) to study the effect of electron correlations on the relaxation dynamics of classical impurity spins. This type of problem can be addressed within the presented LRT and ART frameworks. It essentially requires a computation of the zero-temperature (or the finite-temperature

equilibrium) retarded magnetic susceptibility close to $\omega = 0$. In a first attempt to address a weakly correlated conduction-electron system, here we have applied the RPA to the half-filled Hubbard model at finite next-nearest-neighbor hopping T'. This is already interesting since with increasing U the paramagnetic phase of the electron system becomes unstable towards a $\boldsymbol{k} = (\pi, \pi)$ antiferromagnetic phase. Close to the phase transition, the Gilbert damping matrix $\alpha_{mm'}$ is found to be overall strongly enhanced and strongly nonlocal. The numerical data suggest that right at the phase transition, the distance dependence is simply given by $\alpha(\boldsymbol{R}) \propto e^{i\boldsymbol{k}\boldsymbol{R}}$ with $\boldsymbol{k} = (\pi, \pi)$, which would cause spin dynamics without any dissipation. However, right at the phase transition, the effective spin-only theory itself is expected to break down. Important next steps would therefore be to replace the RPA by a more advanced technique, to study the system for *U above* the critical interaction, and to address the strong-coupling regime.

ACKNOWLEDGMENTS

APPENDIX: REPRESENTATION OF THE NONLOCAL GILBERT DAMPING IN TERMS OF THE NONLOCAL DENSITY OF STATES

To derive Eq. (15) for the Gilbert damping matrix, we start from the definition of the retarded susceptibility given by Eq. (9). The computations are done at finite temperature $1/\beta$, and the zero-temperature limit $\beta \to \infty$ is taken at the end. Since $\langle [s_{i_m}^\alpha(t), s_{i_{m'}}^{\alpha'}(0)] \rangle$ is a free expectation value, Wick's theorem applies and can be used to decompose the two-particle correlation into products of one-particle correlations. A straightforward calculation yields

$$
\chi_{mm'}^{\alpha\alpha'}(t) = \delta^{\alpha\alpha'} \Theta(t) e^{-\eta t}
$$
$$
\times \operatorname{Im}[\langle c_{i_m\sigma}(t) c_{i_{m'}\sigma}^\dagger(0)\rangle \langle c_{i_{m'}\sigma}^\dagger(0) c_{i_m\sigma}(-t)\rangle]. \quad \text{(A1)}
$$

The one-particle correlation functions can be obtained from the (nonlocal) one-particle density of states, given by Eq. (16), as

$$
\langle c_{i\sigma}(t) c_{i'\sigma}^\dagger(0)\rangle = \int dx \, f(-x) A_{ii'}(x) e^{-ixt},
$$
$$
\langle c_{i'\sigma}^\dagger(0) c_{i\sigma}(-t)\rangle = \int dy \, f(y) A_{ii'}(y) e^{iyt}. \quad \text{(A2)}
$$

Here, $f(x) = 1/(e^{\beta x} + 1)$ denotes the Fermi function. Using Eq. (A2), we find, for the frequency-dependent susceptibility,

$$
\chi_{ii'}^{\alpha\alpha'}(\omega) = \delta^{\alpha\alpha'} \iint dx dy \, f(-x) f(y) A_{ii'}(x) A_{ii'}(y) \rho(x, y),
$$
$$ \text{(A3)} $$

with

$$
\rho(x, y) = \int dt \, e^{i\omega t} \Theta(t) e^{-\eta t} \operatorname{Im}(e^{-ixt} e^{iyt})
$$
$$
= \frac{1}{2}\left(\frac{1}{\omega - x + y + i\eta} - \frac{1}{\omega + x - y + i\eta} \right). \quad \text{(A4)}
$$

Note that $A_{ii'}(x)$ is real. Inserting this result in Eq. (A3) and using the identity $f(-x)f(y) - f(x)f(-y) = f(y) - f(x)$, we arrive at

$$
\chi_{ii'}^{\alpha\alpha'}(\omega) = \frac{\delta^{\alpha\alpha'}}{2} \iint dx dy \, [f(y) - f(x)] \frac{A_{ii'}(x) A_{ii'}(y)}{\omega - x + y + i\eta}. \quad \text{(A5)}
$$

For the second representation of the Gilbert damping in Eq. (14), we only need the imaginary part of $\chi_{ii'}^{\alpha\alpha'}(\omega)$. Using the identity $(-1/\pi)\operatorname{Im}(x + i\eta)^{-1} = \delta(x)$, taking the ω derivative of $\operatorname{Im} \chi_{ii'}^{\alpha\alpha'}(\omega)$, and evaluating the result at $\omega = 0$, yields

$$
\alpha_{ii'} = \frac{\pi}{2} J^2 \iint dx dy \, \delta'(y - x)[f(y) - f(x)] A_{ii'}(x) A_{ii'}(y). \quad \text{(A6)}
$$

The prime at the δ function denotes the derivative with respect to the argument. After exchanging the integration variables $x \leftrightarrow y$ for the summand involving $f(x)$ and using $\delta'(-x) = -\delta(x)$, this simplifies to

$$
\alpha_{ii'} = \pi J^2 \iint dx dy \, \delta'(y - x) f(y) A_{ii'}(x) A_{ii'}(y). \quad \text{(A7)}
$$

To carry out the integration over y, we use integration by parts. This leaves us with

$$
\alpha_{ii'} = -\pi J^2 \int dx \, f'(x) A_{ii'}(x)^2
$$
$$
- \pi J^2 \int dx \, f(x) A_{ii'}(x) A_{ii'}'(x). \quad \text{(A8)}
$$

Consider the second term. We have $A_{ii'}(x) A_{ii'}'(x) = \frac{1}{2}(d/dx) A_{ii'}(x)^2$, so that we can use integration by parts once more. For a tight-binding density of states, there is no residual boundary term. Hence, we finally get the result

$$
\alpha_{ii'} = -\frac{\pi}{2} J^2 \int dx \, f'(x) A_{ii'}(x)^2. \quad \text{(A9)}
$$

Since $f'(x) \to -\delta(x)$ in the zero-temperature limit, this gives Eq. (15).

[1] C. Chappert, A. Fert, and F. N. Van Dau, The emergence of spin electronics in data storage, Nat. Mater. **6**, 813 (2007).

[2] A. V. Chumak, V. I. Vasyuchka, A. A. Serga, and B. Hillebrands, The next wave, Nat. Phys. **11**, 437 (2015).

[3] E. V. Gomonay and V. M. Loktev, Spintronics of antiferromagnetic systems, Low Temp. Phys. **40**, 17 (2014).

[4] V. Baltz, A. Manchon, M. Tsoi, T. Moriyama, T. Ono, and Y. Tserkovnyak, Antiferromagnetic spintronics, Rev. Mod. Phys. **90**, 015005 (2018).

[5] G. Tatara, H. Kohno, and J. Shibata, Microscopic approach to current-driven domain wall dynamics, Phys. Rep. **468**, 213 (2008).

[6] B. Skubic, J. Hellsvik, L. Nordström, and O. Eriksson, A method for atomistic spin dynamics simulations: implementation and examples, J. Phys.: Condens. Matter **20**, 315203 (2008).

[7] G. Bertotti, I. D. Mayergoyz, and C. Serpico, *Nonlinear Magnetization Dynamics in Nanosystemes* (Elsevier, Amsterdam, 2009).

[8] R. F. L. Evans, W. J. Fan, P. Chureemart, T. A. Ostler, M. O. A. Ellis, and R. W. Chantrell, Atomistic spin model simulations of magnetic nanomaterials, J. Phys.: Condens. Matter **26**, 103202 (2014).

[9] S. V. Vonsovsky, On the exchange interaction of the valence and inner electrons in ferromagnetic (transition) metals, Zh. Éksp. Teor. Fiz. **16**, 981 (1946); C. Zener, Interaction between the *d* shells in the transition metals, Phys. Rev. **81**, 440 (1951).

[10] H.-T. Elze, Linear dynamics of quantum-classical hybrids, Phys. Rev. A **85**, 052109 (2012).

[11] M. Sayad and M. Potthoff, Spin dynamics and relaxation in the classical-spin Kondo-impurity model beyond the Landau-Lifshitz-Gilbert equation, New J. Phys. **17**, 113058 (2015).

[12] M. Elbracht and M. Potthoff, Accessing long timescales in the relaxation dynamics of spins coupled to a conduction-electron system using absorbing boundary conditions, Phys. Rev. B **102**, 115434 (2020).

[13] M. Elbracht and M. Potthoff, Long-time relaxation dynamics of a spin coupled to a Chern insulator, Phys. Rev. B **103**, 024301 (2021).

[14] A. Kirilyuk, A. V. Kimel, and T. Rasing, Ultrafast optical manipulation of magnetic order, Rev. Mod. Phys. **82**, 2731 (2010).

[15] A. Weiße, Green-function-based Monte Carlo method for classical fields coupled to fermions, Phys. Rev. Lett. **102**, 150604 (2009).

[16] K. Capelle and B. L. Gyorffy, Exploring dynamical magnetism with time-dependent density-functional theory: From spin fluctuations to Gilbert damping, Europhys. Lett. **61**, 354 (2003).

[17] M. Onoda and N. Nagaosa, Dynamics of localized spins coupled to the conduction electrons with charge and spin currents, Phys. Rev. Lett. **96**, 066603 (2006).

[18] S. Bhattacharjee, L. Nordström, and J. Fransson, Atomistic spin dynamic method with both damping and moment of inertia effects included from first principles, Phys. Rev. Lett. **108**, 057204 (2012).

[19] N. Umetsu, D. Miura, and A. Sakuma, Microscopic theory for Gilbert damping in materials with inhomogeneous spin dynamics, J. Appl. Phys. **111**, 07D117 (2012).

[20] L. D. Landau and E. M. Lifshitz, A Lagrangian formulation of the gyromagnetic equation of the magnetization field, Physik. Zeits. Sowjetunion **8**, 153 (1935); T. Gilbert, On the theory of the dispersion of magnetic permeability in ferromagnetic bodies, Phys. Rev. **100**, 1243 (1955); A phenomenological theory of damping in ferromagnetic materials, IEEE Trans. Magn. **40**, 3443 (2004).

[21] M. A. Ruderman and C. Kittel, Indirect exchange coupling of nuclear magnetic moments by conduction electrons, Phys. Rev. **96**, 99 (1954).

[22] T. Kasuya, A theory of metallic ferro- and antiferromagnetism on Zener's model, Prog. Theor. Phys. **16**, 45 (1956).

[23] K. Yosida, Magnetic properties of Cu-Mn alloys, Phys. Rev. **106**, 893 (1957).

[24] U. Bajpai and B. K. Nikolić, Time-retarded damping and magnetic inertia in the Landau-Lifshitz-Gilbert equation self-consistently coupled to electronic time-dependent nonequilibrium Green functions, Phys. Rev. B **99**, 134409 (2019).

[25] F. Reyes-Osorio and B. K. Nikolić, Gilbert damping in metallic ferromagnets from Schwinger-Keldysh field theory: Intrinsically nonlocal, nonuniform, and made anisotropic by spin-orbit coupling, Phys. Rev. B **109**, 024413 (2024).

[26] D. Thonig, J. Henk, and O. Eriksson, Gilbert-like damping caused by time retardation in atomistic magnetization dynamics, Phys. Rev. B **92**, 104403 (2015).

[27] J. Kuneš and V. Kamberský, First-principles investigation of the damping of fast magnetization precession in ferromagnetic 3*d* metals, Phys. Rev. B **65**, 212411 (2002).

[28] V. Kamberský, Spin-orbital Gilbert damping in common magnetic metals, Phys. Rev. B **76**, 134416 (2007).

[29] K. Gilmore, Y. U. Idzerda, and M. D. Stiles, Identification of the dominant precession-damping mechanism in Fe, Co, and Ni by first-principles calculations, Phys. Rev. Lett. **99**, 027204 (2007).

[30] A. Brataas, Y. Tserkovnyak, and G. E. W. Bauer, Scattering theory of Gilbert damping, Phys. Rev. Lett. **101**, 037207 (2008).

[31] M. C. Hickey and J. S. Moodera, Origin of intrinsic Gilbert damping, Phys. Rev. Lett. **102**, 137601 (2009).

[32] I. Garate and A. MacDonald, Gilbert damping in conducting ferromagnets. I. Kohn-Sham theory and atomic-scale inhomogeneity, Phys. Rev. B **79**, 064403 (2009).

[33] A. A. Starikov, P. J. Kelly, A. Brataas, Y. Tserkovnyak, and G. E. W. Bauer, Unified first-principles study of Gilbert damping, spin-flip diffusion, and resistivity in transition metal alloys, Phys. Rev. Lett. **105**, 236601 (2010).

[34] A. Sakuma, First-principles study on the Gilbert damping constants of transition metal alloys, Fe-Ni and Fe-Pt systems, J. Phys. Soc. Jpn. **81**, 084701 (2012).

[35] H. Ebert, S. Mankovsky, D. Ködderitzsch, and P. J. Kelly, *Ab initio* calculation of the Gilbert damping parameter via the linear response formalism, Phys. Rev. Lett. **107**, 066603 (2011).

[36] M. Fähnle and C. Illg, Electron theory of fast and ultrafast dissipative magnetization dynamics, J. Phys.: Condens. Matter **23**, 493201 (2011).

[37] S. Mankovsky, D. Ködderitzsch, G. Woltersdorf, and H. Ebert, First-principles calculation of the Gilbert damping parameter via the linear response formalism with application to magnetic transition metals and alloys, Phys. Rev. B **87**, 014430 (2013).

[38] R. Mondal, M. Berritta, and P. M. Oppeneer, Relativistic theory of spin relaxation mechanisms in the Landau-Lifshitz-Gilbert equation of spin dynamics, Phys. Rev. B **94**, 144419 (2016).

[39] R. Mondal, M. Berritta, A. K. Nandy, and P. M. Oppeneer, Relativistic theory of magnetic inertia in ultrafast spin dynamics, Phys. Rev. B **96**, 024425 (2017).

[40] F. S. M. Guimaraes, J. R. Suckert, J. Chico, J. Bouaziz, M. dos Santos Dias, and S. Lounis, Comparative study of methodologies to compute the intrinsic Gilbert damping: interrelations, validity and physical consequences, J. Phys.: Condens. Matter **31**, 255802 (2019).

[41] I. A. Ado, P. M. Ostrovsky, and M. Titov, Anisotropy of spin-transfer torques and Gilbert damping induced by Rashba coupling, Phys. Rev. B **101**, 085405 (2020).

[42] Y. Tserkovnyak and M. Mecklenburg, Electron transport driven by nonequilibrium magnetic textures, Phys. Rev. B **77**, 134407 (2008).

[43] E. M. Hankiewicz, G. Vignale, and Y. Tserkovnyak, Inhomogeneous Gilbert damping from impurities and electron-electron interactions, Phys. Rev. B **78**, 020404(R) (2008).

[44] S. Zhang and Steven S.-L. Zhang, Generalization of the Landau-Lifshitz-Gilbert equation for conducting ferromagnets, Phys. Rev. Lett. **102**, 086601 (2009).

[45] K.-W. Kim, J.-H. Moon, K.-J. Lee, and H.-W. Lee, Prediction of giant spin motive force due to Rashba spin-orbit coupling, Phys. Rev. Lett. **108**, 217202 (2012).

[46] H. Y. Yuan, Z. Yuan, K. Xia, and X. R. Wang, Influence of non-local damping on the field-driven domain wall motion, Phys. Rev. B **94**, 064415 (2016).

[47] S. Mankovsky, S. Wimmer, and H. Ebert, Gilbert damping in noncollinear magnetic systems, Phys. Rev. B **98**, 104406 (2018).

[48] R. Verba, V. Tiberkevich, and A. Slavin, Damping of linear spin-wave modes in magnetic nanostructures: Local, nonlocal, and coordinate-dependent damping, Phys. Rev. B **98**, 104408 (2018).

[49] M. Elbracht and M. Potthoff, Prerelaxation in quantum, classical, and quantum-classical two-impurity models, Phys. Rev. Res. **6**, 033275 (2024).

[50] M. Campisi, S. Denisov, and P. Hänggi, Geometric magnetism in open quantum systems, Phys. Rev. A **86**, 032114 (2012).

[51] A. Sakuma, Microscopic description of Landau-Lifshitz-Gilbert type equation based on the s-d model, arXiv:cond-mat/0602075.

[52] H. Katsura, A. V. Balatsky, Z. Nussinov, and N. Nagaosa, Voltage dependence of Landau-Lifshitz-Gilbert damping of spin in a current-driven tunnel junction, Phys. Rev. B **73**, 212501 (2006).

[53] A. S. Núñez and R. A. Duine, Effective temperature and Gilbert damping of a current-driven localized spin, Phys. Rev. B **77**, 054401 (2008).

[54] I. Turek, J. Kudrnovský, and V. Drchal, Nonlocal torque operators in *ab initio* theory of the Gilbert damping in random ferromagnetic alloys, Phys. Rev. B **92**, 214407 (2015).

[55] A. Sakuma, Microscopic theory of Gilbert damping for transition metal systems, J. Magnet. Soc. Japan **37**, 343 (2013).

[56] R. Smorka, M. Thoss, and M. Žonda, Dynamics of spin relaxation in nonequilibrium magnetic nanojunctions, New J. Phys. **26**, 013056 (2024).

[57] C. Jarzynski, Nonequilibrium equality for free energy differences, Phys. Rev. Lett. **78**, 2690 (1997).

[58] P. Talkner, E. Lutz, and P. Hänggi, Fluctuation theorems: Work is not an observable, Phys. Rev. E **75**, 050102(R) (2007).

[59] M. Campisi, P. Hänggi, and P. Talkner, Colloquium: Quantum fluctuation relations: Foundations and applications, Rev. Mod. Phys. **83**, 771 (2011).

[60] S. Michel and M. Potthoff, Spin Berry curvature of the Haldane model, Phys. Rev. B **106**, 235423 (2022).

[61] F. D. M. Haldane, Model for a quantum Hall effect without Landau levels: Condensed-matter realization of the "parity anomaly", Phys. Rev. Lett. **61**, 2015 (1988).

[62] C. Stahl and M. Potthoff, Anomalous spin precession under a geometrical torque, Phys. Rev. Lett. **119**, 227203 (2017).

[63] N. Lenzing, A. I. Lichtenstein, and M. Potthoff, Emergent non-Abelian gauge theory in coupled spin-electron dynamics, Phys. Rev. B **106**, 094433 (2022).

[64] N. Lenzing, D. Krüger, and M. Potthoff, Geometrical torque on magnetic moments coupled to a correlated antiferromagnet, Phys. Rev. Res. **5**, L032012 (2023).

[65] M. Berry and J. Robbins, Chaotic classical and half-classical adiabatic reactions: geometric magnetism and deterministic friction, Proc. R. Soc. London A **442**, 659 (1993).

[66] M. V. Berry, Quantal phase factors accompanying adiabatic changes, Proc. R. Soc. London A **392**, 45 (1984).

[67] J. H. Verner, Numerically optimal Runge-Kutta pairs with interpolants, Numer. Algor. **53**, 383 (2010).

[68] C. Rackauckas and Q. Nie, Differential equations - A performance and feature-rich ecosystem for solving differential equations in Julia, J. Open Res. Software **5**, 15 (2017).

[69] G. Steinebach, Construction of Rosenbrock-Wanner method and numerical benchmarks within the Julia differential equations package, BIT Numer. Math. **63**, 27 (2023).

[70] R. Kikuchi, On the minimum of magnetization reversal time, J. Appl. Phys. **27**, 1352 (1956).

[71] J. M. Luttinger and J. C. Ward, Ground-state energy of a many-fermion system. II, Phys. Rev. **118**, 1417 (1960).

[72] T. Moriya, *Spin Fluctuations in Itinerant Electron Magnetism*, Springer Series in Solid-State Sciences, Vol. 56 (Springer, Berlin, 1985).

[73] G. Rohringer, H. Hafermann, A. Toschi, A. A. Katanin, A. E. Antipov, M. I. Katsnelson, A. I. Lichtenstein, A. N. Rubtsov, and K. Held, Diagrammatic routes to nonlocal correlations beyond dynamical mean field theory, Rev. Mod. Phys. **90**, 025003 (2018).

[74] W. Hofstetter and D. Vollhardt, Frustration of antiferromagnetism in the t-t'-Hubbard model at weak coupling, Ann. Phys. **510**, 48 (1998).

[75] M. Sayad, R. Rausch, and M. Potthoff, Relaxation of a classical spin coupled to a strongly correlated electron system, Phys. Rev. Lett. **117**, 127201 (2016).

[76] L. Zhou, J. Wiebe, S. Lounis, E. Vedmedenko, F. Meier, S. Blügel, P. H. Dederichs, and R. Wiesendanger, Strength and directionality of surface Ruderman-Kittel-Kasuya-Yosida interaction mapped on the atomic scale, Nat. Phys. **6**, 187 (2010).

[77] U. Bajpai and B. K. Nikolić, Spintronics meets nonadiabatic molecular dynamics: Geometric spin torque and damping on dynamical classical magnetic texture due to an electronic open quantum system, Phys. Rev. Lett. **125**, 187202 (2020).

[78] J. Fransson, Detection of spin reversal and nutations through current measurements, Nanotechnology **19**, 285714 (2008).

[79] D. Böttcher and J. Henk, Significance of nutation in magnetization dynamics of nanostructures, Phys. Rev. B **86**, 020404(R) (2012).

[80] M. Sayad, R. Rausch, and M. Potthoff, Inertia effects in the real-time dynamics of a quantum spin coupled to a fermi sea, Europhys. Lett. **116**, 17001 (2016).

7 – Summary and Outlook

This thesis analysed the microscopic dynamics of local magnetic impurities coupled to a host system to understand the different effects that are at play on the atomistic level. This analysis covered mainly three effects, namely, the RKKY interaction, the Gilbert damping, and the geometrical spin torque. The second overarching topic is that of the different theories that can be used to describe the spin dynamics: adiabatic spin dynamics (ASD), non-Abelian spin dynamics (NA-SD), linear response theory (LRT), and adiabatic response theory (ART). Throughout this thesis, the impurity spins were approximated as classical vectors to make numerical computations more feasible, while the host system is always quantum mechanical. The first part of the thesis addresses the geometrical spin torque that can be traced back to the spin-Berry curvature $\underline{\Omega}$ and is absent in the standard treatment of spin dynamics using the LLG equations. It arises if the dynamics of the classical impurity spins is treated as slow compared to the dynamics of the host system. On a mathematical level, this is implemented by constraining the host system to always be in the instantaneous ground state corresponding to any given classical spin configuration. The adiabatic constraint, upon being incorporated in a Lagrangian formulation of the theory, results in a geometrical spin torque influencing the dynamics of the classical spins. This adiabatic spin dynamics (ASD) theory was originally formulated in [56] and was discussed in chapter 4. Publication [I] builds upon the Lagrangian formulation and shows that ASD can be expanded to the case where the adiabatic constraint is relaxed. Namely, the state of the host system is not constrained to only the ground state but to a low-energy subspace consisting of the n lowest multi-particle eigenstates for a given spin configuration. This new theory is called non-Abelian spin dynamics (NA-SD) theory with the term non-Abelian stemming from the fact that the spin-Berry curvature and hence the geometrical spin torque is no longer a one-dimensional scalar object but an $n > 1$ dimensional matrix-valued one [105, 106]. In publication [I] NA-SD is tested with the same model system as in [56], a single classical spin coupled to a one-dimensional chain of conduction electrons. Two phenomena that could not be explained within the framework of ASD can now be resolved. Namely, the effective spin dynamics resulting from NA-SD shows spin nutation, which is a higher order effect not present in ASD, and the non-Abelian spin-Berry curvature is nonzero for any number of particles, whereas the Abelian one is only nonzero for an odd number of particles [56]. The latter observation can be explained by the fact that the ground state of the model system for even N is always time-reversal symmetric, irrespective of the strength of the quantum-classical exchange coupling J. In general, the non-Abelian spin-Berry curvature in a time-reversal symmetric system is finite as opposed to the Abelian one, see publication [I].

To build on the findings of publications [I], one can look for more systems to which NA-SD can be applied. Especially considering their physical relevance since [I] mainly builds up the theoretical framework of NA-SD and applies it only to a minimal model. Systems for which the application of NA-SD is expected to be fruitful are systems in which we expect the ground

state to become degenerate with at least one other state at some point throughout the induced dynamics. This includes system with symmetry-induced ground-state degeneracy [107, 108]. In these cases one naturally has to include multiple states when constraining the host system to its ground-state manifold. Additionally, NA-SD can also be used to systematically expand the restriction to the ground-state manifold to include low-lying excitations relevant for the low-energy physics and corresponding dynamics. Another class of interesting systems is that of topological insulators where only a few energy eigenstates are separated from the rest by an energy gap. One example would be a Chern insulator with a boundary and edge states lying in its band gap [109, 110]. At half-filling such a system has a degenerate ground state due to these edge modes. A similar reasoning can be given for topological superconductors with defects featuring Majorana zero modes inside the superconducting gap [111].

While ASD and NA-SD are in principle applicable for all values of J, one is often only interested in the weak-J regime, e.g., weak coupling between classical spin impurities and the host system. In this regime, the natural theory to use is linear response theory. It has been shown that applying a weak-J approximation to ASD [57] and comparing with results from linear response theory with an additional adiabatic approximation [45] yields the same expressions for the geometrical spin torque. However, one has to be careful because for weak J the geometrical spin torque vanishes if the host system is time-reversal invariant. A class of systems that are not time-reversal invariant are systems with spontaneous magnetic order, described, for instance, by a Heisenberg model. Due to the mechanism of spontaneous symmetry breaking, they also exhibit gapless excitations called Goldstone modes. This is important since the Lehmann representation of the spin-Berry curvature features the energy difference between the ground state and excited states as a denominator. Thus, if gapless excitations are present, the Lehmann representation has divergent terms. Of course, for an actual divergent $\underline{\Omega}$ the theory becomes meaningless but for certain systems and dimensions the divergences can be regularised to yield a finite but large quantity. In such systems, the geometrical spin torque is then especially significant. That the spin-Berry curvature can be enhanced by a divergence of an energy-difference denominator was first shown in [57]. The second publication [II] investigates this with an antiferromagnetic Heisenberg model for a host system. In the thermodynamic limit, and using well-known spin wave theory, one gets an analytical expression for the spin-Berry curvature in terms of a $\boldsymbol{k}$ integral, which can be shown to converge in $d = 3$ and produce an exceptionally large result.

While from a purely theoretical point of view the spin-Berry curvature as a concept is already quite interesting, boosting its magnitude is relevant for real world applications. Therefore, the discussed setup may be a good candidate for measuring the geometrical spin torque in an experimental setting. Suitable systems can be atom-by-atom engineered nanomagnets [112, 113]. Measurements might be achieved using ferromagnetic resonance techniques [114, 115], for instance using spin-polarized scanning tunneling microscopy [116, 117]. Looking further ahead, a large geometrical spin torque might prove useful in applications to antiferromagnetic spintronics [15, 118, 119].

Apart from the geometrical spin torque, two other crucial effects govern the microscopic dynamics of local magnetic impurities: the RKKY interaction $\underline{J}^{\mathrm{RKKY}}$ and the Gilbert damping

$\underline{\alpha}$. The former is an indirect exchange interaction between local magnetic entities mediated by conduction electrons. It was absent in the first two studies since these were done for systems with only a single classical impurity spin. The Gilbert damping mechanism, on the other hand, is a phenomenological damping mechanism refining the equations of motion for damped magnetisation dynamics devised by Landau and Lifshitz. Originally, it was used on a macrospin level within the framework of micromagnetics but in recent times it has also been derived from first principles on an atomistic level. The third publication [III] contributing to this thesis analyses the impact of $\underline{J}^{\mathrm{RKKY}}$ and $\underline{\alpha}$ on the spin dynamics of quantum-classical impurity models with one or several impurities in one and two spatial dimensions. Both effects can be computed via the magnetic susceptibility using LRT [45]. Publication [III] also adapts ART to quantum-classical spin systems to compute the microscopic dynamics. ART is suited for describing slow perturbations, as opposed to the weak perturbations of LRT. When putting both theories on equal footing, by applying a weak-J approximation to ART and an adiabatic expansion to LRT, they yield the same results for the spin dynamics. From a physical point of view, the focus of the analysis in [III] is the nonlocality of the Gilbert damping tensor, in contrast to its common treatment as a scalar parameter. Here, the main insight is that the Gilbert damping in $d = 2$ has a strong directional dependence and nonlocalities can have a significant impact on the relaxation dynamics. Counterintuitively, one finds that in some cases the inclusion of nonlocal terms even hinders relaxation. The publication also considers the effect of small correlations U in the host on the values of $\underline{J}^{\mathrm{RKKY}}$ and $\underline{\alpha}$. These lead to an even stronger nonlocality.

Adding to this it would be interesting to see the effect of stronger correlations [55] on the nonlocalities. In the large-U limit it might be possible to apply the spin wave calculations from [II] to the calculation of $\underline{\alpha}$ and get an analytical expression. As in the case of the spin-Berry curvature, an experimental verification of the theoretical results would be significant. The Gilbert damping has already been measured for different materials [114] also including its nonlocalities [120]. Again, atom-by-atom engineered magnetic structures are the most promising candidates for an experimental realization of the spin chain dynamics studied in [III]. In this context the computation of spin relaxation dynamics for real materials is also a worthwhile direction of research.

As described above, the Gilbert damping and the spin-Berry curvature can be seen as different sides of the same coin, since they are respectively proportional to the frequency derivative of the symmetric and the antisymmetric part, or alternatively the real and the imaginary part, of the magnetic susceptibility evaluated at $\omega = 0$. This raises the question of how $\underline{\alpha}$ is connected to the so-called quantum metric $\underline{g}$, because $\underline{g}$ and $\underline{\Omega}$ can be seen as the real and the imaginary part of the quantum geometric tensor [121, 122], reminiscent of the relationship between $\underline{\alpha}$ and $\underline{\Omega}$. A natural follow-up is then to investigate the relation between $\underline{\alpha}$ and $\underline{g}$, and a possible impact of $\underline{g}$ on the spin dynamics. The arguably most important question for all setups considered in this thesis is how to apply timescale separation in the case of quantum impurity spins. To this end, a workable theory concerning the application of an adiabatic constraint to two coupled quantum systems with largely different timescales would have to be worked out [65, 123].

Appendices

Auxiliary Calculations

Homogeneity of the Magnetic Susceptibility

It is

$$
\begin{aligned}
\langle \hat{\boldsymbol{s}}_i(t)\hat{\boldsymbol{s}}_{i'}(t') \rangle &= \frac{1}{Z}\,\mathrm{Tr}\Big[e^{-\beta\hat{H}} e^{i\hat{H}t}\hat{\boldsymbol{s}}_i e^{-i\hat{H}t} e^{i\hat{H}t'}\hat{\boldsymbol{s}}_{i'} e^{-i\hat{H}t'} \Big] \\
&= \frac{1}{Z}\,\mathrm{Tr}\Big[e^{-\beta\hat{H}} e^{i\hat{H}(t-t')}\hat{\boldsymbol{s}}_i e^{-i\hat{H}(t-t')}\hat{\boldsymbol{s}}_{i'} \Big] \\
&= \langle \hat{\boldsymbol{s}}_i(t-t')\hat{\boldsymbol{s}}_{i'}(0) \rangle,
\end{aligned}
\tag{A.1}
$$

where we used the cyclic property of the trace. For the magnetic susceptibility, it follows

$$
\begin{aligned}
\chi_{i\alpha,i'\alpha'}(t,t') &= -i\Theta(t-t')\langle \big[\hat{s}_{i,\alpha}(t),\hat{s}_{i',\alpha'}(t')\big] \rangle \\
&= -i\Theta(t-t')\langle \big[\hat{s}_{i,\alpha}(t-t'),\hat{s}_{i',\alpha'}(0)\big] \rangle,
\end{aligned}
\tag{A.2}
$$

i.e., the susceptibility is homogenous.

Spin-Berry Curvature of a Magnet via the Susceptibility

The frequency representation of the antisymmetric part of the magnetic susceptibility $\chi^A_{i\alpha,i'\alpha'}(\omega)$ is related to the spin-Berry curvature $\Omega_{i\alpha,i'\alpha'}$ via

$$
\Omega_{i\alpha,i'\alpha'} = -iJ^2\partial_\omega \chi^A_{i\alpha,i'\alpha'}(\omega)\Big|_{\omega=0}
\tag{A.3}
$$

with the quantum-classical exchange coupling J. Hence, it is possible to compute $\underline{\Omega}$ by first computing the Fourier transform of $\underline{\chi}^A(t)$ and then taking the derivative, instead of working directly with the Lehmann representation of the spin-Berry curvature. Here this alternative way is explored for the antiferromagnetic system discussed in publication [II]. To this end, the ground-state expectation values $\langle \hat{s}_{i,\alpha}(t)\hat{s}_{i',\alpha'}(0) \rangle$ are needed. First the expectation values for $t=0$ will be calculated. The step to the time-dependent quantities is then simple. For zero temperature and in the spin-wave approximation, it is

$$
\begin{aligned}
\langle s_i^+ s_{i'}^- \rangle &= \frac{4s}{L}\sum_{\boldsymbol{k},\boldsymbol{k}'} e^{-i(\boldsymbol{k}\boldsymbol{R}_i-\boldsymbol{k}'\boldsymbol{R}_{i'})}\Big\langle (u_{\boldsymbol{k}}\alpha_{\boldsymbol{k}}+v_{\boldsymbol{k}}\beta_{\boldsymbol{k}}^\dagger)(u_{\boldsymbol{k}'}\alpha_{\boldsymbol{k}'}^\dagger+v_{\boldsymbol{k}'}\beta_{\boldsymbol{k}'})\Big\rangle \\
&= \frac{4s}{L}\sum_{\boldsymbol{k},\boldsymbol{k}'} e^{-i(\boldsymbol{k}\boldsymbol{R}_i-\boldsymbol{k}'\boldsymbol{R}_{i'})}u_{\boldsymbol{k}}u_{\boldsymbol{k}'}\Big\langle \alpha_{\boldsymbol{k}}\alpha_{\boldsymbol{k}'}^\dagger \Big\rangle \\
&= \frac{4s}{L}\sum_{\boldsymbol{k}} e^{-i\boldsymbol{k}(\boldsymbol{R}_i-\boldsymbol{R}_{i'})}u_{\boldsymbol{k}}^2,
\end{aligned}
\tag{A.4}
$$

where the spin operators are expressed in terms of Bogoliubov operators and the expectation

value is taken in the corresponding vacuum state. Analogously, one gets

$$\left\langle s_i^- s_{i'}^+ \right\rangle^{(0)} = \frac{4s}{L} \sum_{\boldsymbol{k}} e^{i\boldsymbol{k}(\boldsymbol{R}_i - \boldsymbol{R}_{i'})} v_{\boldsymbol{k}}^2 \tag{A.5}$$

$$\left\langle s_i^+ s_{i'}^+ \right\rangle^{(0)} = \left\langle s_i^- s_{i'}^- \right\rangle^{(0)} = \left\langle s_j^+ s_{j'}^+ \right\rangle^{(0)} = \left\langle s_j^- s_{j'}^- \right\rangle^{(0)} = 0 \tag{A.6}$$

$$\left\langle s_j^+ s_{j'}^- \right\rangle^{(0)} = \frac{4s}{L} \sum_{\boldsymbol{k}} e^{-i\boldsymbol{k}(\boldsymbol{R}_j - \boldsymbol{R}_{j'})} v_{\boldsymbol{k}}^2 \tag{A.7}$$

$$\left\langle s_j^- s_{j'}^+ \right\rangle^{(0)} = \frac{4s}{L} \sum_{\boldsymbol{k}} e^{i\boldsymbol{k}(\boldsymbol{R}_j - \boldsymbol{R}_{j'})} u_{\boldsymbol{k}}^2 \tag{A.8}$$

$$\left\langle s_i^+ s_j^- \right\rangle^{(0)} = \frac{4s}{L} \sum_{\boldsymbol{k},\boldsymbol{k}'} e^{-i\boldsymbol{k}\boldsymbol{R}_i} e^{i\boldsymbol{k}'\boldsymbol{R}_j} \left\langle (u_{\boldsymbol{k}} \alpha_{\boldsymbol{k}} + v_{\boldsymbol{k}} \beta_{\boldsymbol{k}}^\dagger)(u_{\boldsymbol{k}'} \beta_{\boldsymbol{k}'} + v_{\boldsymbol{k}'} \alpha_{\boldsymbol{k}'}^\dagger) \right\rangle^{(0)}$$

$$= \frac{4s}{L} \sum_{\boldsymbol{k}} e^{-i\boldsymbol{k}(\boldsymbol{R}_i - \boldsymbol{R}_j)} u_{\boldsymbol{k}} v_{\boldsymbol{k}} \tag{A.9}$$

$$\left\langle s_j^- s_i^+ \right\rangle^{(0)} = \frac{4s}{L} \sum_{\boldsymbol{k}} e^{-i\boldsymbol{k}(\boldsymbol{R}_i - \boldsymbol{R}_j)} u_{\boldsymbol{k}} v_{\boldsymbol{k}} \tag{A.10}$$

$$\left\langle s_j^+ s_i^- \right\rangle^{(0)} = \left\langle s_i^- s_j^+ \right\rangle^{(0)} = \frac{4s}{L} \sum_{\boldsymbol{k}} e^{-i\boldsymbol{k}(\boldsymbol{R}_j - \boldsymbol{R}_i)} u_{\boldsymbol{k}} v_{\boldsymbol{k}} \tag{A.11}$$

$$\left\langle s_i^+ s_j^+ \right\rangle^{(0)} = \left\langle s_i^- s_j^- \right\rangle^{(0)} = \left\langle s_j^+ s_i^+ \right\rangle^{(0)} = \left\langle s_j^- s_i^- \right\rangle^{(0)} = 0 \tag{A.12}$$

$$\langle s_i^z \rangle^{(0)} = - \langle s_j^z \rangle^{(0)} = s - \frac{2}{L} \sum_{\boldsymbol{k}} v_{\boldsymbol{k}}^2. \tag{A.13}$$

The time evolution of the spin operators can be computed straight forwardly as

$$s_i^+(t) = e^{iHt} s_i^+ e^{-iHt} = \sqrt{\frac{4s}{L}} \sum_{\boldsymbol{k}} e^{i\boldsymbol{k}\boldsymbol{R}_i} (u_{\boldsymbol{k}} e^{iHt} \alpha_{\boldsymbol{k}} e^{-iHt} + v_{\boldsymbol{k}} e^{iHt} \beta_{\boldsymbol{k}}^\dagger e^{-iHt}), \tag{A.14}$$

where the time evolution of the Bogoliubov operators is

$$e^{iHt} \alpha_{\boldsymbol{k}} e^{-iHt} = \sum_m^\infty \frac{1}{m!} [iHt, \alpha_{\boldsymbol{k}}]_m = e^{-it J_H s \omega(\boldsymbol{k})} \alpha_{\boldsymbol{k}} \tag{A.15}$$

with $\omega(\boldsymbol{k}) := \sqrt{(\Delta z)^2 - \gamma_{\boldsymbol{k}}^2}$ and the m times nested commutator $[\cdot, \cdot]_m$. In deriving (A.15), it was used that $[H, \alpha_{\boldsymbol{k}}] = -J_H s \omega(\boldsymbol{k}) \alpha_{\boldsymbol{k}}$, which in turn follows from $[\hat{n}_{\boldsymbol{k}}^\alpha, \alpha_{\boldsymbol{k}'}] = -\delta_{\boldsymbol{k}\boldsymbol{k}'} \alpha_{\boldsymbol{k}'}$ and $\left[\hat{n}_{\boldsymbol{k}}^\beta, \alpha_{\boldsymbol{k}'}\right] = 0$. For $\alpha_{\boldsymbol{k}}^\dagger, \beta_{\boldsymbol{k}}, \beta_{\boldsymbol{k}}^\dagger$ analogous results hold. Therewith:

$$\left\langle s_i^+(t) s_{i'}^-(0) \right\rangle^{(0)} = \frac{4s}{L} \sum_{\boldsymbol{k}} e^{-i\boldsymbol{k}(\boldsymbol{R}_i - \boldsymbol{R}_{i'})} u_{\boldsymbol{k}}^2 e^{-it\omega'(\boldsymbol{k})} \tag{A.16}$$

$$\left\langle s_i^-(t) s_{i'}^+(0) \right\rangle^{(0)} = \frac{4s}{L} \sum_{\boldsymbol{k}} e^{i\boldsymbol{k}(\boldsymbol{R}_i - \boldsymbol{R}_{i'})} v_{\boldsymbol{k}}^2 e^{-it\omega'(\boldsymbol{k})} \tag{A.17}$$

$$\left\langle s_j^+(t) s_{j'}^-(0) \right\rangle^{(0)} = \frac{4s}{L} \sum_{\boldsymbol{k}} e^{-i\boldsymbol{k}(\boldsymbol{R}_j - \boldsymbol{R}_{j'})} v_{\boldsymbol{k}}^2 e^{-it\omega'(\boldsymbol{k})} \tag{A.18}$$

$$\left\langle s_j^-(t) s_{j'}^+(0) \right\rangle^{(0)} = \frac{4s}{L} \sum_{\boldsymbol{k}} e^{i\boldsymbol{k}(\boldsymbol{R}_j - \boldsymbol{R}_{j'})} u_{\boldsymbol{k}}^2 e^{-it\omega'(\boldsymbol{k})} \tag{A.19}$$

$$\left\langle s_i^+(t)s_j^-(0)\right\rangle^{(0)} = \left\langle s_j^-(t)s_i^+(0)\right\rangle^{(0)} = \frac{4s}{L}\sum_{\boldsymbol{k}} e^{-i\boldsymbol{k}(\boldsymbol{R}_i-\boldsymbol{R}_j)}u_{\boldsymbol{k}}v_{\boldsymbol{k}}e^{-it\omega'(\boldsymbol{k})} \tag{A.20}$$

$$\left\langle s_j^+(t)s_i^-(0)\right\rangle^{(0)} = \left\langle s_i^-(t)s_j^+(0)\right\rangle^{(0)} = \frac{4s}{L}\sum_{\boldsymbol{k}} e^{-i\boldsymbol{k}(\boldsymbol{R}_j-\boldsymbol{R}_i)}u_{\boldsymbol{k}}v_{\boldsymbol{k}}e^{-it\omega'(\boldsymbol{k})} \tag{A.21}$$

with the definition $\omega'(\boldsymbol{k}) = J_H s\omega(\boldsymbol{k})$. One can use those expectation values to compute the elements of the magnetic susceptibility

$$\chi_{i\alpha i'\alpha'}(t) = -i\Theta(t)e^{-\eta t}\left\langle\left[s_i^\alpha(t), s_{i'}^{\alpha'}(0)\right]\right\rangle^{(0)}. \tag{A.22}$$

In the spin-wave approximation it is

$$\langle[s_i^x(t), s_{i'}^x(0)]\rangle^{(0)} = \left\langle\left[s_i^y(t), s_{i'}^y(0)\right]\right\rangle^{(0)}$$
$$= \frac{1}{4}\left[\left\langle s_i^+(t)s_{i'}^-(0)\right\rangle^{(0)} + \left\langle s_i^-(t)s_{i'}^+(0)\right\rangle^{(0)} - \left\langle s_{i'}^+(0)s_i^-(t)\right\rangle^{(0)} - \left\langle s_{i'}^-(0)s_i^+(t)\right\rangle^{(0)}\right]$$
$$\left\langle\left[s_i^x(t), s_{i'}^y(0)\right]\right\rangle^{(0)} = -\left\langle[s_i^y(t), s_{i'}^x(0)]\right\rangle^{(0)}$$
$$= -\frac{i}{4}\left[\left\langle s_i^-(t)s_{i'}^+(0)\right\rangle^{(0)} - \left\langle s_i^+(t)s_{i'}^-(0)\right\rangle^{(0)} + \left\langle s_{i'}^-(0)s_i^+(t)\right\rangle^{(0)} - \left\langle s_{i'}^+(0)s_i^-(t)\right\rangle^{(0)}\right],$$

which is true even if i and i' are not from the same sublattice. Thus, one has

$$\chi_{ixi'x}(t) = -\frac{is}{L}\Theta(t)e^{-\eta t}\sum_{\boldsymbol{k}}\left(u_{\boldsymbol{k}}^2\left(e^{-i\boldsymbol{k}(\boldsymbol{R}_i-\boldsymbol{R}_{i'})}e^{-it\omega'(\boldsymbol{k})} - e^{i\boldsymbol{k}(\boldsymbol{R}_i-\boldsymbol{R}_{i'})}e^{it\omega'(\boldsymbol{k})}\right)\right.$$
$$\left. -v_{\boldsymbol{k}}^2\left(e^{-i\boldsymbol{k}(\boldsymbol{R}_i-\boldsymbol{R}_{i'})}e^{it\omega'(\boldsymbol{k})} - e^{i\boldsymbol{k}(\boldsymbol{R}_i-\boldsymbol{R}_{i'})}e^{-it\omega'(\boldsymbol{k})}\right)\right)$$
$$\chi_{jxj'x}(t) = -\frac{is}{L}\Theta(t)e^{-\eta t}\sum_{\boldsymbol{k}}\left(v_{\boldsymbol{k}}^2\left(e^{-i\boldsymbol{k}(\boldsymbol{R}_j-\boldsymbol{R}_{j'})}e^{-it\omega'(\boldsymbol{k})} - e^{i\boldsymbol{k}(\boldsymbol{R}_j-\boldsymbol{R}_{j'})}e^{it\omega'(\boldsymbol{k})}\right)\right.$$
$$\left. -u_{\boldsymbol{k}}^2\left(e^{-i\boldsymbol{k}(\boldsymbol{R}_j-\boldsymbol{R}_{j'})}e^{it\omega'(\boldsymbol{k})} - e^{i\boldsymbol{k}(\boldsymbol{R}_j-\boldsymbol{R}_{j'})}e^{-it\omega'(\boldsymbol{k})}\right)\right)$$
$$\chi_{ixjx}(t) = -\frac{is}{L}\Theta(t)e^{-\eta t}\sum_{\boldsymbol{k}}u_{\boldsymbol{k}}v_{\boldsymbol{k}}\left(e^{-i\boldsymbol{k}(\boldsymbol{R}_i-\boldsymbol{R}_j)} + e^{i\boldsymbol{k}(\boldsymbol{R}_i-\boldsymbol{R}_j)}\right)\left(e^{-it\omega'(\boldsymbol{k})} - e^{it\omega'(\boldsymbol{k})}\right)$$
$$= -\frac{4s}{L}\Theta(t)e^{-\eta t}\sum_{\boldsymbol{k}}u_{\boldsymbol{k}}v_{\boldsymbol{k}}\cos(\boldsymbol{k}(\boldsymbol{R}_i-\boldsymbol{R}_j))\sin(\omega'(\boldsymbol{k})t)$$
$$\chi_{ixi'y}(t) = \frac{s}{L}\Theta(t)e^{-\eta t}\sum_{\boldsymbol{k}}\left(u_{\boldsymbol{k}}^2\left(e^{-i\boldsymbol{k}(\boldsymbol{R}_i-\boldsymbol{R}_{i'})}e^{-it\omega'(\boldsymbol{k})} + e^{i\boldsymbol{k}(\boldsymbol{R}_i-\boldsymbol{R}_{i'})}e^{it\omega'(\boldsymbol{k})}\right)\right.$$
$$\left. -v_{\boldsymbol{k}}^2\left(e^{-i\boldsymbol{k}(\boldsymbol{R}_i-\boldsymbol{R}_{i'})}e^{it\omega'(\boldsymbol{k})} + e^{i\boldsymbol{k}(\boldsymbol{R}_i-\boldsymbol{R}_{i'})}e^{-it\omega'(\boldsymbol{k})}\right)\right)$$
$$\chi_{jxj'y}(t) = \frac{s}{L}\Theta(t)e^{-\eta t}\sum_{\boldsymbol{k}}\left(v_{\boldsymbol{k}}^2\left(e^{-i\boldsymbol{k}(\boldsymbol{R}_j-\boldsymbol{R}_{j'})}e^{-it\omega'(\boldsymbol{k})} + e^{i\boldsymbol{k}(\boldsymbol{R}_j-\boldsymbol{R}_{j'})}e^{it\omega'(\boldsymbol{k})}\right)\right.$$
$$\left. -u_{\boldsymbol{k}}^2\left(e^{-i\boldsymbol{k}(\boldsymbol{R}_j-\boldsymbol{R}_{j'})}e^{it\omega'(\boldsymbol{k})} + e^{i\boldsymbol{k}(\boldsymbol{R}_j-\boldsymbol{R}_{j'})}e^{-it\omega'(\boldsymbol{k})}\right)\right)$$
$$\chi_{ixjy}(t) = \frac{s}{L}\Theta(t)e^{-\eta t}\sum_{\boldsymbol{k}}u_{\boldsymbol{k}}v_{\boldsymbol{k}}\left(e^{-i\boldsymbol{k}(\boldsymbol{R}_i-\boldsymbol{R}_j)} - e^{i\boldsymbol{k}(\boldsymbol{R}_i-\boldsymbol{R}_j)}\right)\left(e^{-it\omega'(\boldsymbol{k})} - e^{it\omega'(\boldsymbol{k})}\right) = 0,$$

i.e., the susceptibilities on the different sublattices are connected by exchanging $u_{\boldsymbol{k}}$ and $v_{\boldsymbol{k}}$. Calculating the Fourier transform $\int_{-\infty}^\infty dt\Theta(t)e^{i(\omega\pm\omega(\boldsymbol{k})+i\eta)t}$ and evaluating it at $\omega = 0$ yields

$$\chi_{ixi'x}(\omega = 0) = -\frac{s}{L} \sum_{\boldsymbol{k}} \frac{u_{\boldsymbol{k}}^2 + v_{\boldsymbol{k}}^2}{\omega'(\boldsymbol{k})} \left(e^{-i\boldsymbol{k}(\boldsymbol{R}_i - \boldsymbol{R}_{i'})} + e^{i\boldsymbol{k}(\boldsymbol{R}_i - \boldsymbol{R}_{i'})} \right) \tag{A.23}$$

$$\chi_{jxj'x}(\omega = 0) = -\frac{s}{L} \sum_{\boldsymbol{k}} \frac{u_{\boldsymbol{k}}^2 + v_{\boldsymbol{k}}^2}{\omega'(\boldsymbol{k})} \left(e^{-i\boldsymbol{k}(\boldsymbol{R}_j - \boldsymbol{R}_{j'})} + e^{i\boldsymbol{k}(\boldsymbol{R}_j - \boldsymbol{R}_{j'})} \right) \tag{A.24}$$

$$\chi_{ixjx}(\omega = 0) = -\frac{s}{L} \sum_{\boldsymbol{k}} \frac{2u_{\boldsymbol{k}}v_{\boldsymbol{k}}}{\omega'(\boldsymbol{k})} \left(e^{-i\boldsymbol{k}(\boldsymbol{R}_i - \boldsymbol{R}_j)} + e^{i\boldsymbol{k}(\boldsymbol{R}_i - \boldsymbol{R}_j)} \right) \tag{A.25}$$

$$\chi_{ixi'y}(\omega = 0) = -i\frac{s}{L} \sum_{\boldsymbol{k}} \frac{u_{\boldsymbol{k}}^2 + v_{\boldsymbol{k}}^2}{\omega'(\boldsymbol{k})} \left(e^{-i\boldsymbol{k}(\boldsymbol{R}_i - \boldsymbol{R}_{i'})} - e^{i\boldsymbol{k}(\boldsymbol{R}_i - \boldsymbol{R}_{i'})} \right) = 0 \tag{A.26}$$

$$\chi_{jxj'y}(\omega = 0) = -i\frac{s}{L} \sum_{\boldsymbol{k}} \frac{u_{\boldsymbol{k}}^2 + v_{\boldsymbol{k}}^2}{\omega'(\boldsymbol{k})} \left(e^{-i\boldsymbol{k}(\boldsymbol{R}_j - \boldsymbol{R}_{j'})} - e^{i\boldsymbol{k}(\boldsymbol{R}_j - \boldsymbol{R}_{j'})} \right) = 0, \tag{A.27}$$

where η was set to zero after doing the integral. Some components of the susceptibility become zero due to the summand being antisymmetric regarding $\boldsymbol{k}$. The derivative with respect to ω evaluated at $\omega = 0$ gives

$$-iJ^2 \partial_\omega \chi_{ixi'x}(\omega)\Big|_{\omega=0} = i\frac{sJ^2}{L} \sum_{\boldsymbol{k}} \frac{1}{\omega'(\boldsymbol{k})^2} \left(e^{-i\boldsymbol{k}(\boldsymbol{R}_i - \boldsymbol{R}_{i'})} - e^{i\boldsymbol{k}(\boldsymbol{R}_i - \boldsymbol{R}_{i'})} \right)$$
$$= \frac{2sJ^2}{L} \sum_{\boldsymbol{k}} \frac{\sin(\boldsymbol{k}(\boldsymbol{R}_i - \boldsymbol{R}_{i'}))}{\omega'(\boldsymbol{k})^2} = 0 \tag{A.28}$$

$$-iJ^2 \partial_\omega \chi_{jxj'x}(\omega)\Big|_{\omega=0} = -\frac{2sJ^2}{L} \sum_{\boldsymbol{k}} \frac{\sin\big(\boldsymbol{k}(\boldsymbol{R}_j - \boldsymbol{R}_{j'})\big)}{\omega'(\boldsymbol{k})^2} = 0 \tag{A.29}$$

$$-iJ^2 \partial_\omega \chi_{ixjx}(\omega)\Big|_{\omega=0} = 0 \tag{A.30}$$

$$-iJ^2 \partial_\omega \chi_{ixi'y}(\omega)\Big|_{\omega=0} = -\frac{sJ^2}{L} \sum_{\boldsymbol{k}} \frac{1}{\omega'(\boldsymbol{k})^2} \left(e^{-i\boldsymbol{k}(\boldsymbol{R}_i - \boldsymbol{R}_{i'})} + e^{i\boldsymbol{k}(\boldsymbol{R}_i - \boldsymbol{R}_{i'})} \right)$$
$$= -\frac{2sJ^2}{L} \sum_{\boldsymbol{k}} \frac{\cos(\boldsymbol{k}(\boldsymbol{R}_i - \boldsymbol{R}_{i'}))}{\omega'(\boldsymbol{k})^2} \tag{A.31}$$

$$-iJ^2 \partial_\omega \chi_{jxj'y}(\omega)\Big|_{\omega=0} = \frac{2sJ^2}{L} \sum_{\boldsymbol{k}} \frac{\cos\big(\boldsymbol{k}(\boldsymbol{R}_j - \boldsymbol{R}_{j'})\big)}{\omega'(\boldsymbol{k})^2}, \tag{A.32}$$

where due to $\big\langle \big[s_i^x(t), s_{i'}^x(0) \big] \big\rangle^{(0)} = \big\langle \big[s_i^y(t), s_{i'}^y(0) \big] \big\rangle^{(0)}$ the xx elements have the same value as the yy elements. One sees that the only nonvanishing components are the xy terms and their value is the same as the one calculated via the Lehmann representation of the spin-Berry curvature in publication [II].

Bibliography

[1] R. A. Millikan, The Isolation of an Ion, a Precision Measurement of Its Charge, and the Correction of Stokes's Law, Science **32**, 436 (1910).

[2] S. A. Wolf, D. D. Awschalom, R. A. Buhrman, J. M. Daughton, S. von Molnár, M. L. Roukes, A. Y. Chtchelkanova, and D. M. Treger, Spintronics: A Spin-Based Electronics Vision for the Future, Science **294**, 1488 (2001).

[3] I. Žutić, J. Fabian, and S. Das Sarma, Spintronics: Fundamentals and applications, Reviews of Modern Physics **76**, 323 (2004).

[4] A. Fert, Nobel Lecture: Origin, development, and future of spintronics, Reviews of Modern Physics **80**, 1517 (2008).

[5] S. D. Bader and S. S. P. Parkin, Spintronics, Annual Review of Condensed Matter Physics **1**, 71 (2010).

[6] A. Fert and I. A. Campbell, Two-Current Conduction in Nickel, Physical Review Letters **21**, 1190 (1968).

[7] M. N. Baibich, J. M. Broto, A. Fert, F. N. Van Dau, F. Petroff, P. Etienne, G. Creuzet, A. Friederich, and J. Chazelas, Giant Magnetoresistance of (001)Fe/(001)Cr Magnetic Superlattices, Physical Review Letters **61**, 2472 (1988).

[8] G. Binasch, P. Grünberg, F. Saurenbach, and W. Zinn, Enhanced magnetoresistance in layered magnetic structures with antiferromagnetic interlayer exchange, Physical Review B **39**, 4828 (1989).

[9] B. Dieny, Giant magnetoresistance in spin-valve multilayers, Journal of Magnetism and Magnetic Materials **136**, 335 (1994).

[10] A. Hirohata, K. Yamada, Y. Nakatani, I.-L. Prejbeanu, B. Diény, P. Pirro, and B. Hillebrands, Review on spintronics: Principles and device applications, Journal of Magnetism and Magnetic Materials **509**, 166711 (2020).

[11] T. Miyazaki and N. Tezuka, Giant magnetic tunneling effect in Fe/Al2O3/Fe junction, Journal of Magnetism and Magnetic Materials **139**, L231 (1995).

[12] C. Chappert, A. Fert, and F. N. Van Dau, The emergence of spin electronics in data storage, Nature Materials **6**, 813 (2007).

[13] R. Sbiaa, H. Meng, and S. N. Piramanayagam, Materials with perpendicular magnetic anisotropy for magnetic random access memory, physica status solidi (RRL) – Rapid Research Letters **5**, 413 (2011).

[14] S. Ikegawa, F. B. Mancoff, J. Janesky, and S. Aggarwal, Magnetoresistive Random Access Memory: Present and Future, IEEE Transactions on Electron Devices **67**, 1407 (2020).

[15] A. A. Khajetoorians, J. Wiebe, B. Chilian, and R. Wiesendanger, Realizing All-Spin–Based Logic Operations Atom by Atom, Science **332**, 1062 (2011).

[16] B. Behin-Aein, J.-P. Wang, and R. Wiesendanger, Computing with spins and magnets, MRS Bulletin **39**, 696 (2014).

[17] A. A. Khajetoorians, S. Lounis, B. Chilian, A. T. Costa, L. Zhou, D. L. Mills, J. Wiebe, and R. Wiesendanger, Itinerant Nature of Atom-Magnetization Excitation by Tunneling Electrons, Physical Review Letters **106**, 037205 (2011).

[18] L. D. Landau and E. M. Lifshitz, On the theory of the dispersion of magnetic permeability in ferromagnetic bodies, Physik. Zeits. Sowjetunion **8**, 153 (1935).

[19] T. Gilbert, A phenomenological theory of damping in ferromagnetic materials, IEEE Transactions on Magnetics **40**, 3443 (2004).

[20] A. Brataas, Y. Tserkovnyak, and G. E. W. Bauer, Scattering Theory of Gilbert Damping, Physical Review Letters **101**, 037207 (2008).

[21] D. Thonig and J. Henk, Gilbert damping tensor within the breathing Fermi surface model: anisotropy and non-locality, New Journal of Physics **16**, 013032 (2014).

[22] F. Reyes-Osorio and B. K. Nikolić, Gilbert damping in metallic ferromagnets from Schwinger-Keldysh field theory: Intrinsically nonlocal, nonuniform, and made anisotropic by spin-orbit coupling, Physical Review B **109**, 024413 (2024).

[23] M. Elbracht and M. Potthoff, Prerelaxation in quantum, classical, and quantum-classical two-impurity models, Physical Review Research **6**, 033275 (2024).

[24] G. Bertotti, I. D. Mayergoyz, and C. Serpico, *Nonlinear Magnetization Dynamics in Nanosystemes* (Elsevier, Amsterdam, 2009).

[25] E. Butikov, Precession and nutation of a gyroscope, European Journal of Physics **27**, 1071 (2006).

[26] M. Fähnle, D. Steiauf, and C. Illg, Generalized Gilbert equation including inertial damping: Derivation from an extended breathing Fermi surface model, Physical Review B **84**, 172403 (2011).

[27] S. Bhattacharjee, L. Nordström, and J. Fransson, Atomistic Spin Dynamic Method with both Damping and Moment of Inertia Effects Included from First Principles, Physical Review Letters **108**, 057204 (2012).

[28] J.-E. Wegrowe and M.-C. Ciornei, Magnetization dynamics, gyromagnetic relation, and inertial effects, American Journal of Physics **80**, 607 (2012).

[29] T. Kikuchi and G. Tatara, Spin dynamics with inertia in metallic ferromagnets, Physical Review B **92**, 184410 (2015).

[30] M. Sayad, R. Rausch, and M. Potthoff, Inertia effects in the real-time dynamics of a quantum spin coupled to a Fermi sea, Europhysics Letters **116**, 17001 (2016).

[31] U. Bajpai and B. K. Nikolić, Time-retarded damping and magnetic inertia in the Landau-Lifshitz-Gilbert equation self-consistently coupled to electronic time-dependent nonequilibrium Green functions, Physical Review B **99**, 134409 (2019).

[32] M. A. Ruderman and C. Kittel, Indirect Exchange Coupling of Nuclear Magnetic Moments by Conduction Electrons, Physical Review **96**, 99 (1954).

[33] T. Kasuya, A Theory of Metallic Ferro- and Antiferromagnetism on Zener's Model, Progress of Theoretical Physics **16**, 45 (1956).

[34] K. Yosida, Magnetic Properties of Cu-Mn Alloys, Physical Review **106**, 893 (1957).

[35] J. Kuneš and V. Kamberský, First-principles investigation of the damping of fast magnetization precession in ferromagnetic 3d metals, Physical Review B **65**, 212411 (2002).

[36] K. Gilmore, Y. U. Idzerda, and M. D. Stiles, Identification of the Dominant Precession-Damping Mechanism in Fe, Co, and Ni by First-Principles Calculations, Physical Review Letters **99**, 027204 (2007).

[37] G. Tatara, H. Kohno, and J. Shibata, Microscopic approach to current-driven domain wall dynamics, Physics Reports **468**, 213 (2008).

[38] B. Skubic, J. Hellsvik, L. Nordström, and O. Eriksson, A method for atomistic spin dynamics simulations: implementation and examples, Journal of Physics: Condensed Matter **20**, 315203 (2008).

[39] M. C. Hickey and J. S. Moodera, Origin of Intrinsic Gilbert Damping, Physical Review Letters **102**, 137601 (2009).

[40] A. A. Starikov, P. J. Kelly, A. Brataas, Y. Tserkovnyak, and G. E. W. Bauer, Unified First-Principles Study of Gilbert Damping, Spin-Flip Diffusion, and Resistivity in Transition Metal Alloys, Physical Review Letters **105**, 236601 (2010).

[41] M. Fähnle and C. Illg, Electron theory of fast and ultrafast dissipative magnetization dynamics, Journal of Physics: Condensed Matter **23**, 493201 (2011).

[42] A. Sakuma, First-Principles Study on the Gilbert Damping Constants of Transition Metal Alloys, Fe–Ni and Fe–Pt Systems, Journal of the Physical Society of Japan **81**, 084701 (2012).

[43] S. Mankovsky, D. Ködderitzsch, G. Woltersdorf, and H. Ebert, First-principles calculation of the Gilbert damping parameter via the linear response formalism with application to magnetic transition metals and alloys, Physical Review B **87**, 014430 (2013).

[44] R. F. L. Evans, W. J. Fan, P. Chureemart, T. A. Ostler, M. O. A. Ellis, and R. W. Chantrell, Atomistic spin model simulations of magnetic nanomaterials, Journal of Physics: Condensed Matter **26**, 103202 (2014).

[45] M. Sayad and M. Potthoff, Spin dynamics and relaxation in the classical-spin Kondo-impurity model beyond the Landau–Lifschitz–Gilbert equation, New Journal of Physics **17**, 113058 (2015).

[46] J. Kondo, Resistance Minimum in Dilute Magnetic Alloys, Progress of Theoretical Physics **32**, 37 (1964).

[47] A. C. Hewson, *The Kondo Problem to Heavy Fermions* (Cambridge University Press, Cambridge, 1993).

[48] R. Smorka, P. Baláž, M. Thoss, and M. Žonda, Nonequilibrium dynamics in a spin valve with noncollinear magnetization, Physical Review B **106**, 144435 (2022).

[49] R. Smorka, M. Thoss, and M. Žonda, Dynamics of spin relaxation in nonequilibrium magnetic nanojunctions, New Journal of Physics **26**, 013056 (2024).

[50] A. Suresh, R. D. Soares, P. Mondal, J. P. S. Pires, J. M. V. P. Lopes, A. Ferreira, A. E. Feiguin, P. Plecháč, and B. K. Nikolić, Electron-mediated entanglement of two distant macroscopic ferromagnets within a nonequilibrium spintronic device, Physical Review A **109**, 022414 (2024).

[51] R. Kubo, Statistical-Mechanical Theory of Irreversible Processes. I. General Theory and Simple Applications to Magnetic and Conduction Problems, Journal of the Physical Society of Japan **12**, 570 (1957).

[52] V. Kamberský, On ferromagnetic resonance damping in metals, Czechoslovak Journal of Physics B **26**, 1366 (1976).

[53] V. Kamberský, Spin-orbital Gilbert damping in common magnetic metals, Physical Review B **76**, 134416 (2007).

[54] H. Ebert, S. Mankovsky, D. Ködderitzsch, and P. J. Kelly, Ab Initio Calculation of the Gilbert Damping Parameter via the Linear Response Formalism, Physical Review Letters **107**, 066603 (2011).

[55] M. Sayad, R. Rausch, and M. Potthoff, Relaxation of a Classical Spin Coupled to a Strongly Correlated Electron System, Physical Review Letters **117**, 127201 (2016).

[56] C. Stahl and M. Potthoff, Anomalous Spin Precession under a Geometrical Torque, Physical Review Letters **119**, 227203 (2017).

[57] S. Michel and M. Potthoff, Spin Berry curvature of the Haldane model, Physical Review B **106**, 235423 (2022).

[58] D. Marx and J. Hutter, *Ab initio molecular dynamics: Theory and Implementation,* In: *Modern Methods and Algorithms of Quantum Chemistry* NIC Series, Vol. 1, Ed. by J. Grotendorst, p. 301 (John von Neumann Institute for Computing, Jülich, 2000).

[59] Q. Zhang and B. Wu, General Approach to Quantum-Classical Hybrid Systems and Geometric Forces, Physical Review Letters **97**, 190401 (2006).

[60] M. Born and R. Oppenheimer, Zur Quantentheorie der Molekeln, Annalen der Physik **389**, 457 (1927).

[61] M. Born and V. Fock, Beweis des Adiabatensatzes, Zeitschrift für Physik **51**, 165 (1928).

[62] T. Kato, On the Adiabatic Theorem of Quantum Mechanics, Journal of the Physical Society of Japan **5**, 435 (1950).

[63] G. Rigolin and G. Ortiz, Adiabatic theorem for quantum systems with spectral degeneracy, Physical Review A **85**, 062111 (2012).

[64] M. V. Berry, Quantal phase factors accompanying adiabatic changes, Proceedings of the Royal Society of London. A. Mathematical and Physical Sciences **392**, 45 (1997).

[65] H. Kuratsuji and S. Iida, Effective Action for Adiabatic Process: Dynamical Meaning of Berry and Simon's Phase, Progress of Theoretical Physics **74**, 439 (1985).

[66] J. Moody, A. Shapere, and F. Wilczek, Realizations of Magnetic-Monopole Gauge Fields: Diatoms and Spin Precession, Physical Review Letters **56**, 893 (1986).

[67] X. G. Wen and A. Zee, Spin Waves and Topological Terms in the Mean-Field Theory of Two-Dimensional Ferromagnets and Antiferromagnets, Physical Review Letters **61**, 1025 (1988).

[68] Q. Niu and L. Kleinman, Spin-Wave Dynamics in Real Crystals, Physical Review Letters **80**, 2205 (1998).

[69] Q. Niu, X. Wang, L. Kleinman, W.-M. Liu, D. M. C. Nicholson, and G. M. Stocks, Adiabatic Dynamics of Local Spin Moments in Itinerant Magnets, Physical Review Letters **83**, 207 (1999).

[70] M. Elbracht, S. Michel, and M. Potthoff, Topological Spin Torque Emerging in Classical Spin Systems with Different Timescales, Physical Review Letters **124**, 197202 (2020).

[71] M. V. Berry and J. M. Robbins, Chaotic classical and half-classical adiabatic reactions: geometric magnetism and deterministic friction, Proceedings of the Royal Society of London. Series A: Mathematical and Physical Sciences **442**, 659 (1997).

[72] M. Campisi, S. Denisov, and P. Hänggi, Geometric magnetism in open quantum systems, Physical Review A **86**, 032114 (2012).

[73] F. Garcia-Gaitan and B. K. Nikolić, Fate of entanglement in magnetism under Lindbladian or non-Markovian dynamics and conditions for their transition to Landau-Lifshitz-Gilbert classical dynamics, Physical Review B **109**, L180408 (2024).

[74] S. V. Vonsovsky, Zh. Éksp. Teor. Fiz. **16**, 981 (1946); C. Zener, Phys. Rev. **81**, 440 (1951); S. V. Vonsovsky and E. A. Turov, Zh. Éksp. Teor. Fiz. **24**, 419 (1953).

[75] U. Schollwöck, The density-matrix renormalization group in the age of matrix product states, Annals of Physics **326**, 96 (2011).

[76] C. A. Büsser, G. B. Martins, and A. E. Feiguin, Lanczos transformation for quantum impurity problems in d-dimensional lattices: Application to graphene nanoribbons, Physical Review B **88**, 245113 (2013).

[77] A. Allerdt and A. E. Feiguin, A Numerically Exact Approach to Quantum Impurity Problems in Realistic Lattice Geometries, Frontiers in Physics **7** (2019).

[78] A. Heslot, Quantum mechanics as a classical theory, Physical Review D **31**, 1341 (1985).

[79] M. J. W. Hall, Consistent classical and quantum mixed dynamics, Physical Review A **78**, 042104 (2008).

[80] H.-T. Elze, Linear dynamics of quantum-classical hybrids, Physical Review A **85**, 052109 (2012).

[81] K.-H. Yang and J. O. Hirschfelder, Generalizations of classical Poisson brackets to include spin, Physical Review A **22**, 1814 (1980).

[82] M. Lakshmanan and M. Daniel, Comment on the classical models of electrons and nuclei and the generalizations of classical Poisson brackets to include spin, The Journal of Chemical Physics **78**, 7505 (1983).

[83] G. Czycholl, *Theoretische Festkörperphysik*, Springer-Lehrbuch (Springer, Berlin, Heidelberg, 2008).

[84] W. Nolting and A. Ramakanth, *Quantum Theory of Magnetism*, (Springer, Berlin, Heidelberg, 2009).

[85] T. Moriya, Anisotropic Superexchange Interaction and Weak Ferromagnetism, Physical Review **120**, 91 (1960).

[86] I. Dzyaloshinsky, A thermodynamic theory of "weak" ferromagnetism of antiferromagnetics, Journal of Physics and Chemistry of Solids **4**, 241 (1958).

[87] D. Treves and S. Alexander, Observation of Antisymmetric Exchange Interaction in Yttrium Orthoferrite, Journal of Applied Physics **33**, 1133 (1962).

[88] G. C. Wick, The Evaluation of the Collision Matrix, Physical Review **80**, 268 (1950).

[89] L. G. Molinari, Notes on Wick's theorem in many-body theory, arXiv:1710.09248 (2023).

[90] A. Bohm, A. Mostafazadeh, H. Koizumi, Q. Niu, and J. Zwanziger, *The Geometric Phase in Quantum Systems* (Springer, Berlin, 2003).

[91] H. Reinhardt, *Band 2 Pfadintegralformulierung und Operatorformalismus*, (De Gruyter Oldenbourg, 2020).

[92] J. Goldstone, Field theories with « Superconductor » solutions, Il Nuovo Cimento (1955-1965) **19**, 154 (1961).

[93] Y. Nambu and G. Jona-Lasinio, Dynamical Model of Elementary Particles Based on an Analogy with Superconductivity. I, Physical Review **122**, 345 (1961).

[94] P. C. Hohenberg, Existence of Long-Range Order in One and Two Dimensions, Physical Review **158**, 383 (1967).

[95] N. D. Mermin and H. Wagner, Absence of Ferromagnetism or Antiferromagnetism in One- or Two-Dimensional Isotropic Heisenberg Models, Physical Review Letters **17**, 1133 (1966).

[96] V. L. Berezinsky, Destruction of Long-range Order in One-dimensional and Two-dimensional Systems Possessing a Continuous Symmetry Group. II. Quantum Systems., Sov. Phys. JETP **34**, 610 (1972).

[97] T. Holstein and H. Primakoff, Field Dependence of the Intrinsic Domain Magnetization of a Ferromagnet, Physical Review **58**, 1098 (1940).

[98] T. Brauner, Spontaneous Symmetry Breaking and Nambu–Goldstone Bosons in Quantum Many-Body Systems, Symmetry **2**, 609 (2010).

[99] P. W. Anderson, An Approximate Quantum Theory of the Antiferromagnetic Ground State, Physical Review **86**, 694 (1952).

[100] A. Beekman, L. Rademaker, and J. van Wezel, An introduction to spontaneous symmetry breaking, SciPost Physics Lecture Notes p. 011 (2019).

[101] C. Jarzynski, Nonequilibrium Equality for Free Energy Differences, Physical Review Letters **78**, 2690 (1997).

[102] P. Talkner, E. Lutz, and P. Hänggi, Fluctuation theorems: Work is not an observable, Physical Review E **75**, 050102 (2007).

[103] M. Campisi, P. Hänggi, and P. Talkner, Colloquium: Quantum fluctuation relations: Foundations and applications, Reviews of Modern Physics **83**, 771 (2011).

[104] D. Andrieux and P. Gaspard, Quantum Work Relations and Response Theory, Physical Review Letters **100**, 230404 (2008).

[105] F. Wilczek and A. Zee, Appearance of Gauge Structure in Simple Dynamical Systems, Physical Review Letters **52**, 2111 (1984).

[106] D. Xiao, M.-C. Chang, and Q. Niu, Berry phase effects on electronic properties, Reviews of Modern Physics **82**, 1959 (2010).

[107] A. Zee, Non-Abelian gauge structure in nuclear quadrupole resonance, Physical Review A **38**, 1 (1988).

[108] D. R. Yarkony, Diabolical conical intersections, Reviews of Modern Physics **68**, 985 (1996).

[109] N. H. Le, A. J. Fisher, N. J. Curson, and E. Ginossar, Topological phases of a dimerized Fermi–Hubbard model for semiconductor nano-lattices, npj Quantum Information **6**, 1 (2020).

[110] R. Quade and M. Potthoff, Controlling the real-time dynamics of a spin coupled to the helical edge states of the Kane-Mele model, Physical Review B **105**, 035406 (2022).

[111] S. Nadj-Perge, I. K. Drozdov, B. A. Bernevig, and A. Yazdani, Proposal for realizing Majorana fermions in chains of magnetic atoms on a superconductor, Physical Review B **88**, 020407 (2013).

[112] R. Wiesendanger, Spin mapping at the nanoscale and atomic scale, Reviews of Modern Physics **81**, 1495 (2009).

[113] A. A. Khajetoorians, J. Wiebe, B. Chilian, S. Lounis, S. Blügel, and R. Wiesendanger, Atom-by-atom engineering and magnetometry of tailored nanomagnets, Nature Physics **8**, 497 (2012).

[114] M. Oogane, T. Wakitani, S. Yakata, R. Yilgin, Y. Ando, A. Sakuma, and T. Miyazaki, Magnetic Damping in Ferromagnetic Thin Films, Japanese Journal of Applied Physics **45**, 3889 (2006).

[115] J. C. Sankey, P. M. Braganca, A. G. F. Garcia, I. N. Krivorotov, R. A. Buhrman, and D. C. Ralph, Spin-Transfer-Driven Ferromagnetic Resonance of Individual Nanomagnets, Physical Review Letters **96**, 227601 (2006).

[116] R. Wiesendanger, Single-atom magnetometry, Current Opinion in Solid State and Materials Science **15**, 1 (2011).

[117] M. Hervé, M. Peter, T. Balashov, and W. Wulfhekel, Towards Laterally Resolved Ferromagnetic Resonance with Spin-Polarized Scanning Tunneling Microscopy, Nanomaterials **9**, 827 (2019).

[118] T. Jungwirth, X. Marti, P. Wadley, and J. Wunderlich, Antiferromagnetic spintronics, Nature Nanotechnology **11**, 231 (2016).

[119] V. Baltz, A. Manchon, M. Tsoi, T. Moriyama, T. Ono, and Y. Tserkovnyak, Antiferromagnetic spintronics, Reviews of Modern Physics **90**, 015005 (2018).

[120] Y. Li and W. Bailey, Wave-Number-Dependent Gilbert Damping in Metallic Ferromagnets, Physical Review Letters **116**, 117602 (2016).

[121] J. P. Provost and G. Vallee, Riemannian structure on manifolds of quantum states, Communications in Mathematical Physics **76**, 289 (1980).

[122] W. Chen and G. von Gersdorff, Measurement of interaction-dressed Berry curvature and quantum metric in solids by optical absorption, SciPost Physics Core **5**, 040 (2022).

[123] K. Fujikawa and K. Umetsu, Path-integral derivation of the equations of the anomalous Hall effect, Physical Review B **105**, 155118 (2022).

Never confuse education with intelligence,
you can have a PhD and still be an idiot.

— **RICHARD FEYNMAN**

☐

Eidesstattliche Versicherung

Hiermit versichere ich an Eides statt, die vorliegende Dissertationsschrift selbst verfasst und keine anderen als die angegebenen Hilfsmittel und Quellen benutzt zu haben.

Sofern im Zuge der Erstellung der vorliegenden Dissertationsschrift generative Künstliche Intelligenz (gKI) basierte elektronische Hilfsmittel verwendet wurden, versichere ich, dass meine eigene Leistung im Vordergrund stand und dass eine vollständige Dokumentation aller verwendeten Hilfsmittel gemäß der Guten wissenschaftlichen Praxis vorliegt. Ich trage die Verantwortung für eventuell durch die gKI generierte fehlerhafte oder verzerrte Inhalte, fehlerhafte Referenzen, Verstöße gegen das Datenschutz- und Urheberrecht oder Plagiate.

Hamburg, den   _____

                                                            Nicolas Lenzing